Growth and Maintenance of the Mouse Adrenal Cortex

by

Su-Ping Chang
MSc in Reproductive Biology
BSc (Honours) in Medical Technology

Division of Reproductive & Developmental Sciences
The University of Edinburgh

Thesis submitted to the University of Edinburgh
for the degree of Doctor of Philosophy

2008

Declaration

The BrdU injections and surgical implantation of osmotic mini pumps were done for me by Mr Keith Chalmers (an animal technician in the Biomedical Research Facility, University of Edinburgh). Some statistical analysis was performed for me by Dr Robert Elton (Medical Statistics Consulting, Edinburgh) and Dr John West (my supervisor) helped with some other statistical tests. My supervisors (Dr John West and Dr Steve Morley) corrected the first draft of all of the chapters to improve the English and provide critical feedback. Otherwise, except where clearly stated elsewhere, the experiments described in this thesis are my own work.

No part of this work has been submitted in support of another degree or qualification.

Su-Ping Chang
2008

Abstract

The adrenal cortex is classically divided into three morphologically and biochemically distinct zones, covered by a thin, cellular capsule. The adult adrenal cortex is a dynamic tissue in which distinct regions of cell proliferation, movement and death have been identified. Several models for stem cell maintenance of the adult adrenal cortex have been proposed, but adrenocortical stem cells have not yet been identified. Adrenal cortices of *21OH/LacZ* transgenic mice show similar mosaic patterns of β-galactosidase staining to X- inactivation mosaics and *LacZ* ↔ wildtype chimeras. *21OH/LacZ* mice provide a tool for lineage analysis, which may help to i) identify clones of cells produced by stem cells in the adult, ii) determine when stem cells begin to function and iii) evaluate different models of how stem cells maintain the adrenal cortex. Analysis of *21OH/LacZ* transgenic adrenal cortices showed that the randomly orientated clusters of fetal patches change progressively during the perinatal period to adult radial stripes. Correlation of changes in mosaic patterns and the locations of cell proliferation suggests that the stripes arise by edge-biased growth during the perinatal growth period. Although stem cells may not be involved in the initial formation of stripes, it seems likely that stem cells later maintain the stripes by producing clones of cells that move centripetally to displace the earlier fetal patterns and later replace aging cells. Various combinations of BrdU labelling and chase periods demonstrated that most cell division occurred in the outer 40% of the adrenal cortex, confirmed that cells moved towards the medulla and identified a population of label-retaining cells near the capsule, which could include stem cells. (Stem cells have been recognised as BrdU label-retaining cells in other tissues because they divide less frequently than their daughter cells so dilute the incorporated BrdU more slowly.) Stripe patterns in adult *21OH/LacZ* transgenic adrenal cortices were examined to try to distinguish between various models proposed for stem cell maintenance of the adrenal cortex. The observed continuous radial stripe pattern favours the general hypothesis that a single population of stem cells in the periphery maintains the entire adrenal cortex,

although other explanations are possible. Quantitative analysis of adult stripe patterns did not show the reduction in stripe number that might be predicted if an age-related decline in adrenocortical stem cell function occurs, as may happen in some other tissues.

Acknowledgements

My special thanks go to my supervisors Dr John West, Dr Steve Morley and all members of the West lab (past and present) for their help and support. I am grateful for an award from the University of Edinburgh Scholarships and Student Finance Office which allowed me to complete the writing of this thesis. I would also like to express my appreciation to my family and friends for their support and concerns, especially my father.

List of posters, presentations and published abstracts

1. Chang S-P, Morley SD, West JD (2004). Evaluation of the suitability of mosaic *21OH/LacZ* transgenic mice for lineage analysis in the adrenal cortex. Abstract for a poster: Scottish Society for Experimental Medicine, Edinburgh, UK, 12th November 2004. Published in the *Scottish Medical Journal*.

2. Chang S-P, Morley SD, West JD (2005). Preliminary evidence for maintenance of the adrenal cortex by bi-directional cell migration from distinct stem cell populations located in the undifferentiated zone. Poster: Scottish Stem Cell Network: Stem Cells 2005: Progress to therapy? Edinburgh, UK, 4-5th March 2005.

3. Chang S-P, West JD, Morley SD (2006). Changes in mosaic patterns of transgene expression during organogenesis and growth of the adrenal cortex. Poster: British Society for Developmental Biology/British Society for Cell Biology joint spring meeting, York, UK; 20-23rd March 2006.

4. Chang S-P, West JD, Morley SD (2006). Preliminary evidence for the mechanism of mouse adrenal cortex maintenance from mosaic stripe pattern analysis. Abstract for an invited talk: 15th Simpson Symposium 'Reproductive Recycling: Germ Cells to Stem Cells', Edinburgh, UK; 3-5th September 2006.

5. Chang S-P, West JD, Morley SD (2007). The mosaic patterns of *21OH/LacZ* transgene expression changes during organogenesis and growth of the adrenal cortex. Abstract for a poster: Society for Endocrinology/British Endocrine Societies meeting, Birmingham, UK; 5-8th March 2007. Published in *Endocrine Abstracts* 13 P133.

6. Chang S-P, West JD, Morley SD (2007). Clues about organogenesis and maintenance of the adult mouse adrenal cortex from analysis of mosaic patterns of expression of a *21OHase/LacZ* transgene. Abstract for a poster: Anatomical Society Meeting 'Advances in stem Cell Biology', Durham 3-5th July 2007. Published in *Journal of Anatomy* 212, 86.

Table of contents

List of Abbreviations

°C	Degree Celsius
µm	Micrometer
21OH	21-hydroxylase
21OH/LacZ	21-hydroxylase/LacZ reporter transgene
ABCG2	ATP-binding cassette, sub-family G (White), member 2
ACTH	Adrenocorticotrophic hormone
ANOVA	Analysis of variance
BrdU	Bromodeoxyuridine (5-bromo-2-deoxyuridine)
C-19	Carbon 19
CRF	Corticotropin-releasing factor
CRH	Corticotrophin-releasing hormone
Cx43	Connexin 43 (or gap junction protein, alpha 1, 43kDa; Gja1)
d.p.i.	Dots per inch
DAB	3,3'-diaminobenzidine
DHEA	Dehydroepiandrosterone
E	Embryonic day
ES cells	Embryonic stem cells
F1	First filial generation or initial hybrid progeny of cross-breeding (Latin, filial = son)
FACS	Fluorescent-activated cell sorting
G0 phase	Period in the cell cycle where cells exist in a quiescent state
G1 phase	Gap 1 (after M phase and before S phase in the cell cycle)
G2 phase	Gap 2 (after S phase and before M phase in the cell cycle)
GFP	Green fluorescent protein
h	Hour
H & E	Haematoxylin and eosin
HPA	Hypothalamic-pituitary-adrenal axis
HSC	Haematopoietic stem cell
i.p.	Intraperitoneal

IddU	Iododeoxyuridine
ISC	Intestinal stem cell
K12	Keratin 12
K3	Keratin 3
Ki67	Ki67 protein is present during all active phases of the cell cycle (G1, S, G2 & M) and is also known as antigen identified by monoclonal antibody Ki67 (MKI67)
LSC	Limbal stem cell (limbus is at the periphery of the corneal epithelium)
M phase	Mitosis
min	Minute
P	Postnatal day
PBS	Phosphate buffered saline
PCNA	Proliferating cell nuclear antigen
PFA	Paraformaldehyde
S phase	Synthesis phase of the cell cycle
SCC	Cholesterol side chain cleavage enzyme (also known as CYP11A1 or cytochrome P450, family 11, subfamily A, polypeptide 1)
SF-1	Steroidogenic factor 1
TA cell	Transient amplifying cell (or Transit amplifying cell)
TBS	Tris buffered saline
Tris	Tris(hydroxymethyl)aminomethane
TUNEL	Terminal deoxynucleotidyl transferase mediated dUTP Nick End Labeling
v/v	Volume for volume
w/v	Weight for volume
X-gal	5-bromo-4-chloro-3-indolyl-beta-D galactopyranoside
ZF	Zona Fasciculata
ZG	Zona glomerulosa
ZR	Zona reticularis

ZU(ZI)	Undifferentiated zone (Zona intermedia)
β-gal	β-galactosidase

1 Introduction

1.1 The adrenal gland

1.1.1 Location and anatomy of the adrenal gland

Mammals have two adrenal glands, which are also known as the suprarenal glands because of their anatomical location. They are embedded in the perirenal fat at the superior pole of the kidneys. Individual glands are covered with a connective tissue capsule from which trabeculae (small tissue extensions) penetrate into the parenchyma, carrying blood vessels and nerves. Adrenal glands of different species vary in shape from ovoid (mouse), through a rounded pyramidal shape (rat) to a flattened triangular pancake (human).

The adrenal gland is essentially two endocrine glands in one and comprises two distinct structures of different embryological origin and function, namely the outer cortex and inner medulla (Fig. 1.1). The adrenal medulla is an extension of the sympathetic nervous system and is composed of irregularly packed neurosecretory chromaffin cells distinguished by their dense-cored vesicles, containing the catecholamines adrenalin (epinephrine) and noradrenalin (norepinephrine), connective tissue, blood capillaries and nerves. The adult adrenal cortex is composed of 3 concentric definitive zones of steroid-synthesizing cells, the zona glomerulosa, zona fasciculata, and zona reticularis. Each zone displays a characteristic arrangement of cells but the boundaries between zones are somewhat indistinct. Cells of the adrenal cortex are characterised by abundant mitochondria with highly branched cristae and ample smooth endoplasmic reticulum. In the adult mouse, cells in the outer zona glomerulosa (ZG) are small, basophilic and arranged in arches. Cells of the zona fasciculata (ZF) contain abundant lipid droplets, the substrate for steroid hormone synthesis, and are eosinophilic and arranged in columns. The zona reticularis (ZR) is the innermost

zone of the adrenal cortex (adjacent to the adrenal medulla) and ZR cells display a characteristically compacted morphology. The existence of a mouse ZR has sometimes been controversial but its presence can clearly be documented on morphological criteria, although the thickness of the zone can be highly variable between individual mouse strains (Tanaka and Matsuzawa, 1995).

Based on immunohistochemical staining, some authors have described a zona intermedia (ZI) or undifferentiated zone (ZU), located between the ZG and ZF of rats and mice, that does not express cortical zone-specific enzymes (aldosterone synthetase in ZG and 11β-hydroxylase in ZF) (Mitani et al., 2003; Mitani et al., 1994; Mukai et al., 2002). However these non-staining cells may be more properly associated with the inner cell layers of the morphological zona glomerulosa (Vinson, 2003).

The human fetal adrenal gland consists principally of a special fetal zone, that synthesises precursor steroids which can be converted to oestrogen by the placenta, surrounded by a 'rim' of definitive tissue. The fetal zone 'involutes' or disappears rapidly after birth to be replaced by the expanding definitive zone (Winter, 1985). Recent evidence suggest that the developing mouse adrenal cortex may also mainly comprise a fetal zone, the residue of which forms the so-called X zone from around P10, following its replacement by definitive tissue around birth (Zubair et al., 2006). Cells of the mouse X zone appear highly basophilic (highly stained with haematoxylin) following histological staining with haematoxylin and eosin (Nyska and Maronpot, 1999).

The adrenal gland is highly vascular and in humans receives a rich blood supply from the superior, middle and inferior adrenal arteries. These usually arise from the inferior phrenic, abdominal aorta and renal arteries respectively, although individual variations in vascular connections are common within species (Ganong, 1997). Blood in the arteries is dispersed into a network of arterioles in the adrenal capsule. Two types of arteries arise from the arteriolar capsular plexus and penetrate the cortex and medulla: (1) The *arteriae medullae* supply the medulla, passing through the cortex without branching and divide into arterioles and capillaries in the medulla. (2) The *arteriae corticis* arise directly from the capsule and form a network surrounding the clusters of glomerulosa cells and continue as centripetal capillaries lining the fasciculata cell columns. These cortical capillaries open into a sinusoidal plexus in the ZR. Both cortical and medullary arteries drain into the peripheral radicles of the central medullary vein. The left and right adrenal medullary veins drain respectively into the left renal vein and the inferior vena cava (Thomas et al., 2003).

The adrenal gland is well supplied with nerves and is innervated through a subcapsular plexus. The adrenal medulla is an extension of the sympathetic nervous system comprised mainly of neurosecretory chromaffin cells that secrete the catecholamines adrenalin and noradrenalin, which regulate the so-called 'fight or flight' response, but this is beyond the scope of this thesis, which is focused on the adrenal cortex. With a few exceptions, the historical view was that the nerve supply to the medulla passed through the cortex with little if any connection to adrenocortical cells and therefore that the adrenal cortex was not directly innervated. However, since the 1970s, clear descriptions of a richly innervated adrenal cortex have emerged for a variety of species, including rat and also sympathetic and sensory regulation of cortisol release (reviewed in Ehrhart-Bornstein et al., 1998). Briefly, the adrenal cortex is innervated by several types of nerve fibres of both extrinsic and intrinsic origin (extrinsic nerves have their cell bodies outside the adrenal gland while intrinsic nerves are wholly contained within the adrenal gland). The principal source of extrinsic adrenal innervation is

the thoracic splanchnic nerve that carries both sympathetic and sensory nerve fibres which form a subcapsular plexus in association with the capillary vasculature. Some nerve fibres from the subcapsular region pass radially between the cell columns of the ZF, terminating adjacent to steroid producing cells. Other sympathetic nerve fibres pass directly through the cortex in association with the medullary arterioles and terminate within the medulla. Intrinsic innervation of the cortex originates from the medulla from where nerve fibres radiate out, terminating in the cortex. It is notable that the arrangement of the nerves innervating the adrenal cortex and medulla parallel the centripetal organisation of the adrenocortical vasculature and the columnar arrangements of cells in the ZF (Fig. 1.2), and it may well be that each capillary is associated with at least one fine nerve (Teitelbaum, 1942).

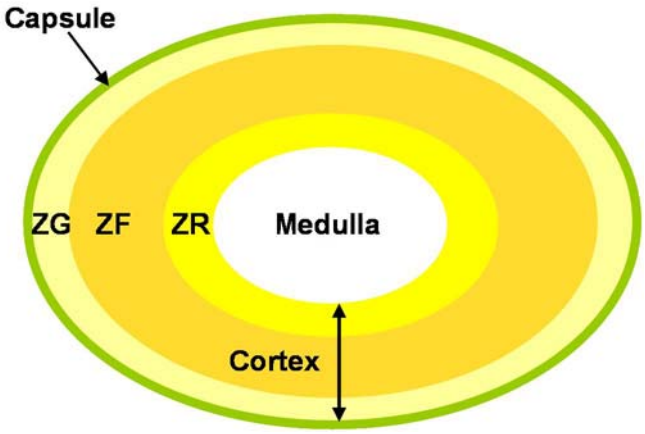

Fig. 1.1. Anatomical arrangement of mouse adrenal gland. The adrenal gland comprises an inner medulla and an outer cortex, which is covered by a thin cellular capsule. The cortex has three classical zones, the ZG (zona glomerulosa), ZF (zona fasciculata), and ZR (zona reticularis), showing distinct morphology.

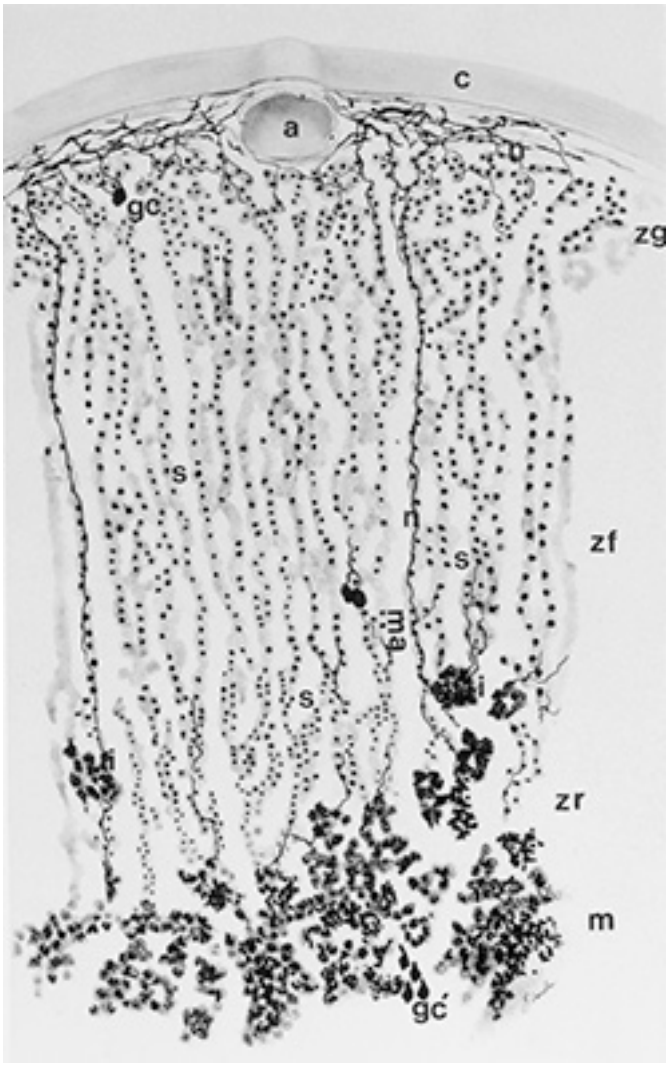

Fig. 1.2. Relationship of the adrenal innervation of the rat adrenal gland to the vasculature. Diagram showing both intrinsic innervation (from medulla to cortex) and extrinsic innervation (from outside adrenal to medulla via capsular plexus). Most of the nerve fibres are located in the capsular (c) and subcapsular region and some extend radially across the cortex. zg, Zona glomerulosa; zf, zona fasciculata; zr, zona reticularis; m, medulla; n, nerve fibers; a, arteriole; ma, medullary artery; s, sinusoids; i, isolated islets of chromaffin cells within the cortex; gc, ganglionic cells. (Reproduced from Ehrhart-Bornstein et al., 1998.)

1.1.2 Function of the adrenal gland

As noted above, the secretory parenchymal tissue of the adrenal gland is classically organized into an inner catecholamine-producing medulla and an outer cortex which synthesises steroid hormones using cholesterol lipid as substrate. However, more recent evidence has identified a certain amount of intermixing of medulla and cortical cells (Ehrhart-Bornstein et al., 1998). The chromaffin cells of the adrenal medulla are characterised functionally by their expression of the enzyme tyrosine hydroxylase and can be divided to two types based on the nature of their membrane-bound catecholamine storage granules. One population with large dense cored granules secretes noradrenalin while the other with smaller and less dense granules secretes adrenalin. The sudden release of catecholamines from these storage granules into the circulation primes the so-called acute 'fight or flight' response to physiological stress by promoting conditions for maximum utilization of energy. Both noradrenalin and adrenalin stimulate glycogenolysis (breakdown of glycogen stored in the liver to glucose and release into the blood stream) and mobilization of free fatty acids from adipose tissue. The release of catecholamines also causes a rise in blood pressure, dilation of coronary blood vessels, vasodilation of the vessels supplying skeletal muscle, vasoconstriction of vessels supplying blood to the gut and skin, an increase in heart rate and output and an increase in the rate and depth of breathing (Ganong, 1997; Ross et al., 1995).

The three principal anatomical zones of the adrenal cortex, the outer ZG, the ZF, and the inner ZR are also distinguished by their different endocrine functions and production of distinct steroid hormones. As described below, the ZG and ZF/ZR respond to distinct physiological stimuli with the result that production of the mineralocorticoid aldosterone in the ZG is stimulated by the peptide hormone angiotensin II and elevated plasma K^+, while synthesis of the glucocorticoid cortisol (corticosterone in rats and mice) in the ZF is regulated principally by the pituitary peptide hormone adrenocorticotrophic hormone (ACTH) (Fig. 1.3). In humans, C-19 adrenal androgens are also produced in the ZF/ZR as a result of the

conversion of 17-OH pregnenolone by the enzyme 17, 20 lyase, but this does not occur in rats and mice (Fig. 1.4). (For reviews see Hinson et al., 2007; Keegan and Hammer, 2002).

The principal mineralocorticoid, aldosterone, is secreted from glomerulosa cells and regulates salt and water balance. It acts on mineralocorticoid receptors in the distal tubules and collecting tubules of the kidney nephron, on gastric mucosa, and on salivary and sweat glands to stimulate the reabsorption of sodium. Mineralocorticoid synthesis in the ZG is under feedback control of the renin-angiotensin system (Ganong, 1997; Ross et al., 1995). The juxtaglomerular cells in the kidney release renin into the blood circulation when blood pressure or plasma sodium concentration falls. Renin then catalyses the conversion of angiotensinogen released from the liver to angiotensin I, which is subsequently converted by angiotensin converting enzyme I to angiotensin II in the lung. Angiotensin II stimulates peripheral vasoconstriction and synthesis and release of aldosterone secretion from zona glomerulosa cells in the adrenal gland. Release of renin from juxtaglomerular kidney cells is then inhibited when blood pressure and sodium level are restored (Ross et al., 1995).

As part of the physiological stress response, the glucocorticoid cortisol, synthesised and secreted from zona fasciculata cells, stimulates gluconeogenesis (glucose synthesis) in the liver to maintain plasma glucose levels. Cortisol also promotes protein mobilisation from skeletal muscle and fat mobilisation from peripheral stores and increases the rate of amino acid transport to the liver and the availability of glycerol from triglyceride breakdown as substrates for gluconeogenesis. Glucocorticoids suppress the immune response by inhibiting the actions of prostaglandins and leukotrienes, the two main products of inflammation and inflammatory responses by inhibiting macrophage recruitment and migration. The ZF is under feedback control of the hypothalamic-pituitary-adrenal (HPA) axis in which hypothalamic corticotrophin-releasing hormone (CRH) stimulates the release of ACTH from the pituitary gland, that then acts on the ZF to stimulate synthesis of cortisol which, in turn, feeds back on the hypothalamus and pituitary

to respectively inhibit CRH and ACTH release. ACTH not only stimulates corticosteroid synthesis, but is also necessary for maintaining adrenocortical cells and also increasing blood flow through the adrenal gland (Ross et al., 1995).

The main secretions of cells in the ZR are the weak androgens, dehydroepiandrosterone (DHEA) and androstenedione. These are also, under feedback regulation of the HPA axis (Ross et al., 1995).

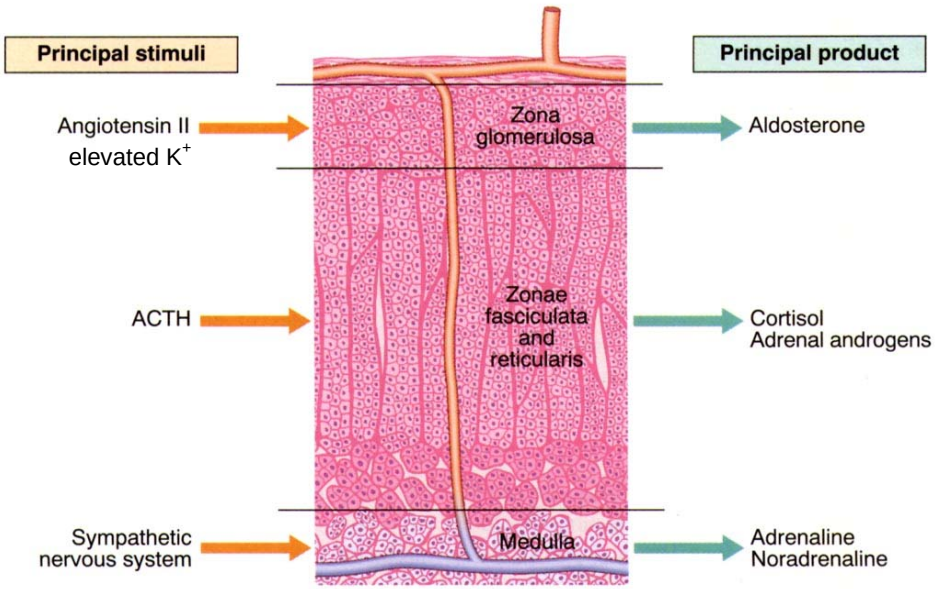

Fig. 1.3. Principal stimuli of the adrenal cortex and its products. The renin-angiotensin-aldosterone system is stimulated in response to low plasma sodium levels and low extracellular fluid volume to produce the peptide hormone angiotensin II. This causes contraction of the peripheral vasculature and acts directly via angiotensin II receptors on the ZG cells of the adrenal cortex to stimulate aldosterone production. Elevated plasma potassium levels will also directly stimulate aldosterone release from the ZG. The ZF synthesizes mainly glucocorticoids (cortisol in humans but corticosterone in rats and mice) in response to ACTH stimulation from the anterior pituitary. Adrenal androgens are produced mainly in the ZR in primates but are not produced in rats and mice.

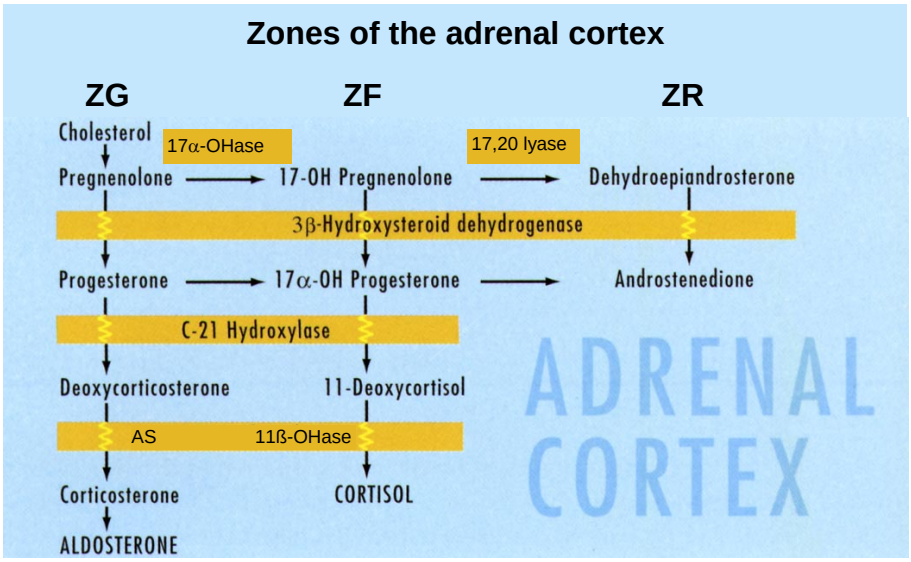

Fig. 1.4. Pathways of adrenocortical steroidogenesis. Cholesterol is processed variously to produce different steroidogenic products including glucorticoids (cortisol in humans and corticosterone in rats and mice), mineralocorticoids (aldosterone) and adrenal androgens. *Abbreviation:* AS, aldosterone synthetase. (Modified after Levy and Lightman, 1997)

1.2 Adrenal development

1.2.1 Description of adrenal development

As mentioned previously (Section 1.1.1), the adrenal gland is composed of two endocrine tissues of different embryological origins, namely a steroid hormone-producing outer cortex derived from mesoderm and an inner medulla, that originates from migratory neural crest cells, which later differentiate into chromaffin cells under the influence of adrenocortical steroids (reviewed in Ehrhart-Bornstein et al., 1998).

Five landmark phases in the development of the human adrenal gland have been identified (Mesiano and Jaffe, 1997; Sucheston and Cannon, 1968). (1) The anlage of the human adrenal cortex is first identified at 3-4 weeks of gestation, as a condensation of the coelomic epithelium. (2) Coelomic epithelial cells proliferate and migrate to the superior end of the mesonephros, and the adrenal gland is first recognizable at 4-6 weeks of gestation. (3) Fetal adrenal cortex cells differentiate into 2 morphologically distinct zones (fetal zone and definitive zone) at 8-10 weeks of gestation. By late gestation the fetal adrenal begins to develop into the early form of the adult adrenal cortex and the morphology of ZF and ZG begin to appear. (4) The fetal zone declines and disappears during the first 3 postnatal months. (5) The final adult zonal pattern is established and stabilised between 10-20 years of age. In primates, a distinct centrally-located medulla is absent throughout most of gestation. Neural crest cells migrate into the developing adrenal gland at around 9 weeks of gestation, followed by the formation of a capsule by specalised mesenchymal cells migrating from the region of Bowman's capsule (Mesiano and Jaffe, 1997). Subsequently, at this stage and beyond, small islets of chromaffin cells can be seen scattered through the body of the cortex (Mesiano and Jaffe, 1997). Later on, the chromaffin cells begin to condense into an early medulla after degeneration of the fetal zone and the medulla forms a cluster of cells in the centre of the gland by postnatal week 4 (Mesiano and Jaffe, 1997). As noted previously, the adrenal cortex and medulla

are both highly innervated (reviewed in Ehrhart-Bornstein et al., 1998), but little has been reported on the developmental timing of innervation in humans. The adrenocortical vasculature first develops around 9 weeks of gestation and persists throughout fetal life in the adrenal of the rhesus monkey, with distinct vascular networks present in the inner fetal and outer definitive zones by midgestation (Mesiano and Jaffe, 1997). Adrenocorticotropic hormone (ACTH) is thought to control the coordinated development of vasculature and endocrine tissue mass during this period (Thomas et al., 2003).

While some developmental waymarks and details of timing may vary between species, adrenocortical development processes in rats and mice are broadly similar to those in humans (Keegan and Hammer, 2002). Several researchers have reported that the precursors of steroidogenic tissues first appear in the mouse and rat embryo as an SF-1-positive adrenogenital primordium at around E8.5-E9.5 in the mouse and E11.5 in the rat (Hatano et al., 1996; Ikeda et al., 1994). This separates into distinct adrenal and gonadal primordia at around E10.5-E11.5 (Fig. 1.5) in the mouse and E12.5 to E14.5 in the rat. Medullary precursor cells migrate into the adrenal primordium at around E12.5 in the mouse and E15 in the rat (Bland et al., 2003; Okamoto and Takemori, 2000). After that, the adrenal becomes encapsulated at around E14.5 in the mouse and E16.5 in the rat (Bland et al., 2003; Okamoto and Takemori, 2000). Development of adrenal innervation in the rat has been studied by several groups (reviewed by Holgert et al., 1998), showing that while sensory innervation is already relatively well developed at birth, intrinsic and extrinsic sympathetic neurons first migrate into the adrenal cortex at E18 and just after birth respectively and then mature postnatally to establish functional innervation by around P10. While little data has been reported for mouse, an immature microvasculature can first be detected morphologically in the rat adrenal gland at E16, although capillaries can only be distinguished histochemically by E19 (alkaline phosphatase and dipeptidyl aminopeptidase IV are used as markers for developing arteries and veins respectively) (Mitani et al., 1999).

In the rat and probably also in the mouse, zone formation (zonation) in the adrenal cortex begins in late gestation (Mitani et al., 1999; Wotus et al., 1998). In addition to the three principal definitive zones, the mouse adrenal cortex also has a so-called ‘X zone’ (Howard-Miller, 1927; Nyska and Maronpot, 1999; Okamoto and Takemori, 2000) located in the innermost region of cortex surrounding the medulla. The X zone first appears in both sexes at about 10 days after birth and reaches a maximum volume in males by weaning. It degenerates at puberty (approximately 5-6 weeks of age) in males, under the influence of male sex hormones. In females, it reaches its maximum size at about 9 weeks of age and degenerates gradually with age or rapidly during the first pregnancy, under the influence of female sex hormones (Nyska and Maronpot, 1999). The function of the X zone remains unknown (Nyska and Maronpot, 1999), but it is thought to be equivalent to the fetal zone that occurs in human adrenals (Zubair et al., 2006).

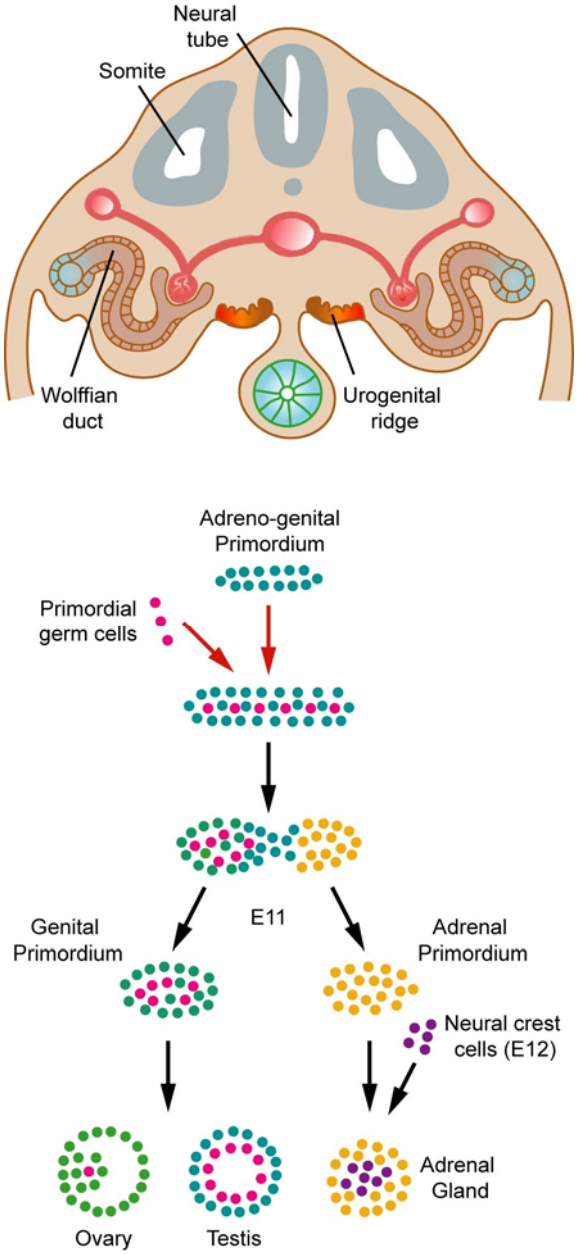

Fig. 1.5. Separation of the mouse adrenogenital primordium into adrenal and genital primordia. The precursors of steroidogenic tissues first appear as an SF-1-positive adrenogenital primordium at around E8.5-E9.5 in the urogenital ridge and separates into adrenal and genital primordia at around E10.5-E11.5. Medullary precursors of neural crest cells migrate into the adrenal primordium at around E12.5 while the genital primodium develops into a testis or ovary in the presence of the absence specific developmental actions of the *SRY* gene. (Figure courtesy of Dr S.D. Morley.)

1.2.2 Adrenal growth

Adrenal growth plays an important part in adrenal development. At around 4-5 weeks of gestation, cells of the human adrenal anlage begin to migrate and condense at the cranial end of the mesenephros to form an 'adrenal blastema', which continues to grow both by inward cell migration and cell proliferation. By 8 weeks of gestation, cells of the adrenal blastema organise into cords and differentiate into large polyhedral cells that become the fetal zone primordium. About a week later the primordial fetal zone is surrounded by a primordial definitive zone, derived either from the same or possibly from a distinct progenitor population in the coelemic epithelium. At this point, cell division becomes confined to the definitive zone which apparently, however, does not grow significantly because differentiating cells migrate into the quiescent fetal zone. The subsequent rapid increase in human adrenal weight beginning from week 10 of gestation and continuing to term is almost entirely due to enlargement of the fetal zone by a combination of cell migration and hypertrophy (increase in cell size) (reviewed in Mesiano and Jaffe, 1997).

The primate adrenal cortex then undergoes substantial postnatal remodelling during which the fetal zone atrophies and is replaced by an expanding definitive zone which begins to display the classical adult zonal structure. The significant decrease in adrenal weight seen soon after birth is accounted for by degeneration of the fetal zone (Mesiano and Jaffe, 1997).

Growth of the mouse adrenal gland has been described in terms of adrenal volume from E15.5 to P7 (Eguchi, 1960) and increase in weight from birth to day 60 (Moog et al., 1954), and together, these studies suggest an initial lag, followed by rapid postnatal growth. After weaning the adrenal gland grows rapidly in mice (Bielohuby et al., 2007) and rats (Majchrzak and Malendowicz, 1983) until week 7, after which female adrenals maintain a constant weight while male adrenals show a 25% reduction in weight between week 7 and week 9. A gender-specific dimorphism in weight (female adrenals are heavier than male adrenals) is

apparent from around 3 weeks of age in mice (Bielohuby et al., 2007) and after 9 weeks of age in rat (Majchrzak and Malendowicz, 1983). These authors proposed that this gender-specific dimorphism is mostly caused by ZF volume differences between females and males which affect the total adrenal volume and weight.

1.2.3 Cell proliferation during adrenal development

As mentioned in section 1.2.2, growth of the embryonic adrenal is a combination of cell proliferation, migration and hypertrophy. Various markers have been used to study cell proliferation in the developing adrenal gland including incorporation of tritiated thymidine or BrdU into replicating DNA and expression of Ki67 nuclear antigen or PCNA. Ki67 and PCNA are recognised cell proliferation markers which are expressed during specific stages of the cell cycle (Mitani et al., 1999; Schulte et al., 2007; Spencer et al., 1999).

In the human fetal adrenal, mitotic activity can be observed throughout the adrenal anlage at 4-5 weeks of gestation and then in both the primordial fetal and definitive zones of the primate adrenal cortex. Cell division then becomes concentrated primarily in the definitive zone at around 8 weeks of gestation, from where differentiating cells probably migrate into the quiescent fetal zone (reviewed in Mesiano and Jaffe, 1997). Spencer et al., (1999) reported that in both the first and second trimesters, PCNA can be detected in cells of the fetal and definitive zones in human fetal adrenal. Between 10 and14 weeks of gestation, the mitotic indices (percentages of PCNA positive cells) in the fetal and definitive zones are fairly low. After 14 weeks the mitotic index in the definitive zone is significantly greater than that in fetal zone (Spencer et al., 1999) and definitive zone cells continue contributing centripetally to the fetal zone (Mesiano and Jaffe, 1997).

In rat BrdU- or PCNA-labelled cells are scattered throughout the developing embryonic adrenal gland at E16 and E18. From E19, the proliferative cells are found in two regions, namely the outermost region and the central part of gland (Mitani et al., 1999). After postnatal day 7, proliferative cells predominate in the subcapsular region (Mitani et al., 1999). In mouse, the pattern of proliferating adrenocortical cells switches from being scattered throughout growing tissue at E11.5 and E13.5 to being confined to the outer cortex from late gestation (Schulte et al., 2007). Thus a common theme emerges in human, rat and mouse where cell proliferation occurs throughout the developing adrenal primordium but later becomes concentrated in the outer cortex.

1.2.4 Cell death during adrenal development

The type of cell death termed ‘apoptosis’ was first reported in the adrenal gland following ACTH withdrawal (Kerr, 2002; Wyllie et al., 1973a; Wyllie et al., 1973b) and has since been shown occur widely in other tissues. Cell death is usually classified into two alternative types, apoptosis and necrosis. However, Majno and Joris (1995) pointed out that these two processes are not mutually exclusive because cells may die by apoptosis and then undergo necrosis. These authors defined cell death as a process that leads to a lethal ‘point of no-return’, whereas necrosis refers to the irreversible morphological alterations (e.g. karyolysis and pyknosis in the nucleus and loss of structure and fragmentation in the cytoplasm) appearing in cells after cell death, regardless of the pre-lethal process. Majno and Joris (1995) argue that the two major processes resulting in cell death are apoptosis (which they describe as a form of intentional cell suicide) and ‘accidental cell death’, including death by environmental insult, e.g. ischaemia (insufficient blood supply) that involves cell swelling. They also coined the term ‘oncosis’ to describe cell death involving cytoplasmic swelling and karyolysis. This view of cell death has been largely accepted by the Cell Death Nomenclature Committee (Levin, 1998). Morphological and biochemical aspects of apoptosis, oncosis and necrosis have been discussed by Van Cruchten and Van den Broeck (2002).

The key features of apoptosis are distinguishable by morphological and biochemical criteria such as cell shrinkage, chromatin condensation and DNA fragmentation, nucleus break-up (karyorhexis), budding (cell emits processes), dense and rounded apoptotic bodies (consisting of cell organelle and/or nuclear material surrounded by an intact plasma member) (Majno and Joris, 1995; Van Cruchten and Van den Broeck, 2002). Apoptosis can be initiated within the cell or by external cues such as hormones, cytokines and a variety of chemical, physical and viral agents. Three mechanisms have been suggested to direct the apoptotic process: (i) a receptor-ligand mediated mechanism, (ii) a mitochondrial pathway and (iii) an endoplasmic reticulum-mediated mechanism. All three of these mechanisms activate the caspase protease cascade associated with apoptosis (Van Cruchten and Van den Broeck, 2002), which leads to breakdown of specific intracellular components, e.g. nuclear lamins and cleavage of the DNA repair enzyme poly-(ADP-ribose) polymerase (though the exact contribution that the cleavage of many caspase substrates makes to the biochemistry and morphology of apoptosis is presently unclear), leading ultimately to cell death. Apoptosis can be detected experimentally by several methods including directly monitoring the activity of the caspase proteases or by TUNEL (terminal deoxynucleotidyl transferase mediated dUTP nick end-labelling), which involves immunohistochemical detection of the characteristic 3' hydroxyl ends of DNA fragmentation break points ('nicks') that are produced by degradation of cellular DNA during apoptosis. Apoptosis is regarded as a crucial mechanism in cellular turnover in the adult tissue and also in tissue genesis during development. It is likely to be regulated by hormones in endocrine-dependent tissues (Kerr, 2002).

Several types of cell death have been described in the adrenal cortex (Ba-Omar and Downie, 2006; Chen-Pan et al., 1996) but most reports focus on apoptosis. In human fetal and perinatal adrenals, Spencer et al., (1999) reported the absence of apoptotic nuclei in the definitive zone of the human adrenal cortex during all stages of gestation. However, apoptotic indices were scattered in the inner cortical compartment (fetal zone), increasing with advancing gestation and reaching a

peak during the first month after birth (Spencer et al., 1999). Significantly, this coincides with the period when the fetal zone degenerates and suggests that fetal zone degradation in the human is driven by apoptosis. It has long been known in the rat that ACTH promotes growth of the adrenal cortex by both hypertrophy (increase in cell size) and hyperplasia (increase in cell numbers). Conversely, withdrawal of ACTH reverses these processes, causing a reduction in adrenocortical size due to atrophy and elimination of cells, by apoptosis (Wyllie et al., 1973a; Wyllie et al., 1973b). Furthermore, this occurred in both fetal and adult adrenal glands, despite their widely differing mitotic activities while, in adults, apoptotic 'indices' were concentrated in the inner zones of the adrenal cortex.

Consistent with the above observations, more recent work, utilising TUNEL as the assay method, revealed that apoptosis was scattered throughout the normal adrenal cortex of rats at perinatal stages, but by postnatal day 10 and also at weaning age (approximately 25 days) apoptosis was localised to the inner cortex (Carsia et al., 1996; Mitani et al., 1999). It is therefore apparent that apoptosis must play a role in the normal physiological turnover of the adrenocortical cell population. To date, apoptosis in the mouse embryonic and adult adrenal cortex has been less well studied, but Breidert and colleagues have reported that apoptotic nuclei were detected in mice aged between 3 and 30 weeks at a very low level, mainly occurring within the connective tissue at the medulla and cortex boundary (Breidert et al., 1998).

1.3 Adult stem cells

Mouse embryonic development starts from a zygote (fertilised oocyte) which undergoes several cell divisions before it forms an 8-16 cell compacted morula and then a 32 cell blastocyst, which produces three primary lineages (epiblast, primitive endoderm and trophectoderm) (Gardner and Papaioannou, 1975). The epiblast produces the entire fetus plus some extraembryonic tissues (e.g. amnion, allantois and yolk sac mesoderm), the primitive endoderm only produces extraembryonic endoderm and the trophectoderm produces extraembryonic trophoblast tissue. Up until the 8-cell stage all the cells are considered to be totipotent (able to form all three of the primary lineages so able to produce all the cell types of the entire organism plus all the extraembryonic tissues) (Kelly, 1975). The developmental potential is gradually restricted during development. Cells of the epiblast and embryonic stem cells (which are derived from the epiblast) are considered to be pluripotent (capable of forming all the cell types derived from the epiblast lineage but not the primitive endoderm or trophectoderm derivatives). As development proceeds, developmental potential is further restricted and cells that can give rise to several different cell types are considered to be multipotent.

Many adult tissues are maintained by adult stem cells (also called somatic stem cells). Stem cells are cells that can divide without limit, replace themselves and also produce more differentiated cells. Adult stem cells may be multipotent (able to generate multiple lineages for an entire tissue), oligopotent (able to generate two or more lineages in a tissue) or unipotent (able to generate a single lineage) (Smith, 2006). In most cases, the tissue-specific stem cells are localised in a specific place, the stem cell ‘niche’, which interacts with the stem cell to maintain its self-renewing properties and probably prevents differentiation or apoptosis (Moore and Lemischka, 2006).

1.3.1 Maintenance of adult tissues by stem cells

Numerous cell divisions (involving replication of trillions of nucleotides) must be performed accurately without any mistakes in a human lifetime. As well as cell divisions that occur during embryonic development, maintenance of an adult tissue often requires cell replenishment to sustain cell numbers and function of a tissue. Various tissues in a complex body shed aging cells and also replace cells after damage. To produce a tissue-specific differentiated cell without any mutations makes a huge demand on accurate genome replication and requires precise controls in expression of specific genes. Adult stem cells provide a mechanism for the maintenance of a specific tissue which minimises the risk of accumulating genetic errors that lead to pathological changes.

The key feature of adult stem cells is that they undergo self-renewal and produce more differentiated cell types. Adult stem cells are also often slow-cycling and may enter a period of quiescence. So, while stem cells have unlimited 'proliferative potential' they do not proliferate frequently (Cotsarelis et al., 1989). In many tissues stem cells produce an intermediate cell type, the transient (or transit) amplifying (TA) cell, which divides a limited number of times to generate a clonal cell lineage before producing fully differentiated cells (Fig. 1.6). TA cells have a lower proliferative potential but typically proliferate more frequently than stem cells (Cotsarelis et al., 1989). Early generation TA cells are also considered to be progenitor cells, which are dividing cells with the capacity to differentiate. (Progenitor cells also include putative stem cells in which self-renewal has not yet been demonstrated.) Later generation TA cells stop proliferating and become fully differentiated cells. Stem cells, their daughter cells and the supporting microenvironment are constructed to coordinate the homeostasis of a tissue. The microenvironment of the stem cell niche sustains the characteristics of stem cells and the balance between quiescence and activity of stem cells that is required for maintenance of a tissue. Stem cells of the haematopoietic system and small intestine have been better characterised than most (Marshman et al., 2002; Wilson and Trumpp, 2006) and are described below. The stem cell system that maintains

the corneal epithelium is also described because this is a unipotent stem cell which may be more similar to the adrenal cortex.

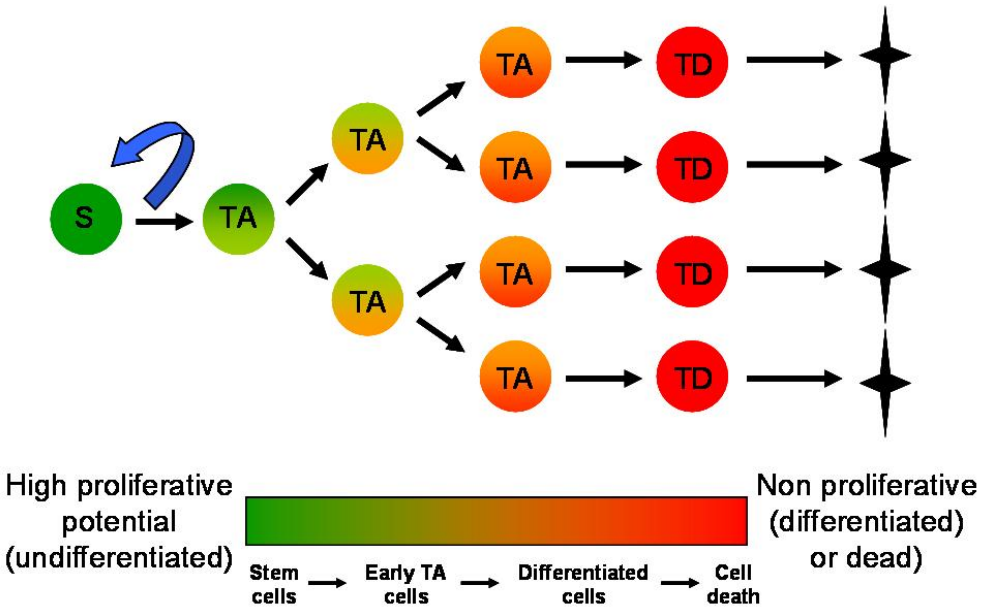

Fig. 1.6. A hierarchy of stem cell, transient amplifying cells and terminally differentiated cells. Stem cell(s) can maintain tissues by asymmetrical divisions which renew themselves and give rise to transient amplifying cells (TA), which lose proliferative potential at successive divisions while evolving and become more differentiated. Eventually, TA cells become terminally differentiated cells (TD) which may be programmed to die (final symbol on right). (Modified after Preston et al., 2003.)

1.3.1.1 Haematopoietic stem cells

The haematopoietic stem cell (HSC) gives rise to all types of blood cells (Fig. 1.7) and is one of best characterised adult stem cell systems. HSCs produce not only lymphoid progenitors to generate lymphoid lineage progeny (T and B lymphocytes) but also myeloid progenitor cells to produce myeloid progeny including basophils, eosinophils, neutrophils, microphages, platelets and erythrocytes (Jackson et al., 2002). HSCs are mostly isolated by fluorescence-activated cell sorting based on their expression of markers Sca-1 (Sca-1^{+}), c-kit (c-kit^{+}), and lack of expression of lineage markers (Lin^{-}) (Jackson et al., 2002). HSCs are mobile and detectable in peripheral blood, fetal liver and fetal spleen as well as their niche in the bone marrow, which sustains their properties (Preston et al., 2003; Wilson and Trumpp, 2006). The osteoblastic niche was the first HSC niche to be identified (Fig. 1.8). HSCs in this niche are associated with the connective tissue lining (endosteal surface) of bone marrow cavities in trabecular bone (e.g. long bones), which is rich in osteoblasts. It has been suggested that these osteoblasts are involved in the maintenance and regulation of HSCs (Moore and Lemischka, 2006). Another HSC niche, the vascular bone-marrow HSC niche, has been identified more recently (Kopp et al., 2005). Here HSCs are associated with the fenestrated endothelium of vascular sinusoids in the bone marrow. Bone-marrow sinusoidal endothelial cells express cytokines and adhesion molecules to regulate mobilization, homing and engraftment of HSCs. It has been suggested that the osteoblastic niche maintains HSCs in a quiescent state whereas the vascular niche promotes proliferation and differentiation (Kopp et al., 2005).

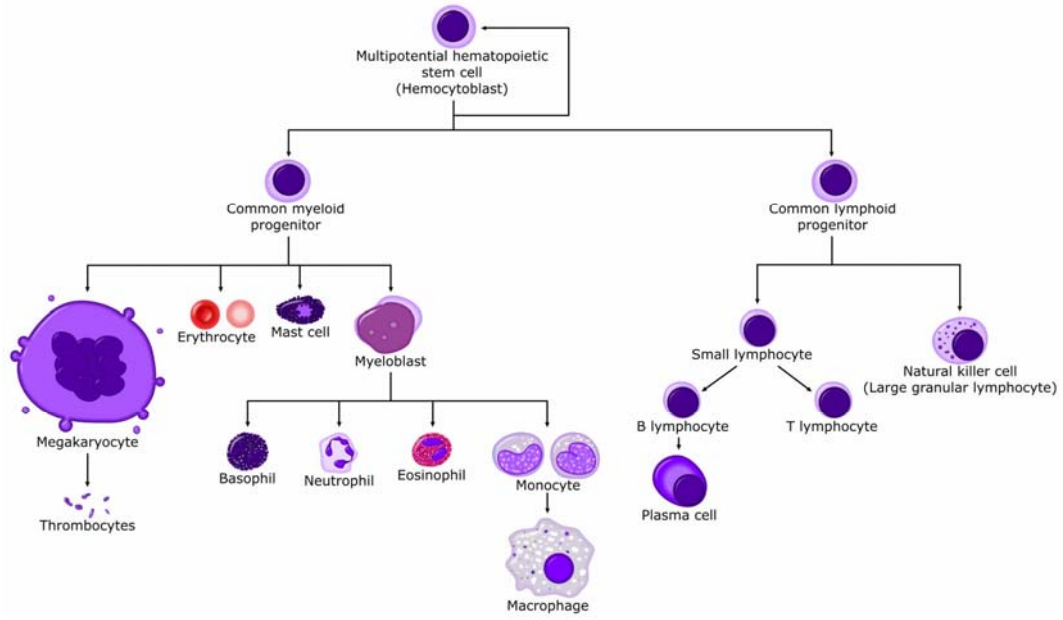

Fig. 1.7. Haematopoietic stem cell lineages. HSCs in the bone marrow can give rise to myeloid and lymphoid progenitors which differentiate into different types of mature blood cells. Note that both stem cells and progenitor cells can produce differentiated cell types but only stem cells can divide without limit and replace themselves. (Reproduced from Wikipedia: http://en.wikipedia.org/wiki/Haematopoiesis)

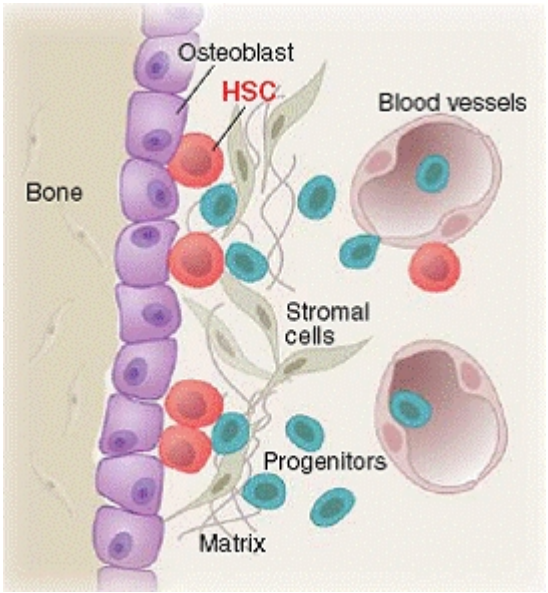

Fig. 1.8. Components of the haematopoietic stem cell (HSC) osteoblastic niche. (Reproduced from Moore and Lemischka, 2006)

1.3.1.2 Stem cells in the small intestine

The small intestine is composed of a series of villi and surrounding crypts (Fig. 1.9). The epithelium of the small intestine is one of fastest tissues to replenish itself and maintenance of the mouse small intestine by intestinal stem cells (ISCs) has been well characterised (Fig. 1.9). The cellular lining of the small intestine comprises columnar epithelial cells, which are replenished when shed into the intestinal lumen. The small intestine crypt epithelium together with its surrounding pericryptal fibroblasts and mesenchyme generates four cell lineages: absorptive enterocytes, goblet cells, enteroendocine cells and paneth cells (at the lowest part of the crypt) (Moore and Lemischka, 2006). Villi are maintained by ISCs and TA cells and it has been suggested that about 4-6 ISCs are actually active per crypt (Moore and Lemischka, 2006). It is widely accepted that ISCs are located in a stem cell niche between the bottom paneth cells and their proliferating progenitors within the crypt at about position 4, as shown in Fig. 1.9 (Marshman et al., 2002; Wilson and Trumpp, 2006). The crypt is derived from ISCs and the cells of a villus are derived from several adjacent crypts (Moore and Lemischka, 2006). Progeny of ISCs move upward to become TA cells (proliferating progenitors). At the top of the crypt, TA cells stop proliferating and differentiate into various types of villus cells.

The location of stem cells about 4 cells above the base of the crypt has recently been challenged (Barker et al., 2007). *Lgr5* (a target gene in the Wnt pathway), is expressed in cells at the base of the intestinal crypts but not in the villi. Further analysis showed *Lgr5* expression was restricted to crypt base columnar (CBC) cells interspersed between paneth cells (importantly below position 4) but *Lgr5* was not expressed in the cells at position 4. Mice, in which an inducible *Lgr5*-CreERT2 transgene was used to activate a Rosa26-*LacZ* reporter transgene, produced clones of ß-gal positive cells that identified Lgr5-positive cells and their daughter cells. Sixty days after induction, the ß-gal positive cells formed a clone of cells that extended up the villus and included all epithelial cell types. This provides evidence that Lgr5-positive cells are stem cells and demonstrates their

oligopotent capacity to maintain the lining of the small intestine (Barker et al., 2007). This new finding that CBC cells in the crypt are putative stem cells, disagrees with the traditional view that the ISCs are located at position 4. However, this does not affect the traditional view that, in the small intestine, cell fate is organised by asymmetrical division along with upward migration in the crypt, which sets up the correct localisation of distinct differentiated cells.

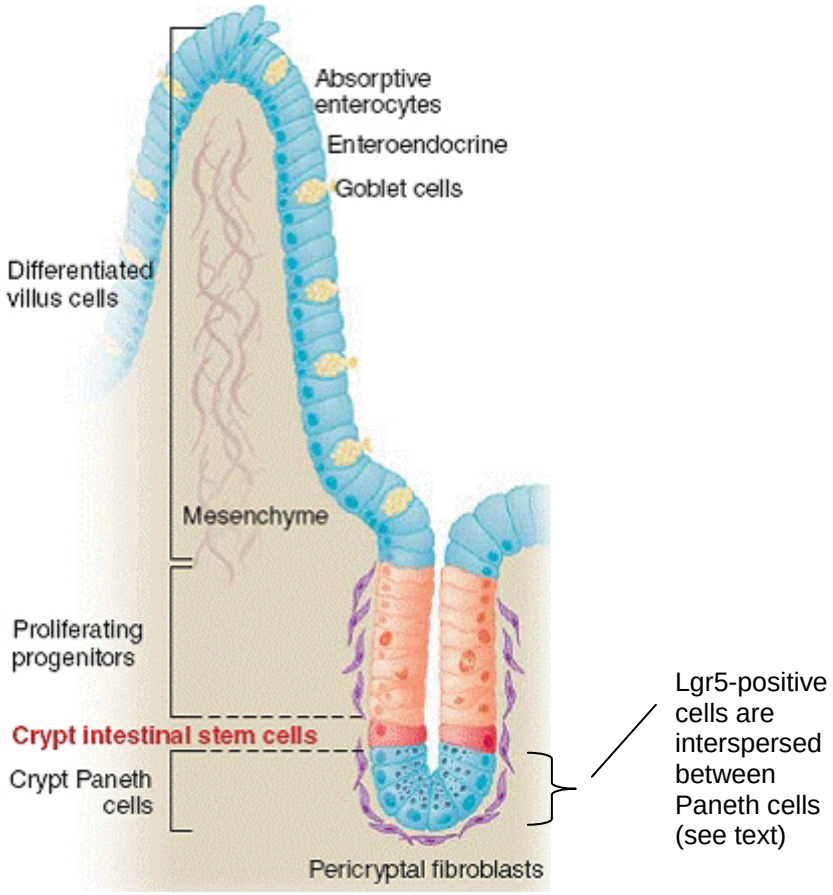

Fig. 1.9. Stem cell maintenance of the small intestine. The villus of small intestine contains four cell types: absorptive enterocytes, goblet cells, enteroendocine cells and paneth cells (at the lowest part of the crypt). Note that the cells shown here as 'crypt intestinal stem cells' are the position 4 stem cells identified by label-retaining studies not the Lgr5-positive cells which are below position 4 (see text for discussion). (Reproduced, with modification from Moore and Lemischka, 2006)

1.3.1.3 Limbal stem cells that maintain the corneal epithelium

The cornea is composed of a superficial corneal epithelium, a thick middle layer of stroma and an inner endothelium (Fig. 1.10A). The corneal epithelium is 4-6 layers of squamous stratified cuboidal epithelium, derived from the surface ectoderm. It is fast growing and quickly regenerated; superficial cells are shed (desquamation) and replaced by progeny of the basal limbal stem cells; LSCs (Cotsarelis et al., 1989). The niche of basal limbal stem cells is in the 'limbus' at the periphery of the cornea (between corneal epithelium and conjunctiva) and, unlike the cornea, the limbus has a blood supply. The limbal stem cells produce transient amplifying (TA) cells which divide several times as they migrate from the periphery towards the centre of the cornea, along the basal layer of epithelium (Fig. 1.10B). After the final division, both daughter cells migrate upwards to the superficial area (Beebe and Masters, 1996), becoming gradually more differentiated and are finally shed.

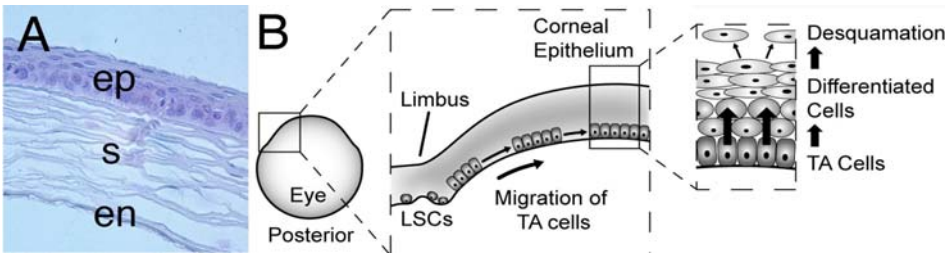

Fig. 1.10. Corneal epithelial maintenance by limbal stem cells. (A) The cornea comprises an outer epithelium (ep), a thick stroma (s) and a single layer of endothelium (en). (**B)** Limbal stem cells (LSCs) in the limbus (between the cornea & conjunctiva) produce transient amplifying (TA) cells, which populate the basal epithelial layer. These replicate, migrate centrally and produce differentiated cells in the outer layers, which are desquamated. (Part A was provided by Dr J. D. West; part B is reproduced from Collinson et al., 2002)

1.3.2 Identification of adult stem cells

1.3.2.1 Stem cell markers

Adult stem cells can be identified by their ability to maintain tissues and form clonal lineages (see above discussion of Lgr5-positive cells in the small intestine) and, in some cases, their multi- or oligo-potency with engraftment of lethally irradiated animal (e.g. haematopoietic stem cells; Jackson et al., 2002). In some cases stem cells can be identified and isolated by expression of specific combinations of genes. For example, as discussed above, HSCs may be isolated by FACS sorting based on expression of c-Kit and Sca-1 plus the absence of expression of lineage markers (Lin^-). The same strategy of identifying specific markers or combinations of markers has been used for several other types of adult stem cells (Table 1.1).

Table 1.1 Examples of mouse tissue-specific stem cells mentioned in the text

Tissue and/or stem cells	Marker or method	Reference
Tissue-specific stem cell markers		
Haematopoietic stem cells	$Sca\text{-}1^+$, $c\text{-}kit^+$, Lin^-	1
Small intestine crypt base columnar cells	$Lgr5^+$	2
Tissues with no specific stem cell markers		
Small intestine crypt +4 cells	label retaining cells	3
Corneal epithelium (limbal stem cells)	label retaining cells	4
Tissues in which stem cells have not been identified		
Adrenal gland		

References: 1, (Jackson et al., 2002); 2, (Barker et al., 2007); 3, (Booth and Potten, 2000); 4, (Cotsarelis et al., 1989).

Specific markers have not yet been identified for many types of stem cells. Until recently no marker was known for stem cells in the mouse colon and small intestine but it now seems that Lgr5 may be a stem cell marker for these tissues (Barker et al., 2007). There are still no known markers for limbal stem cells that maintain the corneal epithelium. Efflux of the vital dye Hoechst 33342 from cells is mediated by the membrane transporter ABCG2 and ABCG2-positive cells may be detected either by immunohistochemistry or as a 'side population' of cells by FACS sorting after loading a cell suspension with the dye. ABCG2 has been proposed as a conserved marker for several types of stem cells (Zhou et al., 2001), including limbal stem cells (Budak et al., 2005) but it is probably not sufficiently specific to be considered a genuine limbal stem cell marker. Combinations of markers may enrich for limbal stem cells that maintain the corneal epithelium (e.g. ABCG2$^+$, p63$^+$, vimentin$^+$, integrin $\alpha9^+$. K19$^+$, Cx43$^-$, involucrin$^-$, K12$^-$, K3$^-$; Schlotzer-Schrehardt and Kruse, 2005), but those proposed so far are probably also characteristic of some other cells (e.g. early TA cells).

More generic methods including cell culture and identification of label-retaining cells (discussed below) have also been used to identify the presence of stem cells. For example, the production of holoclones from cultures of skin (Barrandon and Green, 1987) and the human limbus (Pellegrini et al., 2001) implies the presence of stem cells, but because mouse limbal cells are difficult to culture this approach has not yet been successful in mouse. Similarly, neurospheres (spherical clusters of cells grown in suspension culture) derived from stem cells among dissociated neural cells can maintain multipotentiality during several passages in vitro (Bez et al., 2003; Reynolds and Rietze, 2005).

1.3.2.2 Identification of putative-stem cells as label-retaining cells

Although mouse haematopoietic stem cells have been identified by the expression of specific markers (see above), specific stem cell markers are less well established for other systems. However, more generic methods can be utilised to help identify the stem cells. Even when they are not quiescent, stem cells are slow

cycling and this characteristic can be used to help identify them. Bromodeoxyuridine (BrdU), an analogue of thymidine, can be incorporated into the newly synthesised DNA strands of all dividing cells during S phase of the cell cycle, including dividing stem cells. BrdU incorporation can be detected by immunohistochemistry and this provides a method of identifying dividing cells. Once cells are labelled with BrdU, it is retained in the nuclei and gradually diluted at each cell division. Putative stem cells can be identified as 'label-retaining cells' because they dilute the label more slowly than most cells. A prolonged exposure of BrdU is needed to increase the probability of labelling stem cells unless they are induced to proliferate by wounding the tissue. This approach has been used successfully to identify several different types of putative stem cells including intestinal stem cells (Booth and Potten, 2000) (but see section 1.3.1.2 and discussion below of the status of these cells), and limbal stem cells that maintain the corneal epithelium (Cotsarelis et al., 1989).

However, not all label-retaining cells are stem cells as, for example, terminally differentiating cells will also retain BrdU. In addition, some types of stem cells may not be identifiable as label-retaining cells. For example, it was recently shown that haemotopoietic stem cells (HSCs) sorted on the basis of expression of established markers (see above) did not retain BrdU after a 70 day chase (Kiel et al., 2007). Similarly, another recent study (discussed above) suggests that the cells originally identified as stem cells in the +4 position of the small intestine by label-retaining experiments may represent TA cells rather than true stem cells (Barker et al., 2007). While label-retaining cells may identify putative stem cells, more specific approaches must be used to identify and purify them with more certainty and to test their capacity for self renewal and for maintenance of a tissue.

1.4 Maintenance of the adult mouse adrenal cortex

1.4.1 Cell proliferation, centripetal cell movement and cell death

The adrenal cortex is a dynamic organ and responds to various stimuli to maintain physiological homeostasis (see Section 1.1). As a dynamic tissue, the adrenal cortex is maintained by a balance of cell proliferation, cell movement and cell death. Various proliferative markers, such as tritiated thymidine, BrdU, Ki67 and PCNA, have been utilised to locate the proliferating cells in adrenal cortex. The distribution of dividing cells has been reported in various studies which have shown that the majority of cell divisions occur in the peripheral region, although cells can proliferate in all 3 cortical zones (Race and Green, 1955). This peripheral proliferation occurs mostly in or near the ZG/ZF border, sometimes referred to as the zona intermedia (ZI) or undifferentiated zone (ZU), but it may also occur in the sub-capsular region or within the capsule. (As mentioned in section 1.1.1, the terms zona intermediata and undifferentiated zone have been used for a region between the ZG and ZF in rats and mice that does not express either the ZG-specific enzyme, aldosterone synthetase, or the ZF-specific enzyme, 11β-hydroxylase.) In addition, pulse-labelling of proliferative cells (e.g. incorporation of tritiated thymidine in S phase) suggests that peripherally labelled cells move centripetally (Zajicek et al., 1986). The location of cell death has been revealed mainly by studies of apoptosis (e.g. by microscopic morphology or detection of DNA fragmentation). These studies showed that apoptotic cell death occurs mostly around the boundary of the cortex and medulla (Section 1.2.4). Overall these studies show that most cell proliferation occurs in the outer cortex, cells move or are displaced inwards and die in the ZR close to the medulla boundary. Several hypotheses of adrenal maintenance have been proposed based on these observations and are described in section 1.4.3 below.

1.4.2 Experimental regeneration of the adrenal cortex

If the rat adrenal gland is enucleated (removal of most of the adrenal gland) by extruding most of it through a slit in the capsule, leaving only the capsule and underlying subcapsular cells, it is able to regenerate a new cortex but not the medulla (Perrone et al., 1986; Skelton, 1959 reviewed in Kim and Hammer, 2007). The remaining capsule and subcapsular cells proliferate, spread beneath the capsule and expand towards the centre. After 30 days the normal histological appearance, cortical zonation and steroidogenic functions are restored.

Moreover, clonally derived cultured adrenal cortex cells can produce a functional adrenal cortex when transplanted to another site or another animal. For example, cloned bovine adrenocortical cells transplanted to polycarbonate cylinders under the kidney capsule of adrenalectomised SCID (severe combined immunodeficient) mice proliferated and after 36-41days formed a vascularised tissue mass that was functionally equivalent to an adrenal cortex and able to replace the mouse's own adrenal cortex (Thomas et al., 1997). The transplant had a normal adrenocortical histological appearance and performed the normal endocrine functions of the ZG and ZF.

1.4.3 Hypotheses of adrenal maintenance

Various studies have proposed different locations of putative stem cells in the adrenal cortex and five hypotheses of adrenocortical maintenance have been suggested previously (reviewed in Estivarez et al., 1992; Kim and Hammer, 2007): (1) centripetal cell movement; (2) 'walking stick' shaped movement; (3) zonal maintenance; (4) bi-directional maintenance from the zona intermediata (undifferentiated zone) and (5) maintenance by the capsule. These hypotheses are described below and illustrated by the models shown in Fig 1.11. They are based on evidence gathered from histological and biochemical observations of the adrenocortical zones, adrenocortical localisation of cell proliferation, movement and death and experimentally induced regeneration of the adrenal cortex.

(1) Centripetal cell movement hypothesis (Fig. 1.11a). Gottschau first proposed the centripetal cell movement hypothesis of adrenocortical maintenance, based on morphological observations including the columnar arrangement of cells in the zona fasciculata (Gottschau, 1883; reviewed in Estivarez et al., 1992). This suggests that proliferative cells located peripherally displace existing cells centripetally and give rise to cell populations in all three adrenocortical zones. In the stem cell model based on this hypothesis (Fig. 1.11a) a single population of stem cells would be located in the outer ZG and migrating cells would die near the medullary boundary. In most adult stem cell systems the stem cells produce transient amplifying cells, which can also proliferate, so proliferation need not be limited to the stem cell zone. This idea was supported by later pulse chase experiments showing that tritiated thymidine initially labelled cells at the periphery and this was followed by an increase in labelled cells proceeding centripetally towards the medulla where apoptosis occurs (see section 1.4.1).

This suggested that adrenocortical cells cross all three zones and change their pattern of gene expression and cell biochemistry in each zone (Zajicek et al., 1986). Studies of chimeric and mosaic adrenal cortices provides additional

support for the idea that clones of cells span the whole cortex (Morley et al., 1996; see section 1.5.4) but other interpretations are possible (see section 1.5.4).

(2) 'Walking stick' shaped movement hypothesis (Fig. 1.11b). This hypothesis is partly derived from the evidence for centripetal cell movement and partly from the evidence that cell proliferation mostly occurs in a broad region in the outer cortex. Belloni et al., (1978) proposed that adrenocortical cells were maintained within a histological cord unit, many of which were shaped like a walking stick (Fig. 1.12) and that proliferating cells were at the end of the 'walking stick handle'. To fit better with current concepts of stem cells and TA cells we can update this to suggest that the putative stem cells are at the end of the 'walking stick handle' and proliferating cells (stem cells plus early TA cells) are throughout the handle and upper part of the 'walking stick'. Thus, some of the putative stem cells at the ends of the chords of cells would be in the inner half of ZG or outer third of ZF (near the ZI) as shown in Fig. 1.11b and others would be near the capsule (if the 'walking stick' was straight and similar to Fig. 1.11a) (Belloni et al., 1978). This hypothesis also fits with the arch-like histological appearance of the zona glomerulosa. The main difference between hypotheses (1) and (2) is that in hypothesis (2) the proliferative progenitor cell may initiate an outward movement before centripetal movement. Both hypotheses propose that cells undertake different roles, depending on which zone they are in.

(3) Zonal maintenance hypothesis (Fig. 1.11c): The zonal theory for adrenocortical maintenance was proposed to explain the distinct morphological appearance, steroid production and response to physiological stimuli of the different adrenocortical zones (Deane et al., 1948 ; Swann, 1940). Based on this evidence Race and Green (1955) proposed that each zone maintains its own population of cells by local proliferation within the zone (Fig. 1.11 c). The original idea did not include stem cells but it could be modified to include 3 separate populations of stem cells, each of which were randomly distributed within one of the zones. However, irrespective of whether stem cells are involved, this model is not supported by the evidence that cells move inward to maintain the

adrenal cortex or the adrenal cortical regeneration study discussed above (Perrone et al., 1986; Skelton, 1959).

(4) Zona intermedia maintenance hypothesis (Fig. 1.11d). Mitani and colleagues reported that BrdU- or PCNA-positive proliferating cells in rats were mostly located in or near the zone between the ZG and ZF, that expressed neither aldosterone synthetase nor 11β-hydroxylase (Mitani et al., 2003; Mitani et al., 1994). They named this the zona intermedia (ZI) or undifferentiated zone (ZU) and proposed that this was a stem cell zone. This stem cell zone might contain either one or 2 populations of stem cells that maintain the adrenal cortex bidirectionally, with cells moving outwards to maintain the ZG and inwards for the ZF/ZR. However, stem cells are not usually the most rapidly proliferating cells in a tissue so the proliferating cells in the ZU region may represent the early generation TA cells, which are likely to divide more frequently.

(5) Capsule maintenance hypothesis (Fig. 1.11e). Kim and Hammer have recently revived the suggestion that the adrenal cortex is maintained by stem cells in the capsule (Kim and Hammer, 2007). This is based partly on older work where trypan blue was used to pulse-label cells in the capsule (Salmon and Zwemer, 1941; Zwemer et al., 1938). This showed that initially the trypan blue label was exclusively in capsular cells but later appeared in ZG cells, eventually reaching towards the medulla, which suggests that the labelled cells came from the capsule. Other evidence consistent with stem cells in the capsule includes experiments showing that induction of cell proliferation with ACTH was detected in the capsule and, to a lesser extent, in the ZG and ZI by PCNA (Pignatelli et al., 2002). This supports the idea that stem cells in the capsule could either be fibroblast-like cells capable of transforming into adrenocortical cells (Pignatelli et al., 2002) or producing proliferative progenitor cells (early generation TA cells) in the capsule and outer cortex and that these differentiate into steroidogenic cells (Kim and Hammer, 2007). Another immunohistochemical study showed that the SF-1-positive steroidogenic cells occurred within hyperplastic regions of the capsule (which is otherwise SF-1-negative) that extended into the ZG, implying that

differentiated adrenocortical cells may be derived from the capsule (Bielinska et al., 2003).

Most studies of cell proliferation, movement and death in the adrenal cortex reported so far, support the idea that stem cells are most likely to be located towards the periphery and are less consistent with the model shown as Fig. 1.11c, which includes a stem cell population in the ZR. Although the idea of stem cells in the zona intermedia (model d) has been advocated in the last 5-10 years (Mitani et al., 2003; Mitani et al., 1994), the idea of a peripheral population of stem cells (models a, b and e) are better supported by the adrenal cortical regeneration studies (Perrone et al., 1986; Skelton, 1959).

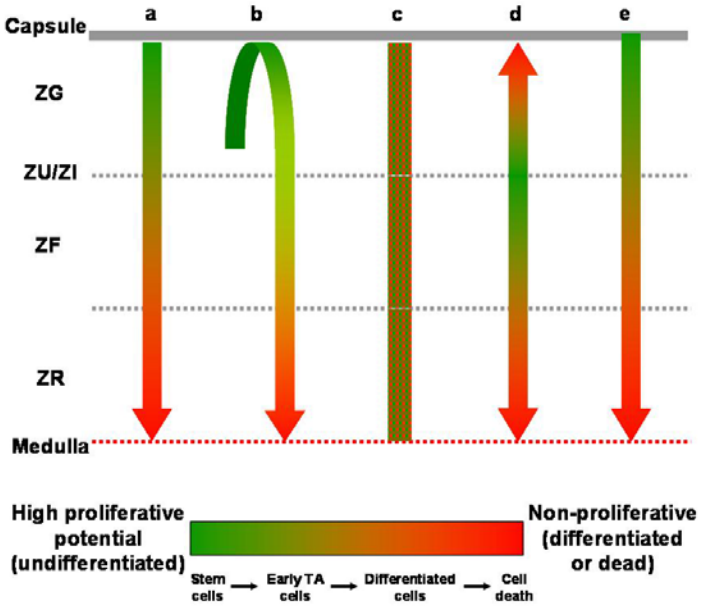

Fig. 1.11. Stem cell models based on published hypotheses of adrenal cortex maintenance. Models a-e are based on hypotheses developed from previous studies (see text). In each case the putative stem cells are located in regions coloured dark green. They produce transient amplifying cells that can divide several times and move away from the stem cell region. As they move and divide they become more differentiated and eventually would be expected to die in the regions coloured red. Movement occurs in the direction green to red. Cell proliferation occurs both in the dark green stem cell zone and the transient amplifying cell zone (intermediate colour) but more cell proliferation is likely among early generation transient amplifying cells (more green than red in colour). After the final cell division TA cells become fully differentiated (red colour). **Model a** represents the centripetal movement hypothesis, where all three zones are maintained by a single population of stem cells in the outer cortex. New cells produced in the subcapsular region of the outer ZG move centripetally and die near the boundary of the cortex and medulla. As cells move centripetally through the zones they play different roles in response to their location. **Model b** represents the 'walking stick-shaped' cell movement hypothesis. This is similar to model a except that many of the stem cells lie deeper in the cortex and initiate an outward movement before centripetal movement. **Model c** shows zonal maintenance, where zones are maintained separately and stem cells (if present) are scattered through the three individual cortical zones (with proliferation and apoptosis within each zone). **Model d** is derived from the idea that the zona intermedia is a stem cell zone and newly formed cells move either outwards to maintain the ZG or inwards to maintain the ZF/ZR. **Model e** represents maintenance by stem cells located in a specific niche within the capsule. Daughter cells move to capsular extensions in the outer ZG and then centripetally through the different zones. **Models a** & **e** are distinguished by different locations of the putative stem cells. In **model a** stem cells are located in the outer cortex whereas in **model e** they are within the capsule (reviewed in Kim and Hammer, 2007).

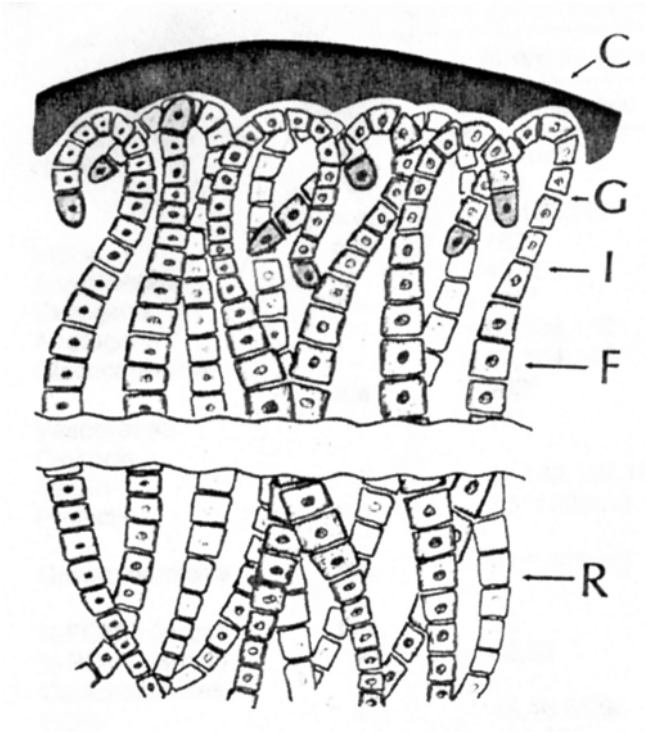

Fig. 1.12. 'Walking stick' shaped movement hypothesis. Stem cells are assumed to be located at the tips of basic cord units which may be straight or curved (like the handle of a walking stick). Some stem cells will be close to the zona intermedia. Eventually, cells move towards the medulla with different roles in the three zones and die around the boundary of cortex and medulla. Abbreviations: C, capsule; G, zona glomerulosa, I, zona intermedia,; F, zona fasciculata; R, zona reticularis. (Reproduced from Estivarez et al., 1992.)

1.4.4 Is the adrenal cortex maintained by stem cells?

The above hypotheses are all consistent with the idea that the adrenal cortex is maintained by stem cells but somatic adrenocortical stem cells have yet to be identified. Stem cells in other tissues have been studied and identified by a combination of characteristics (e.g. self renewal and tissue maintenance) and in some cases specific stem cell markers have been identified (Section 1.3). In the adrenal cortex, existence of stem cells has been proposed in various places based on their proliferation (Kim and Hammer, 2007; Mitani et al., 2003). However in most tissues early generation TA cells proliferate more frequently than stem cells so proliferation is not necessarily a good marker for stem cells. Studies of tissue regeneration by adrenal enucleation (Perrone et al., 1986; Skelton, 1959) and xenografted transplantation (Thomas et al., 1997) discussed above also support the hypothesis that stem cells exist in the cortex. However, to date, no systematic label-retaining studies have been reported to try to identify putative stem cells in the adrenal cortex and further studies are needed to identify them and determine where they are located.

1.5 Mosaic patterns in development and tissue maintenance

Genetic mosaics have two genetically distinct cell populations that arise from the same zygote. Chimeras also have two genetically distinct cell populations but they arise from more than one zygote (e.g. by experimental combination of cells from more than one embryo). Several methods have been developed to produce low-grade genetic mosaics for marking a small number of founder cells for lineage analysis. These methods include incorporation of retroviral marker genes into cells (Huszar et al., 1991; McCarthy et al., 2001) and production of low frequency genetic recombinants that express marker genes using *LaacZ/LacZ* mosaics (Nicolas et al., 1996; Wilkie et al., 2002) or low frequency inducible Cre-*loxP* transgenic systems (Badea et al., 2003). The most common models of mosaicism for the studies of embryonic development and tissue maintenance in the mouse are X-inactivation mosaics and multizygotic chimeras, both of which usually produce variegated patterns with more evenly balanced proportions of the two cell populations.

1.5.1 Use of mouse X-inactivation mosaics and chimeras to study organogenesis

During mammalian development, spontaneous X-chromosome inactivation causes mosaicism in female tissues because one of two X chromosomes in female cells is inactivated in order to perform gene dosage compensation. Paternal and maternal X chromosomes are both functional in female mouse embryos at the mid cleavage stage. At the E3.5-E4.5 blastocyst stage, the paternal X chromosome becomes preferentially inactivated in two extraembryonic lineages (the trophectoderm and primitive endoderm), whereas random inactivation of either the paternal or maternal X chromosome occurs in the epiblast (primitive ectoderm) lineage at a later stage (after E5.5) (Hajkova and Surani, 2004). This produces mosaicism in all derivatives of the epiblast lineage (including the whole fetus). There is some evidence that X-inactivation progresses with different schedules in different somatic tissues, and the notochord, heart, cranial mesoderm and hindgut are

among the last tissues to undergo X inactivation (Tam et al., 1994; Tan et al., 1993). This process of X inactivation is irreversible and stable so that the same X chromosome is inactive in all progeny cells and X chromosome expression shows lineage specific activity.

Mosaicism can be studied in X inactivation mice carrying the X-linked *LacZ* transgene H253 which is under control of a ubiquitously active promotor (Tam et al., 1994; Tan et al., 1993). In H253 mice, ß-gal expression is localized in the nucleus and can be visualized in single cells following X-gal histochemistry, so this provides a good marker for lineage studies. Expression of the *LacZ* transgene appears in around 50 percent of cells in female hemizygotes, which is consistent with random X inactivation of the *LacZ* transgene. Older studies made use of a translocation (Cattanach's translocation) of part of chromosome 7, carrying the wild-type allele of the Tyr^{+} gene encoding tyrosinse, into the X-chromosome of an albino mouse. In pigmented tissues, such as the coat and retinal pigment epithelium, random X-chromosome inactivation produces a mosaic of pigmented (X chromosome carrying the translocation is active) and unpigmented (normal X chromosome is active) cells (Bodenstein and Sidman, 1987b; Nesbitt, 1974).

Mouse chimaeras are usually produced either by injecting embryonic stem (ES) cells into a host blastocyst or by aggregating two embryos at the 8 cell stage after removal of the zonae pellucidae. The chimeric embryo is surgically implanted in the uterus of pseudopregnant surrogate mother to continue development to term. If one of the two cell populations (embryo or ES cells) that are combined to produce the chimera carries a suitable genetic marker, such as *LacZ* or GFP, that is detectable in tissue sections this can be used to detect cell lineages and study the manner in which cells assort themselves during embryogenesis.

Analysis of the distributions of the two cell populations in variegated tissues of mouse X-inactivation mosaics and chimeras can provide information on the extent of cell mixing and cell movement during tissue formation. Less cell mixing is likely to have occurred in formation of mosaic tissues that show a course-grained

distribution of the two cell populations (with large patches) than one that shows a fine-grained distribution (with small patches). For some studies is helpful to distinguish between the terms ‘patch’, ‘descendent clone’ and ‘coherent clone’ (Nesbitt, 1974; West, 1978a). A *patch* is a group of cells of like genotype (or phenotype) that are contiguous at the time of consideration. A *descendent clone* is any group of clonally related cells irrespective of whether they have remained contiguous throughout development. A *coherent clone* is a group of clonally-related cells that have remained contiguous throughout development. Patches can be identified in mosaic tissues but the boundaries of coherent clones and descendent clones cannot usually be identified directly. For example, the number of coherent clones per patch depends partly on the proportions of the two cell populations in the mosaic.

Both X-inactivation mosaics and chimeras have provided insights into the development of tissues and their maintenance in adults. Coat pigmentation provided one of the first markers for analysing variegated patterns in chimeras. Early studies of coat patterns of adult pigmented↔albino chimeric mice suggested the presence of discontinuous dorso-ventral stripes of pigmented and albino hairs, which helped identify how melanoblasts colonised the hair (Mintz, 1967). The stripes on one side of the body did not match with ones on the other side, implying that the stripes on the two sides were independently established by two strings of melanoblasts migrating from the neural crest on either side of the dorsal midline. The significance of stripes that occur in the retinal pigment epithelium, corneal epithelium and adrenal cortex of mosaic and chimeric mice is discussed below.

1.5.2 Mosaic analysis of the mouse retinal pigment epithelium

The retinal pigment epithelium (RPE) is a cup-shaped single layer of pigmented cells at the outside of the neural retina. The retinal pigment epithelia of adult pigmented↔albino chimeric mice and pigmented/albino X-inactivation mosaics, that were heterozygous for Cattanach's translocation (see above), showed a variegated pattern of black and white patches. The chimeric and mosaic RPEs had different mosaic patterns in different regions (Bodenstein, 1986; Bodenstein and Sidman, 1987b). Small irregularly distributed patches occurred in the proximal retinal pigmented epithelium (near the optic nerve head) while radial pigmented stripes appeared in the distal retinal pigmented epithelium (towards the iris). This was explained using a combination of computer modelling and mitotic cell labelling analysis. A computer simulation model was used to compare the effects of growing a two-dimensional mosaic tissue in three ways: edge growth (only cells at the edge divided), edge-biased growth (most cell divisions occurred at the edge) and interstitial growth (cells could divide throughout the tissue) (Bodenstein, 1986). Interstitial growth gradually generated a pattern of cell mixing between the two cell populations in the simulated mosaic tissue whereas edge growth produced little cell mixing and edge-biased growth produced an intermediate amount of cell mixing. Analysis of the locations of proliferating cells during development of the RPE revealed a switch from interstitial growth to edge-biased growth during the later stages of development (Bodenstein and Sidman, 1987a). Thus, during early development of a mosaic retinal pigment epithelium, cell proliferation is widespread throughout the tissue (interstitial growth) so cells mix up to form small black and white patches. At later stages, cell division is more restricted to the edge of the growing tissue (edge-biased growth) so less cell mixing occurs and black and white stripes form at the edge of the RPE as the tissue enlarges. This shows that edge-biased growth can produce stripes in mosaic or chimeric tissues during organogenesis.

1.5.3 Mosaic analysis of the mouse corneal epithelium

During postnatal development of the corneal epithelia of X-inactivation mosaic and chimeric mice there is a transition from an initially randomly orientated mosaic pattern (age of 3 weeks), emergence of radial stripes at the periphery (age of 5 weeks), to complete radial stripes (8-10 weeks), which then persists in the adult stage (Collinson et al., 2002). In this case the likely explanation is that the initial randomly orientated mosaic pattern at 3 weeks is replaced once stem cells in the limbal region (at the periphery of the cornea) are activated. The stem cells produce transient amplifying cells (TA cells) which move inward along the basal epithelial layer for maintenance of the corneal epithelium (Cotsarelis et al., 1989). They divide several times as they migrate inwards and after the final division both daughter cells enter the more superficial layers (Beebe and Masters, 1996). (The adult corneal epithelium is about 5 cells thick and the outer cells become progressively more differentiated until they are lost from the surface by desquamation. See section 1.3.1.3.) The postnatal formation of stripes in the mosaic corneal epithelium shows that stripes can form during the maintenance of an adult tissue even if stripes are not formed during organogenesis. In addition a quantitative analysis of the striped pattern suggested that stem cell function declined with age up to 39 weeks (Collinson et al., 2002).

1.5.4 Mosaic analysis of the mouse and rat adrenal cortex

The continuous radial striped pattern seen in the adrenal cortex of adult mosaic and chimeric rats and mice was demonstrated initially in adult chimeric rats by immunohistochemistry for major histocompatibility antigens within two distinguishable cell populations of cells (Iannaccone, 1987). Analysis of radial stripes revealed that clonal lineages were maintained across three cortical zones and supported the hypothesis that maintenance of adrenal cortex is the result of cell division at the outside of the cortex and movement of cells towards the inner cortex (Iannaccone and Weinberg, 1987). However, if the striped pattern was established before stem cells were active, the zones could be maintained independently without disrupting the full span of the stripes. Later, Morley et al., (2004) reported that X inactivation mosaic, *LacZ*↔wildtype chimeric and *21OH/LacZ* transgenic mosaic mice displayed similar striped patterns, supporting the idea that the stripes are features of clonal lineages in the adrenal cortex.

At fetal stages, *21OH/LacZ* mosaic adrenals had a randomly orientated variegated pattern rather than the adult striped pattern (Morley et al., 1996). One plausible explanation is that the prenatal pattern was replaced with the adult striped pattern when centripetal movement begins. However, others have suggested that the stripes may arise by changes in the constraints on cell proliferation (Landini and Iannaccone, 2000).

The randomly orientated pattern seen in mosaic fetal adrenal cortices is similar to that seen in some other adult tissues (such as the liver) in chimeras and mosaics. Differences between randomly orientated and striped chimeric and mosaic patterns were investigated by computer simulation of a growing mosaic tissue and fractal analysis (Landini and Iannaccone, 2000). The computer simulation varied the ‘pushing force’ exerted by a dividing cell. When the pushing force was low, daughter cells tended to remain together so cell mixing was low resulting in coherent clonal growth and production of large patches. When the pushing force was high, cell mixing was more extensive and this produced simulations with a

larger number of small irregular-shaped patches. The fractal dimension of the patches was used to compare the irregularity of their shapes because patches with more irregular perimeters have higher fractal dimensions. This analysis showed that the large patches produced by a low pushing force had smaller fractal dimensions than those produced by a high pushing force so simulations of more cell mixing produced more irregular shaped patches. This led to the suggestion that the change from randomly orientated mosaic patterns in the mosaic fetal adrenal cortex to the striped pattern seen in adults could involve a change from unconstrained to more constrained cell divisions rather than the onset of centripetal cell migration (Iannaccone et al., 2003; Landini and Iannaccone, 2000). This is similar to the change in variegated patterns that occurs during development of the RPE in chimaeras and X-inactivation mosaics, which has been attributed to a switch from interstitial growth to edge-biased growth (Bodenstein, 1986; Bodenstein and Sidman, 1987a,b,c; see section 1.5.2).

1.6 Use of *21OH/LacZ* transgenic adrenal for cell linage studies

1.6.1 *21OH/LacZ* transgenic mice

The mouse steroid 21-hydroxylase A (*21OHase*) gene is normally expressed throughout the adrenal cortex, where the steroid 21-hydroxylase enzyme mediates the penultimate step in both glucocorticoid and mineralocorticoid synthesis (Fig. 1.4). The *21OHase* gene is now known as cytochrome P450, family 21, subfamily a, polypeptide 1 (gene symbol *cyp21a1*) but the commonly used abbreviation '*21OHase'* is used throughout this thesis. Morley and colleagues reported that a steroid 21-hydroxylase A gene promoter/*LacZ* reporter *(21OH/LacZ)* transgene (Fig. 1.13), was expressed specifically in the adrenal cortex of transgenic mice (Morley et al., 1996). However, instead of being expressed throughout the adult adrenal cortex, like the endogenous gene, the *21OH/LacZ* transgene displayed a strikingly variegated pattern of expression in all ten transgene-expressing lines examined. The reason why the *21OH/LacZ* transgene shows mosaic expression is unclear but it might involve some type of stochastic inactivation of the transgene in some cells early in development (Dobie et al., 1997).

The variegated pattern of expression presented as radial mosaic stripes of β-gal staining spanning the classical adrenocortical zonal structure, but paralleling the columnar arrangement of cells of the zona fasciculata and the centripetal organisation of the adrenocortical blood supply. As previously discussed for mosaic analysis of the rat adrenal cortex in section 1.5.4, if cells within a radial mosaic stripe were clonally related, this would suggest that cells of all three adult adrenocortical zones share a common clonal origin (Iannaccone and Weinberg, 1987; Morley et al., 1996). While this pattern suggests that all three zones are maintained by cellular migration it does not exclude other possibilities if stem cells are activated after stripes are established (see section 1.5.4).

The specificity of *21OH/LacZ* transgene expression was further confirmed by detection of β-gal staining specifically in the adrenal primordium of partially dissected embryos from line 7911 *21OH/LacZ* transgenic mice at E11.5 and E12.5, mirroring the developmental onset of expression of the endogenous *21OHase* gene (Morley et al., 1996). Staining became more intense by E15.5 and E17.5 (80-90% of cells appeared β-gal-positive positive in the outer part of the intact adrenal). However, in contrast to adult radial stripes, this presented as 'islands' of β-gal staining within the developing adrenal gland, suggesting that embryonic adrenal growth may occur by a different mechanism. It is not yet known over which developmental period the transition from an embryonic pattern of 'islands' to adult radial stripes of β-gal staining takes place, or by what mechanism the adult adrenocortical radial stripe pattern emerges (Morley et al., 1996).

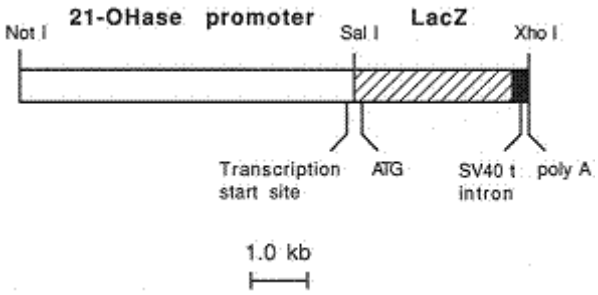

Fig. 1.13. Steroid 21-hydroxylase A gene promoter/*LacZ* reporter *(21OH/LacZ)* transgene construct. (Reproduced from Morley et al., 1996)

1.6.2 The mosaic patterns in adrenal cortices of X-inactivated mosaics, chimeras and *21OH/LacZ* transgenic mice

As described previously (section 1.5), the mosaic patch patterns seen in aggregation chimeras of genetically distinguishable mouse or rat strains and X-inactivation mosaics are known to have a lineage basis and have been used as model systems for analysing cell lineages in a variety of tissues. The mosaic patch patterns of radial β-gal staining stripes seen in adult adrenal cortices of *21OH/LacZ* transgenic mice appear qualitatively similar to those seen in adrenal cortices of adult X inactivation mosaics and *LacZ* ↔ wild type mouse chimeras. Quantitative comparison of the *21OH/LacZ* adrenocortical mosaic stripe patterns with those seen in chimeras and X inactivation mosaics demonstrated that the 'corrected stripe numbers' were similar in all three groups (Morley et al., 2004; see also Figs. 1.14 and 1.15). This supports the hypothesis that the stripes in *21OH/LacZ* adrenal cortices may be formed in the same way as in aggregation chimeras and X-linked inactivation mosaics (i.e. they have a lineage basis). This suggests that *21OH/LacZ* transgenic mice could be used to study steroidogenic cell lineage relationships in the mouse adrenal cortex (Morley et al., 2004). These mice also have the additional advantage of displaying a reproducible mosaic pattern in both males and females and not requiring extensive experimental manipulation to produce material for study.

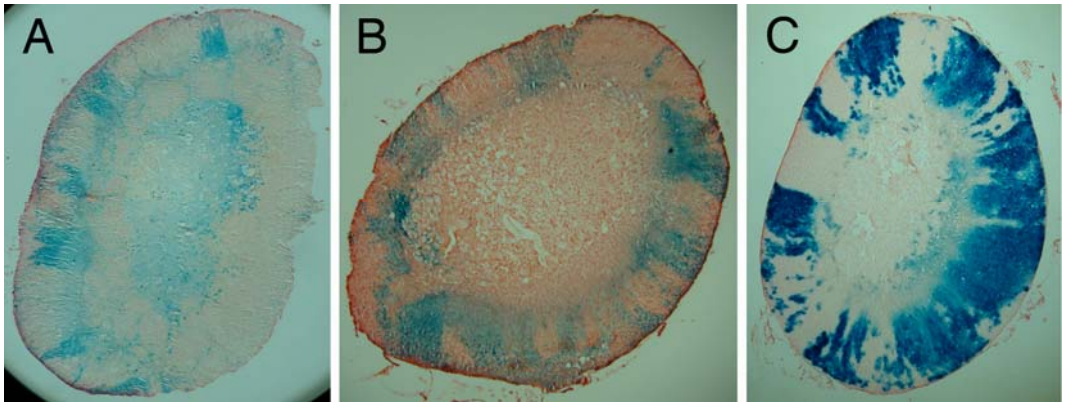

Fig. 1.14. Similar mosaic patterns in mouse adrenal cortices from LacZ↔wild type chimeras, X-inactivation mosaics, and *21OH/LacZ* transgenic mice. Chimeric, X-inactivation mosaic, and *21OH/LacZ* transgenic mice display similar patterns of ß-gal positive (blue) and ß-gal negative (unstained) radial stripes spanning the adult adrenal cortex. (A) Adult LacZ ↔ wild type female chimeric adrenal; (B) Adult female X-inactivation mosaic adrenal and (C) Adult *21OH/LacZ* female transgenic adrenal (line 7911). (Reproduced from Morley et al., 2004)

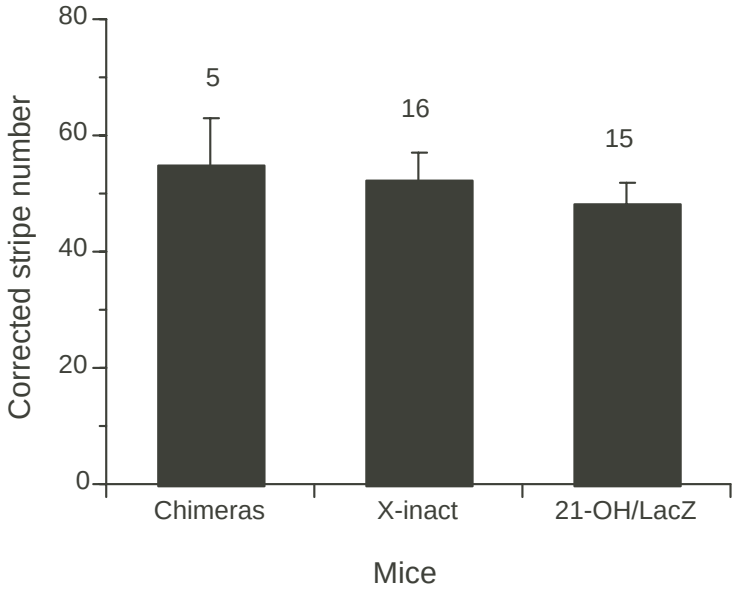

Fig. 1.15. Comparison of the corrected stripe number in adult mouse LacZ↔wild type chimeras, X-inactivation mosaics, and *21OH/LacZ* transgenic mice. Three groups of chimeric, X-inactivation, and *21OH/LacZ* transgenic mice shows quantitatively similar corrected stripe numbers (mean±SEM; number of adrenals shown above each bar). Abbreviations: X-inact, adult X-inactivation mosaic female and *21OH/LacZ*, adult *21OH/LacZ* transgenic female (line 7911). (Reproduced from Morley et al., 2004)

1.7 Aims

The overall aims of the work presented in the thesis were to better characterise some cellular aspects of organogenesis during growth of the mouse adrenal cortex (chapters 3 and 4) and its maintenance in the adult (chapters 5 and 6). An important aspect of this was to try to determine whether the steroidogenic cell population in the adult adrenal cortex is maintained by stem cells and, if so, to identify their likely location. These aims were addressed by analysing mosaic patterns in the adrenal cortex of *21OH/LacZ* transgenic mice and by analysing the distribution of cell proliferation. Specific experimental aims of each chapter were as follows.

- In chapter 3, the main aim was to characterise when and how the mosaic pattern in *21OH/LacZ* transgenic adrenals changes from randomly orientated spots to adult radial stripes by comparing patterns of mosaicism at different ages. It was hoped that characterising the emergence of radial stripes would identify whether stripes emerge during growth or only during maintenance of the adult adrenal and that this might suggest when stem cells become active in maintaining the adrenal cortex.

- The aim of chapter 4 was to test the hypothesis, developed in chapter 3, that stripes emerged by edge-biased growth with proliferation largely restricted to the outer part of the adrenal cortex during the period of adrenal growth.

- The aim of chapter 5 was to evaluate several hypotheses suggesting how stem cells might be involved in maintaining the adrenal cortex. This was addressed using BrdU labelling to study adrenal dynamics (cell proliferation and movement) and to evaluate the location of putative stem cells for adrenocortical maintenance by identifying label retaining cells.

- In chapter 6, the aim was to use the stripe patterns in adult *21OH/LacZ* adrenals to help evaluate the different adrenal stem cell hypotheses by investigating whether the stripes always spanned the entire radial width of the

adrenal cortex and by testing for age-related changes in the adult mosaic pattern, which might reflect age-related changes in stem cell function.

2 Materials and methods

2.1 Mice

2.1.1 Mouse husbandry

Until December 2004 all experimental mice were kept under conventional conditions in the Medical Faculty Animal Area at the University of Edinburgh but after this date mice were housed in individually ventilated cages (IVCs) in the Biological Research Facility at Little France Phase 1 (BRF-LF1), University of Edinburgh. Males and females were separated at weaning (3~4 weeks) and caged in single-sex groups. Mouse colony management and also mating and plug-checking procedures described below were carried out by the staff of the Medical Faculty Animal Area and BRF-LF1.

Before the adrenal glands were dissected, mice were killed by cervical dislocation or decapitation (fetuses). The gender of the mice was confirmed while the adrenal glands were dissected. Animal work was performed in accordance with University of Edinburgh guidelines and UK Home Office regulations as stipulated by the Animals (scientific procedures) Act 1986. Regulated procedures were carried out under Dr John West's Home Office Project Licences PPL 60/2887 and PPL 60/3635.

Adult male and female mice were caged together for breeding and for production of fetuses. To identify the day of mating, vaginal plugs were checked each morning and the females with plugs were earclipped and removed. Mating was assumed to occur in the middle of the dark period and fetal age was timed from the day of the vaginal plug, which was taken to be embryonic (E) day 0.5. The normal gestation period of mice is 19-20 days and the date of birth was regarded as postnatal day 0 (P0).

2.1.2 Mouse strains

21OH/LacZ transgenic mice from line 7911 (Morley et al., 1996) were maintained as a non-inbred, homozygous stock using male x female pairs but avoiding brother x sister matings. Hemizygous *21OH/LacZ* transgenic mice were produced by crossing homozygotes to non-transgenic, wild-type (C57BL/6 x CBA/Ca)F1 hybrid mice. Wild-type (C57BL/6 x CBA/Ca)F1 mice were used for BrdU studies and fetuses were also produced from crosses between C57BL/6 males and CBA/Ca females.

2.1.3 Injections

The animal technician (Mr Keith Chalmers) performed the BrdU injections. 12 week old (C57BL/6 x CBA/Ca) F1 mice were given single intraperitoneal (i.p.) injections of BrdU (10 mg BrdU/ml saline; 0.2ml/mouse).

2.1.4 Implantation of osmotic mini-pumps

Alzet osmotic mini-pumps were filled with BrdU solution (50mg BrdU/ml saline). Alzet model 1007D was filled with 0.1ml BrdU solution for 1 week of BrdU labelling and model 2002 was filled with 0.2ml BrdU solution for 2 weeks labelling. One mini-pump was surgically implanted into each 12 week old (C57BL/6 x CBA/Ca)F1 mouse by the animal technician (Mr Keith Chalmers). An area of back fur (about a quarter of way up from the base of the tail) was shaved, the skin was wiped with 70% ethanol and a small incision made. The incision was enlarged with forceps to make a pocket and the mini-pump inserted and the wound closed with wound clips. After 7 or 14 days (depending on the type of mini-pump), the clips and pump were removed, the wound was closed again with clips which were removed 7 days later. After removal of the mini-pumps, mice were left for various chase periods before they were killed and the adrenals were removed for BrdU immunohistochemistry.

2.2 Measurement of adrenal size and adrenal weight

The adrenal glands were dissected out on a Wild M5A dissecting microscope immediately after the mice were sacrificed. The connective tissue and adipose tissue were trimmed off on a paper towel soaked with PBS and adrenals were either blotted dry and weighed with an electronic balance or placed on moist paper towel for measuring. The lengths and widths of perinatal adrenals were measured on a Wild M5A dissecting microscope fitted with a calibrated eyepiece graticule. The adrenal area and its volume were estimated from the measurements of length and width by assuming the adrenal was an ellipsoid and using the following equations:

ellipse area = $^1/_2$ length × $^1/_2$ width × π

volume of an ellipsoid = $^1/_2$ length × $^1/_2$ width × $^1/_2$ depth × π

(The depth was assumed to be equal to the measured width.)

2.3 Adrenal processing for cryosection (cryostat) and wax-embedded section (microtome)

2.3.1 Preparation of frozen sections for β-galactosidase (β-gal) staining

The mice were culled at specific ages and adrenal glands were dissected out immediately. Adrenals were weighed (adult) or measured (embryos and perinatal mice), then orientated for cutting longitudinal sections and embedded in OCT compound (Tissue-Tek) embedding medium in plastic moulds. The moulds containing OCT and samples were frozen on dry ice to form solid OCT blocks and either cryosectioned immediately or stored at –70°C. 10 μm frozen tissue sections were cut longitudinally with a cryostat (Leica CM 1900), and deposited on Polysine slides (VWR Laboratory Supplies). Slides with adherent frozen sections were either stored in a frost-free freezer at –20°C or stained immediately for β-galactosidase activity.

2.3.2 Wax embedding and sectioning of samples

Mice were culled at specific ages and adrenal glands dissected out immediately. Adrenals were fixed for 2 hours (perinatal adrenals) or for 4 hours (adult adrenals) with freshly prepared 4 % (w/v) paraformaldehyde (PFA) in PBS at 4°C. (Solid PFA was weighed in a fume cupboard, PBS was added and the PFA dissolved by warming it in a 60^{o}C water bath for two hours.) After fixation, adrenal glands were washed in PBS two or three times for 10-15 minutes, then once in isotonic saline (0.9% w/v NaCl) for 15 minutes, once in 50 % (v/v) ethanol, once in isotonic saline for 10 minutes and, finally, once in 70 % (v/v) ethanol for 30 minutes. Adrenals were stored in 70 % (v/v) ethanol until embedding.

Adrenal glands were processed through a routine histological protocol by the histology lab technician, as follows, before being embedded in paraffin wax: 15 minutes in 85 % (v/v) ethanol, 15 minutes in 95 % (v/v) ethanol, three times in 100 % (v/v) ethanol for 15 minutes, twice in xylene for 15 minutes, followed by storage in xylene overnight. Adrenals were placed in molten Paraplast Plus embedding wax at 45°C for 1 hr and then transferred into fresh molten wax for 2 hrs to displace the xylene in the samples. Adrenals were next transferred into a third dish of molten wax, adrenals were orientated for cutting longitudinal sections and solid wax blocks were prepared. Longitudinal, 7 µm sections of adrenals were cut from the wax blocks with a microtome (Leica Jung biocut 2035), mounted on microscope slides (by floating them in 45°C warm water on the slides) and air-dried. (The histology technician prepared the wax blocks but I cut and stained the sections.)

2.4 β-galactosidase staining

Longitudinal, 10 μm frozen sections of adrenal glands from *21OH/LacZ* transgenic mice were soaked for 5-10 minutes in freshly made fix solution (0.1M Na phosphate; pH 7.3, containing 0.2% (w/v) glutaraldehyde, 5mM-EGTA and 2mM-magnesium chloride) at room temperature, followed by washing tissue sections three times for 5 minutes in washing buffer (0.1M-Na phosphate; pH 7.3, containing 2mM-magnesium chloride, 0.01% (v/v) sodium deoxycholic acid, and 0.02% (v/v) nonidet-P40) at room temperature. Sections were then incubated in X-gal staining solution (0.1M Na phosphate; pH 7.3, containing 1mg/ml X-gal; 5-bromo-4-chloro-3-indolyl-beta-D galactopyranoside, Sigma), 5mM-potassium ferrocyanide, 5mM-potassium ferricyanide, 0.01% (v/v) sodium deoxycholic acid, 0.02% (v/v) nonidet-P40 and 2mM-magnesium chloride) for 12-16 hrs at room temperature. After X-gal staining, slides were briefly rinsed in washing buffer and transferred to fresh washing buffer for 2-16 hrs at 4°C. Samples were counterstained in 0.01-0.0125 % neutral red for 30 seconds. Slides were air-dried and mounted with Histoclear mounting medium and cover slips. Mounted slides were air-dried prior to examination with a Zeiss Axioplan 2 compound microscope and images were captured with a Nikon Coolpix 995 digital camera.

2.5 Measurement of stripes in the adrenal cortex

The proportions of β-gal positive and β-gal negative regions along a measured circumference (see below) were used to represent the expression pattern in the intact adrenal cortex. The method of analysis chosen makes two assumptions. (i) The radial stripe pattern seen in β-gal stained tissue sections is a reproducible two dimensional representation of three dimensional columns of cells in the intact gland. (ii) The two dimensional pattern can be subjected to one dimensional measurement of stripe width as the variable because most stripes are continuous across the depth of the cortex and therefore, are approximately constant in length.

Middle β-gal-stained sections of adrenal glands, identified as containing a large area of central medulla, were selected and photographed. In most cases the blue β-gal staining occurred as clear radial stripes across the cortex and the boundary of each stripe was well defined. Following optimisation of measurement methodology (described below), stripes were measured, in the outer third of the adrenal cortex (within the zona fasciculata). Any diffuse pale blue staining in this region was included with the unstained β-gal-negative tissue because this was likely to be a technical artefact (e.g. it could result from diffusion or smearing of stain from a neighbouring β-gal-positive region). Pale blue staining was consistently exhibited in the X zone so was unlikely to be an artefact but this region was not measured.

Digital images of β-gal-stained adrenal gland sections were captured as described in section 2.11 using a 5x objective and analysed on a computer using UTHSCSA Image Tool software for Microsoft Windows. The final on-screen magnification of the calibrated image was approximately 70-90x. First a line was drawn, parallel to the circumference at the perimeter of the adrenal gland, at a pre-determined distance from the perimeter. Initial trials compared measurements at different depths in the cortex (20% and 33% from the capsule towards the inner margin of the cortex; see results, chapter 6) but for the main analysis the width of each stripe was measured at a depth equivalent to 33% of the distance from the capsule (perimeter) to the inner margin of cortex, excluding any X zone (Fig. 2.1). All measured values were standardised to μm with a calibrated scale bar. Measurements were started at one radial boundary between a blue stained, β-gal positive stripe and an unstained, β-gal negative stripe and each stripe was measured following the line in a clockwise direction around the cortex back to the start position. In this way a table with 2 columns of stripe widths (β-gal positive and β-gal negative) was produced. These primary data were used to analyse the stripe patterns in more detail as discussed in section 2.6 below.

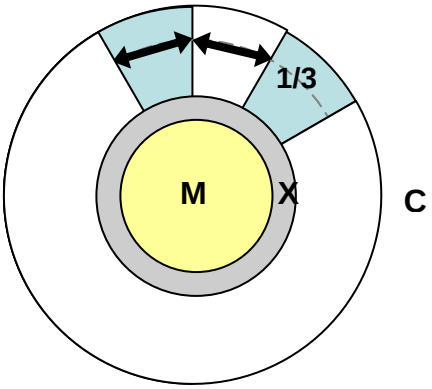

Fig.2.1. Stripe widths were measured at a depth equivalent to 33% of the distance from the capsule to the inner margin of cortex, excluding any X zone (grey ring labelled 'X'). The dashed line shows the line of measurement parallel to the capsule at a depth of 33% of the thickness of the cortex. The double-headed arrows show the width of two stripes. M: medulla (yellow); C: capsule.

2.6 Analysis of stripes width in adrenal cortex

The table of β-gal positive and β-gal negative stripe widths (produced as described in section 2.5) for each measured adrenal provided the uncorrected number of β-gal positive, transgene-**e**xpressing stripes (**S_e**) and the uncorrected number of β-gal negative stripes (**S_n**). Since the measured line is a closed circle, $S_e = S_n$. The **l**ength of the circumference along the measured line (**L**) was obtained by adding up all the stripe widths (both β-gal positive and β-gal negative). The β-gal positive (transgene-**e**xpressing) part of the circumference (**L_e**) was obtained by adding up all the β-gal positive stripe widths. The β-gal **n**egative part of the circumference (**L_n**) was obtained by adding up all the β-gal negative stripe widths. Thus, $L = L_e + L_n$. The **p**roportion of β-gal positive cells (transgene-**e**xpressing) around the measured circumference (**p_e**) was calculated as $p_e = L_e/L$, and the proportion of β-gal negative cells is calculated simply as $p_n = 1 - p_e$. The uncorrected mean width of β-gal positive stripes is given by L_e/S_e but is more usefully expressed as a percentage of the adrenal circumference [$C_e(\%) = p_e \times 100/S_e$] because the uncorrected stripe width and measured circumference both vary according to the depth of cortex where the circumference is measured. Equivalent calculations can be used to derive the mean uncorrected width of the β-gal negative stripes.

One visible, β-gal-positive radial stripe in the adrenal cortex may consist of several adjacent β-gal-positive radial coherent clones (Fig. 2.2). (A coherent clone is defined as group of clonally related cells that have remained contiguous throughout development.) The width of a stripe will depend both on number of radial coherent clones and the width of the radial clones. The number of β-gal-positive coherent clones per stripe will vary with the proportion of β-gal-positive cells in the adrenal cortex. The analysis of stripes that intersect a line drawn through the adrenal cortex, parallel to the perimeter (described in section 2.5) is equivalent to a 1-dimensional mosaic of two cell populations. Previous analysis of such mosaics, based on the work of Roach (Roach, 1968), has estimated the

number of coherent clones per patch of one cell population as 1/(1-p), where p is the proportion of that cell population in the mosaic, as explained in Fig. 2.2, (Collinson et al., 2002; West, 1976; West, 1978a; West, 1978b; West et al., 1997). In the present analysis of the adrenal cortex the number of coherent clones per stripe would be estimated in a similar way as $1/(1-p_e)$, where p_e is the proportion β-gal-positive cells along the measured line.

Variation in the uncorrected mean width of β-gal-positive stripes (expressed as a percentage of the adrenal circumference; $C_e(\%) = p_e \times 100/S_e$) will be partly caused by variation in the proportion of β-gal-positive cells, because this will affect the mean number of adjacent β-gal-positive coherent clones per stripe. This source of variation can be removed by 'correcting' the mean width by dividing $C_e(\%)$ by $1/(1-p_e)$. The corrected mean width of β-gal-positive stripes is an estimate of the mean width of coherent clones, but the estimate is likely to be imprecise unless two assumptions are correct. (The assumptions are that (i) coherent clones are equal in size, or their sizes are normally distributed, and (ii) β-gal-positive and β-gal-negative coherent clones are randomly distributed around the circumference.)

Assumption (i) may not be valid because, for example, coherent clones in the adult retinal pigment epithelium have been shown to vary in size and follow a skewed, non-random distribution (Schmidt et al., 1986). In this case the mean may not be a good summary of stripe widths so the corrected stripe number (which is derived from the corrected mean stripe width) may not be an accurate estimate of the coherent clone number. If assumption (ii) is not valid (e.g. β-gal-positive clones are clumped together), use of the correction factor $1/(1-p_e)$ will not correct the observed stripe number accurately because it represents the predicted number of clones per stripe if the clones are randomly distributed in a linear array (see Fig 2.2b).

As we do not know whether the assumptions are valid the term 'corrected stripe number' is more appropriate than coherent clone number. This is still likely to be

proportional to the number of coherent clones, so it provides a useful comparative measure even if the assumptions are incorrect.

The correction factors $1/(1-p_e)$ and $1/(1-p_n)$ are not independent and for circular arrays the corrected mean widths of β-gal-positive and β-gal-negative stripes are equal. The reciprocal of the corrected mean width of β-gal-positive stripes (expressed as a percentage of the adrenal circumference) gives the number of such 'corrected stripes' that would fit around the measured circumference. As the corrected mean widths of β-gal-positive and β-gal-negative stripes are equal the mean corrected stripe number per circumference applies to the total number rather than specifically β-gal-positive or β-gal-negative stripes.

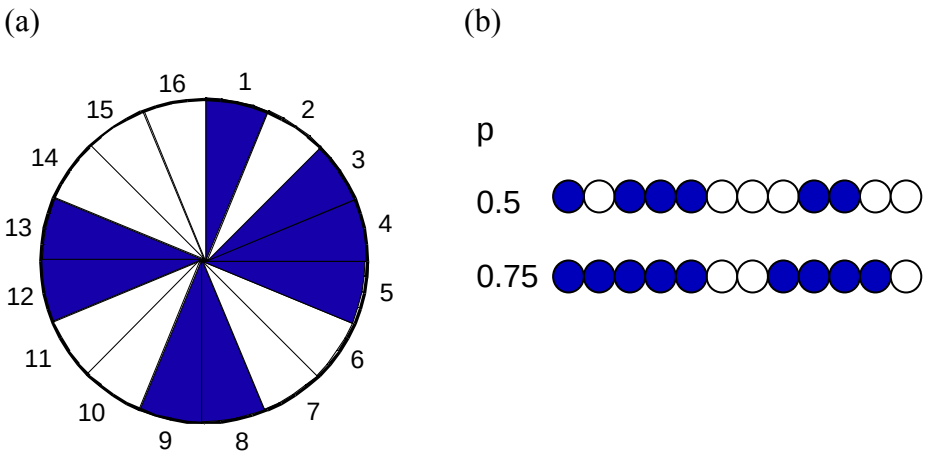

Fig. 2.2. Relationship between radial clones and stripes. (a) A hypothetical circular tissue comprising 8 blue and 8 white radial clones arranged in a random order. One visible stripe can be composed of more than one clone. If neighbouring clones are of the same type (colour) they form wider stripes (e.g. clones 3-5 form a wide stripe of 3 clones). (b) In a linear array of blue and white balls the mean number of blue balls in a row increases as the proportion of blue balls increases from 0.5 to 0.75. If each ball represents a radial coherent clone in the adrenal, a string (or patch) of blue balls represents the width of a stripe. p= proportion of blue balls (or β-gal-expressing cells around the measured adrenal circumference).

In (b) the expected mean number of blue balls per patch (equivalent to the expected number of blue radial coherent clones per stripe in the adrenal) is given by the function $^{1}/_{(1-p)}$, which may be derived as follows. The mean number of blue balls in a patch is equal to the total number of blue balls divided by the number of blue patches. If the total number of balls (blue plus white) in the linear array is N, the number of blue balls is Np, where p is the proportion of blue balls. The frequency of blue patches is equal to the frequency of right hand boundaries of blue patches or the frequency that a blue ball (p) is followed by a white ball (1-p). This is equal to the p(1-p) so the number of blue patches is equal to Np(1-p). The mean number of blue balls per patch is then $^{Np}/_{Np(1-p)}$ which is $^{1}/_{(1-p)}$.

2.7 Haematoxylin and eosin staining

Haematoxylin and eosin (H & E) staining was used for routine histological examination of the adrenal cortex (chapter 4). The 7 μm, wax-embedded, longitudinal tissue sections were mounted on microscope slides, dewaxed (2 x 10 min in xylene; Genta Environmental Ltd.) and rehydrated [2 x 5 min each in 100% ethanol, 70% (v/v) ethanol and PBS, and finally distilled water (2-5 min)]. The slides were immersed in Gill's haematoxylin (Vector, H3401) for 3-5 min, which stains cell nuclei blue and rinsed in tap water (3-5 min**)**. The slides were then briefly immersed (10 dips; 2-3 sec) in 2% (v/v) acid solution (2ml glacial acetic acid + 98ml of distilled H_2O) to remove non-specific cytoplasmic staining, rinsed in tap water (10 dips; 2-3 sec) and immersed in Blueing solution (1.5ml 30% NH_4OH + 98.5ml of 70% ethanol) for 1-2 mins to allow the blue colour to develop. Slides were then rinsed in tap water (10 dips; 2-3 sec), immersed in eosin Y (Surgipath) for 30 sec to stain the cytoplasm pink and rinsed in tap water (3-5 mins). Sections were then dehydrated in a series of graded alcohols (5 mins twice each in 70%, 85%, 95% and 100% v/v ethanol) and cleared in xylene for 5 mins. Coverslips were mounted with DPX mounting medium and left to air dry and slides were stored in slide boxes before observation.

2.8 Ki67 nuclear antigen immunohistochemistry

Immunohistochemistry for Ki67 nuclear antigen was used to detect cells that were in late G1, S, G2 and M phases (but not G0) of the cell cycle, as a marker of cell proliferation (chapter 4, section 4.3.3). Wax-embedded, longitudinal tissue sections were mounted on Polysine slides (VWR laboratory supplies) slides (section 2.3.2) and dewaxed (xylene, twice for 10 min). After two 5 min washes in 100% (v/v) ethanol, slides were immersed in 3% (v/v) hydrogen peroxide (H_2O_2; Sigma H1009) in methanol (Fisher) for 30 min in the dark at room temperature to block endogenous peroxidase activity, which would interfere with

the horseradish peroxidase signal. Slides were then rehydrated in 70% (v/v) ethanol (twice for 5 min) and washed in PBS (twice for 5 min).

Some antibodies require a heat-induced antigen retrieval step to break the cross-links that form during fixation which may mask antigenic sites (Norton et al., 1994). For this purpose slides were placed in a glass rack in a glass dish, covered with citrate buffer (0.01M citrate pH 6). The dish was wrapped with clingfilm and a small hole pierced in each of the 4 corners of the clingfilm. The dish was placed in a microwave oven and microwaved at full power (800 Watts) for 4 periods of 5 min. The level of citrate buffer was topped up with warm water each time to maintain the concentration of citrate buffer. After 4 periods of microwave heating, the buffer was topped up and slides were then left to cool in the buffer at room temperature for 20 minutes.

The slides were then washed in PBS for 5 min and the sections immunostained as follows to detect Ki67 expression. Slides were first treated with blocking serum; 20% (v/v) Rabbit serum (SAPU) in 1×TBS (10×TBS is 15.18g Tris base and 90g sodium chloride in 1 litre water, adjusted to pH 7.6 with HCl) for 30 min then primary anti Ki67 antibody (Novocastra Lab Ltd; NCL-Ki67-MM1; lyophilized mouse monoclonal antibody IgG; 5µl/ml in blocking serum) for 2 hours. This was washed off by pouring TBS over the slides and then immersing them in TBS (2 x 5 min). The sections were then treated with biotinylated secondary antibody (Rabbit antimouse IgG biotin, Dako E0354; 5µl/ml in blocking serum) for 30 min, after which slides were washed in TBS (2 x 5 min). The sections were treated with avidin-biotin-horseradish peroxidase solution (ABComplex/HRP kit; Dako K0355; made up with TBS as per manufacturers instructions) for 30 min at room temperature followed by washing twice for 5 min in TBS.

Sections were incubated for 3 min with 3,3'-diaminobenzidine solution (DAB isopac, Sigma D9015), comprising 25µl DAB (2mg/ml) + 5.9 mls 0.2M TBS + 1µl 30% H_2O_2. After staining, the DAB solution was poured into a beaker containing bleach (to neutralise it before disposal) and the slides were rinsed in

water to stop the reaction. The reaction produces a stable, dark brown insoluble precipitate at sites of antibody localisation.

Sections were lightly counterstained by immersion in haematoxylin (Vector, H3401) for 10 seconds, then rinsed in tap water, dehydrated in graded alcohols and cleared in xylene (as described in section 2.7). Coverslips were mounted in DPX mounting medium and the slides were air dried before analysis.

2.9 BrdU immunohistochemistry

Bromodeoxyridine (BrdU) is incorporated into DNA during cell division and used to label the cells that pass through S-phase in the cell division cycle during the period of exposure to BrdU. In experiments reported in chapter 5, BrdU single injections were used for the analysis of cell movement and longer exposures with BrdU minipumps were used to detect retention in slow-cycling cells of adrenal cortex.

Wax-embedded, longitudinal tissue sections were mounted on Polysine slides (VWR laboratory supplies) slides (section 2.3.2), followed by standard procedures for dewaxing in xylene, blocking endogenous peroxidise activity in 3% H_2O_2, rehydrating in 70% (v/v) ethanol and washing in PBS (as described in section 2.8). Slides were then treated with citrate buffer (0.01M citrate; pH 6) and microwaved at full power (800 Watts) for 4 periods of 5 min. for heat-induced antigen retrieval, as described in section 2.8 for Ki67 immunohistochemistry.

The slides were then washed in PBS for 5 min and the sections immunostained to detect the presence of BrdU. Slides were first treated with blocking serum (20% Rabbit serum; see section 2.8) for 30 min then primary anti BrdU antibody (Beckton Dickinson 347580; 5µl/ml in blocking serum) for 2 hours. The subsequent procedure was same as described for Ki67 immunhistochemistry in section 2.8. Slides were treated with biotinylated secondary antibody (Rabbit

antimouse IgG biotin, Dako E0354; 5µl/ml in blocking serum) for 30 min, and then treated with avidin-biotin-horseradish peroxidase (ABComplex/HRP; Dako K0355) for 30 min at room temperature. After each conjugation the excess reagents were washed off with TBS.

The BrdU-positive cells were visualised by staining for 3 min with 3,3'-diaminobenzidine solution (DAB isopac, Sigma D9015), comprising 25µl DAB (2mg/ml) + 5.9 mls 0.2M TBS + 1µl 30% (v/v) H_2O_2, after which slides were rinsed in water to stop the reaction. The reaction produces a stable, dark brown insoluble precipitate at sites of antibody localisation.

Sections were lightly counterstained by immersion in haematoxylin for 10 seconds, then rinsed in tap water, dehydrated in graded alcohols and cleared in xylene (as described in section 2.7). Coverslips were mounted in DPX mounting medium and the slides were air dried before analysis.

2.10 Analysis of BrdU immunohistochemistry

When analysing BrdU-labelled tissue sections, BrdU-positive cells are identified as having nuclear-localised brown DAB staining.

2.10.1 Image analysis of location of BrdU-positive cells in adrenal cortex by measuring distances from capsule and medulla

Longitudinal mid-sections of adrenals from mice treated with single BrdU injections were used to analyse (i) the main location of proliferating cells (soon after the injection) and (ii) the direction and rate of cell movement, by identifying the main location of BrdU-positive cells at intervals after the injection.

One problem in interpreting distance moved is that the cortex varies in thickness and that the cell movement path (distances from positive cell to capsule and to inner cortex boundary) will, therefore, also vary. If the rate of movement is

constant, cells moving towards the medulla will obviously reach it more quickly if the cortex is thinner or the cell movement path is shorter. To try to minimise this problem, the position of each positive cell was measured relative to both the capsule and the inner cortical boundary. In this way the location could be expressed either as an absolute distance from either boundary or as a percentage of the distance from the capsule to the inner cortical boundary.

Another problem is that the route taken by each cell cannot be known from an observation at a single time point. For simplicity it is assumed that a cell will travel the shortest distance but for a cell that has already moved some of the way, the exact locations of the start and end of the movement path are unknown. To avoid making too many assumptions about the movement path, two different methods of measuring the distances from the capsule and medulla to the BrdU-positive cells were compared. These are shown in Fig. 2.3 as (a) dark blue route (dark blue double arrow): the shortest distances between the BrdU-positive cell and the capsule plus the shortest distances between the BrdU positive-cell and the boundary of the cortex and medulla and (b) pale blue route (pale blue dotted double arrow in Fig. 2.3): the shortest straight line distance between the capsule and the inner boundary of the cortex that includes the position of the BrdU-positive cell.

Calibrated digital images were captured with a Nikon Coolpix 995 digital camera mounted on a Zeiss Axioplan 2 compoind microscope and ImageJ software was used to measure the distances illustrated in Fig. 2.3.

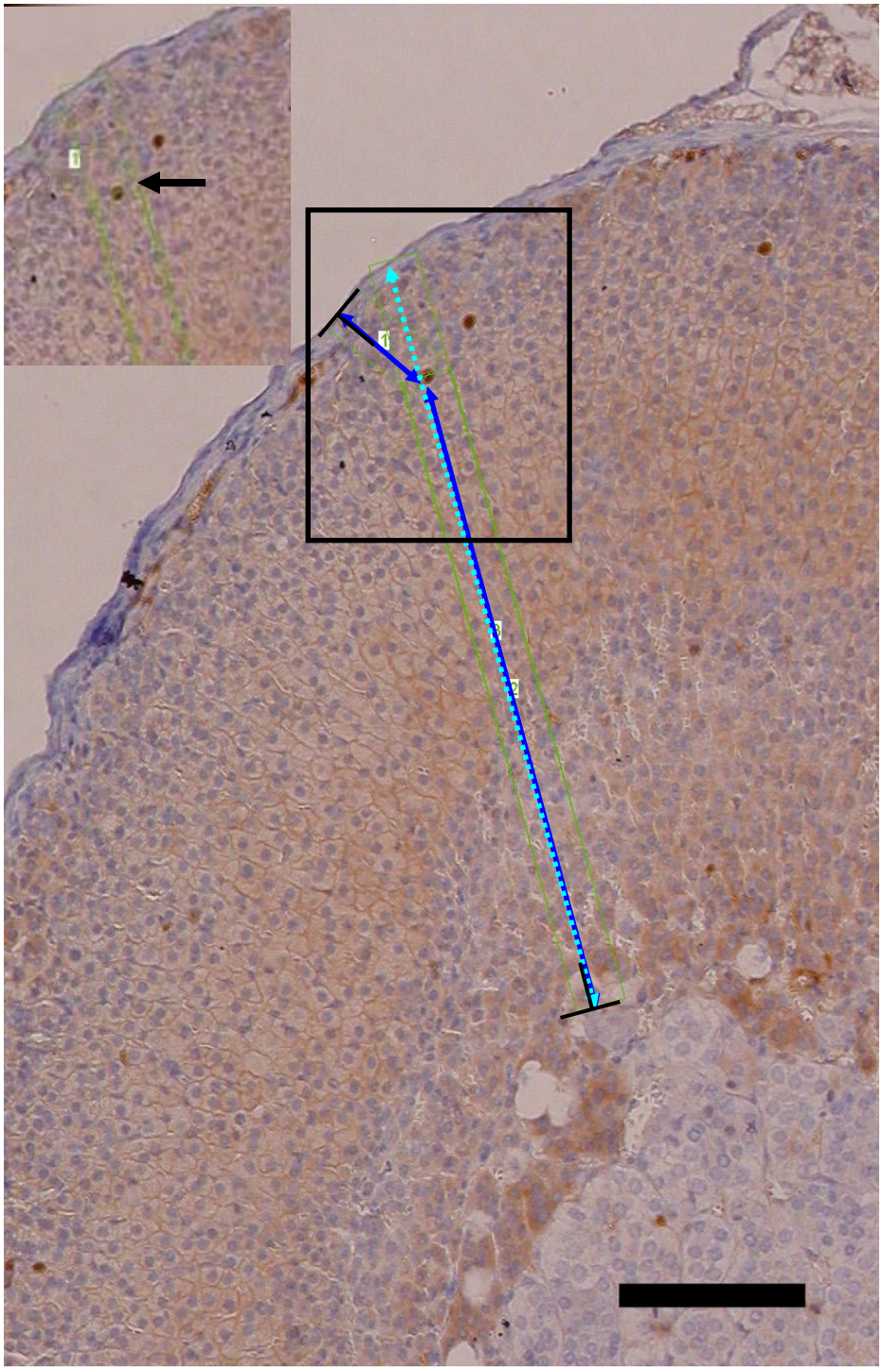

Fig. 2.3. Two different measurements of the location of a BrdU-positive cell in the adrenal cortex. (a) dark blue route (dark blue double arrow): the shortest distances between the BrdU-positive cell (black arrow in inset of boxed area) plus the shortest distances between the BrdU-positive cell and the boundary of the cortex and medulla and (b) pale blue route (pale blue dotted double arrow): the shortest straight line distance from the capsule to the inner boundary of cortex that intersects the BrdU-positive cell. ⊥: right angle. Scale bar = 0.1mm**.**

2.10.2 Image analysis of location of BrdU-positive cells in adrenal cortex using a grid

Middle longtitudinal sections of adrenals from mice exposed to BrdU for two weeks from an osmotic mini-pump were used to identify the BrdU label-retaining cells in order to count them and analyse their location. In most cases there were too many BrdU-positive cells to measure their location individually by the method described in section 2.10.1, so a 10 × 10 grid was superimposed on the calibrated image to define different locations in the adrenal cortex.

As noted previously, the adrenal cortex varies in thickness (between the medulla and capsule). If the 10 × 10 grid is made to span the distance between the capsule and medulla its size will vary according to the thickness of the cortex and sampling bins in a specific row will also vary in size and distance from the capsule and medulla. Alternatively, if the grid is kept at a constant size with its outer edge at the capsule, the inner edge may be in the cortex, at the boundary or in the medulla, so cells near the medulla will appear in different sampling rows depending on the cortical thickness. Some of the variation in cortical thickness may be caused by technical artefacts such as oblique sections and this may affect the analysis of the distribution of labelled cells in the cortex. For example, the proportion of label-retaining cells could be over-estimated in an oblique section if they were located in a narrow band. To minimise this problem the analysis was restricted to regions of adrenal cortex which were 330-400μm thick and where the capsule was approximately parallel to the cortical-medullary boundary (Fig. 2.4).

ImageJ software was used to count the number of BrdU-positive cells separately in 10 rows of the 10 × 10 grid. Firstly, a suitable cortex area (with a thickness of 330-400 μm between the inner and outer boundary was selected and the image was cropped with ImageJ (Fig. 2.4). ImageJ was then used to divide the selected area into 10 rows and 10 columns of a 10 × 10 grid so that row 1 bordered the capsule and row 10 bordered the medulla. The computer mouse was used to ‘click’ on the BrdU-positive cells which highlighted them with different colours

according to their row in the 10 × 10 grid (Fig. 2.5). The numbers of BrdU-positive cells in each row were automatically entered into a spreadsheet. The process was then repeated for the remaining (BrdU-negative) cells in each row to give final counts of BrdU-positive, BrdU-negative and total cell numbers in each of the 10 rows.

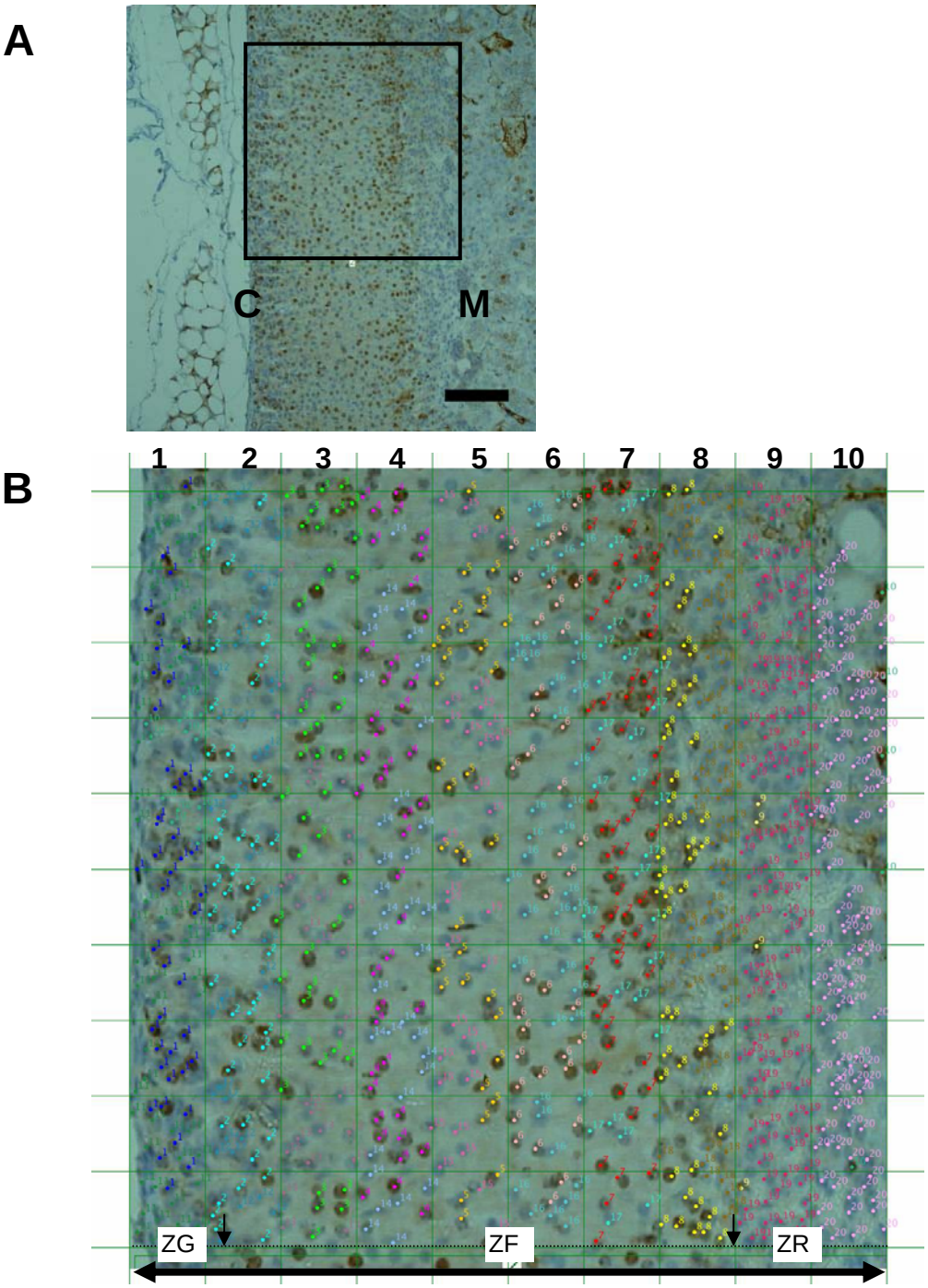

Fig. 2.4. (A) A square of adrenal cortex (330-400 µm deep between the medulla and capsule) was measured with ImageJ software and selected (black outline). Scale bar = 0.1mm; C: capsule; M: medulla. **(B)** The square area shown in **(A)** was cropped and a 10 × 10 grid was superimposed. Double-headed arrow shows depth of cortex. BrdU-positive and BrdU-negative cells were counted in each of 10 rows on-screen and highlighted with different colours for each row. Approximate positions of ZG, ZF and ZR boundaries are shown by arrows.

2.11 Image acquisition

Histological sections were photographed on a Zeiss Axioplan 2 compound microscope (usually using ×10, ×20 or ×40 objective lenses) and images were captured with a Nikon Coolpix 995 digital camera (3.34 megapixels). A calibrated stage micrometer was photographed at the same magnification, at the same time to work out final magnifications so that scale bars could be drawn for each figure (see individual figures). Most images were captured as jpeg files at full image size and 'normal' quality. This gives a final image size of 26×20 cm at 200dpi (dots per inch). For example, with a ×5 objective the image resolution was approximately 2 μm/pixel. Images were uploaded into Adobe Photoshop© software, cropped, scale bars inserted and compiled into montages. Images (and scale bars) were reduced in size for final printing.

2.12 Statistical analysis

Most statistical tests, including chi-square test**,** paired t-test, unpaired t-test, and analysis of variance (ANOVA), were performed using StatView software (SAS Institute Inc., Cary, NC, USA). When a 1-way ANOVA test indicated that there were significant differences among multiple groups (e.g. multiple ages), Scheffe's post hoc test was used for pairwise comparisons to identify which pairs of groups differed from one another. Adrenal growth curves (chapter 4) were analysed by a professional statistician, Dr Robert Elton (Rob Elton Medical Statistics Consulting), using SPSS software (SPSS Inc, Chicago, Illinois, USA) and statistical modelling (see appendix 1).

3. Changes in mosaic β-gal staining patterns in *21OH/LacZ* transgenic adrenal cortices between fetal and adult stages

3.1 Introduction

Mouse genetic mosaics and chimeras with suitable cell markers are useful for studies of developmental lineages (Iannaccone, 1987). Female mice heterozygous for a ubiquitously-expressed, X-linked *LacZ* transgene (Tan et al., 1993) are X-inactivation mosaics. Mosaic transgene expression is produced by random X chromosome inactivation, which results in inactivation of the X chromosome carrying the transgene in approximately 50% of the cells early in development. Mouse chimeras produced by aggregation of genetically distinct embryos, one of which carries a cell marker (such as a ubiquitously-expressed reporter transgene), produce similar mosaic expression patterns. Both X-inactivation mosaics and chimeras are recognised models for studying cell lineages. The mosaic patterns produced by these mice can be used to study tissue organisation during development and tissue maintenance in the adult (Collinson et al., 2004).

Some transgenic mice show mosaic transgene expression and may also be useful for studies of cell lineage (Dobie et al., 1997). For example, as discussed in section 1.6, *21OH/LacZ* transgenic mice, in which a 6.4kb fragment of the mouse steroid 21-hydroxylase A gene promoter directs *LacZ* transgene expression, show mosaic expression of the β-galactosidase reporter (β-gal) in the adrenal cortex (Morley et al., 1996). In a previous study, the stripe patterns of adrenal cortices of adult X-inactivation mosaics, chimeras and *21OH/LacZ* transgenics were shown to be quantitatively similar (Morley et al., 2004), implying that *21OH/LacZ* transgenic mice can be used as a model for studies of cell linage in the adrenal cortex. Mouse chimeras are difficult to produce and in the adrenal cortex mosaic patterns were clearer in *21OH/LacZ* transgenic mice than the X-inactivation mosaics because β-gal reporter expression was stronger (Morley et al., 2004). The

expression of the *21OH/LacZ* transgene in adrenal cortex is first detectable at embryonic day 11.5 (E11.5) and persists in the adult adrenal (Morley et al., 1996).

Radial striped patterns have been reported in the adrenal cortex of chimeric rats and mice (Iannaccone and Weinberg, 1987), mouse X-inactivation mosaics (Morley et al., 2004) and *21OH/LacZ* mice (Morley et al., 1996) but only *21OH/LacZ* mouse transgenics have been used to investigate mosaicism in the fetal adrenal cortex. The mosaic pattern in fetal *21OH/LacZ* transgenic adrenal cortices was different from the adult radial stripes and appeared as randomly orientated (non-radial) spots at embryonic day 15.5 (E15.5). It is not clear whether the transition from embryonic randomly orientated spots to adult radial stripes reflects patterns of adrenal organogenesis and growth or whether the radial stripes are only formed once stem cells are activated to maintain the adrenal cortex at a later stage.

Developmental changes in mosaic patterns have been demonstrated in other tissues (see Chapter 1). The retinal pigment epithelia of adult pigmented↔albino chimeric mice had different mosaic patterns in different regions (Bodenstein and Sidman, 1987b). Small irregularly distributed patches occurred in the proximal retinal pigmented epithelium (near the optic nerve head) while radial pigmented stripes appeared in the distal retinal pigmented epithelium (towards the iris). This was accounted for by a switch from interstitial growth to edge-biased growth during the later stages of development using a combination of computer modelling and cell labelling studies (see Chapter 1). During postnatal development of the corneal epithelia of X-inactivation mosaic and chimeric mice there is a transition from an initially randomly orientated mosaic pattern to radial stripes which then persists in the adult stage (Collinson et al., 2002). In this case the likely explanation is that the initial pattern is produced during fetal development but is replaced once stem cells are activated and maintain the tissue.

In the *21OH/LacZ* transgenic mouse, transgene expression in the adrenal primordium begins at E11.5 and a randomly orientated variegated pattern has

been demonstrated in the adrenal at E15.5 but this is replaced by a radial stripe pattern in the adult (Morley et al., 1996). The timing of this change in mosaic pattern and the possible mechanisms involved remain unknown.

3.1.1 Experimental aims

The main aim of the investigations described in this chapter was to characterise when and how the mosaic pattern of β-gal reporter expression changes from randomly orientated spots at E15.5 to adult radial stripes by comparing patterns of mosaicism at different ages. Characterisation of the emergence of stripes may provide clues about possible mechanisms involved (e.g. whether stripes emerge during development or only during maintenance of the adult adrenal).

3.2 Materials and methods

21OH/LacZ transgenic mouse embryos and pups at specific developmental stages were obtained from timed mating crosses of homozygous *21OH/LacZ* transgenic males and (C57BL/6 × CBA/Ca)F1 wild-type female mice. Dissected adrenal glands were frozen-sectioned (10 μm) and stained histochemically for β-gal activity as described in *Materials and Methods* (section 2.4) and counterstained with neutral red. In each case 5 serial longitudinal sections from the middle of the gland were photographed and analysed. The adrenals were grouped by gender (female and male) from E17.5 to postnatal day 21 (P21) and anatomical location (right and left) for all experiment ages (E14.5, E15.5, E16.5, E17.5, E18.5, P0, P1, P2, P3, P5, P7, P10, P14 and P21). From E17.5 to P21 at least 3 adrenals were analysed in each group of a specific age, sex and location and, from E14.5 to E16.5, 6 to 8 adrenals were examined in every group of a specific age and location.

3.3 Results

Mosaic β-gal staining patterns observed at each stage were classified on the basis of their orientation (radial or non-radial) and the shape ('spot', 'patch' or 'stripe'). A 'spot' is defined as a single dot of staining which could represent either a single cell or a cluster of cells. (Possible diffusion of β-gal reaction product during the staining and fixation processes makes it difficult to distinguish between these alternatives). A 'radial array of spots' is defined as a grouping of discrete spots elongated along the radial axis of the adrenal cortex. A 'non-radial patch' is defined as an area of staining larger than a single cell that is not elongated along the radial axis of the adrenal cortex (it is either symmetrical or elongated in a non-radial direction). A 'radial patch' is defined as an area of staining larger than a single cell that is elongated along the radial axis of the adrenal cortex. A 'stripe' is defined as an uninterrupted radially-oriented elongated area of staining crossing much of cortex.

3.3.1 The mosaic β-gal staining pattern in the *21OH/LacZ* transgenic adrenals between E14.5 and P21

Fig. 3.1 shows typical mosaic staining patterns of fetal adrenal glands from E14.5 to E18.5. At E14.5 the mosaic β-gal staining pattern of the *21OH/LacZ* transgenic adrenals appeared predominantly as randomly orientated spots of blue staining. From E15.5 to E18.5 the spots tended to be more clustered and in some cases the clusters appeared to be aligned radially but these tiny orientated clusters were not seen clearly until later prenatal stages (from E17.5). The overall proportion of β-gal staining appeared lower in E14.5 specimens than at later stages.

Mosaic staining patterns of early postnatal stages (P0-P5) are shown in Fig. 3.2. After birth, elongated patches and radial arrays become progressively clearer with age. By P2 the β-gal staining pattern shows a mixture of spots and patches and by

P5 radial patches are predominant but it is doubtful whether any fully formed stripes are present as early as P5.

Individual fully formed stripes are first recognised at P7 and radial patches and stripes constitute the main mosaic pattern at P7 and P10 (Fig. 3.3) and at later stages. From P14 radial stripes form the predominant pattern (Fig. 3.4) and by P21 the β-gal staining pattern appears identical to the adult mosaic stripe pattern with fully formed stripes predominant.

From E14.5 to E18.5, blue β-gal stained cells are seen in the inner region (putative medulla) as well as the outer region (putative cortex) (Fig. 3.1). The 21OH promoter driving the *21OH/LacZ* transgene is expected to be active in the adrenal cortex but not the medulla so the presence of β-gal staining in the inner part of the adrenal implies that cells of adrenal medulla and cortex are not completely separated at these stages. After birth the blue staining of cells in the central adrenal (medulla region) still occurs but gradually disappears with age (Figs. 3.2-3.4) and very few β-gal stained cells remain in the central region after P14 (Fig. 3.4).

A diffuse pale blue region of β-gal staining was first noted at the inner boundary of the adrenal cortex and medulla in *21OH/LacZ* transgenic females at P7 (Fig. 3.3K) and P10 in males (Fig. 3.3l) and became more clearly delineated at P14 (Fig. 3.4M/m) and afterwards. This pale blue β-gal staining occurs in the region where the X zone develops and persists in the inner adrenal cortex of adult females but not in males (Fig 3.5; see Chapter 6) and is therefore hypothesised to mark the X zone.

Overall, the predominant pattern of the β-gal staining in the *21OH/LacZ* transgenic adrenals changes over the period between E14.5 and P21. The *21OH/LacZ* transgenic adrenal shows a random pattern of spots at E14.5, which changes first to clusters of spots and patches before birth, then radial arrays around birth (P0 ~ P5), combinations of radial patches and stripes (P7 and P10), predominantly stripes (P14) and finally entirely complete stripes (P21) like the adult. At most stages more than one kind of mosaic pattern was present but one main pattern predominated at each stage (as summarised in Tables 3.1 and 3.2).

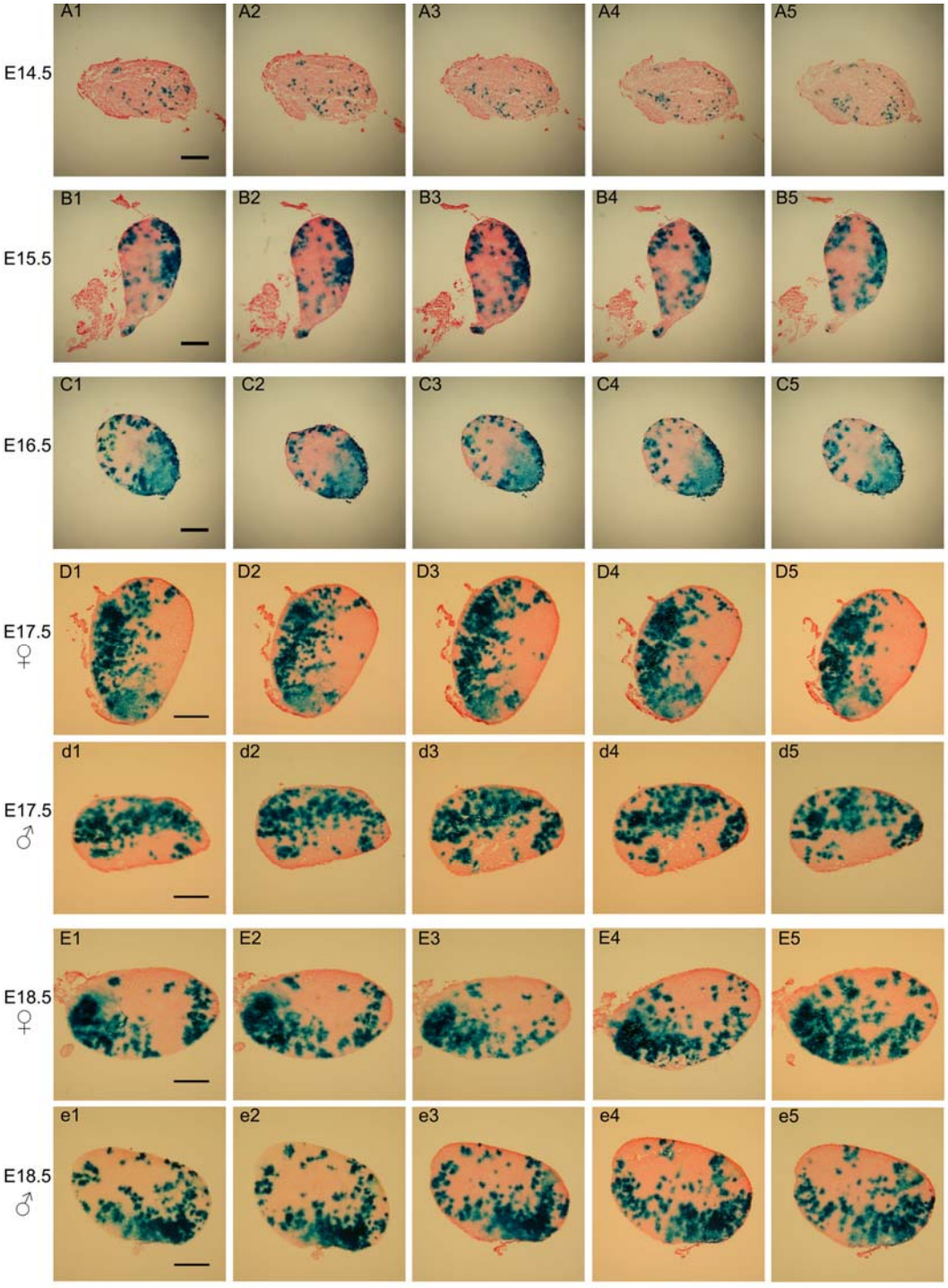

Fig. 3.1. β-gal reporter activity displays a predominantly non-radial mosaic staining pattern between E14.5 and E18.5.

Mosaic β-gal staining patterns in middle section of *21OH/LacZ* transgenic adrenal glands at E14.5 (A), E15.5 (B), E16.5 (C), E17.5 (D/d) and E18.5 (E/e). A, B and C: gender not identified; D and E = females (♀); d and e = males (♂). Scale bars = 200μm.

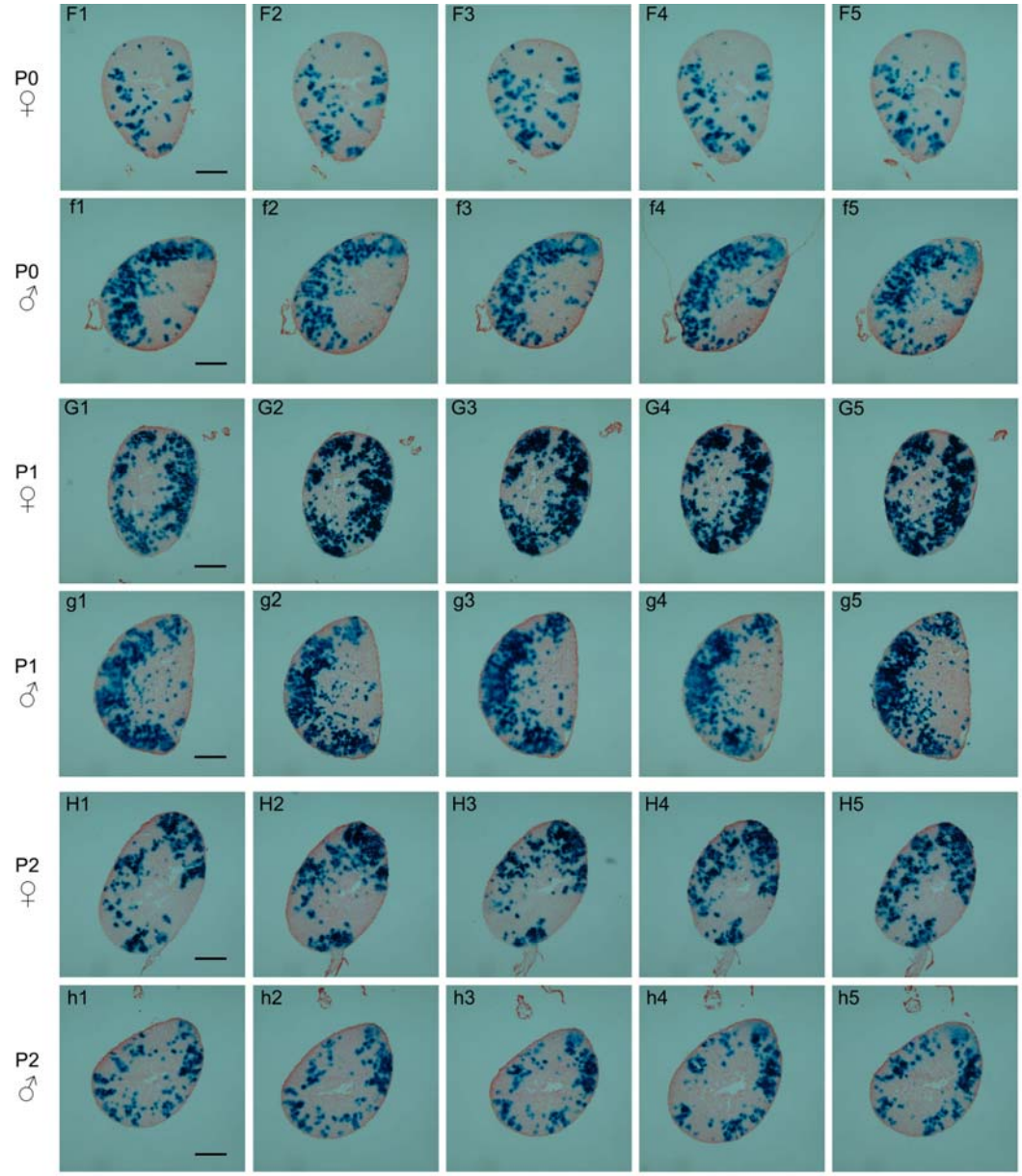

Fig. 3.2. See opposite page for continuation of figure and the legend.

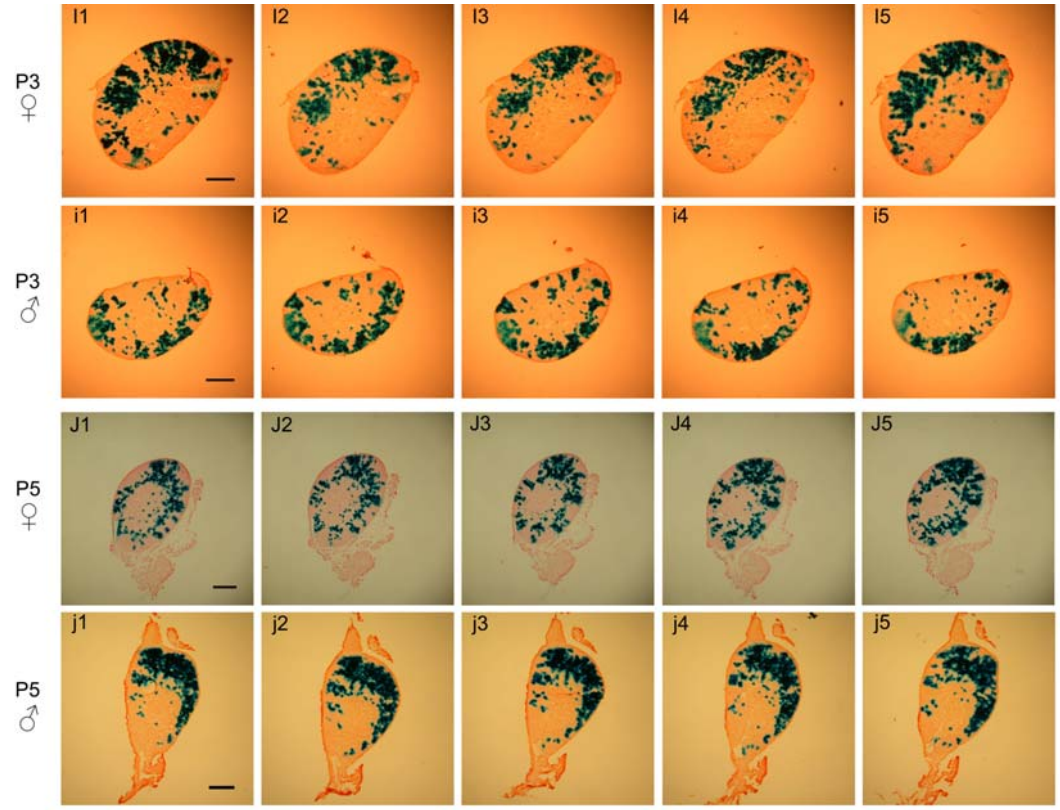

Fig. 3.2 (continued). Mosaic radial patch patterns of β-gal staining are apparent at P0 and predominate at P5.

Mosaic β-gal staining patterns in middle section of *21OH/LacZ* transgenic adrenal glands at P0 (F/f), P1 (G/g), P2 (H/h), P3 (I/i) and P5 (J/j). F-J = females (♀); f-j = males (♂). Scale bars = 200μm.

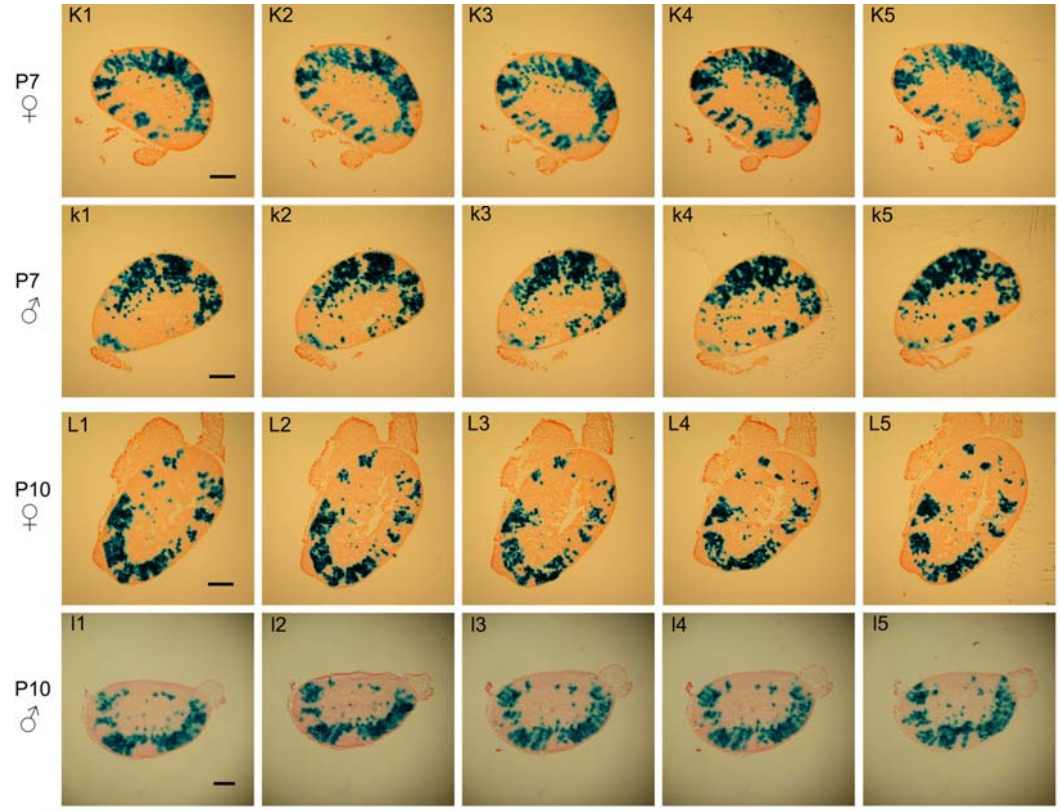

Fig. 3.3. Continuous radial stripes of β-gal staining first become apparent within the mosaic staining pattern at P7 and P10.

Mosaic β-gal staining patterns in middle section of *21OH/LacZ* transgenic adrenal glands at P7 (K/k) and P10 (L/l). K-L = females (♀); k-l = males (♂). Scale bars = 200μm.

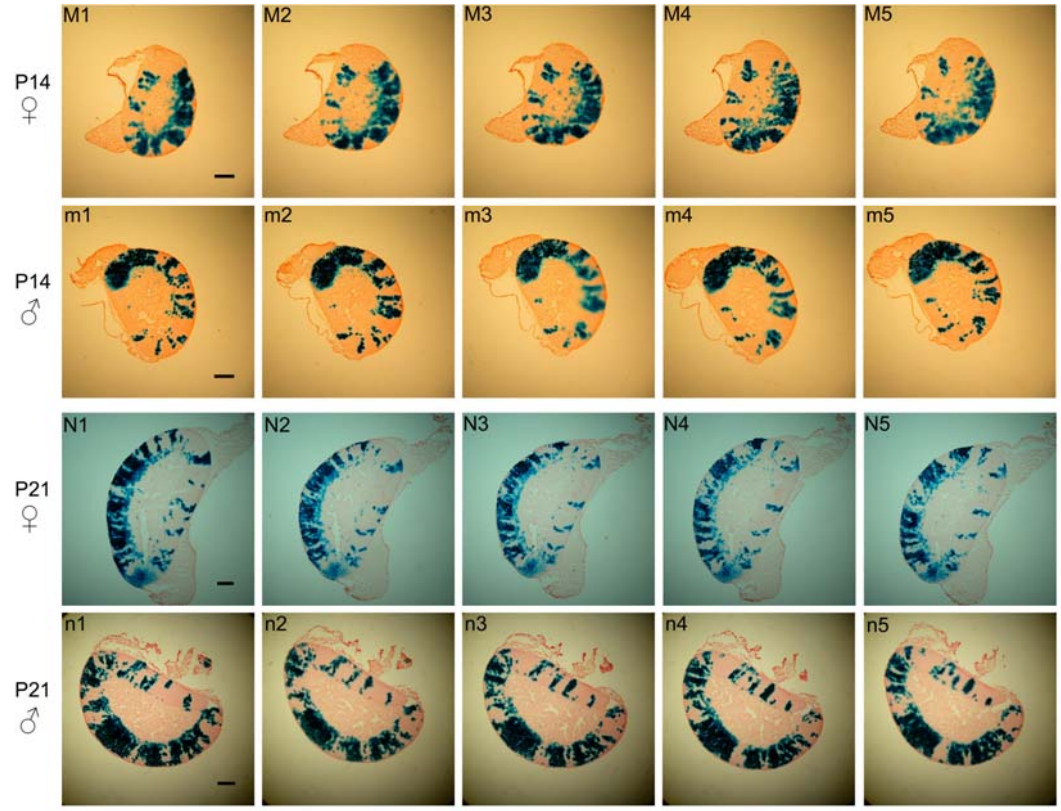

Fig. 3.4. Mosaic continuous radial stripes of β-gal staining predominate at P14 and are essentially equivalent to the adult mosaic stripe pattern at P21. Mosaic β-gal staining patterns in middle section of *21OH/LacZ* transgenic adrenal glands at P14 (M/m) and P21 (N/n). M and N = females (♀); m and n = males (♂). Scale bars = 200μm.

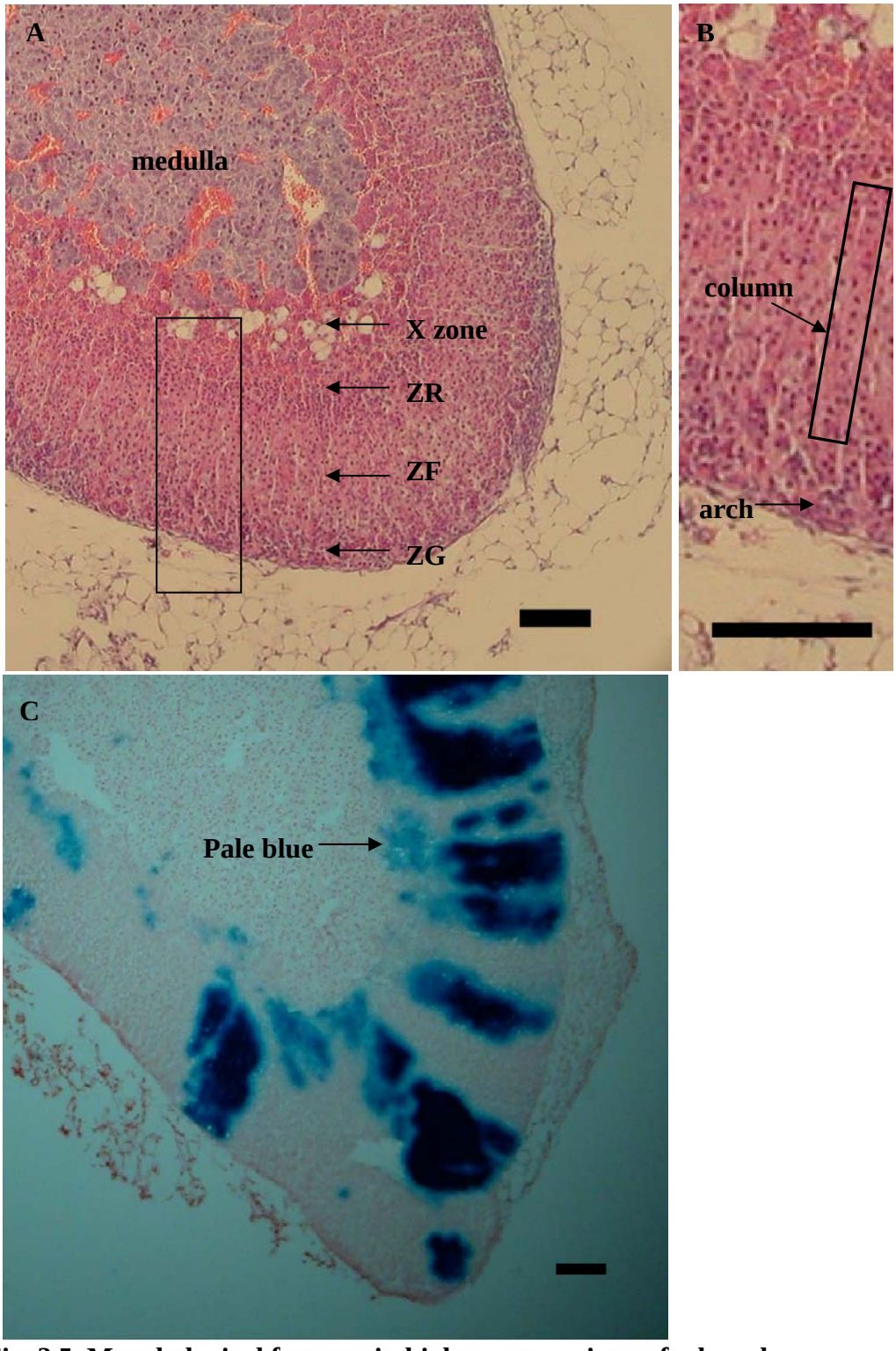

Fig. 3.5. Morphological features in higher power views of adrenal cortex
A. Haematoxylin and eosin stained section showing different cortical zones**. B.** High power view of boxed area in A showing arch-like ZG and columnar ZF structures. **C**. Mosaic β-gal staining showing pale blue presumptive X zone. Scale bars = 100μm.

3.3.2 The effects of gender and anatomical location on the mosaic pattern of the *21OH/LacZ* transgenic adrenals

This study showed that the prevailing mosaic pattern changes with age from a random pattern of spots at E14.5 to the radial stripes as shown at P21 and in the adult adrenal cortex. Tables 3.1 and 3.2 shows that the predominant mosaic pattern changes gradually with age regardless of gender (male and female) or adrenal anatomical location (left and right). Although a few small differences in mosaic patterns occurred among adrenals no consistent effects of gender or location were observed.

However, two features did vary with sex. Pale blue β-gal staining near the boundary of the medulla and cortex, that was attributed to the X zone, seemed to appear earlier in female adrenals (at P7) and was more obvious in females than males at P21 (Fig. 3.4N/n). This is consistent with the known patterns of X zone development in male and female mice (Howard-Miller, 1927; Keegan and Hammer, 2002). The presence of blue β-gal stained cells in the inner part of adrenal gland (developing medulla) showed no obvious difference between male and females or left and right adrenals by P10 but were eliminated more quickly in males than females. The blue β-gal stained cells were still abundant in the medulla region of females at P14 (Fig. 3.4M) but dramatically reduced in male adrenals (serial sections m1-m5 in Fig. 3.4) and eliminated by P21 (Fig. 3.4n).

Table 3.1 Tabulated distribution of mosaic β-gal staining patterns in *21OH/LacZ* transgenic female embryonic and postnatal adrenal glands from E17.5 to P21.

Perinatal female	Classification of mosaic patterns in adrenal cortex					ß-gal staining in medulla	ß-gal stained X-zone
Age	Stripe	Radial patch	Non-radial patch	Radial array of spots	Spot		
E17.5(L)		+	+	+	++	++	
E17.5(R)		+	+	+	+	++	
E18.5(L)		+	±	+	++	++	
E18.5(R)		++	±	+	+	++	
P0(L)		+	±	++	+	++	–
P0(R)		++	±	++	+	++	–
P1(L)	±	++	±	+	+	++	–
P1(R)	±	++	+	++	+	++	–
P2(L)	+	+++		+	+	++	–
P2(R)	±	++		++	+	+	–
P3(L)	+	+++		+	+	++	–
P3(R)	+	+++		+	+	+	–
P5(L)	+	+++		+	+	+	–
P5(R)	+	+++		+	+	+	–
P7(L)	+++	+		+	±	+	±
P7(R)	++	++		+	±	+	±
P10(L)	++	++		+	±	+	±
P10(R)	++	++		+		+	Y
P14(L)	+++	+				+	Y
P14(R)	+++	+		+		+	Y
P21(L)	++++	±				±	Y
P21(R)	++++	±				±	Y

Summary of the mosaic β-gal staining patterns in *21OH/LacZ* transgenic female embryonic and postnatal adrenal glands from E17.5 to P21.

Classifications of the mosaic β-gal staining patterns seen in adrenal cortices from left and right *21OH/LacZ* transgenic adrenal glands (illustrated in Figs. 3.1-3.4) are shown for the different embryonic and postnatal developmental stages. The subjective frequencies of scores for each mosaic pattern are indicated by symbols ('+', '-', etc.) for each stage. Where a pattern changes in frequency between stages, this is highlighted by different shading. The presence of β-gal staining in adrenal medullae (possibly indicating isolated islands of cortical tissue) and the X zone at the cortical medulla boundary are also noted for different developmental stages. Mosaic patterns in the adrenal cortex were qualitatively similar in males and females of the same age (compare Tables 3.1 and 3.2).
Abbreviations: L, left adrenal; R, right adrenal; Y, yes (feature present)

Table 3.2 Tabulated distribution of mosaic β-gal staining patterns in *21OH/LacZ* transgenic male embryonic and postnatal adrenal glands from E17.5 to P21.

Perinatal male	Classification of mosaic patterns in adrenal cortex					ß-gal staining in medulla	ß-gal stained X-zone
Age	Stripe	Radial patch	Non-radial patch	Radial array of spots	Spot		
E17.5(L)		+	+	+	++	++	
E17.5(R)		+	+	++	++	++	
E18.5(L)		+	±	+	++	+	
E18.5(R)		+	+	+	+	++	
P0(L)		+++	+	++	+	++	–
P0(R)		+++	±	++	+	++	–
P1(L)	±	++	+	++	+	++	–
P1(R)	±	+++	±	++	+	++	–
P2(L)	+	++	+	++	+	++	–
P2(R)	±	++	±	++	+	+	–
P3(L)	+	+++		+	±	+	–
P3(R)	+	+++	±	+	±	+	–
P5(L)	+	+++		+	±	+	–
P5(R)	+	+++		+	±	+	–
P7(L)	++	++		+	+	+	–
P7(R)	++	++		+	+	+	–
P10(L)	++	++		±		±	±
P10(R)	+++	++		±	+	+	±
P14(L)	+++	+				±	±
P14(R)	+++	+		±		–	±
P21(L)	++++	±				–	Y
P21(R)	++++	±				–	Y

Summary of the mosaic β-gal staining patterns in *21OH/LacZ* transgenic male embryonic and postnatal adrenal glands from E17.5 to P21.

Classifications of the mosaic β-gal staining patterns seen in adrenal cortices from left and right *21OH/LacZ* transgenic adrenal glands (illustrated in Figs. 3.1-3.4) are shown for the different embryonic and postnatal developmental stages. The subjective frequencies of scores for each mosaic pattern are indicated by symbols ('+', '-', etc.) for each stage. Where a pattern changes in frequency between stages, this is highlighted by different shading. The presence of β-gal staining in adrenal medullae (possibly indicating isolated islands of cortical tissue) and the X zone at the cortical medulla boundary are also noted for different developmental stages. Mosaic patterns in the adrenal cortex were qualitatively similar in males and females of the same age (compare Tables 3.1 and 3.2).
Abbreviations: L, left adrenal; R, right adrenal; Y, yes (feature present)

3.4 Discussion

3.4.1 Developmental changes in β-gal staining patterns in the central part of the adrenal gland (future medulla and X zone)

Investigations of β-gal staining patterns in the adrenal cortices of *21OH/LacZ* mice during development from E14.5 fetuses to P21 mice revealed changes in the pale blue area adjacent to the medulla, changes in the frequency of β-gal stained cells in the central adrenal as well as changes in the nature of the mosaic pattern throughout the adrenal cortex.

Although the mouse X zone may represent a postnatal derivative of the fetal zone (Zubair et al., 2006), the area of diffuse pale blue β-gal staining did not appear in the inner cortex of *21OH/LacZ* mice until P7 in females and P14 in males. This is consistent with the histological appearance of the X zone in the mouse adrenal at 10-14 days (Howard-Miller, 1927; Keegan and Hammer, 2002), which is after the cortex and medulla separate. This conclusion is supported by the persistence of the pale blue β-gal staining and appearance of X zone vacuoles in adult females but not in adult males (see chapter 6). A different intensity of β-gal staining in the X zone has previously been reported for female adult *SCC-LacZ* transgenic adrenals (Hu et al., 1999) as delineating the X zone. The different intensity of β-gal staining between the X zone, derived from the fetal zone, and definitive zone may relate to their different origins (Zubair et al., 2006), possibly indicating differing levels of steroid 21-hydroxylase gene expression in each of these tissues. This is supported by the transition from relatively weak β-gal staining at E14.5 to a more intense staining at later embryonic and postnatal stages (Figs. 3.1-3.4). A similar trend was reported by Morley et al., (1996). The occurrence of intense blue cells may reflect the emergence of the definitive zone while the paler blue cells represent embryonic fetal zone. The above evidence supports the idea that the pale blue β-gal staining delineates the X zone in juvenile *21OH/LacZ* transgenic mice and demonstrates the emergence of a distinct X zone at 1-2 weeks.

The appearance of blue β-gal stained cells in the inner part of the adrenal gland (before the boundary is established between the medulla and cortex) can be explained by mixing of medulla and cortex cells when the neural crest-derived medulla cells migrate into the mesoderm-derived adrenal primordium at E12.5 (Nyska and Maronpot, 1999). The gradual elimination of the blue cortical cells from the inner region of adrenal gland (future medulla) may reflect their movement into the cortex or their death by apoptosis when the boundary of cortex and medulla is set up. The alternative possibility of transdifferentiation of cortical cells into medulla cells seems less likely due to their distinct embryonic origins but this needs further investigation. It is not clear why blue cells are eliminated from the centre region at an earlier stage in males than females.

3.4.2 Developmental changes in adrenal cortex mosaic patterns (transition from randomly orientated spots to radial stripes)

The β-gal staining pattern in the *21OH/LacZ* transgenic adrenals changes gradually over the period from E14.5 to P21, which is a period of adrenal growth (see chapter 4). The random spots at E14.5 changed to clusters of patches and spots (before birth), radial arrays (P0-P5), combinations of radial patches and stripes (P7 and P10), predominantly stripes (P14) and finally entirely stripes (P21) as seen in the adult (Morley et al., 1996). This sequence was unaffected by gender or anatomical location (left versus right) and is shown diagrammatically as 5 stages in Fig. 3.6A. Possible explanations of how patterns might change between stages are discussed below.

(a) Changes from E14.5 to E18.5 (i-ii in Fig. 3.6A)

The change from (i) randomly orientated spots at E14.5 to (ii) clusters of patches and spots at E18.5 may partly reflect an increase in the proportion of β-gal-stained cells. This could be caused by an increase in the number of cells that express the *21OH/LacZ* transgene (new activation of transgene) and/or an increase in transgene expression level so that more cells that express the transgene produce β-gal at a detectable level.

Morley et al., (1996) reported that the transgene in *21OH/LacZ* transgenic adrenals (from line 7911) is first expressed at E11.5 and that the β-gal staining becomes more intense at E15.5 and E17.5 (Morley et al., 1996), which is consistent with the increase in steroidogenic enzyme expression occurring before birth. This is reflected by the increasing levels of endogenous *21OH* mRNA detected by in situ hybridisation in the developing adrenal gland at E11.5, E14.5 and E17.5 (Morley et al., 1996). The above evidence is consistent with the results from E14.5 to E18.5 shown in section 3.3.1, which suggest that expression of *21OH/LacZ* increases between E14.5 and E15.5. It would be of interest to further investigate quantitatively how the levels of *21OH/LacZ* transgene expression change during development – e.g. by using QRT-PCR (quantitative real time polymerase chain reaction).

The E14.5-E16.5 fetal adrenals were analysed last so it is also possible that the lower proportion of β-gal stained cells at E14.5 is attributable to drift in genetic background, which affected the probability of *21OH/LacZ* transgene silencing. Further studies are needed to investigate this possibility.

(b) Changes from E18.5 to P5 (ii-iii in Fig. 3.6A)

The change of mosaic pattern from (ii) clusters of patches and spots at E18.5 to (iii) radial arrays of spots and patches at P5 could be explained by onset of radial cell proliferation, radial cell elongation or by radial information influencing transgene expression. (Radial information might include changes in histology and the integration of radial blood vessels and nerves when the cortex organises as a

functional unit and forms the cortical zones but it is not clear how this could affect transgene expression.) It seems much more likely that the formation of radial mosaic patterns involves radial cell elongation or radial cell proliferation (either with or without apoptosis). The radial mosaic patterns might be established by radially orientated cell division so that β-gal-positive cells at any position (e.g. blue cells **a**, **b** and **c** in Fig. 3.6A(ii) could proliferate radially to generate a blue radial elongation shown as **A**, **B** and **C** in Fig. 3.6A(iii)). The emergence of radial arrays at the outer edge could also be explained if proliferation was largely confined to the outer growing edge (edge-biased growth), as discussed in *(c)* below.

(c) Changes from P5 to P7 (iii-iv in Fig. 3.6A)

The change from (iii) radial arrays of spots and patches at P5 to (iv) radial elongation to form a mixture of radial patches and emerging stripes at P7 may result from (1) radial cell elongation, (2) radially orientated proliferation causing radial elongation of the patches and spots that exist before P7 or (3) edge biased growth of the adrenal cortex (Fig. 3.7).

Edge-biased growth causes stripes to be generated while cells in the outer cortex proliferate. (The role of edge-biased growth in generating striped mosaic patterns is discussed in chapter 1.)

In Fig. 3.6A(iv) stripe formation is illustrated as occurring both by radial proliferation at different specific locations in the cortex and by edge-biased growth. Radial proliferation (e.g. by radially orientated mitotic divisions) is shown as stars 1a, 1b and 1c at inner, outer and intermediate cortical positions in Fig. 3.6Aiv and double-headed arrows 1a, 1b and 1c in Fig. 3.6B. Edge biased growth is shown as star 2 in Fig. 3.6Aiv and the outward-pointing arrow 2a in Fig. 3.6B. The blue cell, labelled by star 2 in Fig. 3.6Aiv (at P7), is located where the outer edge of the cortex would have been at P5 (grey oval line). Its division generated the stripe when the adrenal grows from P5 to P7 and proliferation would then be confined to the outermost cells (at the blue oval line).

(d) Changes from P7 to P21 (iv-vi in Fig. 3.6A)

As the adrenal continues to grow, the dominant pattern changes from a mixture of radial patches and emerging stripes at P7 (Fig. 3.6A iv) to fully formed stripes at P21 (Fig. 3.6Av), which reflects continuing radial elongation to form the striking adult striped pattern. The clusters of spots seen at P7 (e.g. Fig. 3.3 k4) are eliminated by the time the mature striped pattern arises at P21.

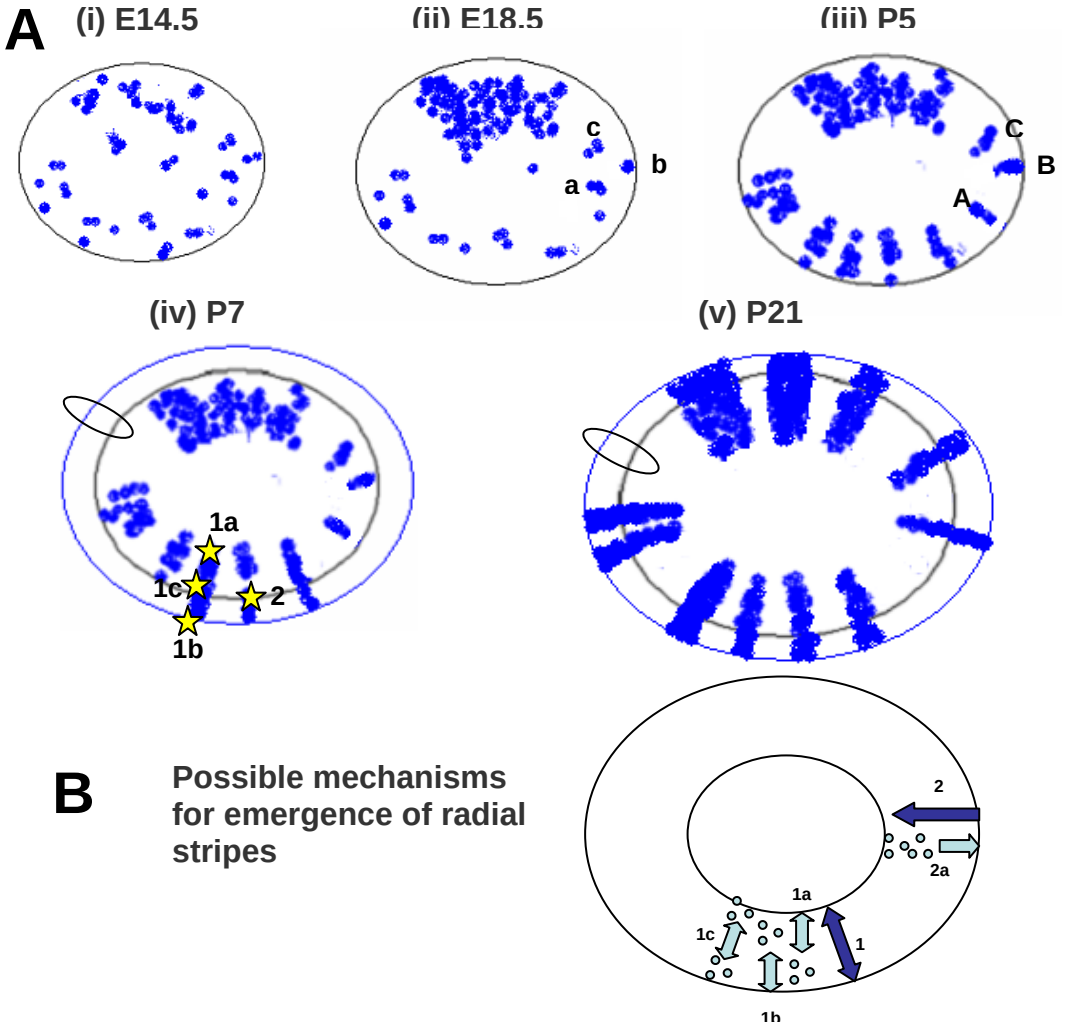

Fig. 3.6. Diagrammatic representations of mosaic β-gal patterns at five representative developmental stages (i-v)

A (i-v). The predominant mosaic β-gal staining patterns for each of five representative developmental stages are shown diagrammatically (i-v). These show (i) random orientated spots at E14.5, (ii) clusters of patches and spots at E18.5, (iii) radial arrays of spots and patches at P3, (iv) emerging radial stripes at P7 and (v) radial stripes at P21. Possible explanations for the changes in mosaic patterns between stages shown are discussed in the text. The inner oval shapes in (iv) and (v) represent the adrenal gland in the previous diagram and the difference between inner and outer adrenal outlines (also encircled) represents the increase in adrenal size (see text for explanation). Possible fates of blue (β-gal-stained) spots a, b and c in (ii) are shown as A, B and C in (iii). Possible mechanisms of stripe formation at 1a, 1b and 2 in (iv) are discussed in the text.

B. Diagram showing possible mechanisms for emergence of radial stripes. See text and Fig. 3.7 for further details.

☆ represents proliferation in (iv); ⁘ represents clusters of spots in (B)

3.4.3 Emergence of stripes

Possible ways that stripes may emerge by radial proliferation are shown in Fig. 3.6B (arrows at 1a-c). If proliferation is restricted to only (or mainly) the cells in the outer cortex (arrow at 2a in Fig. 3.6B) this is known as edge growth (or edge-biased growth if a few interstitial cells also divide) and has been shown to result in stripe formation in other mosaic systems (Bodenstein, 1986; Bodenstein and Sidman, 1987a; Bodenstein and Sidman, 1987b; Bodenstein and Sidman, 1987c). In this case the stripe would extend to the outside of the cortex but the original mosaic pattern would persist in the inner cortex (also see Fig. 3.7B). Similar stripes could also arise by localised radial proliferation deeper in the adrenal cortex (arrows 1a and 1c in Fig. 3.6B) but, if the original mosaic pattern is fine-grained, proliferation would have to be restricted to a small region along the radial axis to form a single-coloured stripe. This is illustrated in more detail in Fig. 3.7.

In each case it is predicted that the initial stripe would not span the whole adrenal cortex but a residual mosaic region would be left in the outer and/or inner cortex. The mosaic patterns illustrated in Figs. 3.2-3.4 do not provide adequate resolution to distinguish between these different possibilities but this is considered further in chapter 4.

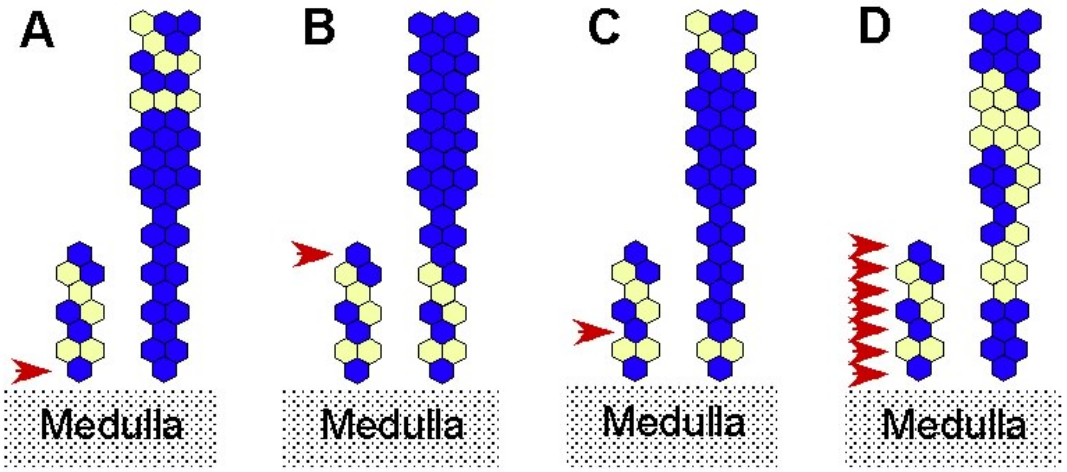

Fig. 3.7. Alternative patterns of growth that could produce a blue (β-gal-positive) stripe in the developing adrenal cortex.

In each diagram (A-D) the group of 10 hexagons on the left represents a column of cells spanning the adrenal cortex (from medulla boundary at the bottom to capsule at the top) at around birth. The red arrowheads indicate the proliferating cell(s) and the taller groups of hexagons represent the enlarged column of cells at a later stage (but before P21). In A-C proliferation is restricted to a specific region (only one of the 10 original cells shown). (**A**) Only the blue cell adjacent to the medulla proliferates and this produces a blue stripe with a mosaic region in the outer cortex (top). (**B**) Only the outermost blue cell proliferates and this produces a blue stripe with a mosaic region in the inner cortex. This equivalent to strict edge growth but a similar pattern would be expected with edge-biased growth if almost all cell divisions were at the edge. (**C**) A more centrally located blue cell proliferates and produces a blue stripe with mosaic regions in both the inner and outer cortex. (**D**) Proliferation occurs throughout the adrenal cortex so no clear stripe is produced.

3.4.4 Final transition to full stripes

By P21 the stripes span the whole adrenal cortex so we need to explain how the residual mosaic region is replaced by extending the adjacent stripe. This could occur if the older non-proliferative cells died by apoptosis wherever they were located (1a-c in Fig. 3.6B). Alternatively stripes formed by edge-biased growth would be extended if apoptosis occurred only near the boundary with medulla (Fig. 3.8). This would eliminate residual mosaic tissue at the medulla boundary by progressively eroding it from the inner part of the cortex. Eventually apoptosis would reach the stripe and the stripe would then span the cortex. In the rat adrenal cortex most apoptosis occurs close to the medulla at P10 and in the adult but apoptotic cells are scattered throughout the adrenal gland at perinatal stages (Mitani et al., 1999; Wyllie et al., 1973a). The location of apoptosis close to the medulla at P10 in the rat supports the model shown in Fig. 3.8 but it is not known whether apoptosis occurs in the mouse before P21.

If stem cells are specified and activated in the outer cortex they are likely to produce proliferative transient amplifying cells, which are believed to move centripetally to maintain the adult adrenal cortex (Zajicek et al., 1986). Thus a stem cell specified within a blue β-gal-positive stripe will produce a clone of β-gal-positive cells that move centripetally and will eventually reach the medulla and replenish the original blue stripe (stripe 2 in Fig. 3.6B). Fig. 3.8 illustrates both elimination of residual mosaic tissue at the medulla boundary by apoptosis and centripetal movement of cells derived from stem cells in the outer cortex. However, it remains unknown whether stem cell activation or centripetal movement begins before P21 when the stripes already span the entire cortex.

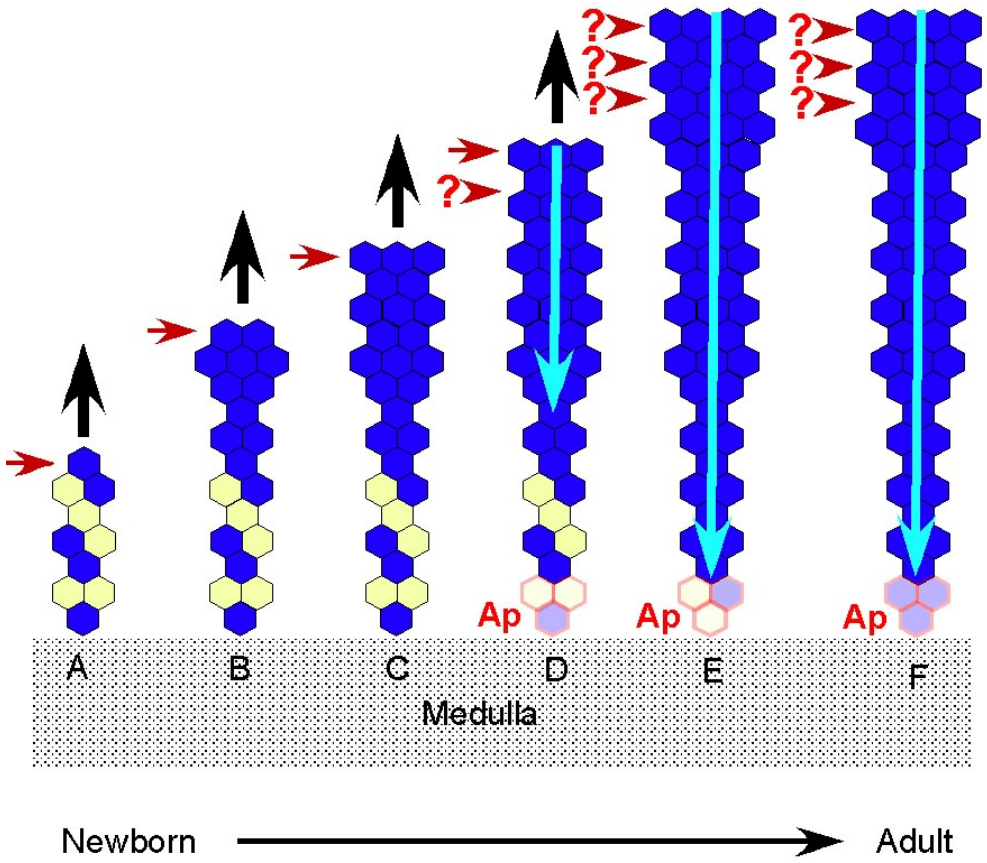

Fig. 3.8. Hypothetical formation of a blue (β-gal-positive) stripe spanning the whole adult adrenal cortex.

Diagrams **A-D** show the production of a blue (β-gal-positive) stripe in the outer adrenal cortex with a mosaic region in the inner cortex (as in Fig. 3.7B). The red arrows indicate the proliferating cell(s) and the vertical black arrows indicate increased radial growth. At the stage reached in diagram **D** the cortex is still growing but cortical cells closest to the medulla are dying by apoptosis. Stem cells have also been specified in the outer cortex, which will produce transient amplifying cells that proliferate and move centripetally (blue arrow). The '?' symbols and red arrowheads indicate the proliferation of stem cells or transient amplifying cells. In **E** the cortex has stopped growing and the original mosaic pattern near the medulla is being lost as cells next to the medulla die by apoptosis and are replaced by adjacent cells. In **F** the original pattern has been entirely replaced and the blue stripe spans the whole adrenal cortex. Abbreviations: Ap, apoptosis.

3.5 Conclusions

The experiments described in this chapter show that the transition from randomly orientated spots to radial stripes is complete by P21. Several hypotheses to explain how this transition may occur have been suggested and are investigated in chapter 4.

4. Changes in growth, morphology and cell proliferation in the mouse adrenal from E14.5 to P21

4.1 Introduction

Chapter 3 demonstrated that the mosaic pattern of β-gal reporter staining in *21OH/LacZ* transgenic adrenal glands changes with age between E14.5 and P21 from a non-radially orientated random pattern of spots to radial patches and finally radial stripes. It is not presently known which of the biological changes occurring during this period could account for the changes in mosaic patterns of reporter staining. Various possible mechanisms, such as radial cell proliferation, edge-biased growth, localised apoptosis and morphogenic factors, including formation of blood vessels and the changes in adrenal histological morphology leading to the appearance of the adrenocortical zones, were mentioned in chapter 3 and may contribute to the changes in mosaic pattern. While chapter 3 focussed on identifying when the radial pattern of stripes formed in *21OH/LacZ* transgenic adrenal glands, this chapter is more concerned with the mechanisms by which they might be formed.

The biochemical and histological features of the adult adrenal glands of human, rat and mouse have been well described previously (Mitani et al., 1999; Nyska and Maronpot, 1999; Vinson, 2003). There are also various detailed descriptions of rat and human adrenal gland development from late gestation, through weaning, to adulthood (Keegan and Hammer, 2002; Mitani et al., 1999).

In the mouse, development of the adrenal cortex begins at day 11 of gestation (E11), after separation from an adrenogenital primordium, followed by integration of neural crest-derived medulla precursors at E12 and formation of the adrenal capsule and cortical capillaries at E14 (Keegan and Hammer, 2002; Nyska and Maronpot, 1999). Growth of the mouse adrenal gland around birth has been

described in terms of weight and adrenal volume (Eguchi, 1960; Moog et al., 1954). The 3 major cortical zones first appear in males and females around birth and share a broadly similar morphology, although the sexes later become distinguished by the variable presence of the so-called X zone at the cortical-medullary boundary (Howard-Miller, 1927; Keegan and Hammer, 2002). Growth continues until around 7 weeks of age but a gender-specific dimorphism in weight is apparent from around 3-4 weeks of age (Moog et al., 1954; Bielohuby et al., 2007).

A recent study has shown that at E15.5 BrdU-labelled cells start to assemble in the outer region of the developing mouse adrenal gland and become progressively more concentrated in the sub-capsular region just before birth (Schulte et al., 2007). Although there is some difference between the figures and text descriptions, the figures in this study also showed that, at P14, proliferating adrenocortical cells were scattered throughout the outer part of the cortex. It is, however, unclear how the patterns of cell proliferation alter between late fetal stages and P14.

Each of the above studies has focussed on dynamic morphological changes occurring in the mouse adrenal cortex at particular stages of development, using a variety of experimental methods but, to date, no single study has consistently compared adrenocortical growth and cell proliferation from fetus, through postnatal stages, to adulthood.

4.1.1 Experimental aims

Some of the possible mechanisms, discussed at the end of chapter 3, that may cause changes in mosaic patterns of β-gal reporter expression in *21OH/LacZ* adrenals will be investigated in this chapter. For example, it has been reported that the size of the adrenal changes little between E18.5 and P4 (Eguchi, 1960), so it is important to determine whether cell proliferation occurs during the period when stripes emerge (P0-P10). Adrenal size, histological morphology and locations of proliferating cells will be compared in mouse adrenals at various ages to try to identify what factors may be associated with the observed changes in mosaic patterns (formation of stripe pattern) and how they may be associated with adrenal growth. Other factors (such as apoptosis and changes in cell shape) may also play significant roles but there was insufficient time to include these in the study.

4.2 Materials and methods

4.2.1 Measurement of adrenal size

The *21OH/LacZ* transgenic adrenal glands analysed for mosaic patterns in chapter 3 were freshly dissected and measured with a dissecting microscope fitted with an eyepiece graticule before processing for frozen sections. Adrenal sizes were compared by measurements of length and width because glands at the youngest ages were too small to weigh accurately. These basic measurements were then converted into estimates of adrenal area and volume by assuming the adrenal is an ellipsoid. The area was estimated as the area of ellipse ($^1/_2$ length $\times$ $^1/_2$ width $\times$ π) and the volume was estimated as the volume of an ellipsoid with a depth that was equal to its width ($^1/_2$ length $\times$ $^1/_2$ width $\times$ $^1/_2$ width $\times$ π).

The adrenals were grouped by gender (female and male) from E17.5 to postnatal day 21 (P21) and anatomical location (right and left) for all experiment ages (E14.5, E15.5, E16.5, E17.5, E18.5, P0, P1, P2, P3, P5, P7, P10, P14 and P21). From E17.5 to P21 at least 3 adrenals were analysed in each group of a specific age, sex and location and, from E14.5 to E16.5, 6 to 8 adrenals were examined in every group of a specific age and location.

4.2.2 Adrenal histological morphology (H&E staining)

Seven micron sections of adrenal glands from (C57BL/6 x CBA/Ca)F1 mice were stained with H&E (see section 2.6) for comparison of histological morphology at E18.5, P1, P3, P10 and adult (8 week old). The middle sections of 2-3 wax-embedded left adrenals were photographed and analysed per stage for both females and males.

4.2.3 Cell proliferation (Ki67 nuclear antigen immunohistochemistry)

Seven micron sections of (C57BL/6 x CBA/Ca)F1 adrenals were labelled by immunohistochemical staining for Ki67 nuclear antigen (brown DAB endpoint in nuclei) as a marker for cell proliferation in the adrenal gland at E18.5, P1, P3, P10 and adult (8 weeks old) and counter-stained with haematoxylin (see section 2.7). The middle longitudinal sections of 3 wax embedded left adrenals were photographed and examined for each stage in both females and males.

4.2.4 Statistical analysis

Growth curves were analysed by a professional statistician, Dr Robert Elton (Rob Elton Medical Statistics Consulting), who used SPSS software (SPSS Inc, Chicago, Illinois, USA) for statistical modelling. Adrenal lengths and widths were $\log_{10}$ transformed because biological growth is often logarithmic. Linear modelling on $\log_{10}$-transformed data was used to test for effects of sex and anatomical location with age on adrenal size. Cubic and quadratic modelling were also used to test whether adrenal growth was likely to be tri-phasic or otherwise non-linear. See Appendix 1 for further details.

4.3 Results

The mosaic pattern of β-gal reporter staining in *21OH/LacZ* adrenals has been shown to change with age from E14.5 to P21. However, it is not known if the changes in mosaic pattern are specifically associated with changes in adrenal size, histological morphology or cell proliferation, and, if so, how they are associated.

4.3.1 Changes in mouse adrenal size from E14.5 to P21

In general, Figs. 4.1A-D show similar trends and, as expected, the length (Fig. 4.1A), width (Fig. 4.1B), area (Fig. 4.1C) and volume (Fig. 4.1D) all increase between E14.5 and P21. Visual inspection suggests that the growth curves might be tri-phasic with a middle plateau period showing little growth from around E16.5 until P5, which could have important implications for the mechanism of stripe formation. For example, if stripes emerged during a period of no net-growth, this could undermine the hypotheses illustrated in Figs. 3.7 and 3.8 (sections 3.4.3 & 3.4.4). The possibility of triphasic growth is considered in more detail in section 4.3.1.1

4.3.1.1 The shape of the growth curve

Fig. 4.1A suggests that adrenal length increases most rapidly after P5 and there may be little net growth between E16.5 and P5. A similar trend was seen for adrenal width (Fig. 4.1B) but the P5 adrenal widths appeared lower than expected by comparison with neighbouring time points and are probably anomalous. This has also affected the estimates of area and volume at P5 (Figs. 4.1C and 4.1D). Although left and right adrenals were analysed from a minimum of 3 female and 3 male mice, in the case of P5 adrenals these were all from one litter so any error in dating that litter could produce a consistent anomaly in the measured adrenal dimensions. (This may not necessarily be the explanation because the P5 adrenal lengths are not obviously anomalous but with hindsight more litters should have been sampled for every age). Furthermore, the P5 litter group was the first to be dissected and analysed so may have taken longer than later dissections once

procedures had become more routine. However, the results for other ages show clear trends.

Biological growth is often logarithmic rather than linear so the data were log transformed to try to visualise the growth trends more clearly. Visually, semi-log plots of $\log_{10}$ length versus age (Fig. 4.1E) and $\log_{10}$ volume versus age (Fig. 4.1F) both suggest that adrenal growth occurs between E16.5 and P5 as well as earlier and later.

Dr Robert Elton used statistical modelling of $\log_{10}$-transformed data to test whether adrenal growth was likely to be tri-phasic or non-linear (see appendix 1). Neither the cubic nor quadratic model provided a significantly better fit to the data. There was no evidence for a plateau in the growth curve or a steadily increasing slope (of logged values). The lack of evidence for a clear plateau implies that the adrenal gland was growing at all stages examined including stages when mosaic stripe patterns first emerge (discussed in Chapter 3).

Fig. 4.1. Change in adrenal size in *21OH/LacZ* transgenic mice from E14.5 to P21. The adrenal glands were dissected and the length and width were measured with a dissecting microscope fitted with an eyepiece graticule. The adrenal glands are grouped into female left (F/L; dark blue), female right (F/R; pink), male left (M/L; yellow) and male right (M/R; light blue) from E17.5 to P21; 3-4 mice were used per gender for each age. Fetuses at E14.5 - E16.5 were not separated by gender but the adrenal glands were separated into left (F+M/L; purple) and right (F+M/R; brown); adrenals from 6-8 E14.5 -E16.5 fetuses were analysed for each group. The Y-axis shows the measured value of adrenal size and the X-axis is the age. (**a**) Adrenal length (mm); (**b**) adrenal width (mm); (**c**) adrenal area (mm^2), estimated as described in the text; (**d**) adrenal volume (mm^3) estimated as described in the text; (**e**) $\log_{10}$ of the adrenal length (mm); (**f**) $\log_{10}$ of the estimated adrenal volume (mm^3).

(A)

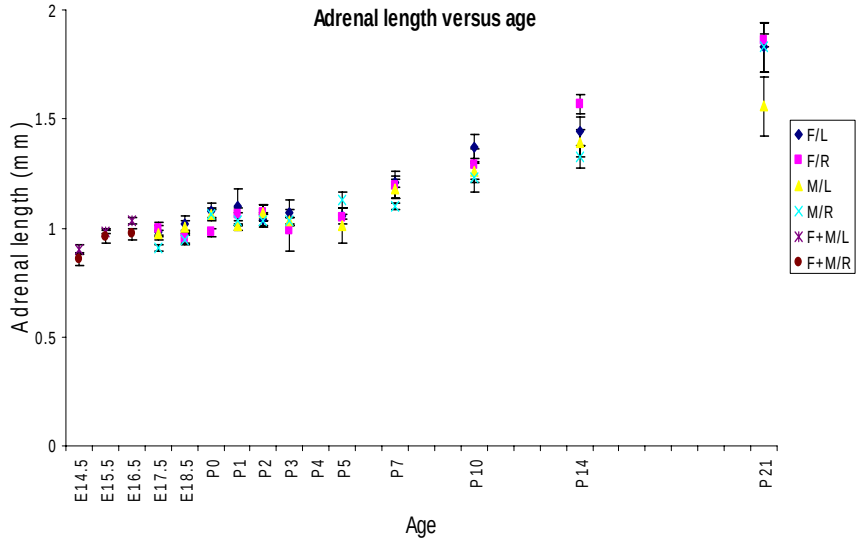
Adrenal length versus age
Adrenal length (mm)
2
1.5
1
0.5
0
E14.5
E15.5
E16.5
E17.5
E18.5
P0
P1
P2
P3
P4
P5
P7
P10
P14
P21
Age
F/L
F/R
M/L
M/R
F+M/L
F+M/R

(B)

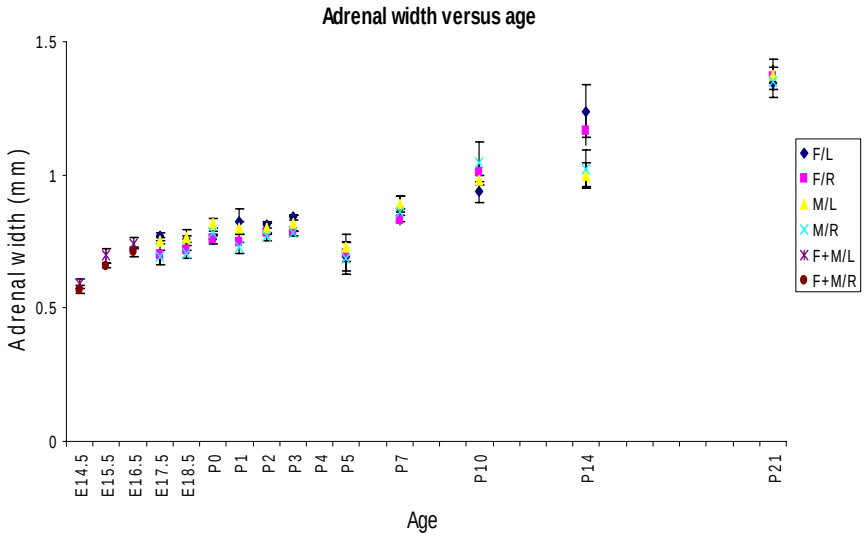
Adrenal width versus age
Adrenal width (mm)
1.5
1
0.5
0
E14.5
E15.5
E16.5
E17.5
E18.5
P0
P1
P2
P3
P4
P5
P7
P10
P14
P21
Age
F/L
F/R
M/L
M/R
F+M/L
F+M/R

(C)

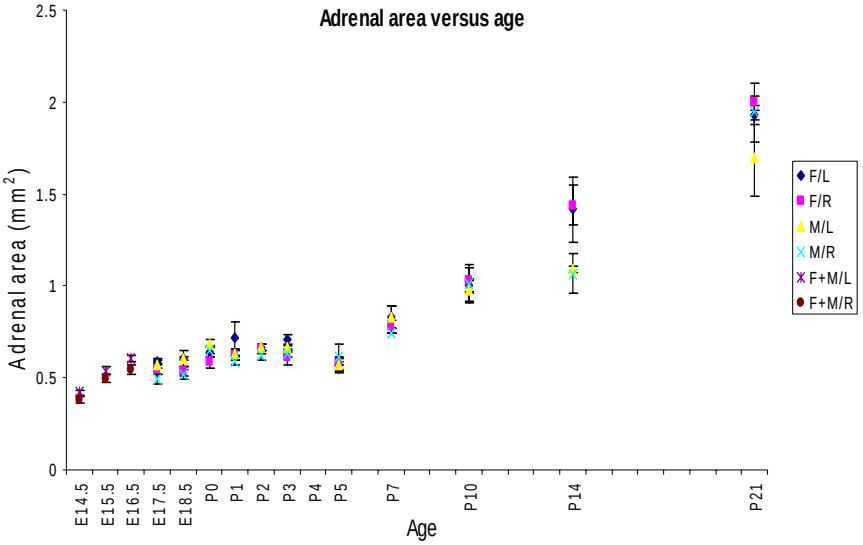
Adrenal area versus age
Adrenal area (mm2)
2.5
2
1.5
1
0.5
0
E14.5
E15.5
E16.5
E17.5
E18.5
P0
P1
P2
P3
P4
P5
P7
P10
P14
P21
Age
F/L
F/R
M/L
M/R
F+M/L
F+M/R

(D)

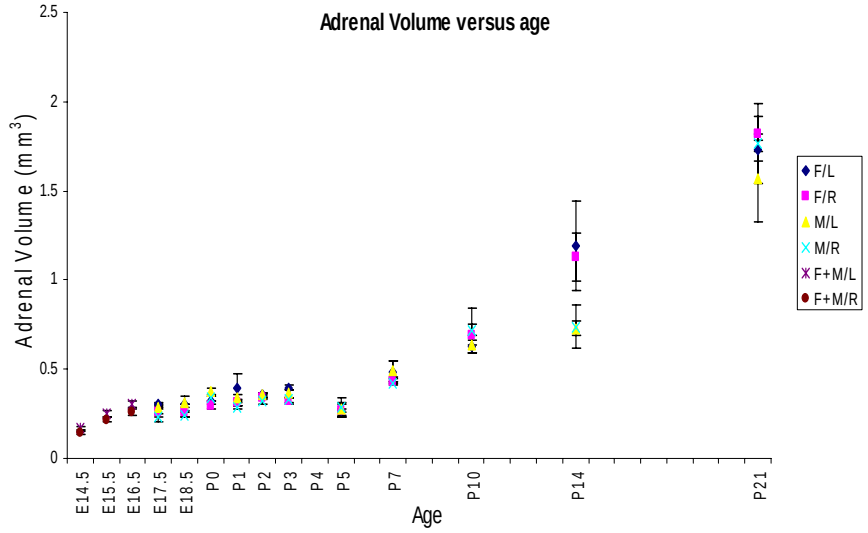
Adrenal Volume versus age
Adrenal Volume (mm3)
2.5
2
1.5
1
0.5
0
E14.5
E15.5
E16.5
E17.5
E18.5
P0
P1
P2
P3
P4
P5
P7
P10
P14
P21
Age
F/L
F/R
M/L
M/R
F+M/L
F+M/R

(E)

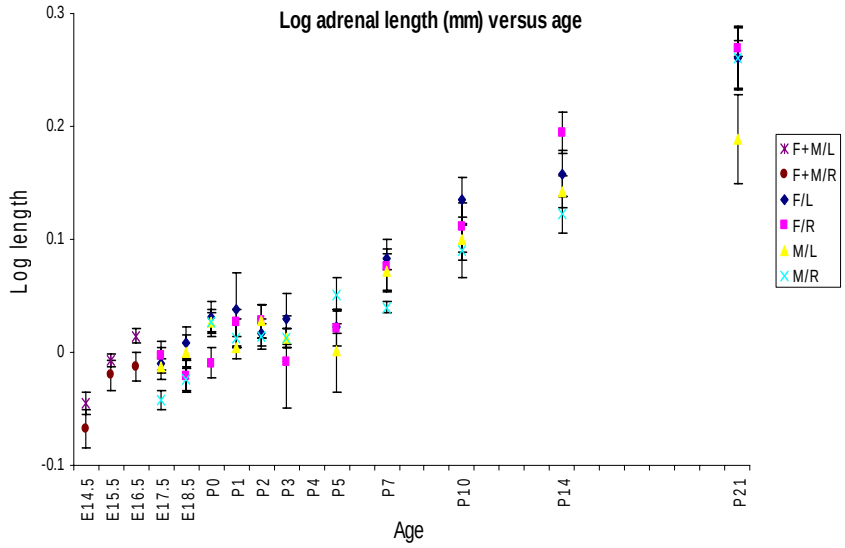
Log adrenal length (mm) versus age
Log length
0.3
0.2
0.1
0
-0.1
E14.5
E15.5
E16.5
E17.5
E18.5
P0
P1
P2
P3
P4
P5
P7
P10
P14
P21
Age
F+M/L
F+M/R
F/L
F/R
M/L
M/R

(F)

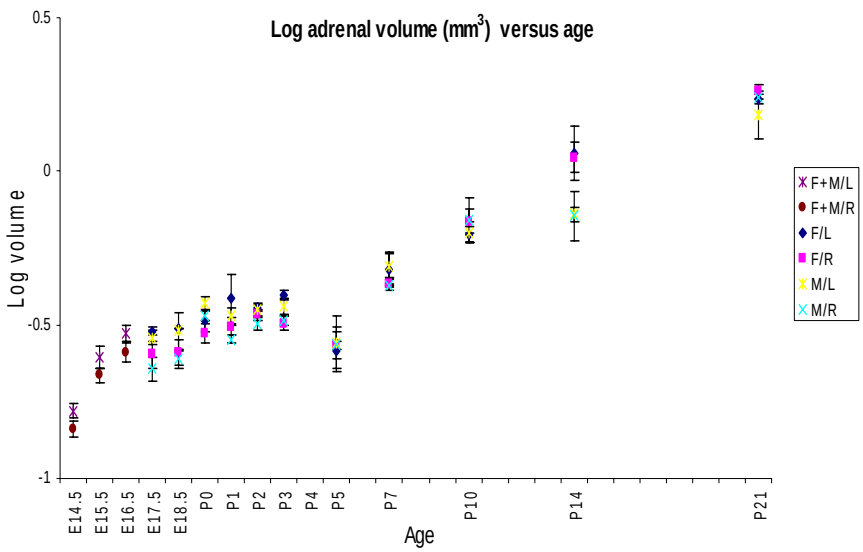
Log adrenal volume (mm3) versus age
Log volume
0.5
0
-0.5
-1
E14.5
E15.5
E16.5
E17.5
E18.5
P0
P1
P2
P3
P4
P5
P7
P10
P14
P21
Age
F+M/L
F+M/R
F/L
F/R
M/L
M/R

4.3.1.2 Effects of gender and anatomical location (left versus right) on adrenal size

Dr Rob Elton used linear modelling of $\log_{10}$ transformation of length and width (excluding P5 results) with age, gender, anatomical position to test statistically whether any of these factors had significant effects on adrenal size (see appendix 1). The analysis showed that females of a given age have longer adrenals than males (P=0.014) but adrenal widths did not differ for males and females (P=0.53). Figs. 4.2 A,B and 4.3A,B show these comparison more clearly than 4.1A but visually the effect appears small. When the interaction of age and gender was examined, there was no evidence that the gender effect on adrenal length is related to age (P=0.26). The analysis also showed that left adrenals of a given age are larger than right ones. This size difference is statistically significant for adrenal width (P<0.001; Fig 4.3 C,D) but not quite significant for adrenal length (P=0.08; Fig. 4.2C,D). It is not clear why gender and anatomical position do not affect length and width similarly.

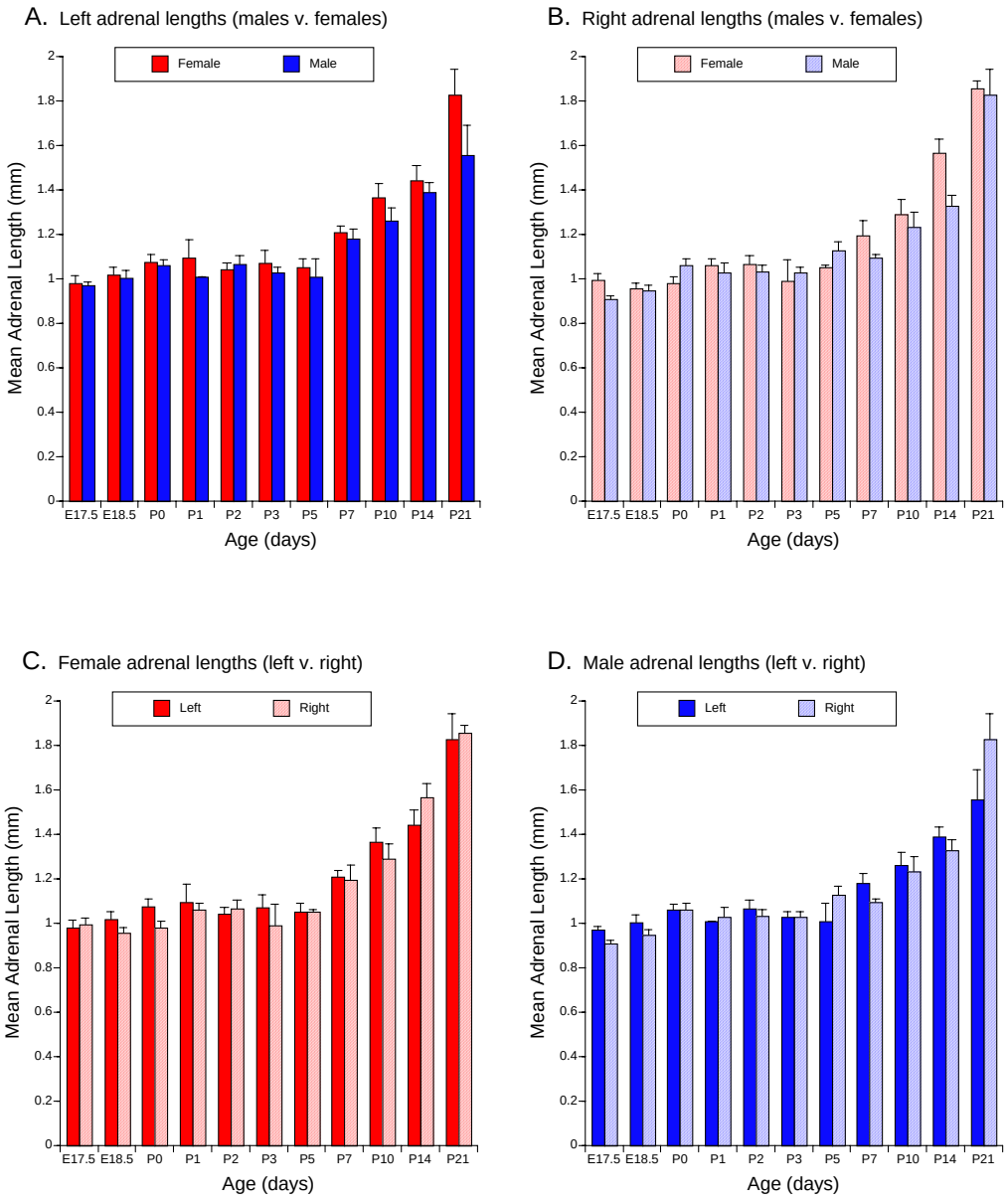

Fig. 4.2. **Comparison of length in different groups (males vs. females and left vs. right) of *21OH/LacZ* transgenic mice from E17.5 to P21**.
Comparisons of left adrenal lengths (A) and right adrenal lengths (B) between male and females. (Females had significantly longer adrenals than males, *P*=0.014; see text.) Comparisons of adrenals in females (C) and males (D) between left and right. (Left and right adrenals did not differ significantly in length, *P*=0.08; see text.) Red-filled bar, female left adrenal; blue-filled bar, male left adrenal; red diagonal bar, female right adrenal; blue diagonal bar, male right adrenal.

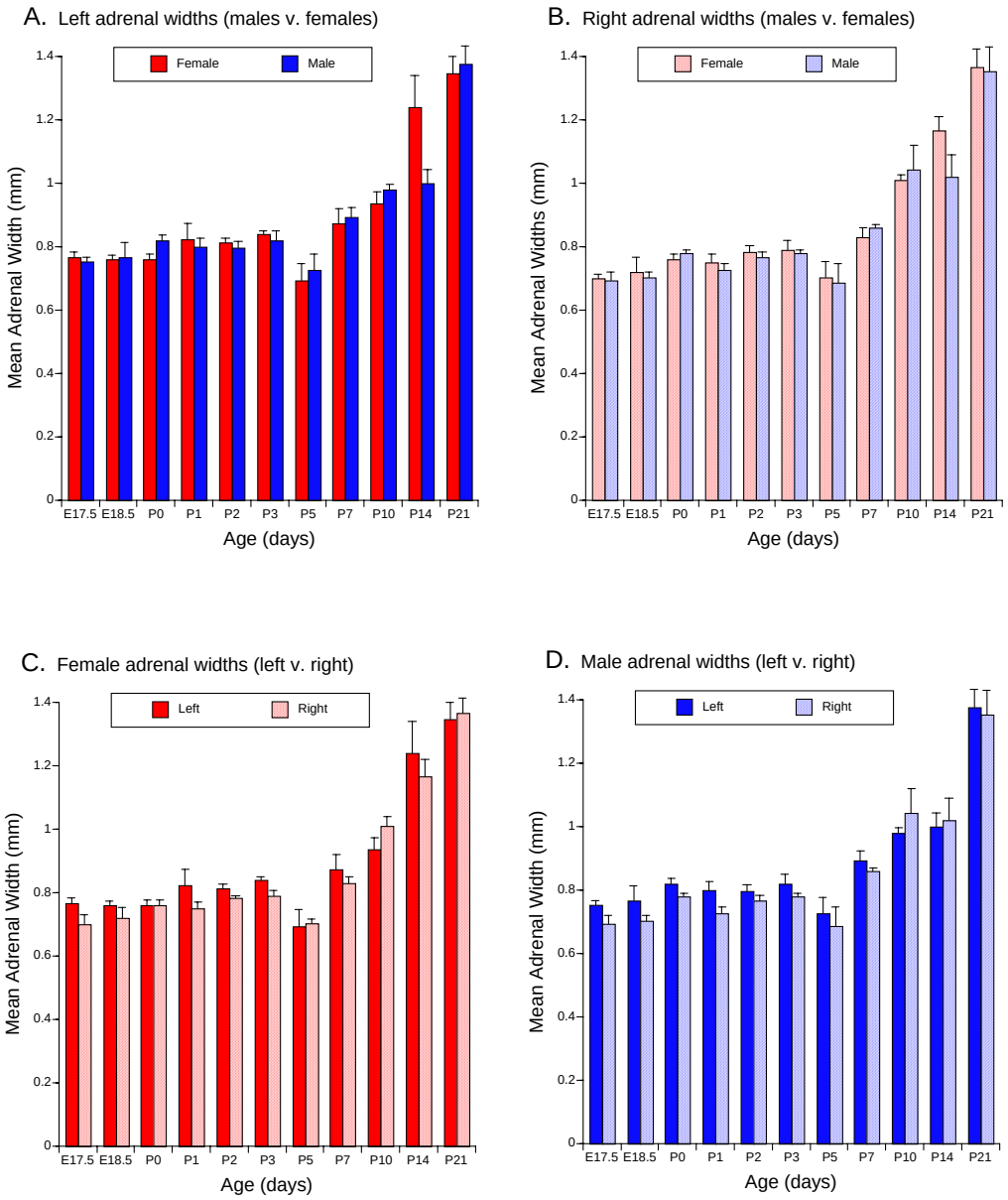

Fig. 4.3. **Comparison of adrenal width in different groups (males vs. females and left vs. right) of *21OH/LacZ* transgenic mice from E17.5 to P21**. Comparisons of left adrenal widths (A) and right adrenal widths (B) between male and females. (Male and female adrenals did not differ significantly in width, P=0.53; see text.) Comparisons of female widths (C) and male widths (D) between left and right adrenals. (Left adrenals were significantly wider than right adrenals, P<0.001; see text.) Red-filled bar, female left adrenal; blue-filled bar, male left adrenal; red diagonal bar, female right adrenal; blue diagonal bar, male right adrenal.

4.3.2 Histological morphology of the developing mouse adrenal gland

The characteristics of H&E staining (basophilic for ZG and eosinophilic for ZF) and histological arrangement (arch-like morphology for ZG, columnar morphology for ZF and compacted morphology for ZR) of the developing mouse adrenal gland were examined at E18.5, P1, P3, P10 and adult (8 weeks old). The purpose of this was to compare the time of development of the three adrenocortical zones with the time of stripe formation (discussed in Chapter 3). Results are illustrated in Figs. 4.4 and 4.5 and the main features of histological morphology are tabulated in Table 4.1.

Fig. 4.4 shows no dramatic differences between males and females in the progressive changes in histological morphology of the 3 definitive adrenocortical zones (ZG, ZF and ZR) and medulla of perinatal adrenal glands over the period E18.5 to P10. In both sexes a morphological ZG first becomes apparent at E18.5 while all 3 cortical zones can be clearly distinguished by P10. The medulla is still intermingled with cortex at E18.5 but the boundary between the cortex and medulla is forming at P3 and is clearly distinguishable by P10. Red blood cells are present in the cortex and medulla at each stage examined from E18.5. The adult female (8 week old) adrenal cortex displays an obvious vacuolated X zone but this is not present in the male, consistent with the observations in the literature that the male X zone has already regressed by this time (Bielohuby et al., 2007; Nyska and Maronpot, 1999).

The greater detail revealed by the higher power images in Fig. 4.5 shows that at E18.5 1-3 layers of basophilic glomerulosa cells are present in the ZG, while the columnar structure in the ZF is not yet complete. At P1 and P3 the beginnings of the arch-like structure of the ZG are visible while the columnar structure in the ZF are incomplete at P1 but are almost complete by P3. The arch-like structure of the ZG, the columnar morphology of the ZF and the compacted morphology of the ZR are clearly formed at P10 and appear similar to the adult morphology.

Fig. 4.4. Low power histology of E18.5, P1, P3, P10 and adult (8 week old) adrenal glands. Low magnification images of 7 μm wax sections of C57BL/6 x CBA/Ca)F1 mouse adrenal glands stained with haematoxylin and eosin as described in *Materials and Methods* (section 2.6). 2-3 adrenals were examined for each age. The main histological features are tabulated in Table 4.1. Boxed area is shown at higher magnification in Fig. 4.5. Scale bars = 100μm.

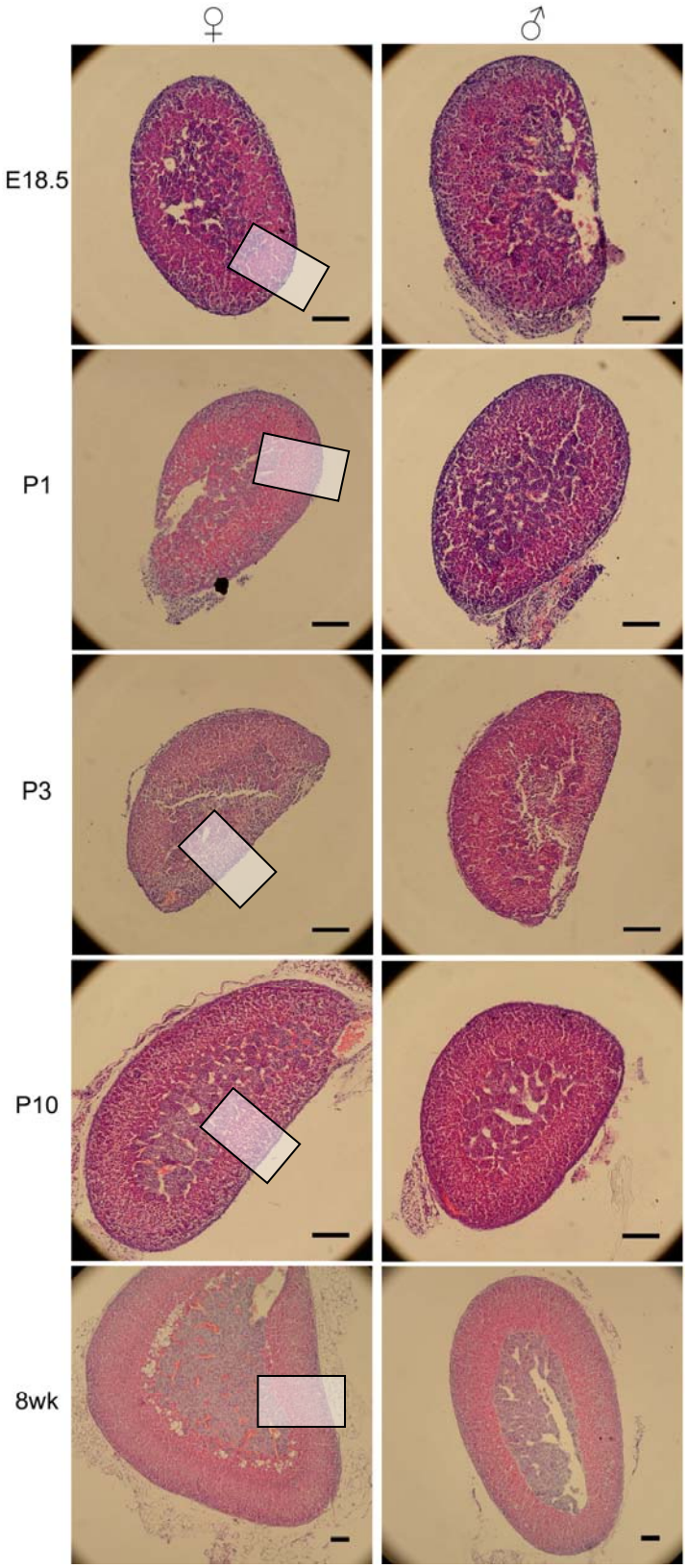
♀
♂
E18.5
P1
P3
P10
8wk

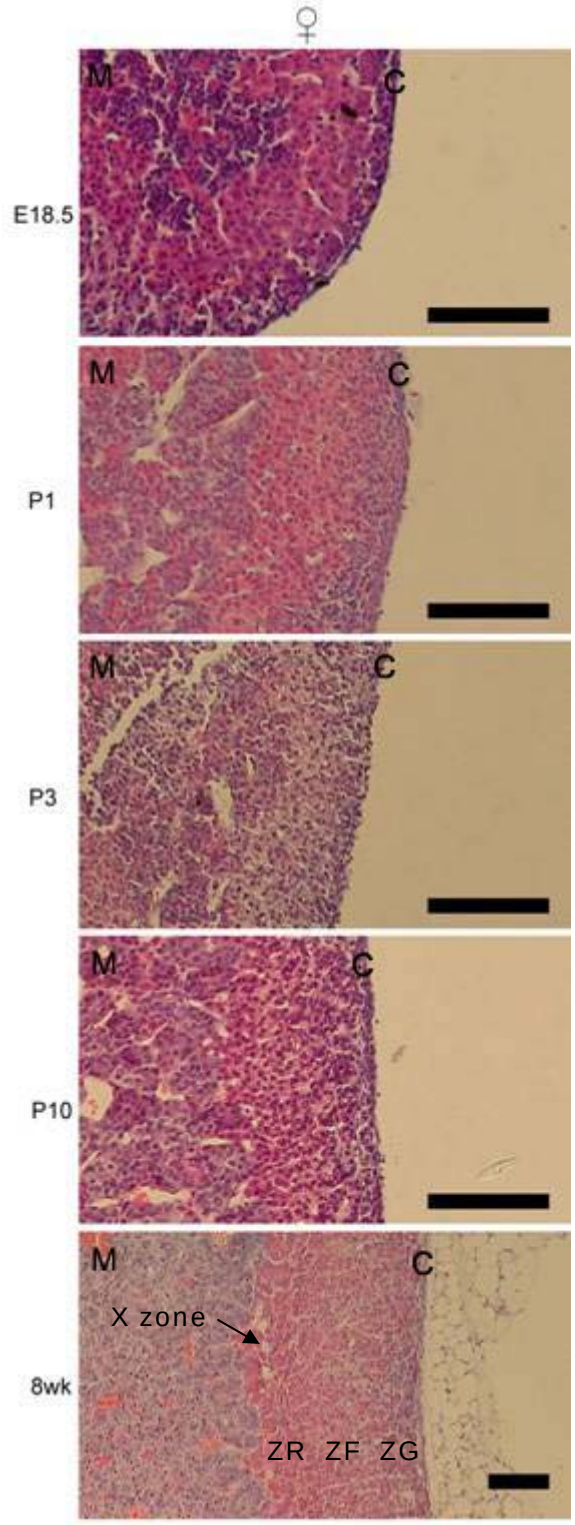

Fig. 4.5. Histology of E18.5, P1, P3, P10 and adult adrenal glands from female mice. Higher magnification images of selected areas of female adrenal glands shown within boxes in Fig. 4.4. See Fig. 3.5 for labelling of morphological arch-like structures in ZG and cell columns in the ZF. Scale bars = 100µm. Abbreviations: M, medulla; zones of the cortex: ZG, ZF, ZR; X-zone; C, capsule.

Table 4.1: Histological characterisation of different zones of (C57BL/6 x CBA/Ca)F1 adrenal glands from E18.5 to adult (8 weeks).

Age	Histological features				
	Adrenocortical Zones				Medulla
	Zona Glomerulosa (basophilic)	**Zona Fasciculata** (eosinophilic)	**Zona Reticularis** (eosinophilic)	**X Zone** (vacuolated)	
E18.5	1-3 layers of basophilic cells	Incomplete columnar structure;	ZR not yet identifiable	absent	Cortex intermingled with medulla
P1	2-4 layers cells start to form arch-like structure	Incomplete columnar structure	ZR not yet identifiable	absent	Cortex intermingled with medulla
P3	2-4 layers of basophilic cells in arch-like structure	Almost completed columnar structure	ZR not yet identifiable	absent	Cortex medulla boundary forming
P10	Fully formed arch structure	Fully formed column	Fully formed compact ZR	absent	Clear cortical medulla boundary
Adult	Fully formed arch structure	Fully formed column	Fully formed compact ZR	vacuolated X zone present	Clear cortical medulla boundary

4.3.3 Location of cell proliferation in the developing mouse adrenal gland from E18.5 to adult

Ki67 nuclear antigen immunohistochemistry can be used as a marker of cell proliferation as Ki67 is present in the nuclei of proliferating cells from late G1, through S and G2 to M phase (but does not label cells in G0). The locations of proliferating cells in mouse adrenal glands from E18.5 to adult (8 week old) are illustrated in Figs. 4.6 and 4.7 and summarised in Table 4.2.

Males and females showed similar distribution patterns of Ki67-positive cells in E18.5, P1, P3, P10 and adult adrenal glands (Fig. 4.6). Fig. 4.7 shows that most of the Ki67-positive cells were concentrated in 1-3 subcapsular layers at E18.5, P1 and P3. At P10 the frequency of Ki67-positive cells increased with their principal location expanding to encompass the ZG and outer half of the ZF. In the adult the frequency of Ki67-positive cells decreased and they were scattered in the outer cortex (ZG and outer ZF). While at all stages the majority of Ki67-positive cells were located in the outer cortex, a small number of Ki67-positive cells were always present in the inner cortex from E18.5 to adult. The medulla contained many Ki67-positive cells from E18.5 to P10 but had fewer positive cells in the adult.

Fig. 4.6. Locations of proliferating cells in whole sections of adrenal glands from E18.5 to adult. Low magnification images of 7 μm wax sections of E18.5, P1, P3, P10 and 8 week (C57BL/6 x CBA/Ca)F1 mouse adrenal glands showing proliferating cells, detected by immunohistochemical staining with anti-Ki67 antibody (brown nuclear staining) as described in section 2.7. 2-3 adrenals were examined for each age. Boxed area is shown at higher magnification in Fig. 4.7. Scale bars = 100μm.

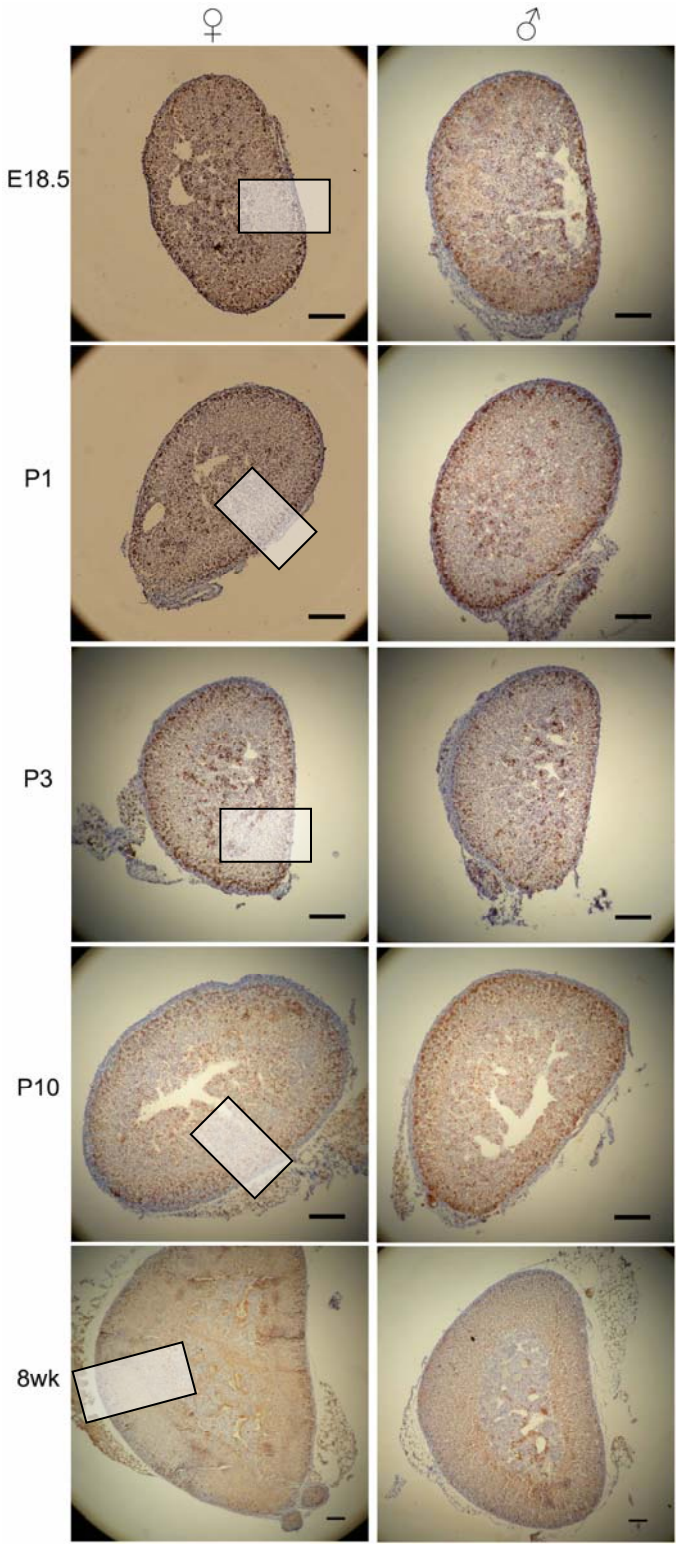
♀
♂
E18.5
P1
P3
P10
8wk

Fig. 4.7. Locations of proliferating cells in magnified section of female adrenal glands from E18.5 to adult. Higher magnification images of selected areas of female adrenal glands at E18.5, P1, P3, P10 and adult (8 weeks old) shown within boxes in Fig. 4.6. (The 8 week image has been rotated approximately 180º to be consistent with the other images.) Proliferating cells are detected by immunohistochemical staining with anti-Ki67 antibody (brown nuclear staining). See Fig. 3.5 for labelling of morphological arch-like structures in ZG and cell columns in the ZF. Scale bars = 100µm. Abbreviations: M, medulla; zones of the cortex: ZG, ZF, ZR; C, capsule.

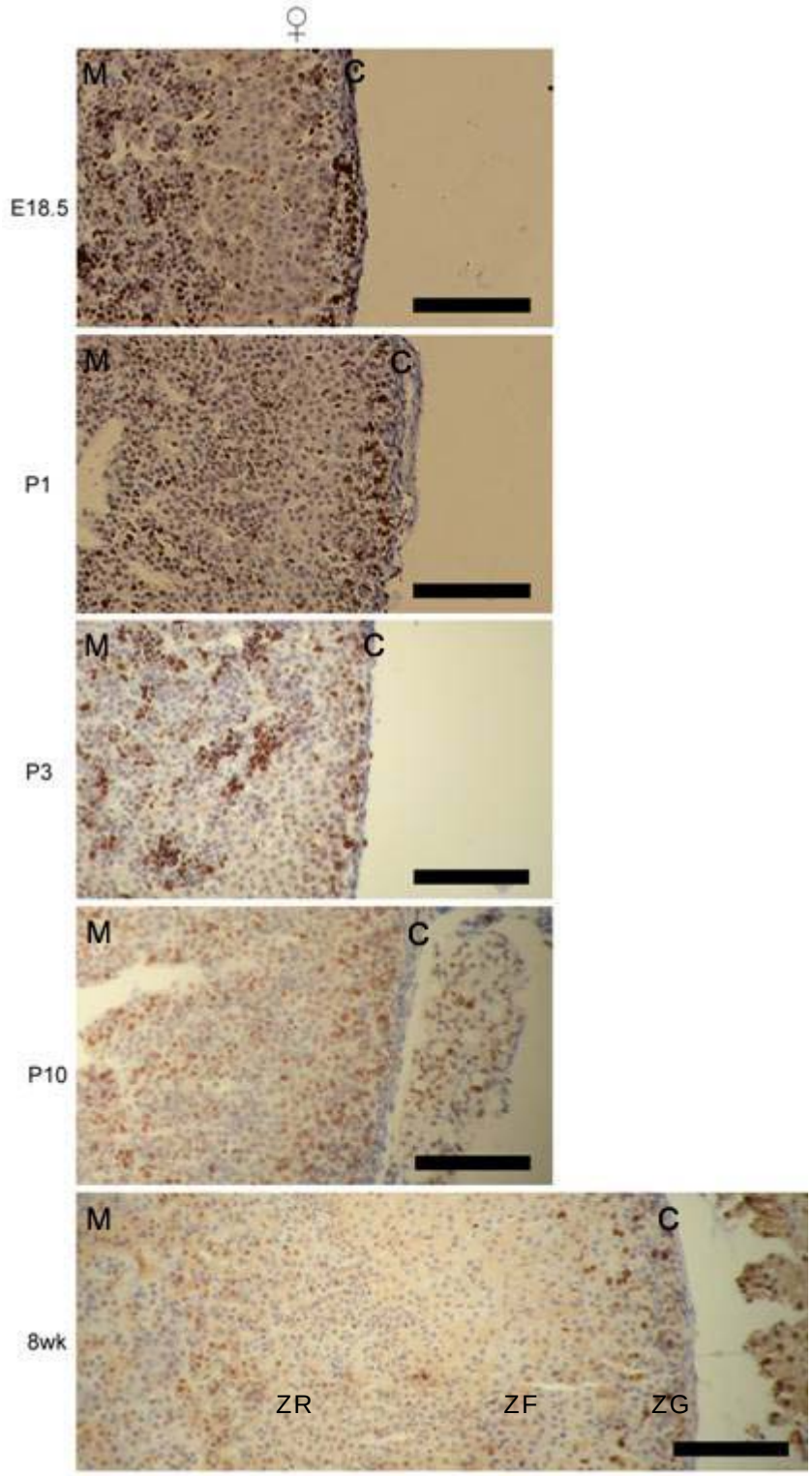
♀
E18.5
P1
P3
P10
8wk
M
C
ZR
ZF
ZG

Table 4.2 The distribution of Ki67-positive cells in adrenal glands of E18.5, P1, P3, P10 and adult (C57BL/6 x CBA/Ca)F1 mice.

Age	**Main location of Ki67-positive cells in cortex**	**Frequency of Ki67-positive cells** (subjective score)		
		Outer cortex	Inner cortex	Medulla
E18.5	1-3 subcapsular cell layers*	+++	+	+++
P1	2-3 subcapsular cell layers (ZG)	+++	+	+++
P3	2-3 subcapsular cell layers (ZG)	+++	+	+++
P10	ZG + outer half of ZF	++++	+	+++
Adult (8 wks)	ZG + outer third of ZF	++	+	++

* The subcapsular region is the most peripheral part of the outer cortex (3 cell layers closest to capsule)

4.4 Discussion

4.4.1 Changes in mouse adrenal size from E14.5 to P21

In humans, embryonic adrenal growth is rapid during the second and third trimester, interrupted by a fall in adrenal weight around birth probably reflecting regression of the fetal zone and its replacement by the expanding definitive zone in preparation for postnatal life. This is followed by a steady postnatal gain in weight and acquisition of a fully zonated morphology (Spencer et al., 1999; Winter, 1985). Prior to the current study, a few researchers had studied specific stages of perinatal and post weaning growth of the adrenal gland in rat (Majchrzak and Malendowicz, 1983; Wright and Voncina, 1977) and mouse (Bielohuby et al., 2007; Eguchi, 1960). In mice, following rapid post-weaning growth to postnatal week 7, female adrenal glands maintain a constant weight while adrenal glands in males lose approximately 25% of their mass before achieving their adult weight.

The study of perinatal and postnatal mouse adrenal sizes presented in this chapter showed similar growth trends for adrenal length, width, area and volume, all of which increased between E14.5 and P21. The lower than expected P5 value for adrenal width relative to neighbouring time points is probably an anomaly arising from an experimental artefact such as tissue shrinkage caused by slow processing of the first tissues dissected (the P5 samples were the first samples dissected) or sampling bias (all the P5 samples were from the same litter). However, the P5 adrenal lengths seem less affected than the widths. It is also possible that adrenal size does decline between P3 and P5 and this is mostly a reduction in width. As noted above, humans show a fall in adrenal weight around the time of birth relating to adaptions for postnatal life. It is possible, therefore, that the fall in mouse P5 adrenal width is a real result but further work is needed to investigate this.

The nature of the growth trend shown in Fig. 4.1 is difficult to determine. Visual inspection of plots in Fig. 4.1A-D suggested that growth might be triphasic with initial rapid growth followed by little net growth from around E16.5 until P5 and then a further period of rapid growth from around P7. However, this appears less convincing when the adrenal sizes are plotted as $\log_{10}$ data (Fig. 1E-F) and it was not supported by statistical analysis (Appendix 1). The simplest interpretation of the present data is of logarithmic growth throughout the E14.5-P21 period studied. This means that the adrenal is growing throughout the time when the stripes emerge (see Chapter 3 and section 4.4.4). Nevertheless, the precise shape of the growth curve remains uncertain and further work would be needed to reduce the experimental variation.

Despite the uncertainty about the shape of the growth curve, the E14.5-P21 data presented here are consistent with earlier separate analyses of perinatal and postnatal stages, showing respectively slow growth between E18.5 and P4 (Eguchi, 1960) and logarithmic growth from around P5 to P21 (Moog et al., 1954). Subsequent growth over the post-weaning period is not investigated here but others have shown that growth continues until around 7 weeks (Bielohuby et al., 2007). The period E14.5-P21 includes tissue remodelling accompanying adrenocortical zonation and the appearance of a morphological X zone and the reorganisation of mosaic patches into continuous stripes. Net growth during this period probably reflects a balance between cell proliferation (discussed in section 4.4.3) and cell apoptosis.

A gender-dependant dimorphism in adrenal weights has been reported (Bielohuby et al., 2007; Moog et al., 1954; Tanaka and Matsuzawa, 1995) with female mice having heavier adrenal glands than males from around three weeks of age (Bielohuby et al., 2007), while newborn male and females have similar adrenal weights (Moog et al., 1954). The results in this chapter show that females had larger adrenals (reflected by significantly larger adrenal lengths but not widths) before P21. The lack of significant difference in adrenal widths may be a consequence of the relatively small sample size.

The observation that right adrenals were significantly smaller than left adrenals from E14.5 to P21 is consistent with observations on adults described in chapter 5. This has not been reported previously but could be explained by anatomical location (for example, the right adrenal gland underlies the liver and the blood supply differs for left and right adrenals).

4.4.2 Histological morphology of the developing mouse adrenal gland

Examination of the morphology of the developing mouse adrenal cortex by H&E staining revealed a rapid perinatal development of the classical zonated adrenocortical structure following the first appearance of a basophilic zona glomerulosa at E18.5 (Table 4.1), broadly consistent with previous studies (Eguchi, 1960; Schulte et al., 2007). Thus the typical morphological structures of ZG, ZF and ZR are completely formed by P10 and are essentially similar to those of the 8 week old adult. One difference is the absence in females of a morphological X zone at P10, compared to adults. At this time diffuse pale blue staining is present in *21OH/LacZ* transgenic adrenals (section 3.3.1). This staining may reveal the presence of an X zone phenotype before the morphology becomes apparent by conventional H& E staining. However, a morphological X zone was clearly present at 8 weeks of age corresponding to pale blue staining patterns seen in adult *21OH/LacZ* transgenic adrenals (section 3.3.1).

4.4.3 Cell proliferation in the developing mouse adrenal gland

Patterns of cell proliferation in the adrenal gland have been reported for both rats and mice at various individual stages before and after birth (Mitani et al., 1999; Schulte et al., 2007) but data has yet to be reported for early postnatal stages in the mouse. Proliferating cells were uniformly distributed in the adrenal primordia at early stages (E11.5 and E13.5 fetal mice) but became concentrated in the subcapsular region in later stage fetal mouse and rat adrenals. In juveniles and adults (P7, P30 and adult rats plus 2 week old and adult mice) proliferating cells were more broadly distributed in the outer half of the cortex and declined in

number with age. (Although proliferation in 2 week old and adult mouse adrenals was described by Schulte et al., (2007) as being in 'the subcapsular layer' their figure 2 actually showed a broader region of proliferation.)

As reported in this chapter, cell proliferation in the mouse adrenal cortex at E18.5, P1 and P3 forms a condensed distribution of Ki67-positive cells that is mostly in the cortical subcapsular cell layers (corresponding to the zona glomerulosa). The proliferative region then expands into the outer half of the zona fasciculata at P10 with a huge increase in proliferating cell numbers. Further studies are needed to investigate whether the increase in cell proliferation coincides with the onset of apoptosis. In the adult (8 weeks) proliferating cells are reduced in number but are still scattered in the ZG and the outer part of the ZF. These distributions are, in each case, similar to published cell proliferation trends shown by data for the rat at E19, P1, P7 and P30 (Mitani et al., 1999), while the later embryonic and perinatal stages reported here resemble the published patterns of cell proliferation for mouse E15.5 and 17.5 (Schulte et al., 2007). The increase in cell proliferation and expansion throughout the outer half of the cortex at P10 is also probably consistent with this other study. (However, as mentioned above, there is a disagreement between the data presented for 2 week old mice by Schulte et al., (2007) and its description.)

Combined with the morphology of the developing adrenal gland reported in section 4.4.2, the cell proliferation results suggest that most zona glomerulosa cells have a significant proliferative ability at E18.5-P3 and that proliferation spreads to the outer part of the zona fasciculata by P10 but is reduced in the adult.

4.4.4 Relevance of adrenal growth, cell proliferation and zonal histology for interpreting changes in mosaic patterns

The experiments reported in Chapter 3 showed that the β-gal staining pattern in the *21OH/LacZ* transgenic adrenals changed between E14.5 and P21. The random spots at E14.5 changed to non-radial clusters of patches and spots (before birth), radial arrays (P0-P5), combinations of radial patches and stripes (P7 and P10), predominantly stripes (P14) and eventually entirely stripes (P21 to adult). Some of the observations made on adrenal growth, histological changes and patterns of cell proliferation help to understand how the changes in mosaic patterns may arise. Table 4.3 relates changes in β-gal staining to changes in adrenal growth, H&E morphology and location of Ki67-positive cells.

Table 4.3 Summary of changes in β-gal staining, H&E morphology and location of Ki67-positive cells

Age	**β-gal staining pattern** (Chapter 3)	**Growth ?**	**H&E morphology**	**Main location of Ki67-positive cells**
E18.5	Non-radial mosaic clusters	Yes	Incomplete outline of column ZF	1-3 subcapsular layers
P1	radial arrays	Yes	Incomplete outline of arch ZG & column ZF	2-3 subcapsular layers (ZG)
P3	radial spots and patches	Yes	Incomplete outline of arch ZG & column ZF	2-3 subcapsular layers (ZG)
P10	Continuous radial stripes and patches	Yes	Fully formed ZG, ZF & ZR. Clear cortical medulla boundary	ZG + outer half of ZF
Adult	Continuous radial stripes	NA	Fully formed ZG, ZF & ZR. Vacuolated X zone	ZG + outer third of ZF

NA = not applicable.

The adrenal gland grows throughout the period when stripes emerge (P0-P10) and the Ki67 experiment proliferation marker shows that adrenocortical cells are proliferating at all stages investigated, although during this period proliferation expands from a subcapsular location to include the outer half of the ZF. This is consistent with a role for cell proliferation and continuing growth of the adrenal cortex in stripe emergence but does not prove that cell proliferation or growth is necessary.

In Chapter 3 it was suggested that the change from clusters of patches and spots at E18.5 to radial arrays of spots and patches at P5 and then the emergence of stripes between P5 and P7 could possibly be explained by radial cell elongation, radial cell proliferation, edge-biased growth or by radial information (e.g. cortical morphology, blood vessel and nerve integration) somehow influencing the radial mosaic pattern. Histology showed that radial columns of cells in the zona fasciculata forming at E18.5, were almost complete by P3 and fully formed by P10. Unfortunately, there was insufficient time to investigate distributions of blood vessels and nerves or whether radial cell-elongation or radially orientated cell divisions occurred (e.g. during ZF column formation).

The possible effects of different cell proliferation distributions on mosaic pattern formation (from around P0 to P10) were considered in Fig 3.7. The subcapsular location of most Ki67-positive cells from E18.5 to P3 excludes the model shown in Fig 3.7D (cell proliferation throughout the cortex) but this model is also inconsistent with stripe formation. More significantly, the subcapsular pattern of proliferation also excludes the models illustrated in Fig. 3.7A (proliferation restricted to inner cortex) and Fig. 3.7C (proliferation restricted to central cortex). The pattern of Ki67-postive cells supports the model illustrated in Fig. 3.7B (proliferation restricted to outer cortex). Ki67-positive cells were not entirely restricted to the sub-capsular region so this represents edge-biased growth rather than strict edge growth. Nevertheless edge-biased growth is proposed to generate stripes in other mosaic systems (see section 1.5). Cell proliferation was predominantly in the sub-capsular region at E18.5 before the first radial patches

emerged at around P3 but there is likely to be a lag of several cell generations between the onset of edge-biased growth and the visible appearance of stripes.

The radial arrays of spots and patches that emerged between P0 and P5 were not clearly confined to the outer edge of the cortex. This may be partly because proliferation was not entirely confined to the edge (as noted above) and partly for other reasons. For example, inclusion of β-gal-positive cortical cells in the central medullary region at early stages will contribute to the impression of a randomly orientated mosaic central region but they will be lost from the centre as the boundary between the cortex and medulla matures (see section 4.3.2). Similarly, the loss of the medulla cells from the cortical region may contribute to the emergence of the radial pattern. Also, changes in morphological constraints (such as blood capillaries, nerves or extracellular matrix) may impose some radial direction to cell proliferation or cell shape and produce a radial arrangement of cells. By the time the Ki67-positive cell region expanded to include the outer half of the ZF as well as the ZG at P10, some continuous radial stripes were already apparent and cortical morphology was clear.

The hypothetical model of stripe formation shown in Fig 3.8 proposed that formation of continuous radial stripes involved several phases. (1) The initial phase involves outward extension of stripes by edge-biased growth (Fig 3.8A-C). (2) Subsequently, inner cells are removed by cell death near the medulla causing the stripes to extend towards the medulla (Fig 3.8D-E). In parallel with this (but not necessarily beginning at the same time) the proliferative region may expand. If proliferation is entirely within the stripe, cell death will eventually remove the inner mosaic pattern so that the stripe will span the entire cortex. (3) In the adult the adrenal stops growing and cell proliferation is balanced by cell death (Fig 3.8F). If cell proliferation is mostly in the outer cortex and cell death is in the inner cortex there will be net inward movement of cells.

The concentration of cell proliferation in the subcapsular region at E18.5 to P3 is consistent with edge-biased growth in the first phase driving stripe formation.

Subsequently the expansion of the proliferative region at P10 probably reflects the onset of cell proliferation associated with inward cell migration. Therefore, because the adrenal is still growing, in phase 2 stripe formation is likely to be driven by a combination of cell migration and edge-biased growth. There was insufficient time to investigate whether cell death occurs near the medulla at around P10 but there is already evidence that apoptosis becomes concentrated towards the inner cortex by postnatal day 10 in the rat (see section 1.2.4), although no comparable studies have been reported for the mouse.

The adult radial stripe pattern is completely formed by P21 and is almost mature by P14 but at P10 it is still a mixture of patches and radial stripes (chapter 3). Cell proliferation in the adult is largely confined to the outer third of the cortex whereas the proliferative region appears broader at P10. However, the apparent decrease in the width of the proliferative region from half to a third of the ZF probably reflects the increase in size of the ZF so that a similar-sized proliferative region occupies a smaller proportion of the outer ZF (Fig. 4.7). The similarity between the width of the proliferative region in the outer cortex between P10 and adult (8 weeks) in the mouse (Fig 4.7) suggests the adult pattern of cell proliferation probably begins to be established before the adult stripe pattern matures between P14 and P21.

4.4.5 Coordination of changes in *21OH/LacZ* mosaic patterns with the physiology of adrenocortical growth and development

The previous section (4.4.4) deals mainly with the timing and possible growth mechanisms underlying emergence of mosaic stripes in the period E14.5-P21. However, because the mouse adrenal cortex undergoes a number of dynamic physiological changes during this period, it is also important to relate the changes in mosaic patterns to adrenocortical physiology. This may identify functional correlations that could be explored in the future. As mentioned in chapter 1, the peptide hormone ACTH has dual roles in the regulation of steroid hormone synthesis in response to physiological stimuli and also in trophic regulation of the adult adrenal cortex. However, ACTH may not be the principal physiological mitogen during adrenocortical development. This role has been attributed to the various peptides produced locally in the adrenal cortex by tissue-specific processing of cleavage products of the pro-opiomelanocortin precursor molecule from which ACTH is also derived. (Published data reviewed in Estivariz et al., 1992; Keegan and Hammer, 2002 are derived mainly from the rat but may also be relevant to mouse.) Nevertheless, ACTH and corticosterone can be measured as circulating hormones in the mouse and can therefore be used as an index of HPA axis maturity during adrenocortical development (Schmidt et al., 2003). In this section, physiological and functional changes occurring in the mouse adrenal cortex over the period E14.5-P21 are compared with changes in *21OH/LacZ* mosaic patterns, as summarised in Table 4.4.

Table 4.4 Coordination of changes in mosaic pattern with the physiology of adrenocortical growth and development

Age	Adrenocortical development and zonation	21OH/LacZ mosaic pattern	Cell division (hyperplasia)	Cell size (hypertrophy)	HPA axis and adrenocortical physiology
Up to E17.5	Integration of medullary precursors (from E12.5). Encapsulation (E14.5). Expansion of definitive cortex (from E14.5).	Randomly orientated patches and spots	Changes from scattered distribution (at E13.5) to subcapsular region (from E15.5) [1].	N/A	Adrenocortical ACTH receptor-positive cell numbers increased[1] **.
E17.5-18.5	First appearance of a basophilic ZG.	Randomly orientated patches and spots	Proliferation in 1-3 subcapsular layers (edge-biased growth).	N/A	Adrenocortical ACTH receptor-positive cell numbers increased[1] **. Increase in serum ACTH and corticosterone levels.
P0-7	Rapid development of classical zonated adrenocortical structure. Columnar ZF structure emerging.	Emergence of radial arrays of patches and spots.	Proliferation in 2-3 subcapsular layers (edge-biased growth).	No apparent change*.	Stress hypo-responsive period (high serum CRH but low ACTH and corticosterone). P1-9 [2].
P8-21	ZG, ZF & ZR similar to adult pattern by P10. First appearance of the X zone (P14).	Predominantly radial stripes by P14 and entirely stripes by P21.	Proliferation in ZG and outer half of ZF (P10)	N/A	Adult-like HPA axis (from P12). Elevated serum ACTH & corticosterone in response to CRH [2]. Adrenocortical ACTH receptor-positve cells further increased (at P14) [1]**.
3-7 weeks	ZG, ZF & ZR similar to adult pattern. X zone regression at puberty in males but maintained until first pregnancy in females.	Radial stripes.	Cell numbers increase in ZF [3].	ZF cells increase in volume in males [3].	Serum corticosterone decreases (weeks 3-11). SCC and 11β-OHase increase [3].
Adult	ZG, ZF & ZR adult pattern. X zone regression in females following first pregnancy.	Radial stripes	Proliferation in outer 40% of cortex. Cell number increases in ZF [3].	ZF cells increase in volume (mostly in females) [3].	Serum corticosterone decreases (weeks 3-11). SCC, 11β-OHase and stored lipid increase between weeks 7 & 11 [3].

* Preliminary cell size measurements on small areas of tissue showed no marked differences between E18.5 and P10 in cell size but this needs to be repeated. ** Adrenocortical ACTH receptor mRNA-positive cells as a proportion of total DAPI-positive cells numbers. *Abbreviations:* N/A, Not available. *References:* 1. Schulte *et al.,* 2007; 2. Schmidt *et al.,* 2003; 3. Bielohuby *et al.,* 2007.

At fetal stages up to E17.5 neural crest-derived medullary precursors are integrated into the adrenal gland, followed by encapsulation. This is accompanied by expansion of the definitive cortex starting around E14.5. This expansion is reflected in the changing pattern of cell division, from scattered proliferation throughout the developing adrenal gland to a subcapsular localisation from around E15.5 (Schulte et al., 2007). Meanwhile, the *21OH/LacZ* mosaic pattern comprises randomly orientated spots and patches during this period. Also, localisation of cell proliferation to the sub-capsular region coincides with an increase in ACTH receptor-positive cells. However, the distributions of proliferative cells and 3β-hydroxysteroid dehydrogenase/ACTH receptor-positive cells indicate that they are different groups of cells, representing distinct non-overlapping populations of relatively undifferentiated precursors and more differentiated steroidogenic cells (Schulte et al., 2007). Between E17.5 and E18.5, an increase in serum ACTH levels, indicating enhanced HPA activity, coincides with a generalised upregulation of steroidogenic gene expression and the emergence of the ZG. It is possible that emergence of the ZG could be driven by the local action of ACTH on a specific group of precursor cells (reviewed in Vinson, 2003), but a functional correlation has yet to be established.

From postnatal P0 to P7, emergence of the radial mosaic pattern is coordinated with formation of the cortical zones and coincides with the so-called 'stress hypo-responsive period', lasting from P1 to P9 in the mouse. This is characterised by low plasma corticosterone levels and little increase in ACTH and corticosterone release in response to stress, though adult-like basal ACTH levels are maintained (Schmidt et al., 2003). However, it is not clear that the stress hypo-responsive period is relevant to the changes in mosaic pattern or zonation, though it would be interesting to investigate whether or not maintenance of basal ACTH levels is important for maintaining adrenal growth during this period. Later on, from P8 to P21, the region of proliferation in the adrenal cortex becomes broader and this occurs around the end of the stress hypo-responsive period (P10). However, since basal ACTH levels are unchanged even beyond the end of the stress hypo-

responsive period (Schmidt et al., 2003), it seems unlikely that ACTH drives the change in distribution of cell proliferation. By P10 the pattern of zonation has matured and is similar to the adult, this coinciding with maturation of the adult-like HPA axis (Schmidt et al., 2003), the change in distribution of cell proliferation and maturation of the mosaic stripe pattern (described in this thesis) over the period P7-14. At around this time, cells from the fetal zone become concentrated at the medullary-cortical boundary (Zubair et al., 2006) and most stripes extend across the full thickness of the cortex. This suggests that stripes extend towards the medulla by inward displacement of cells as older fetal adrenocortical cells condense at the cortical-medullary boundary and/or are removed by apoptosis and that this process may drive the emergence of the morphological X zone.

By post-weaning stages, the HPA axis, stripe pattern and zonation are well-established. The adrenal gland continues to grow until the adult stage and this is involves a combination of hyperplasia and hypertrophy (Bielohuby et al., 2007) rather than primarily hyperplasia (as at earlier stages).

Overall, the dynamic changes in adrenocortical cell proliferation and mosaic stripe patterns between E14.5 and P21 are not well correlated with basal ACTH levels, which remain broadly similar from P1. Also, in general, proliferating cells do not have ACTH receptors. Therefore, it seems probable that steroidogenesis is regulated partly by plasma ACTH levels and partly by ACTH receptor availability but adrenocortical cell proliferation (and by implication the *21OH/LacZ* mosaic pattern) is regulated by other aspects of adrenocortical physiology.

In conclusion, a combination of the results presented in chapters 3 and 4 together with various published studies on mouse adrenal development have revealed the coordination of several different cellular and physiological changes that occur during adrenal development and maturation.

4.5 Conclusions

The experiments described in this chapter support the hypothesis that edge-biased growth contributes to the emergence of stripes described in Chapter 3 but further studies are required to more fully understand how stripes emerge.

5 Maintenance of the adult adrenal cortex

5.1 Introduction

So far, chapters 3 and 4 have focused on organogenesis of the adrenal cortex (when and how the *21OH/LacZ* mosaic pattern changed and radial stripes formed in the adrenal cortex). Chapters 5 and 6 are concerned with the maintenance of the adult adrenal cortex. Chapter 5 also considers whether stem cells are involved in this tissue maintenance process, as they are in many other tissues. Since 1883, when the idea of the centripetal movement was first suggested to have a role in maintenance of the adrenal cortex (Gottschau, 1883; reviewed in Kim and Hammer, 2007), several hypotheses for adrenocortical maintenance have been described. The following five hypotheses were reviewed in section 1.4.3: (a) centripetal movement, where all three zones are maintained by a single population of stem cells in the outer cortex that produces daughter cells which move centripetally; (b) 'walking stick' maintenance where cells from the ZG/ZF boundary region may first move outwards into the ZG and then loop inwards into the ZF; (c) zonal maintenance, where the three zones are maintained separately (e.g. by their own separate stem cell populations); (d) zona intermedia, where stem cells in the zona intermedia maintain the cortex by bidirectional cell movement and (e) maintenance by stem cells located within the capsule.

Most work has shown that the main region of cell proliferation is in the outer cortex (Belloni et al., 1978; Mitani et al., 2003; Zajicek et al., 1986), cells tend to move inwards (Zajicek et al., 1986) and most apoptosis occurs close to the medullary boundary (Breidert et al., 1998; Carsia et al., 1996; Mitani et al., 1999). This makes the zonal maintenance (Fig. 1.11 c) and zona intermedia models (Fig. 1.11 d) less likely. Also, the ability of an enucleated adrenal cortex to regenerate a new cortex with a normal histological appearance and cortical zonation, with the suggestion that all three regenerated zones arise from a common precursor in the

periphery (section 1.4.2), does not support the zonal maintenance and zona intermedia hypotheses.

Most hypotheses for adrenocortical maintenance are based on the location of proliferative cells and the movement of labelled adrenocortical cells, as well as the distinct zonal morphologies and the region of the gland in which cell apoptosis occurs. In several cases in the literature the locations of stem cell populations have been predicted mainly by the location of proliferative cells. However, proliferation is not specific to stem cells and will also identify TA cells, which may in any case proliferate more frequently than stem cells (section 1.3.). There are currently no known cell markers that specifically identify adrenocortical stem cells. However, other methods, based on the general characteristics of adult stem cells have been used to identify stem cells in some other tissues. For example, the infrequent division of many stem cells means they can often be identified as label-retaining cells, following labelling with the thymidine analogue BrdU and a chase period which dilutes the label more slowly in stem cells than most other cell types, (Cotsarelis et al., 1989; see section 1.3.2.2). This provides a useful first step towards trying to identify stem cells in the adrenal cortex.

5.1.1 Experimental aims

The main aim of this chapter was to use BrdU labelling to identify (i) where cells in the adrenal cortex divide, (ii) whether cells move (and, if so, in which direction) and (iii) whether a label-retaining cell population can be identified, to help recognise putative adrenocortical stem cells. It was anticipated that this information would help to distinguish between some of the hypotheses of adrenocortical maintenance discussed in section 1.4.3 and illustrated in Fig. 1.11.

5.2 Materials and methods

5.2.1 Analysis of cell movement with BrdU single injection

Adrenal glands from mice given a single injection of BrdU were used to study (i) the main location of proliferating cells (soon after the injection) and (ii) the direction of cell movement, by identifying the main location of BrdU-positive cells at intervals after the injection. Both male and female wild-type (C57BL/6 x CBA/Ca)F1 mice were given single intraperitoneal (i.p.) injections of BrdU (10 mg BrdU/ml saline; 0.2ml/mouse) at the age of 12 weeks. After specific chase times (4 hours after BrdU injection (0 weeks) and 1, 3, 5, 8 and 15 weeks) the mice were killed and adrenal glands were prepared for immunohistochemical detection of BrdU-labelled proliferative cells, as described in section 2.8. Seven micron sections of wax-embedded adrenals were labelled by immunohistochemical staining for BrdU. Sections were then counterstained with haematoxylin (see section 2.9). The middle longitudinal sections of adrenals were photographed with a Nikon Coolpix 995 digital camera mounted on a Zeiss Axioplan 2 compound microscope. Five adrenals (2 female and 3 male) were analysed for the 8 week chase group and 6 adrenals (3 males and 3 females) were analysed for the other groups.

BrdU-positive cells were identified in calibrated digital images of immunohistochemical staining as having nuclear-localised brown DAB staining. The position of each positive cell was measured relative to the outside of the capsule and the boundary of cortex and medulla by imageJ software, using 2 different methods (see section 2.10.1). In this way the location of BrdU-positive cell could be expressed either as an absolute distance from either boundary or as a percentage of the distance from the capsule to the medullary boundary.

5.2.2 Detection of slow-cycling cells with longer exposure to BrdU

Prolonged exposures of adrenals to BrdU were used to identify and locate the BrdU label-retaining cells. Wild-type (C57BL/6 x CBA/Ca) F1 mice were treated

with BrdU solution (50mg BrdU/ml saline) administered via implanted Alzet osmotic mini-pumps (see section 2.1.4) to label proliferative cells over periods of either one or two weeks (described in section 2.1.4). After specific chase periods, the mice were killed and adrenal glands were dissected and processed for BrdU immunohistochemical staining to detect the BrdU label retaining cells (see section 2.9). In a preliminary study, six adult female mice were exposed to BrdU labelling for one week and adrenals were examined after a chase period of 0 (0), 35 (5), 49 (7), 63 (9), 85 (12.1), 105 (15) or 136 (19.4) days (weeks). In a later experiment, groups of 12 week old (C57BL/6 x CBA/Ca)F1 female and male mice were exposed to BrdU for 2 weeks, and the adrenals were examined after chase periods of 0, 6, 18 or 23 weeks. For groups of female and male mice, adrenals from two mice were examined for 0 and 6 week of chase periods, while adrenals from three mice were examined for 18 weeks and five mice were examined for 23 weeks of chase periods. Because of time constraints only female left adrenals were analysed quantitatively.

For each adrenal gland, an area of cortex that was 330-400µm thick with approximately parallel inner and outer boundaries was selected for measurement, in the calibrated digital images of BrdU immunohistochemical staining. Rounded nuclei, typical of steroidogenic cells, were classified as BrdU-positive or BrdU-negative. Cells with an obviously elongated vascular morphology were excluded from the analysis. The positions of BrdU-positive and negative cells were marked on a superimposed 10 × 10 grid and their numbers counted with imageJ software (see section 2.10.2).

5.3 Results

5.3.1 Dynamics of cell proliferation and movement in the adrenal cortex

Adrenal glands dissected 4 hours following a single injection of BrdU were used to identify sites of proliferation in the adrenal cortex, while glands collected at various intervals (1, 3, 5, 8 and 15 weeks) after a single injection were analysed to monitor possible movement of cells away from sites of proliferation.

Fig. 5.1 and Fig. 5.2 show that BrdU label was retained in cells in the adrenal cortex at various intervals (0, 1, 3, 5, 8 and 15 weeks) after a single BrdU injection. Four hours after the BrdU injection (shown as 0 weeks) labelled cells are located principally in the outer part of the cortex, suggesting that this may be the major site of proliferation, with few if any labelled cells detected in inner region of the cortex. At later times, labelled cells can be detected mainly in mid and inner regions of the cortex implying cell movement has occurred, though a few labelled cells seem to remain in the outer cortex. BrdU-labelled cells appeared in similar locations in left and right adrenals from males and females (compare Figs. 5.1 and 5.2) so, due to time constraints, female left adrenals were used for further quantitative analysis of the positions of labelled cells.

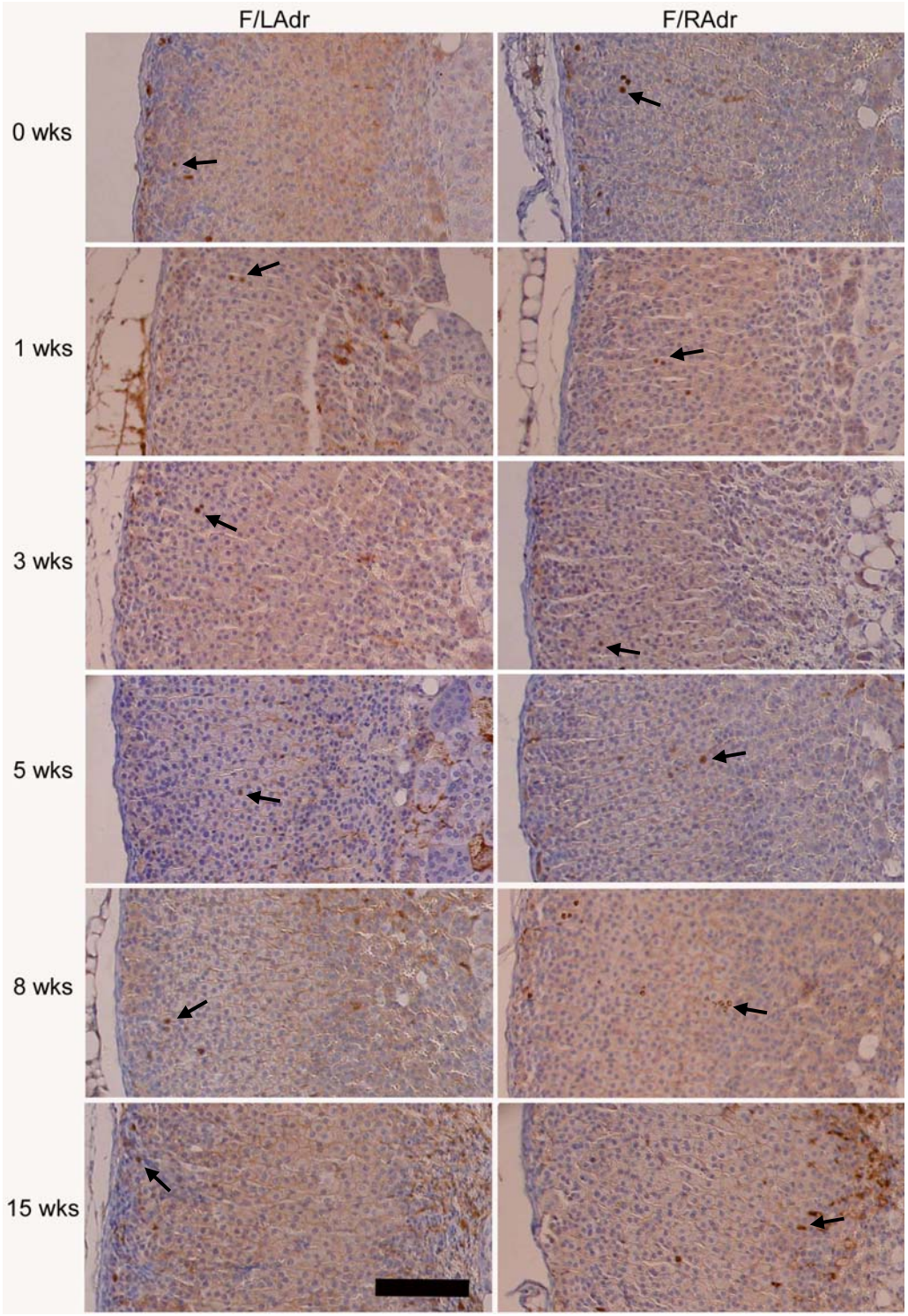

Fig. 5.1. Distribution of BrdU-labelled cells in female adrenals.
Immunohistochemical detection (section 2.9) of BrdU-positive cells in F1 female adrenals at intervals after a single BrdU injection, at the age of 12 weeks. Adrenals were obtained 4 hours after injection (0 weeks) and following chase periods of 1, 3, 5, 8 and 15 weeks. Scale bar = 0.1mm. Arrow, labelled cell.

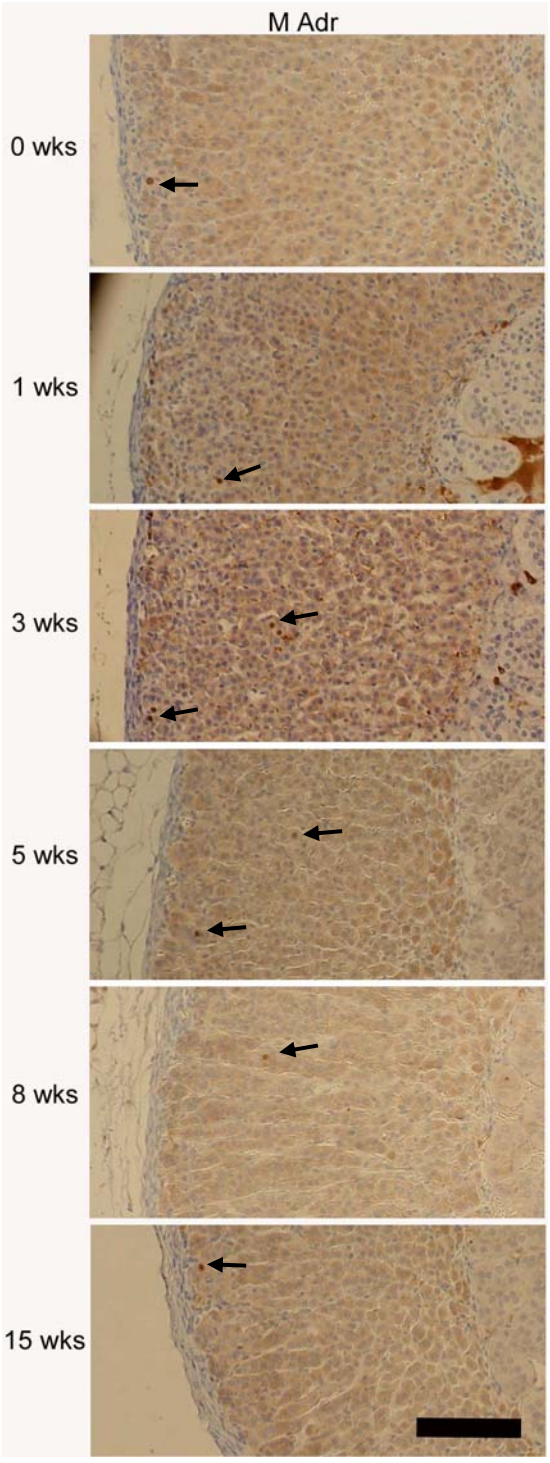

Fig. 5.2. Distribution of BrdU labelled cells in male adrenals.
Immunohistochemical detection (section 2.9) of BrdU-positive cells in F1 male adrenals at intervals after a single BrdU injection, at the age of 12 weeks. Adrenals were obtained 4 hours after injection (0 weeks) and following chase periods of 1, 3, 5, 8 and 15 weeks. Arrow, labelled cell. The distribution is similar to female (Fig. 5.1). Scale bar = 0.1mm.

5.3.1.1 Comparison of different methods of measuring the positions of BrdU-positive cells

As described previously in section 2.10.1, two methods were compared for estimating the positions of BrdU-labelled cells: (a) the shortest distance between the BrdU-positive cell and the outside of the capsule plus the shortest distance between the BrdU-positive cell and the boundary of the cortex and medulla and (b) the shortest straight line distance from the outside of the capsule to the inner boundary of cortex that intersects the BrdU-positive cell. In each case the position of each BrdU-positive cell was measured relative to both the capsule and the inner cortical boundary, so that the location could be expressed either as an absolute distance from boundary or as a percentage of the distance from the capsule to the inner cortical boundary.

Comparison of the percentage distance from the capsule to the inner cortical boundary, produced by the two measurement methods, show that they correlated well (Fig. 5.3). For 3 out of 763 BrdU-positive cells, the two methods estimated positions that differed by more than 10% of the distance from the capsule to the medullary boundary. This arose because these three cells were all from the same region of one adrenal, in which there was a nodule on the outside of the capsule. Method (b) had included the nodule in the distance measurements whereas method (a) had measured BrdU-positive cells to a different part of the capsule to produce the shortest distance. Consequently, these three anomalous cells were excluded from the quantitative analysis.

For the remaining 760 cells the mean differences in estimated position was 0.45% of the distance between the capsule and the medullary boundary and the maximum difference between the two estimates was 5.94%. It was expected that method (b) would, on average, produce slightly higher estimates of the percentage distance from the capsule because method (a) specifically used the shortest distance between the capsule and medulla. For 495 of the 760 cells, method (b) did produce a higher estimate of the percentage distance from the capsule (mean

difference = 0.76%; maximum= 5.94%) but for 150 cells both methods produced exactly the same estimate and in 115 cases method (a) produced a higher estimate (mean difference = 0.33%; maximum= 1.03%). The overall agreement between the two methods was very good (Fig. 5.3) and it was decided to use method (b) (the shortest straight line distance from the outside of the capsule to the inner boundary of cortex that intersects the BrdU-positive cell) because this was simpler. The quantitative analysis of cell position was, therefore, based on the percentage distance from adrenal capsule to medulla estimated by method (b), excluding the three anomalous cells mentioned above.

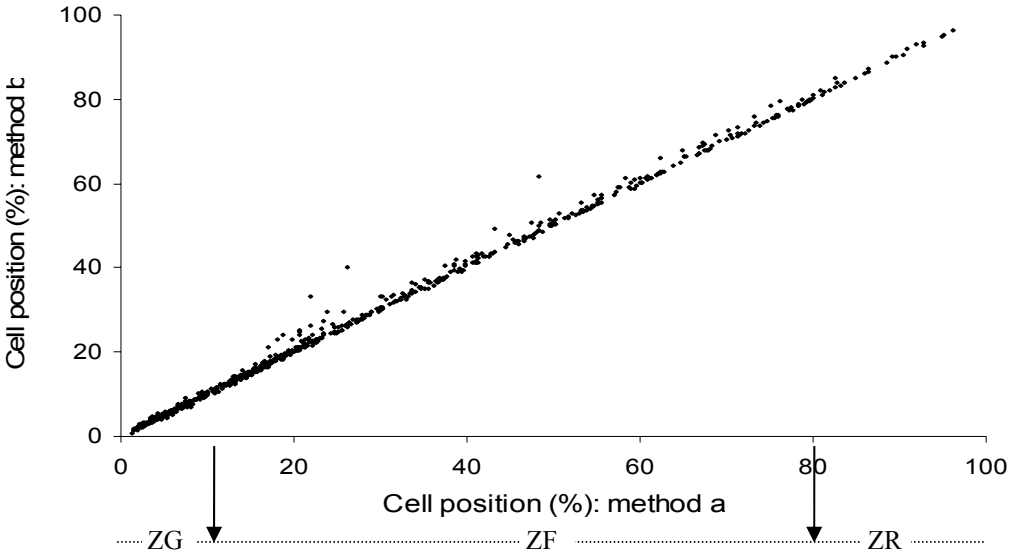

Fig. 5.3. Correlation of 2 methods for estimating positions of 763 labelled cells (percentage distance from capsule). X axis: (a) the shortest distance between the BrdU-positive cell and the capsule plus the shortest distance between the BrdU-positive cell and the boundary between the cortex and medulla. Y axis: (b) the shortest straight line distance from the capsule to the inner boundary of cortex that intersects the BrdU-positive cell. Measurements were carried out on BrdU-labelled sections of female left adrenal glands as described in section 2.10. Approximate positions for boundaries between ZG, ZF and ZR determined during the analysis are shown by arrows. The two methods showed a highly significant correlation ($r=0.999$, $P<0.0001$).

5.3.1.2 Identification of the main region of cell proliferation

Following single BrdU injections and different chase times (0, 1, 3, 5, 8 and 15 week), the positions of BrdU-labelled cells in female left adrenals were estimated as the percentage distance along the shortest straight line distance from the outside of the capsule to the medullary boundary (method b). Figs. 5.4 and 5.5(a) show that at 0 weeks (4 hours after BrdU injection) most labelled cells (147/153= 96%) are within 40% of the distance from the outside of the capsule. This outer 40% will be called the 'proliferative region' and the remainder (≥40% from the capsule) termed the 'non-proliferative region'. The histogram shown as in Fig. 5.5(a) indicates that within this outer 40%, the peak area of cell proliferation occurs between 5% and 25% from the capsule (112/147 cells = 76%).

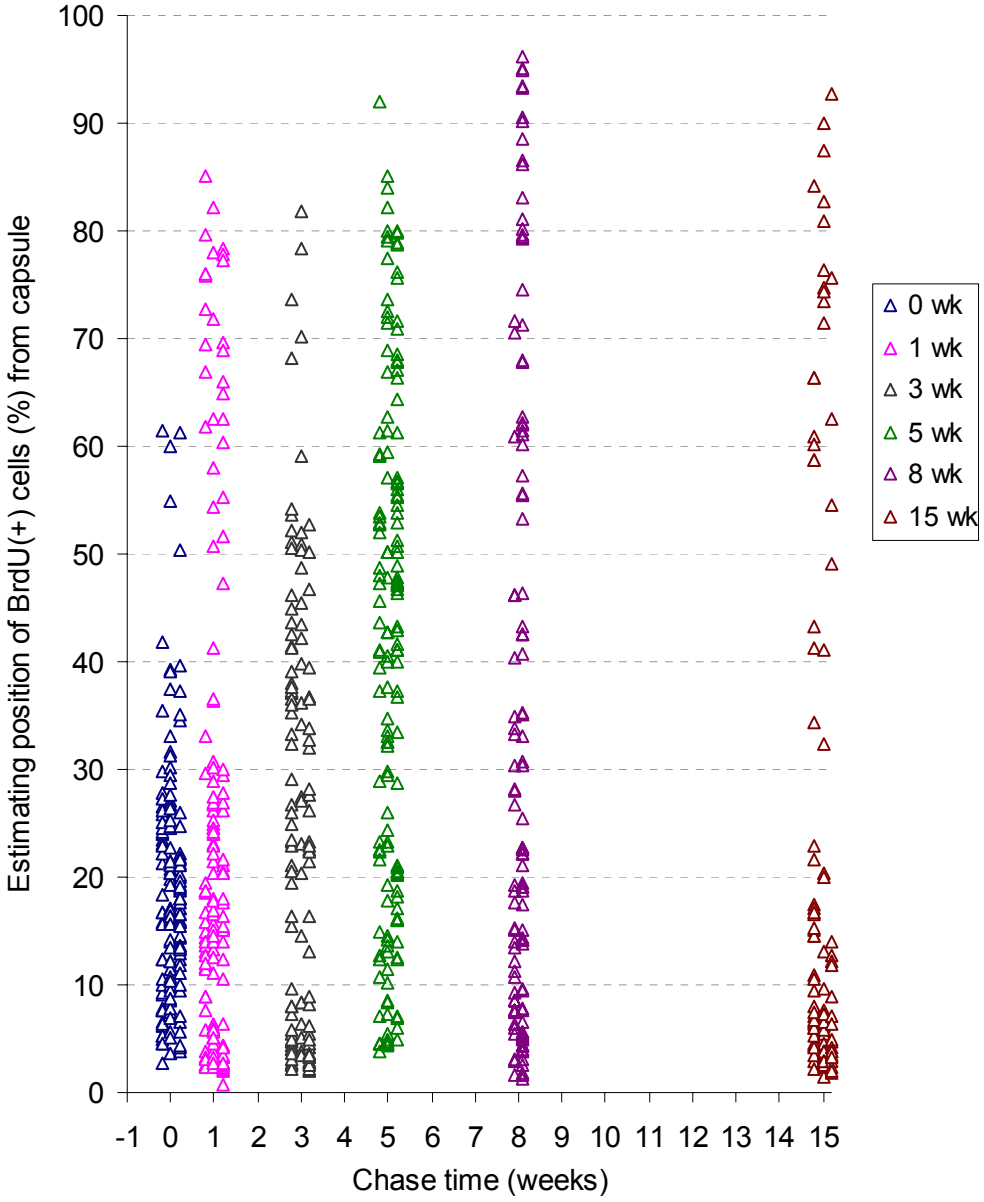

Fig. 5.4. Estimated positions of BrdU-labelled cells in the female left adrenal cortex after different chase periods following a single BrdU injection.
Positions of BrdU-labelled cells (% distance from capsule) were estimated by method (b), as described in section 5.3.1.1. After a single BrdU injection, middle sections of 3 female left adrenals were examined following chase periods of 0, 1, 3, 5 and 15 weeks, while 2 adrenals were examined following 8 week chase time BrdU-labelled cells were detected immunohistochemically as described in section 2.9. Data points are shown as follows: 0 week, blue; 1 week, pink; 3 week, black; 5 week, green; 8 week, purple and 15 week, brown colour.

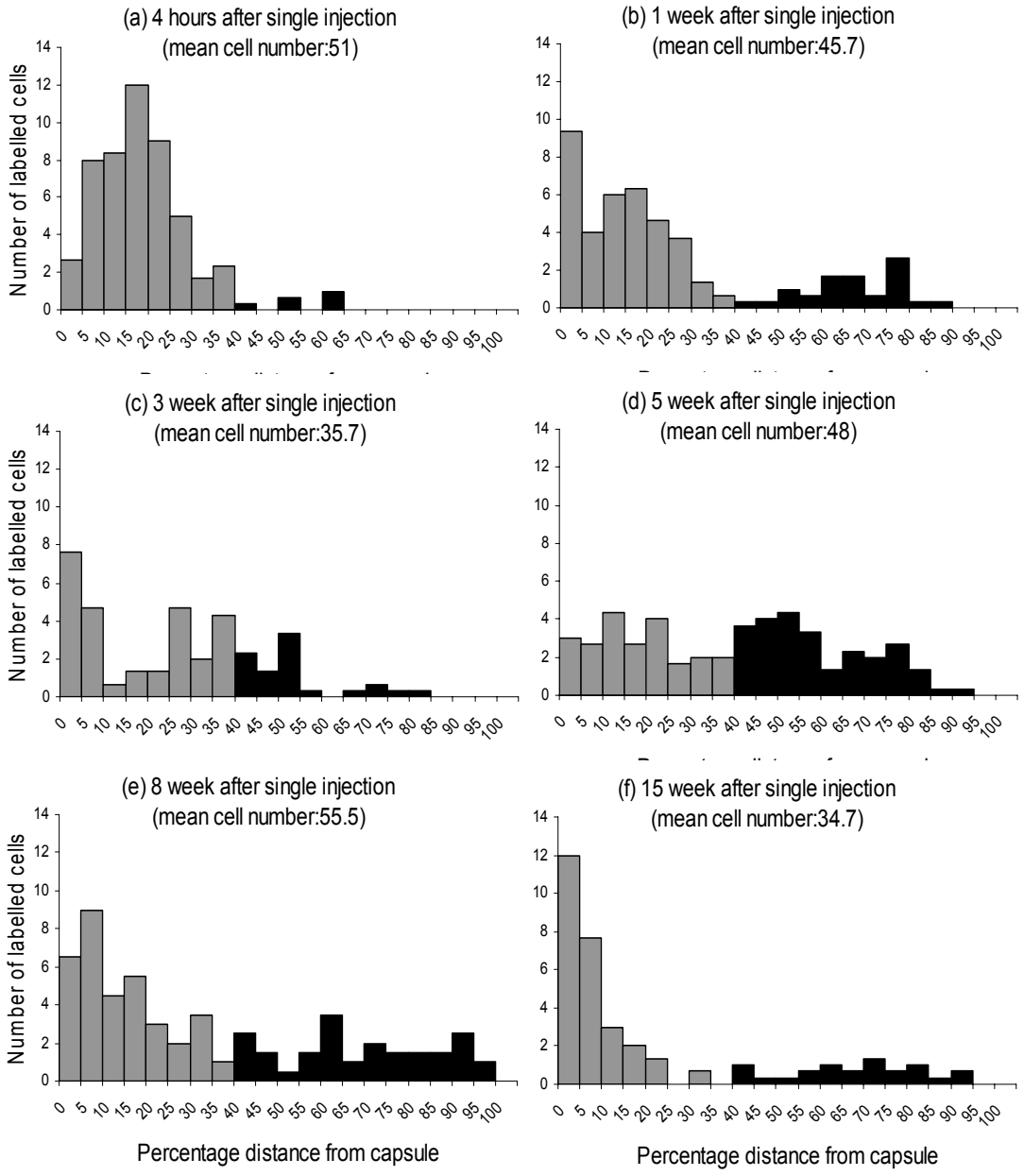

Fig. 5.5. Distribution of BrdU-labelled cells in the female left adrenal cortex following different chase periods after a single BrdU injection. (a) 4 hours, (b) 1 week, (c) 3 weeks, (d) 5 weeks, (e) 8 weeks and (f) 15 weeks. Data from the experiment described in Fig. 5.4 was re-plotted over 5% distance intervals from the outside of the capsule to the cortical medullary boundary. The 'mean cell number' represents the average number of BrdU-postive cells per section. For (e) N=2; for all others N=3. Grey bar, <40% distance from the outside of the capsule; black bar, ≥40% distance from the outside of the capsule.

5.3.1.3 Evidence for cell movement within the adrenal cortex 1 week after BrdU labelling

The positions of BrdU-labelled cells after different chase periods are shown in Fig. 5.4 and plotted as histograms in Fig. 5.5 a-f. After a one week chase period there was a significantly higher frequency of labelled cells in the non-proliferative region (≥40% of the distance from the capsule) than at 0 weeks (29:108 versus 6:147; $\chi^2 = 18.67$; $P<0.001$), suggesting movement towards the medulla (Fig. 5.5 a and b). There were also more labelled cells within 5% of the capsule (28:109 versus 8:145; $\chi^2 = 14.01$; $P<0.001$), suggesting cells may either move towards the capsule or proliferate in this outermost region (the outer 20 μm). However, the overall frequency of labelled cells within 10% of the capsule (outer 40 μm) did not change significantly (40:97 versus 32:121; $\chi^2 = 2.23$; $P>0.05$) during this time period. This implies that there is no net outward movement of labelled cells to the outer 10% of the cortex from regions further into the cortex, but cells may move from a position between 5 and 10% from the capsule to within 5% of the capsule (a mean distance of about 20 μm). The statistical tests were based on the total numbers of labelled cells in each region but only three adrenals were examined for each of these chase periods. This may be too few adrenals to draw reliable conclusions about small movements. In addition, any damage to the capsule will affect the precision of measurements of cells close to the capsule. Further work is needed to evaluate the possibility of outward movement. Therefore, while it is clear that cells move towards the medulla within a week of labelling, it is less clear whether cells also move towards the capsule as predicted by the model illustrated in Fig. 1.11d.

5.3.1.4 Locations of BrdU-positive cells 3-15 weeks after labelling

It is more difficult to interpret the distributions of BrdU-labelled cells after longer chase periods (Fig. 5.4 and Fig. 5.5 c-f) because the number of labelled cells may increase by cell division (until BrdU is diluted below the detectable limit) and the labelled cells may move or die.

Figs. 5.4 and 5.5 show that between 3 and 5 weeks, the BrdU-labelled cells continue to spread towards the inner cortex and by 5 weeks, they are nearly equally distributed throughout most of the cortex (in both proliferative and non proliferative regions). At 8 weeks the BrdU-labelled cells remain spread throughout the cortex but with a slightly increased frequency within 20% of the distance from the capsule. Finally, 15 weeks after BrdU injection, labelled cells are thinly scattered throughout most of the cortex but remain much more abundant close to the capsule.

Several trends are suggested by the results shown in Fig. 5.6. Although only a few adrenals were examined and the trends are not statistically significant they have identified possibilities that could be investigated in more detail in future studies. Between 0 and 3 weeks, the number of BrdU-labelled cells per adrenal section declines in the proliferative region (<40% capsule-medulla distance; grey bars), but increases nearer the medulla (≥40% capsule-medulla distance; black bars), suggesting net movement towards the medulla. Overall, the total number of labelled cells (total height of bars) falls during this period which probably reflects death of cells near the medulla. (This decrease is unlikely to reflect dilution of BrdU below the detectable limit because cells produced by the first few cell divisions are still likely to be detectable as BrdU-positive cells. Therefore cell division should initially cause an increase in the frequency of BrdU-labelled cells, as suggested below for the 3-8 week interval.)

From 3 to 8 weeks the total number of BrdU-labelled cells per section increases, suggesting that BrdU-labelled cells divide again and that the increase in cell number exceeds cell death during this period. The overall increase in labelled cells between 3 and 8 weeks is accompanied first by an increase in numbers in the non-proliferative region at 5 weeks (suggesting that initially the gain of cells by cell division in the proliferative region is exceeded by movement of cells to the non-proliferative region). There is then an increase of labelled cells in the proliferative region at 8 weeks. This is consistent with a second wave of cell proliferation and continued migration towards the medulla.

Between 8 and 15 weeks the total number of labelled cells and the number of labelled cells in the proliferative and non-proliferative regions all fell. Surprisingly, however, some labelled cells remained 15 weeks after the BrdU injection in the proliferative region close to the capsule (at an mean distance of 7.8±1.6% from the capsule; N= 3 adrenals) as shown clearly in Fig. 5.4 and 5.5. These remaining labelled cells close to the capsule may be non-migrating, less proliferative cells. For example dividing cells may have taken up the BrdU but then produced cells which stopped dividing (e.g. terminally differentiated or quiescent cells). It seems less likely that they are cells that are continuously slow cycling (such as putative stem cells, identified as label-retaining cells) because if they divided infrequently they would not be likely to be labelled by a single BrdU injection in the first place.

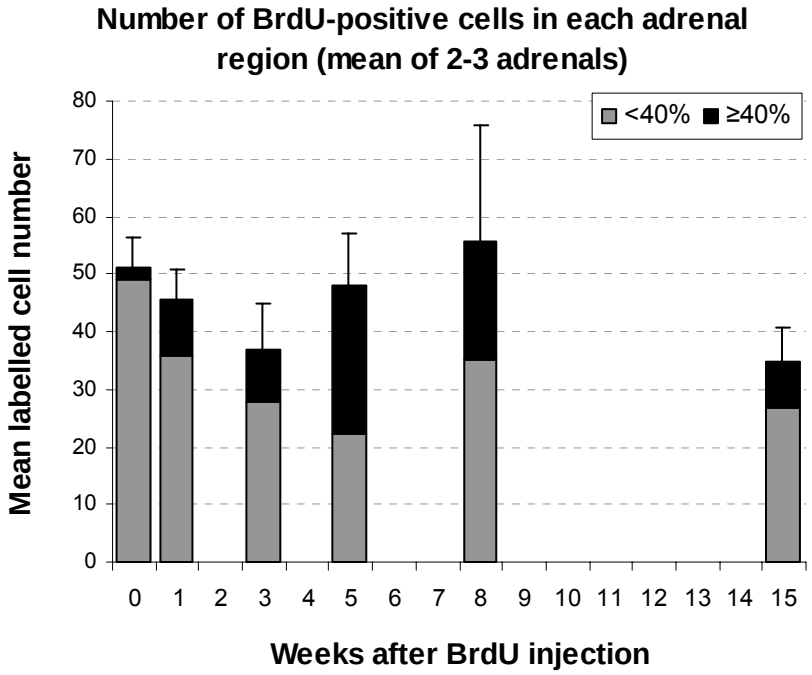

Fig. 5.6. Number of BrdU-positive cells in proliferative and non-proliferative regions of female left adrenal cortices following different chase periods after a single BrdU injection. Data on BrdU-labelled cells in female left adrenal cortices from Fig. 5.5 were grouped into proliferative (<40% capsule-medulla distance) and non-proliferative regions (≥40% capsule-medulla distance), as defined in Section 5.3.1.2. Total height of bars represents the mean number of labelled cells per section (error bars show the standard error of the mean). Grey bars, mean number of labelled cells in the proliferative region; black bars, mean number of labelled cells in non-proliferative region. Analysis of variance showed no overall significant differences for total number of labelled cells (P=0.549), the number of labelled cells in the proliferative region (P=0.060) or the number of labelled cells in the non-proliferative region (P=0.056).

5.3.2 Label-retaining cells in the adrenal cortex

Adrenals were exposed to BrdU for prolonged periods followed by a series of increasing chase periods to try to identify and locate any BrdU label-retaining cells which might include putative stem cells. This study was carried out in two parts. A preliminary experiment using one mouse for each of 7 different chase times was used to identify suitable chase periods. The final study used a longer labelling period and focused on fewer chase periods with several mice per group.

In the preliminary study, adult female mice were each implanted with a mini-pump that released BrdU for a week, and adrenals were obtained after chase periods of 0, 35 (5), 49 (7), 63 (9), 85 (12.1), 105 (15) or 136 (19.4) days (weeks). The distribution of BrdU-labelled cells was analysed in regions using a 10 × 10 grid. The images of BrdU immunohistochemical staining are shown in Fig. 5.7 and distributions of BrdU-labelled cells are shown in Fig. 5.8.

At 0 days (immediately after the one week labelling period), the labelled cells were mostly located in the outer 5 grid rows (Figs. 5.7 and Fig. 5.8), representing the outer 50% of the cortex. After a chase time of 35 days (Fig. 5.8) the overall frequency of labelled cells increased and they had spread to the inner cortex, as shown previously in the BrdU injection study described above (section 5.3.1.4). The frequency of BrdU-labelled cells declined with longer chase periods (Fig. 5.8). However, even after a chase period of 136 days some BrdU-labelled cells remained although these were not localised in a particular region (Fig. 5.8). It was therefore decided to extend the chase period beyond 19 weeks for the main experiment.

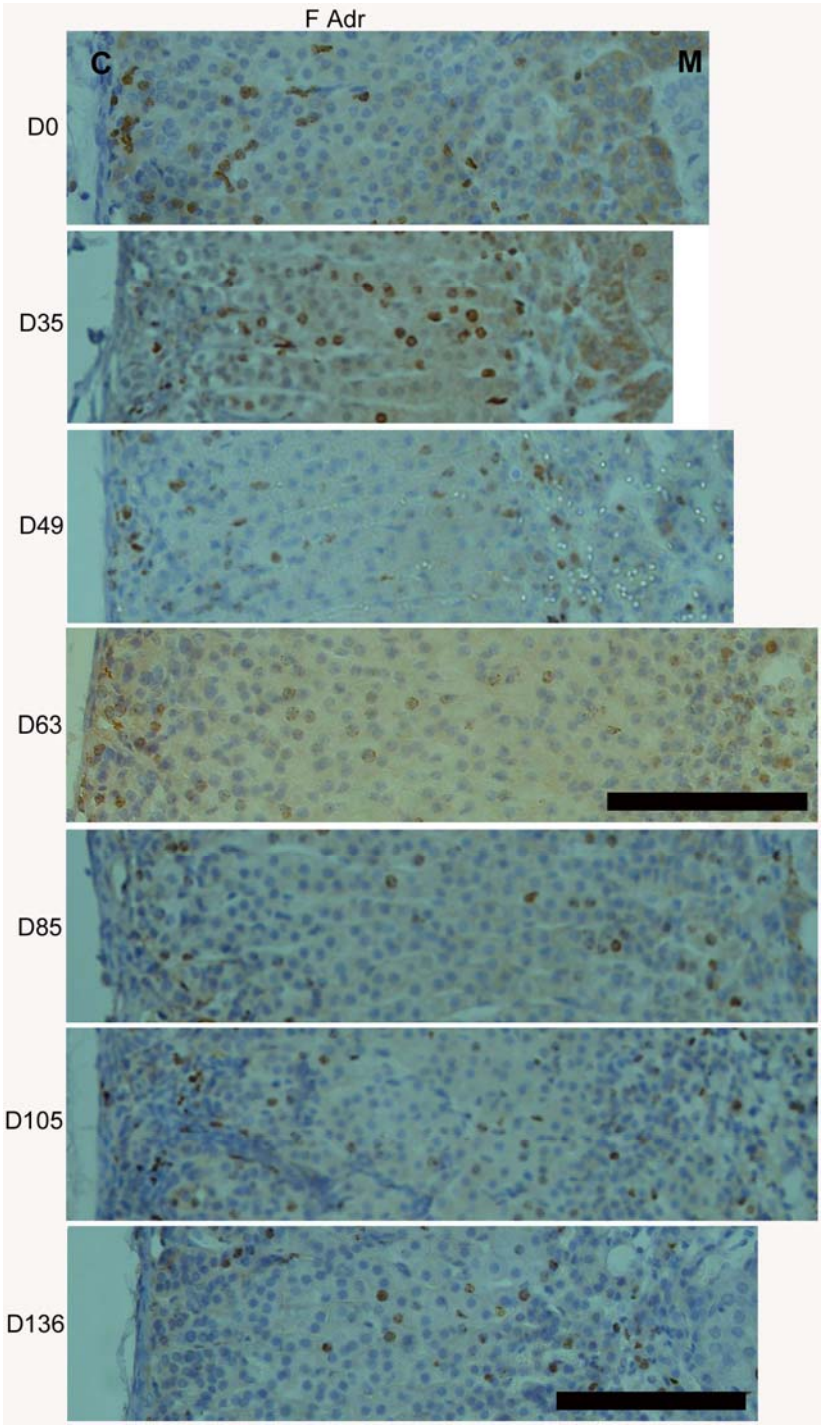

Fig. 5.7. Distribution of BrdU-labelled cells in sections of female adrenals after a series of chase periods following one week exposure to BrdU. Immunohistochemical detection (section 2.9) of BrdU-labelled cells in female adrenals obtained after different chase periods (0, 35, 49, 63, 85, 105 and 136 days) following 1 week exposure to BrdU. The scale bar for 136 day chase experiment applies to all the photographs except for the 63 day chase experiment. Scale bar = 0.1mm. C, capsule; M, medulla.

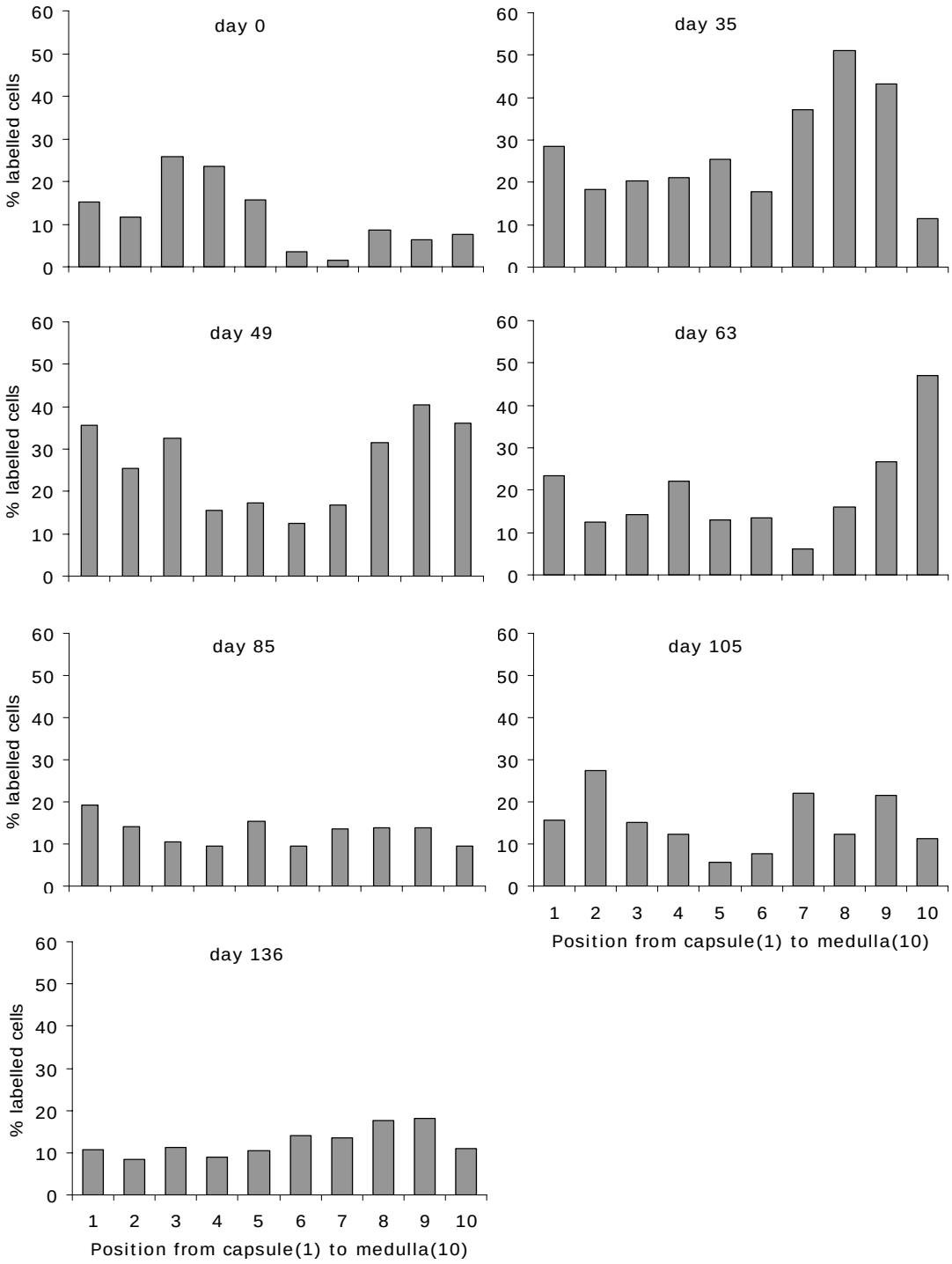

Fig. 5.8. Distribution of BrdU-positive cells across the adrenal cortex after a series of chase periods following one week exposure to BrdU. The percentage of BrdU positive cells (identified by immunohistochemistry) in each row of a 10 × 10 grid is shown after 1 week exposure to BrdU followed by different chase periods (0, 35, 49, 63, 85, 105 and 136 days). Row 1 is close to the capsule and row 10 is close to the medulla.

In the main experiment the period of BrdU exposure was increased to 2 weeks and the longest chase time was extended to 23 weeks to try to identify a specific population of label-retaining cells. Four mice (2 males and 2 females) were examined after chase periods of 0 and 6 weeks, 6 mice (3 males and 3 females) were analysed at 18 weeks and 10 mice (5 males and 5 females) were analysed after a 23 week chase period (Figs. 5.9 and 5.10). When analysed immediately after 2 weeks exposure to BrdU large numbers of BrdU-labelled cells were detected, most of which were located in the outer cortex. After 6 weeks chase, the labelled cells had spread throughout the most of cortex and the intensity of BrdU staining seemed weaker in some cells, which is consistent with evidence discussed earlier (section 5.3.1.4) for a further round of cell division occurring between 3 and 8 weeks. Figs. 5.9 and 5.10 show that between 6 and 18 weeks labelled cell numbers were massively depleted. By 18 weeks most of the remaining labelled cells were located either in the outer cortex (near the capsule or in a group of cells that seemed to extend from the capsule to the outer cortex; this group of cells will be referred to here as a 'capsule extension') or the inner cortex (possibly within a degenerating X zone near the medulla in females). There were also a few labelled cells within the medulla, which presumably represent medullary label-retaining cells. In contrast, few BrdU-labelled cells were visible in the middle of the cortex. After a 23 week chase period very few strongly staining BrdU-positive cells were visible and these were mostly close to the capsule or in the capsule extension (Figs. 5.9 and 5.10).

There was insufficient time to analyse the distribution of BrdU-positive cells in detail in both males and females but visual inspection suggested that they showed similar distributions (Figs. 5.9 and 5.10), so the left adrenals of female mice were chosen for quantitative analysis. The results (Fig. 5.11) are similar to the above description based on the qualitative microscopic analysis for the 0 and 6 week chase periods. However, for the 18 and 23 week chase periods the BrdU-positive cells were scored as being more evenly distributed throughout the cortex rather than being mainly localised close to the capsule, as appears to be the case on

visual inspection. The likely explanation for this is that a proportion of cells throughout the cortex retained low levels of BrdU, having undergone a few but insufficient divisions to completely dilute the label and these weakly positive cells were scored as positive for the quantitative analysis. Nevertheless, the images also show a population of more strongly staining positive cells located mostly close to the capsule or in the capsule extension. Unfortunately, there was insufficient time to investigate this further (e.g. by repeating the quantitative analysis with the addition of a semi-quantitative score of the staining intensity of each BrdU-positive nucleus).

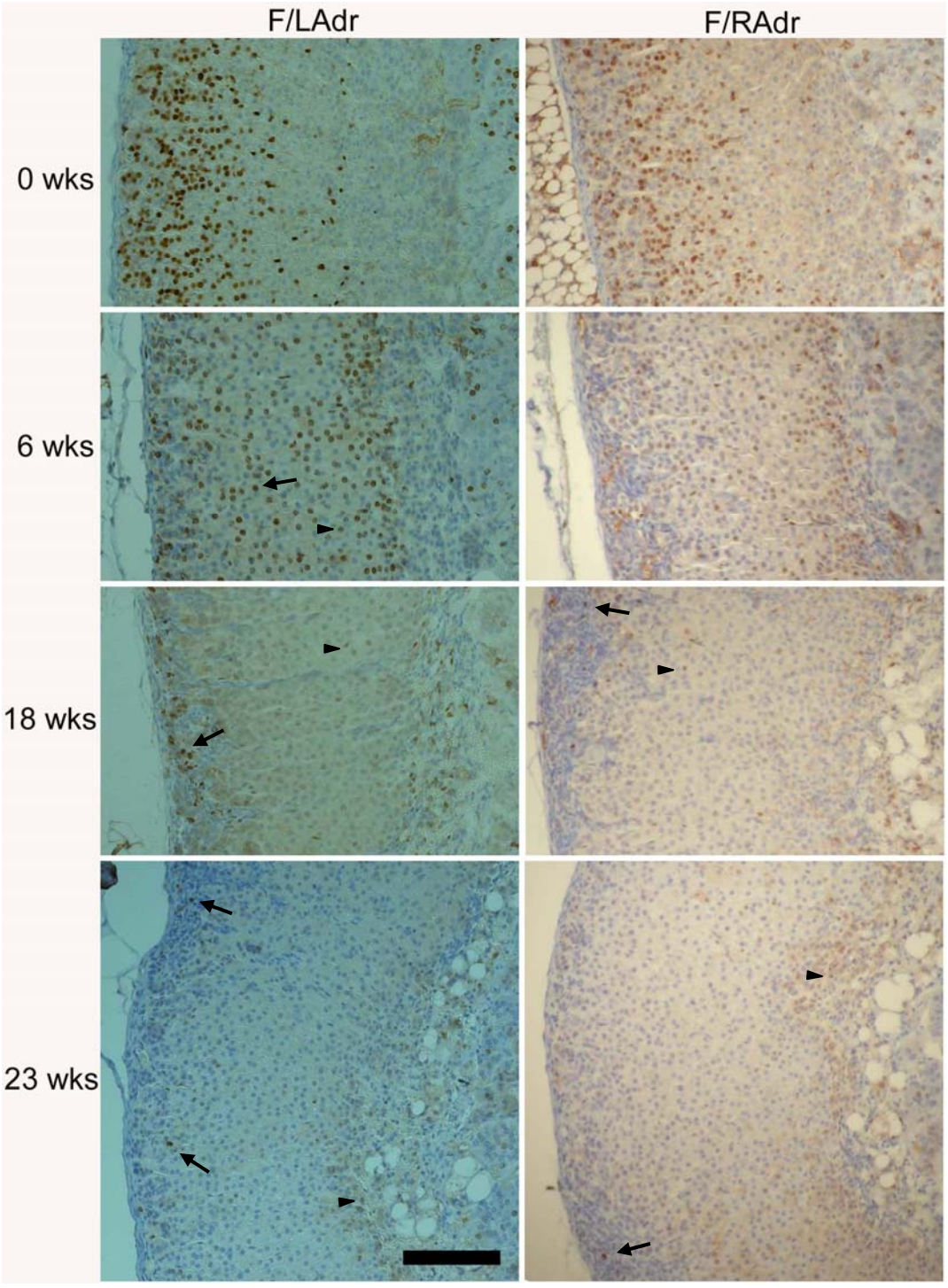

Fig. 5.9. Distribution of BrdU-labelled cells in female adrenals after a series of chase periods following two weeks exposure to BrdU from a mini-pump. Immunohistochemical detection (section 2.9) of BrdU-labelled cells in female adrenals after different chase periods (0, 6, 18, 23 weeks) following two weeks exposure to BrdU. Scale bar = 0.1mm. F/LAdr, female left adrenal; F/RAdr, female right adrenal. Arrowhead, strongly labelled cell; arrow, labelled cell.

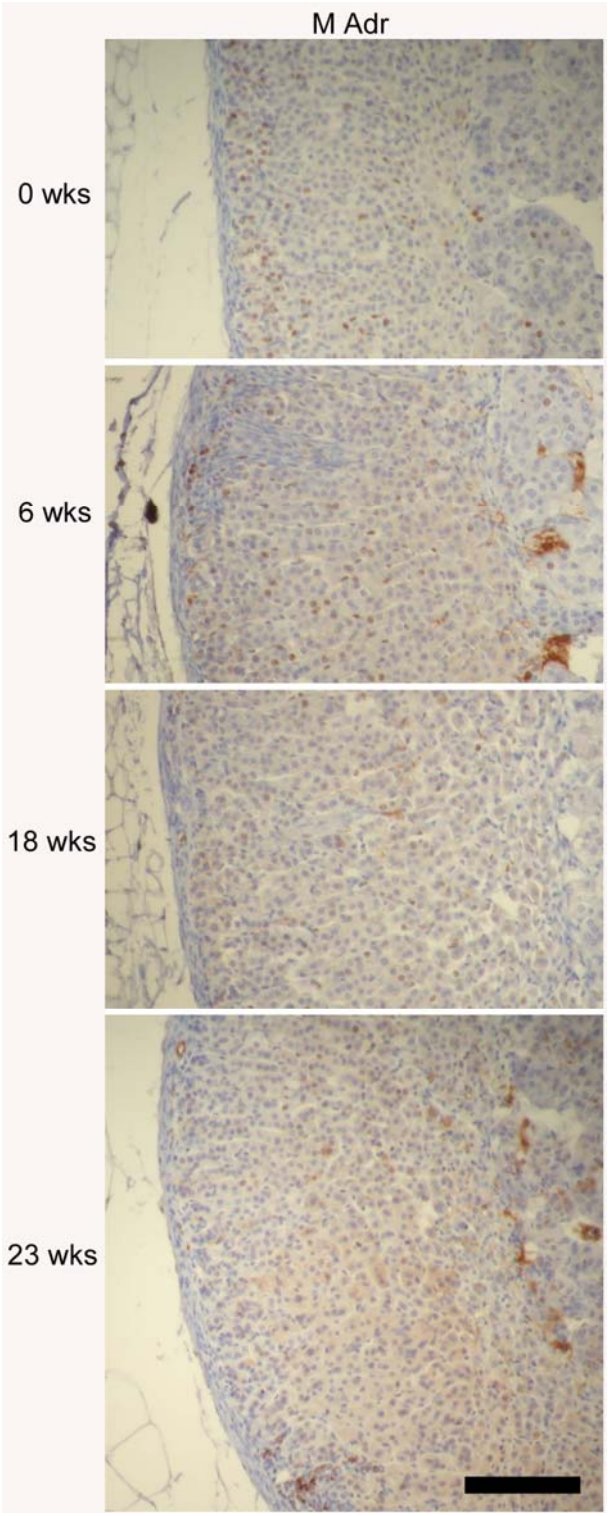

Fig. 5.10. Distribution of BrdU-labelled cells in male adrenals after a series of chase periods following two weeks exposure to BrdU from a mini-pump. Immunohistochemical detection (section 2.9) of BrdU-labelled cells in male adrenals after different chase periods (0, 6, 18, 23 weeks) following two weeks exposure to BrdU. Scale bar = 0.1mm. M Adr, male adrenal.

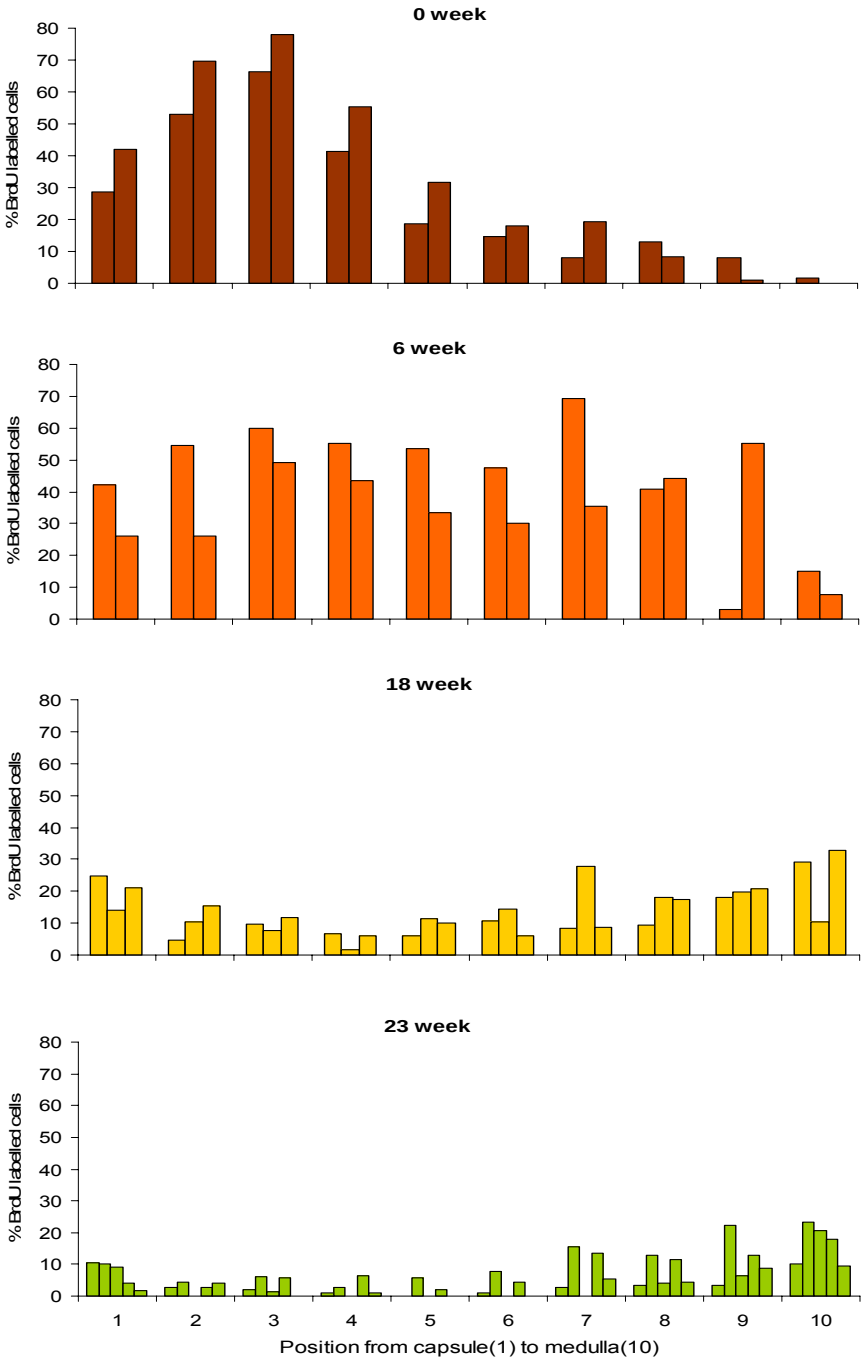

Fig. 5.11. Distribution of BrdU-labelled cells across the adrenal cortex after a series of chase periods following 2 weeks exposure to BrdU. The percentage of BrdU-positive cells (identified by immunohistochemistry) in each row of a 10 × 10 grid is shown for sections of female left adrenals following 2 weeks exposure to BrdU and different chase periods (0, 6, 18, 23 weeks). Row 1 is close to the capsule and row 10 is close to the medulla. The number of bars represents the numbers of adrenals analysed.

5.4 Discussion

5.4.1 Cell proliferation and movement in the adrenal cortex

Analysis of adrenals at different times after single BrdU injection suggested that proliferation occurs predominantly in the outer region of the adrenal cortex. The distribution of BrdU-positive cells will not include any cells that were removed by apoptosis immediately after cell division. While it seems unlikely that apoptosis would be sufficient to explain the restriction of BrdU-positive cells to the outer 40% of the cortex, it will be necessary in the future to confirm this by direct experimental measurement of distribution of apoptotic indices in the adrenal cortex. Cell division is followed by an inward spread of BrdU-labelled cells, indicating that, after division, cells move to the inner, non-proliferative region. This is consistent with most previous studies of cell proliferation (Mitani et al., 2003; Zajicek et al., 1986) and cell movement (Belloni et al., 1978; Kataoka et al., 1996; Zajicek et al., 1986). While 96% of dividing cells were located in the outer 40% of the left adrenal cortex of female mice, 4% were closer to the medulla. This low level proliferation in the inner cortex is consistent with that reported previously in the rat (McNicol and Duffy, 1987). The main region of proliferation may include stem cells and early generation TA cells, while the 4% of labelled cells in the inner 60% of the cortex may reflect later generation TA cells, which may divide as they move centripetally. Unfortunately, due to time restrictions, insufficient adrenals were analysed to determine conclusively whether cell proliferation was restricted to the ZG and ZF or whether some cell proliferation also occurs in the ZR. However, even if proliferation occurs within the ZR it must be at a much lower level than in the ZG or ZF.

Although, the frequency of BrdU-labelled cells within 5% of the capsule increased after 1 week there was no overall increase in labelled cell numbers for the region within 10% of the capsule. For reasons mentioned previously, further work is needed to identify conclusively whether all moving cells move centripetally or if some cells move outwards. This would evaluate the zona

intermedia hypothesis for adrenocortical maintenances which predicts bidirectional movement (Fig. 1.11d).

5.4.2 Identification of BrdU label-retaining cells

Experiments where mice were continuously exposed to BrdU for 1 or 2 weeks and then left for long chase periods were designed to label slow cycling cells to help identify the location of putative stem cells in the adrenal cortex. Immediately after labelling for 1 or 2 weeks most BrdU-labelled cells were in the outer cortex, as was found after labelling by a single BrdU injection. However, the labelled region appeared broader after the longer labelling periods and this is probably because many cells that divided near the beginning of labelling would have moved before the end of the labelling period. The initial mini-pump experiment was designed to optimise conditions for the later experiment. The first experiment showed that BrdU-labelled cells were distributed throughout the adrenal cortex by 7 weeks and remained broadly distributed even after 19 weeks, although they were depleted in number. Consequently a longer labelling period (2 weeks) was used in the second experiment and after a 6 weeks chase period the BrdU-labelled cells were distributed throughout the adrenal cortex, as predicted from the first experiment. Following 18 weeks chase, the reduction in number of labelled cells together with the occurrence of pale labelled cells in the middle of the cortex suggests cell loss and BrdU dilution (by cell division) have both occurred. Between 18 and 23 weeks, the numbers of labelled cells (including those in the outer cortex) decrease further.

After a 23 week chase interval, there were no intensely-labelled BrdU label-retaining cells remaining in the central cortex in positions that would be predicted by the zonal hypothesis or zona intermedia hypothesis of adrenocortical maintenance (Fig. 1.11). Some pale BrdU-labelled cells remained near the cortex-medullary boundary but these are unlikely to be stem cells because stem cells are unlikely to move and immediately after labelling there were few BrdU-positive cells at the cortex-medullary boundary. Therefore, these pale BrdU-labelled cells

following a 23 week chase period must have moved to the boundary after incorporating BrdU elsewhere and maybe have differentiated after several divisions. Other, more strongly BrdU-positive cells remained near the capsule or in the capsule extension.

At 23 weeks most of the cortex is depleted of strongly stained BrdU-positive cells but some intensively labelled cells remained near the capsule or in a group of cells that appears to extend from the capsule to the outer cortex. This group of cells, defined above as a 'capsule extension', may be similar to the groups of cells described as extending from the capsule into the cortex in different species (Bielinska et al., 2003; Kim and Hammer, 2007). The key question is whether these label-retaining cells represent stem cells. As discussed in chapter 1 (section 1.3.2.2) stem cells are likely to be slow cycling and this has enabled identification of stem cells as BrdU label-retaining cells in some tissues. Slow cycling cells should require a prolonged exposure to BrdU to maximise the chance of labelling them and once labelled will dilute the BrdU more slowly than faster cycling cells in the tissue. Thus the BrdU label-retaining cells identified near the capsule or in the capsule extension after 2 weeks exposure to BrdU and a chase period of 23 weeks could be slow cycling cells and these may include stem cells. However, the observation that labelled cells in a similar location remained after a 15 week chase following a single injection casts doubt on this conclusion because only a small proportion of cells that were continuously slow cycling would be likely to be in division during exposure to BrdU from a single injection. Thus it is not yet clear whether all the cells identified as label-retaining cells near the capsule or in the capsule extension are cells that were initially rapidly cycling but then stopped dividing (e.g. became terminally differentiated ZG cells or quiescent cells) or whether they include a sub-population of slow-cycling putative stem cells.

5.5 Conclusions

The experiments in this chapter showed that most cell proliferation occurs in the outer adrenal cortex, cells move centripetally towards the medulla and BrdU label-retaining cells were present in the outer cortex, close to the capsule or in the capsule extension. The low level of proliferation coupled with the reported high level of apoptosis close to the medulla (in the ZR) and the absence of intensely labelled label-retaining cells in the central cortex argue against the zonal hypothesis of adrenocortical maintenance (Fig. 1.11c). The absence of intensely labelled label-retaining cells in the region proposed for the ZI also provides some evidence against the zona intermedia hypothesis (Fig. 1.11d). However, this hypothesis was not adequately tested by cell movement in this chapter, because more work is needed to identify whether any cells migrated towards the capsule, and there was insufficient time to investigate the locations of apoptotic cells. If the BrdU-label-retaining cells close to the capsule or in the capsule extension include stem cells, this would support the hypothesis that stem cells maintain the adrenal cortex and provide preliminary evidence for a population of adrenal cortical stem cells close to the capsule or in the capsule extension (e.g. Fig. 1.11a or e). However, additional experiments are required to establish whether these label-retaining cells do include stem cells.

6. Analysis of mosaic β-gal staining patterns in the adult *21OH/LacZ* transgenic adrenal cortex

6.1 Introduction

In chapter 3 it was shown that the transition from randomly orientated spots to radial stripes in *21OH/LacZ* transgenic adrenals occurred perinatally and was complete by P21. Analysis of the distribution of cell proliferation during the perinatal period (described in chapter 4) supported the hypothesis that the stripes emerged by edge-biased growth. Chapter 5, focused on maintenance of the adult adrenal cortex. BrdU labelling was used to identify the location of dividing cells, whether cells move and whether a label-retaining cell population could be identified to help recognise stem cells and to re-evaluate various hypotheses of stem cell maintenance of the adult adrenal cortex. In this chapter, the radial stripe patterns in adult *21OH/LacZ* transgenic adrenal cortices are analysed to better characterise the maintenance of adrenal cortex and to further help distinguish between different models proposed for adrenocortical maintenance by stem cells.

As discussed in chapters 1 and 3, adult *21OH/LacZ* mice show a mosaic pattern of radiating β-gal positive and β-gal negative stripes crossing the adrenal cortex due to mosaic expression of the *21OH/LacZ* reporter gene (Morley et al., 1996). This also occurs in some other transgenic mice (Hu et al., 1999) and is probably due to random inactivation of the transgene in some progenitor cells at an early developmental stage. The mechanism of transgene inactivation in *21OH/LacZ* mice is not understood and it is not known whether or not it is similar to position effect variegation, which has been suggested for mosaic expression of some other transgenes (Dobie et al., 1997).

Similar stripes occur in the adrenal cortices of chimeras and X-inactivation mosaics (Iannaccone, 1987; Iannaccone and Weinberg, 1987; Morley et al., 2004). The results of previous analysis indicated that the patterns of stripes in the adrenal cortices of adult *21OH/LacZ* transgenic mice were qualitatively and quantitatively similar to those in mouse chimeras and X-inactivation mosaics (Chang, 2003; Morley et al., 2004). There was a close agreement in the 'corrected stripe number' (see section 2.6) among X-inactivation mosaics, chimeras and hemizygous *21OH/LacZ* transgenic mice. As the stripes in chimeras and X-inactivation mosaics are known to represent clonal lineages this is also likely to be true in *21OH/LacZ* transgenics. This suggests that the mosaic stripe patterns in *21OH/LacZ* transgenic adrenals can be used to analyse clonal lineages in the same way as variegated patterns in chimeras and X-inactivation mosaics. Mosaic patterns have been widely used to analyse developmental lineages but can also be used to investigate clonal lineages produced by adult stem cells (Collinson et al., 2002). Randomly orientated clonal expansion would be expected to produce a randomly orientated mosaic pattern of β-gal-positive and β-gal-negative patches whereas directional growth and maintenance of the tissue would be predicted to produce radial stripes. In chapter 3 it was shown that stripes emerged during perinatal growth and were probably formed by edge-biased growth. Although stem cells may not be involved in the initial formation of stripes, it seems likely that stem cells later maintain the stripes by producing clones of cells that move centripetally to displace the earlier fetal patterns and later replace aging cells.

If the cells in the stripes are clonal derivatives of stem cells that maintain the adult adrenal cortex, the radial stripe pattern in the adrenal cortex could be used to evaluate different hypotheses of how stem cells maintain the adrenal cortex. The radial striped patterns in the adrenal cortex of adult mosaic and chimeric rats and mice (Iannaccone and Weinberg, 1987; Morley et al., 2004) and *21-OH/LacZ* transgenic mice (Morley et al., 2004; Morley et al., 1996) appeared to extend across the entire width of the cortex. It is important to establish whether this is always the case because it may help to distinguish between different hypotheses

for maintenance of the adrenal cortex by one or more populations of stem cells located in different regions of the adrenal cortex and/or capsule (see section 1.4). For example, if a single population of stem cells produced new cells in all three zones, stripes would be expected to always span all the zones whereas stripes may not always span the full thickness of the cortex if the zonal maintenance theory is correct.

The maintenance of the corneal epithelium (described in sections 1.3.1.3 and 1.5.3) may have some similarities to the maintenance of the adrenal cortex. For example the initial randomly-orientated mosaic pattern in the corneal epithelium is replaced by radial stripes after birth (Collinson et al., 2002). The time when stripes emerge in the cornea has been interpreted as the time when limbal stem cells at the periphery of the cornea are activated and the stem cells produce clones of daughter cells (transient amplifying cells) that move inwards to maintain the corneal epithelium. In addition, a quantitative analysis of the striped pattern showed that the ‘corrected stripe number’ declined with age up to 39 weeks, which may reflect an age-related decline in stem cell function (section 1.5.3).

6.1.1 Aims

The studies described in this chapter had three aims. Firstly, the mosaic stripe pattern of the adult *21OH/LacZ* transgenic adrenals was used to evaluate different hypotheses of adrenocortical stem cells by examining whether the adult stripes always span the entire cortex radially. Secondly, quantitative analysis of corrected stripe numbers at different ages was used to look for age-related changes in the adult mosaic pattern, which might reflect age-related changes in functional stem cell clones (as seen in the corneal epithelium). Apart from age, other factors (gender and genotype) were also tested for their effects on the stripe pattern. Thirdly, comparison of the proportion of cells showing β-gal staining in homozygous and hemizygous *21OH/LacZ* transgenic adrenals at different ages was used to evaluate whether transgene inactivation continues throughout adult life and is controlled at the cellular or chromosomal level and to identify whether transgene inactivation continues in the adult.

6.2 Materials and methods

Groups of male and female *21OH/LacZ* transgenic mice were sacrificed at 8, 13, 26, 39 and 52 weeks of age and adrenal glands were dissected out immediately under a Wild M5A dissecting microscope. The connective tissue and adipose tissue were trimmed off on a paper towel soaked with PBS, after which adrenals were blotted dry and weighed on an electronic balance. Dissected adrenal glands were frozen-sectioned (10 μm), stained histochemically for β-gal activity as described in section 2.4 and counterstained with neutral red. Several serial longitudinal sections from the middle of the adrenal were photographed and examined. The adrenals were grouped by gender (female or male), age, *21OH/LacZ* genotype (homozygous or hemizygous for the transgene) and anatomical location (right or left). For each group, images of five to ten serial sections from each of four to six adrenal glands were analysed to determine whether any of the stripes were discontinuous. For the quantitative analysis, the widths of alternating β-gal-positive and β-gal-negative stripes in *21OH/LacZ* transgenic adrenals were measured at a position equivalent to one third of the depth of cortex from the capsule to the inner margin of cortex, as described in section 2.5. The total measured stripe numbers in the adrenal cortex were corrected, to allow for differences in proportions of β-gal-positive and β-gal-negative cells affecting the probability clonal stripes of the same colour occurring next to each other (see section 2.6), The percentages of β-gal staining and non-staining cells were also obtained along with the total length measured for the comparison of transgene silencing in homozygous and hemizygous *21OH/LacZ* transgenic adrenals.

6.3 Results

6.3.1 Qualitative analysis of β-gal stripes in the adult *21OH/LacZ* transgenic adrenal cortex

The patterns of β-gal radial stripes of *21OH/LacZ* transgenic adrenal cortices appeared qualitatively similar at all adult ages studied and most stripes appeared to span the entire cortex. Fig. 6.1 shows representative examples of stripes in adrenal cortices at 8 and 52 weeks. The qualitative stripe patterns at these two ages did not differ significantly from each other or from the other ages studied (13, 26 and 39 weeks; pictures not shown) and are equivalent to those reported in chapter 3 for P14-P21 adrenals. The only difference observed, as previously noted for P10-P21 adrenals in section 3.1, was the pale blue β-gal staining seen in the X zone of female adrenals at 8 weeks, gradually degenerating with age (e.g. see Fig. 6.1 female adrenal at 52 weeks old). Adrenal cortices from homozygous *21OH/LacZ* transgenic mice tended to have higher proportions of β-gal-positive cells than adrenals from hemizygotes and this is discussed in more detail in section 6.3.5. Otherwise, the pattern of was similar for all groups.

In most cases, radial stripes extended the full width of the cortex but some discontinuous stripes were found in individual sections. Evidence for discontinuous stripes could be important because they would provide evidence for maintenance of different zones of the adrenal cortex by different populations of stem cells. To identify whether discontinuous regions of staining were real or attributable to technical artefacts, five to ten serial sections near the centre of each of about 200 adrenal glands were examined. In most cases the stripe pattern changed in adjacent sections indicating that stripes were incomplete because they were not parallel to the plane of section. Only three samples from about 200 adrenals consistently showed discontinuous stripes in six to ten serial sections. In all three cases, there were a few cell layers of β-gal negative tissue that covered a fairly large area (Fig. 6.2). Underneath this thin covering of β-gal-negative cells, the rest of the inner cortex was a mixture of β-gal positive and β-gal negative

radial stripes. No cases of the reverse pattern (thin covering of β-gal positive cells overlying β-gal negative tissue) were observed. It is unknown whether these very rare discontinuous stripes in the serial sections were attributable to technical artefacts or another cause (e.g. thick capsule). Closer inspection of the sections failed to resolve whether the unstained areas were predominantly ZG or capsule because of the limited resolution of using frozen sections without zone-specific markers. However, it seems unlikely that these unstained outer regions were maintained by a separate stem cell population from the underlying tissue.

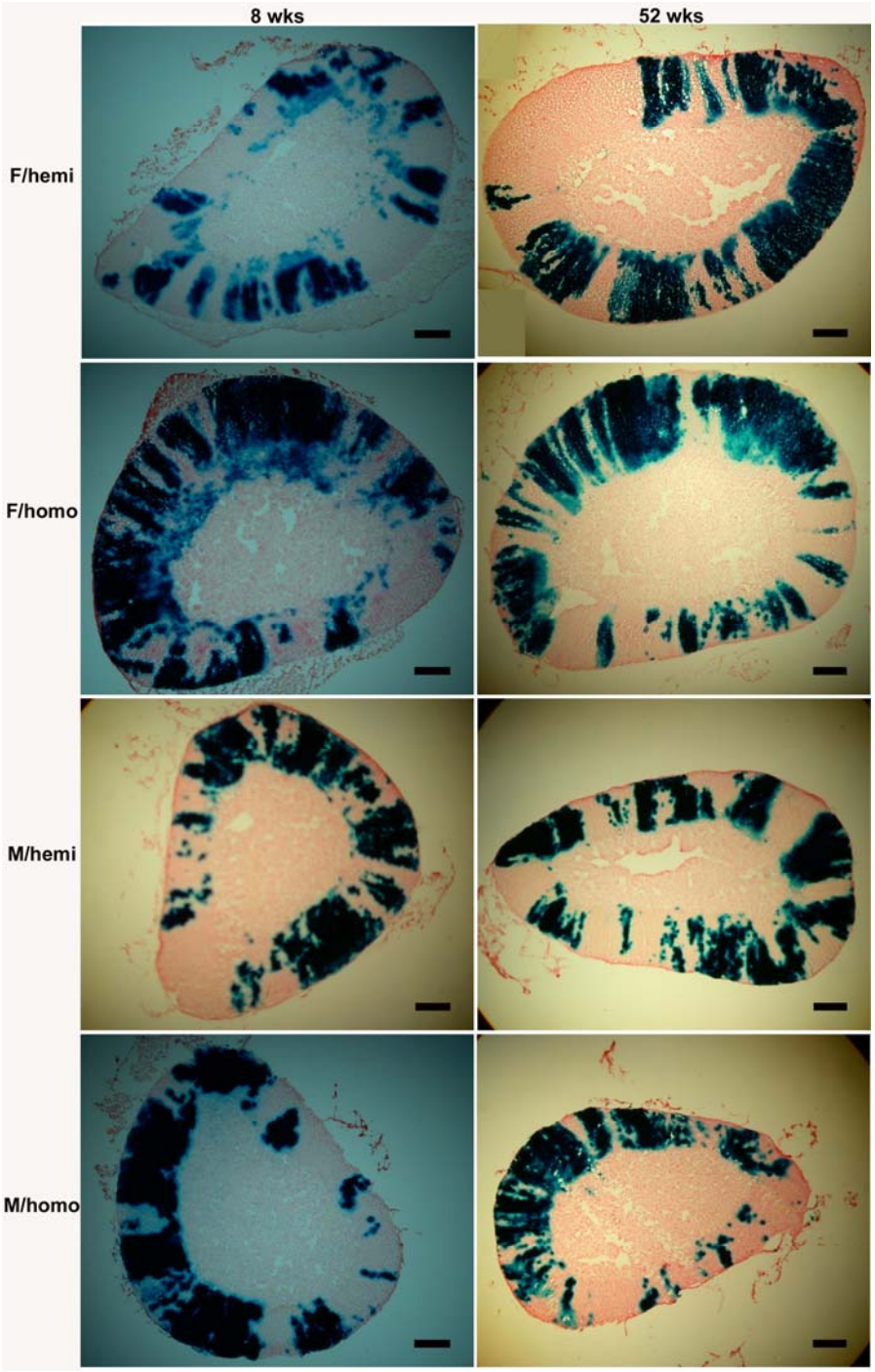

Fig. 6.1. β-gal-positive and β-gal-negative stripes in the adult *21OH/LacZ* transgenic adrenal cortex. Representative images of β-gal-positive and β-gal-negative stripes in adrenal cortices from male and female, homozygous and hemizygous *21OH/LacZ* transgenic mice at 8 and 52 weeks of age. In most cases the stripes are continuous and transect the whole cortex. *21OH/LacZ* adrenals were frozen-sectioned and stained for β-gal as described in sections 2.3 and 2.4. Scale bar, 0.2mm.

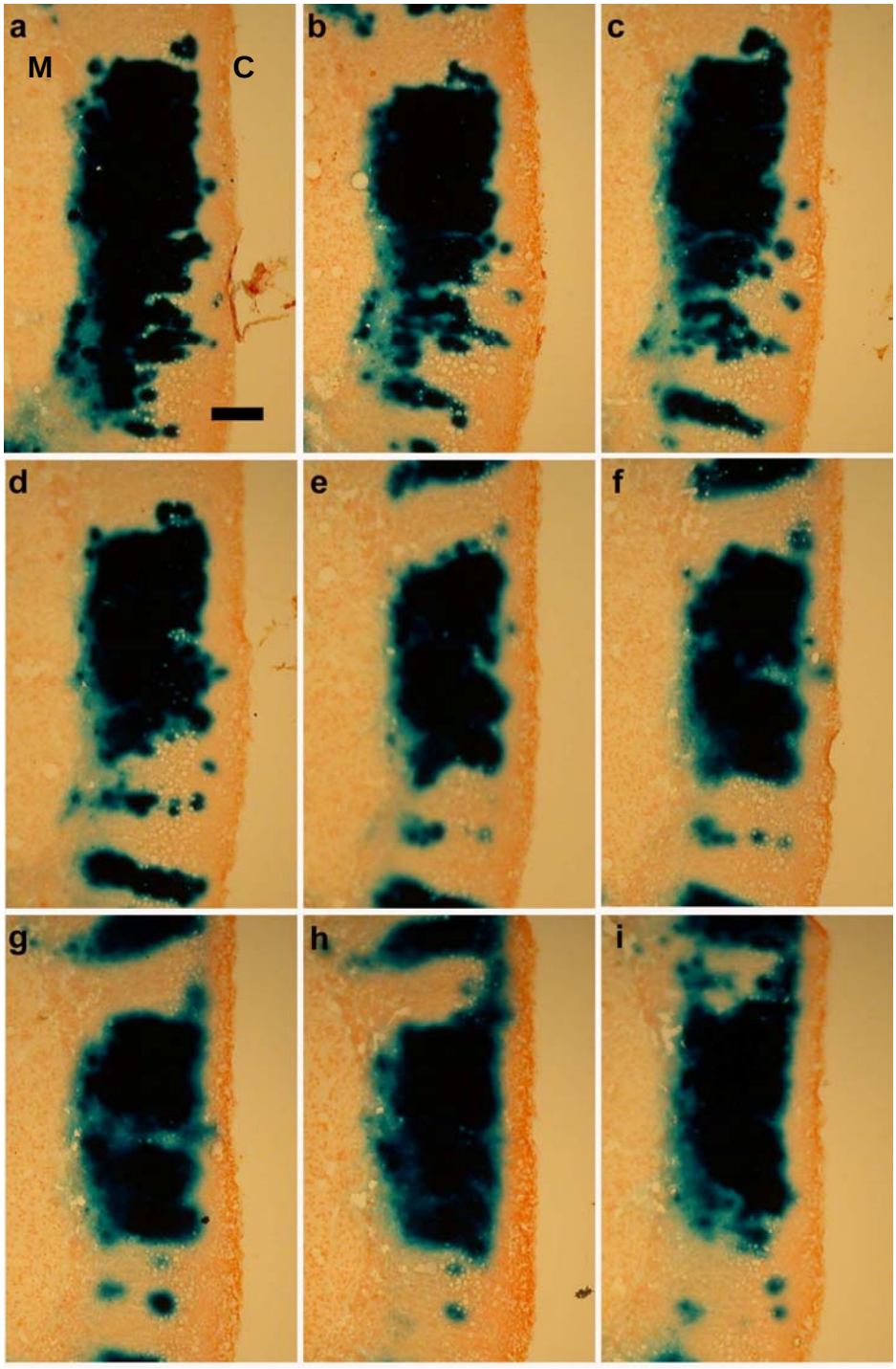

Fig. 6.2. A representative example of discontinuous stripes in the serial sections of *21OH/LacZ* transgenic adrenal cortices. C, capsule; M, medulla. *21OH/LacZ* adrenals were frozen-sectioned and stained for β-gal as described in sections 2.3 and 2.4. In each section a few cell layers of β-gal negative tissue overlie a mixture of β-gal positive and β-gal negative radial stripes. Scale bar, 0.1mm.

6.3.2 Preliminary technical investigations for measurement of β-gal stripes in the adult *21OH/LacZ* adrenal cortex

As a first step, it was desired to compare and validate methods for quantitatively evaluating mosaic β-gal striping patterns in the *21OH/LacZ* adrenal cortex.

6.3.2.1 Regions showing intermediate β-gal staining

The majority of adult *21OH/LacZ* mosaic adrenocortical stripe patterns were either uniformly stained dark blue or unstained. Some areas, however, showed regions of pale blue staining, although these were invariably adjacent to regions that were stained dark blue (Fig. 6.3). Such pale blue regions might reflect boundaries between β-gal-positive and β-gal-negative cells. Frozen sections were only 10 μm thick, so it is unlikely that many sections contained superimposed regions from β-gal-positive and β-gal-negative cells. It seems more likely that the pale blue staining reflects diffusion of stain from the β-gal-positive region. For this reason they were scored as β-gal-negative in the quantitative analysis.

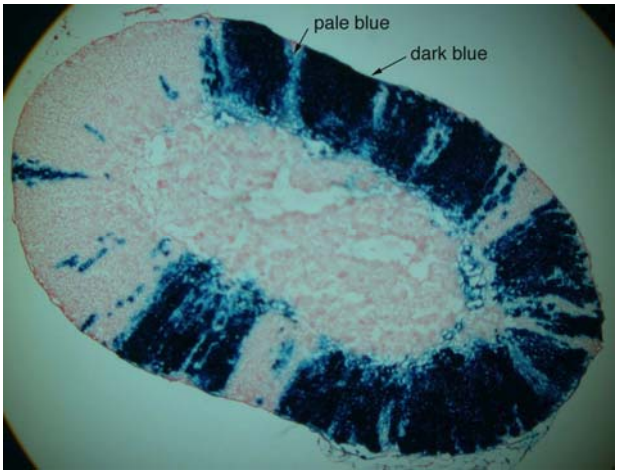

Fig. 6.3. The middle section of a stained *21OH/LacZ* adrenal gland showed pale blue regions as well as the normal dark blue and unstained stripes. *21OH/LacZ* adrenals were frozen-sectioned and stained for β-gal as described in sections 2.3 and 2.4. The pale blue is thought to arise from leakage of β-gal staining and the dark blue is taken as true β-gal-positive staining.

6.3.2.2 Measurement of stripe widths at different depths

For the quantitative analysis, the widths of alternating β-gal-positive and β-gal-negative stripes in *21OH/LacZ* transgenic adrenals were measured along a line parallel to the circumference at the perimeter of the adrenal gland (see section 2.5). Initial trials were carried out to compare stripe measurements at two different depths in the cortex using 13 adrenals from 26-week-old hemizygous *21OH/LacZ* transgenic mice. This was to test whether the mean corrected stripe number was affected by the radial position in the outer cortex. In these preliminary analyses stripe widths were measured at both 20% and 33% depth from the outer edge of adrenal cortex. In each case the mean corrected stripe numbers were calculated as described in section 2.6.

As expected the total circumference measured differed between these two depths ($P<0.0001$ by paired t-test) but there was no significant difference in either the percentage of β-gal-positive staining (Fig. 6.4) or the total number of corrected stripes (Fig. 6.5). Following this initial comparison it was decided to standardise measurements at a distance of 33% from the outer edge of the cortex to ensure that the measurements were consistently within the zona fasciculate and not near the ZU, where stripes might be affected.

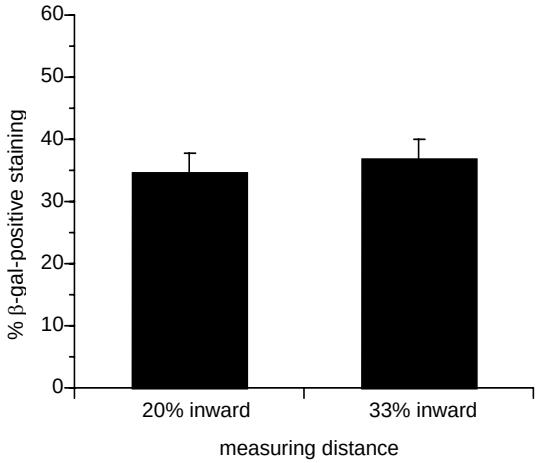

Fig. 6.4. Comparison of percentage of β-gal-positive staining at two depths in the adrenal cortex. β-gal-positive stripe widths were measured along lines parallel to the outer perimeter at different depths from the capsule (as described in section 2.5) and converted into a percentage of the measured circumference. There was no significant difference in percentage β-gal-positive staining between measurements made at depths of 20% and 33% from the capsule for 13 adrenals from 26 week old *21OH/LacZ* transgenic mice. (Means were 34.75±2.86 and 36.94±2.94 for 20% and 33% depths respectively; *P*=0.1039 by paired t-test.)

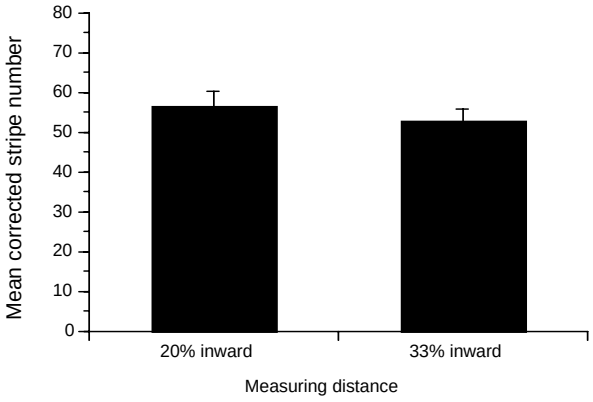

Fig. 6.5. Comparison of mean corrected stripe number at two depths in the adrenal cortex. β-gal-positive and negative stripe widths were measured along lines parallel to the outer perimeter at different depths from the capsule and the mean corrected stripe numbers were calculated as described in section 2.6. There was no significant difference in mean corrected stripe number between measurements made at depths of 20% and 33% from the capsule for 13 adrenals from 26 week old *21OH/LacZ* transgenic mice. (*P*=0.3581 by paired t-test).

6.3.3 Comparison of corrected stripe numbers in male and female homozygous and heterozygous adrenal cortices at different ages

21OH/LacZ radial mosaic β-gal stripes were measured in the middle longitudinal section of the adrenal glands from four groups (hemizygous females, hemizygous males, homozygous females and homozygous males) and the mean corrected number of stripes in mid-sections was calculated (as described in section 2.6). This value refers to total number of β-gal-positive and β-gal-negative radial stripes around in a longitudinal section. As discussed in section 2.6, it is an estimate of the number of 'coherent clones' in the section and the 'correction' allows for the fact that stripes may consist of several adjacent radial coherent clones and the mean number of coherent clones per stripes varies with the proportions β-gal-positive and β-gal-negative cells. The mean corrected stripe number did not differ significantly with age for any of the four groups (Fig. 6.6A-D). Specifically, there was no evidence for a decline in the corrected stripe number with age, so there was no evidence for an age-related decline in stem cell function of the type that has been reported for the corneal epithelium (Collinson et al., 2002). The distributions of individual stripe widths for both β-gal-positive and β-gal-negative stripes were analysed for hemizygous females (chosen as a representative group) and again there were no specific trends with age (Fig 6.6E). The most common stripe widths were 50-99 μm at 8, 26 and 39 weeks.

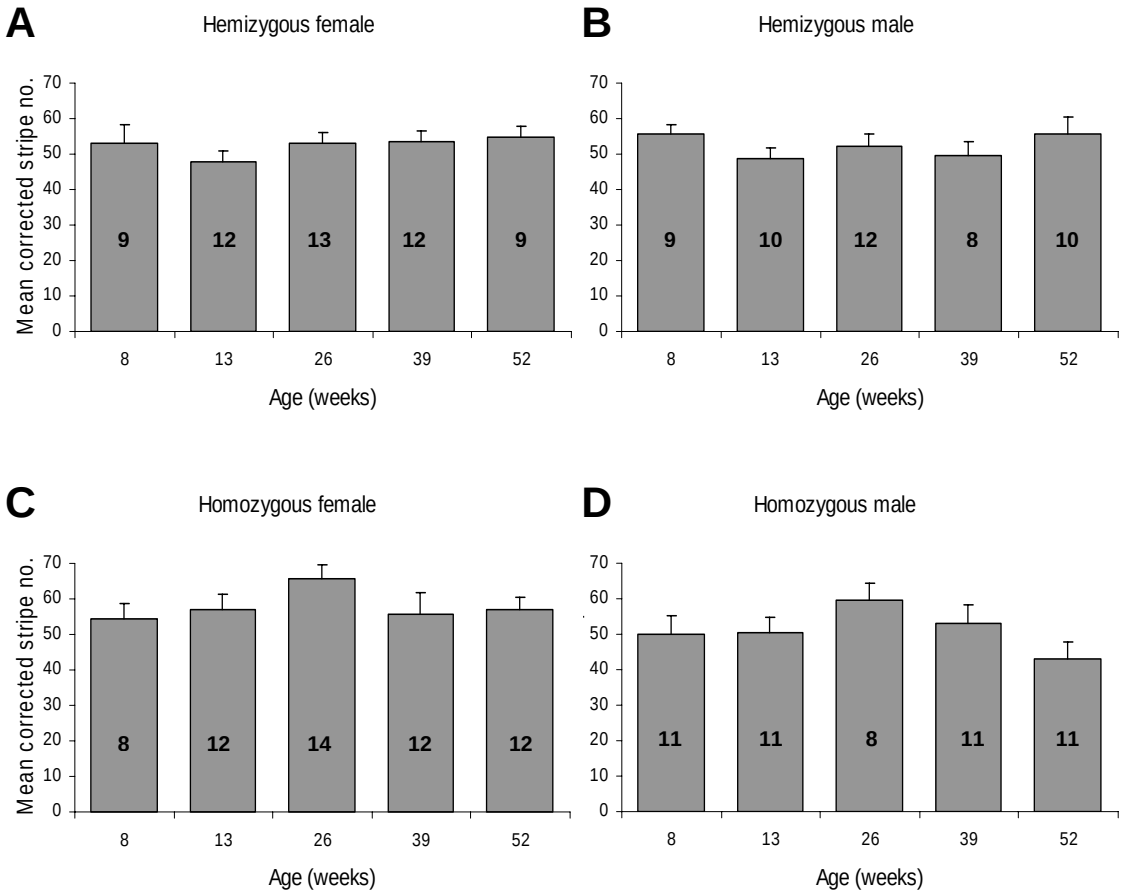

Fig. 6.6A-D. Comparison of the mean corrected stripe number in the adrenal cortices of *21OH/LacZ* transgenics at different ages. No significant variation in mean corrected stripe number with age was found by 1-way ANOVA for hemizygous females (P=0.7704), hemizygous males (P=0.6023), homozygous females (P=0.4178) or homozygous males (P=0.2716). Error bars are standard errors of the mean (SEM). Corrected stripe numbers were calculated from measurement of stripe widths made along a line parallel to the outer perimeter at a depth of 33% from the capsule, as described in section 2.6. The numbers shown in the body of bars are the numbers of adrenals analysed for each group.

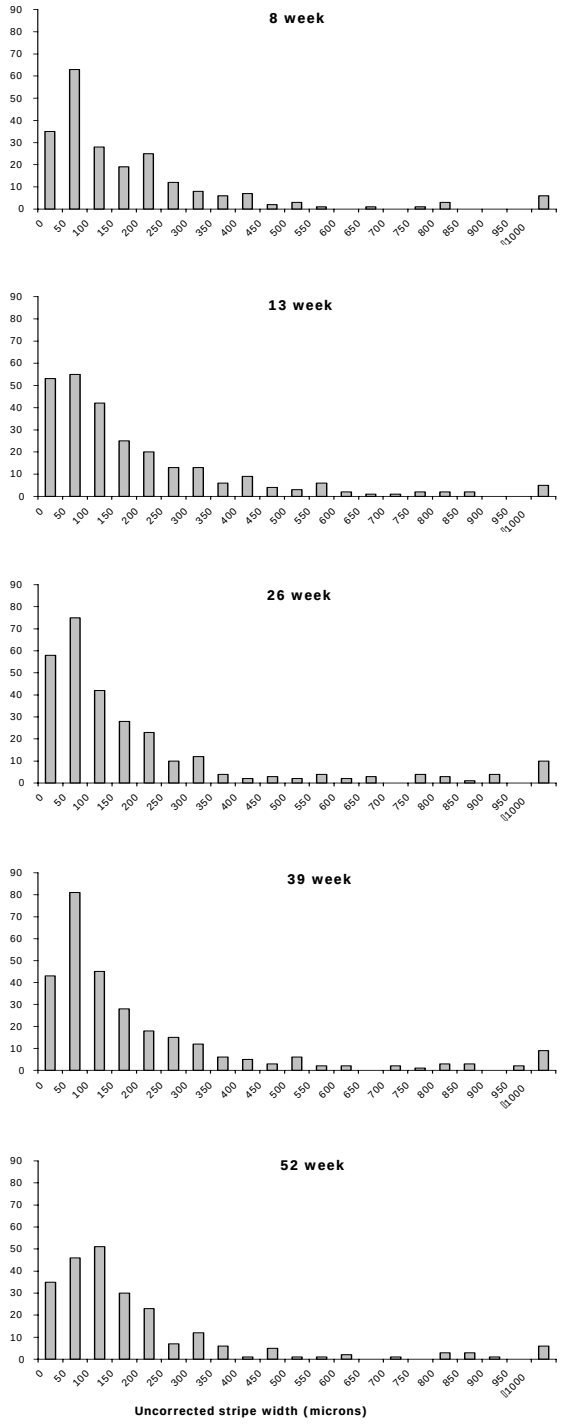

Fig. 6.6E. Comparison of the distributions of individual (uncorrected) stripe widths in female hemizygous *21OH/LacZ* adrenals at different ages. The uncorrected stripe widths for both β-gal-positive and β-gal-negative stripes were obtained directly from measurements along the circumference as described in Chapter 2 and expressed in microns. (See Fig 6.6A for numbers of adrenals.)

6.3.4 Comparison of corrected stripe numbers between different genotypes and ages

The results of the four separate 1-way analyses of variance presented in Fig. 6.6 shows that there was no evidence of age-related variation in corrected stripe numbers within individual groups. To investigate whether the corrected stripe numbers differed between these four groups, four pairs of comparisons were made.

Comparison between hemizygous females and hemizygous males at different ages showed no significant variation in mean corrected stripe number with age or sex (Fig. 6.7). For homozygotes, there was no significant variation in mean corrected stripe number with age for either females or males. However, comparison showed that there was a significant overall difference between homozygous females and homozygous males (Fig. 6.8). This appeared as a general trend for homozygous females to have higher corrected stripe numbers compared to homozygous males but this was only statistically significant at 52 weeks (Fig. 6.8).

Neither hemizygous nor homozygous females showed any significant variation in mean corrected stripe number with age but there was a significant difference between hemizygotes and homozygotes. There was a general trend for homozygous females to have higher corrected stripe numbers and this was significant at 13 and 26 weeks (Fig. 6.9). The comparison of homozygous males and hemizygous males showed no significant variation in mean corrected stripe number with age or homozygous versus hemizygous genotype (Fig. 6.10).

These comparisons between the four groups showed that overall the mean corrected stripe number per section was similar (close to 50) for both genotypes in both sexes at all ages. However, there was some variation associated with sex and hemizygous versus homozygous genotype but this was only significant at specific ages. In these cases, with the exception of the 8 week hemizygous male group, the trend was for the mean corrected stripe number per section to be higher in

homozygous females than the other three groups. The significance of this variation is not presently clear, but is discussed below.

To consider whether weight (and therefore size) could affect the corrected stripe number and in particular to test whether adrenals from homozygous females were consistently larger than the others, weights of the adrenals from the four groups were compared (Fig. 6.11). Both female homozygous and hemizygous adrenals were heavier than male adrenals at each age ($P<0.0001$ for homozygotes and $P<0.0001$ for hemizygotes by 2-way ANOVA) but adrenals from homozygous females were not significantly heavier than adrenals from hemizygous females ($P=0.5341$ by 2-way ANOVA). Therefore the larger size of female adrenals may not be a major factor because hemizygous males and females had similar mean corrected stripe numbers per section. Although it remains unclear why the mean corrected stripe number was higher for homozygous females than hemizygous females it was only significant at 13 and 26 weeks. In conclusion, however, it is clear that there is no overall age-related change in mean corrected stripe number per section that could be interpreted as an age-related change in stem cell function.

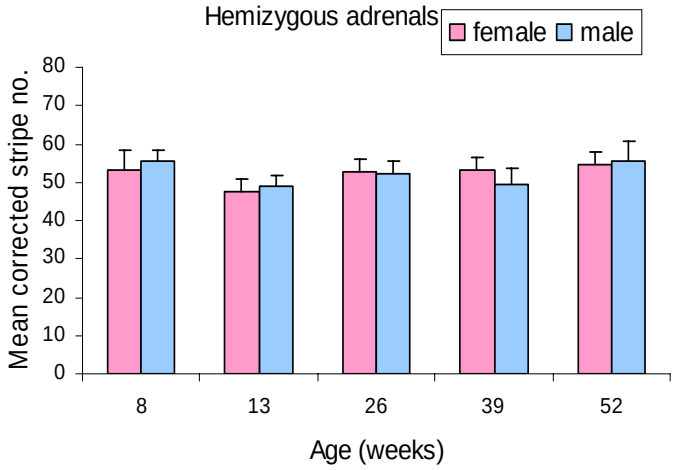

Fig. 6.7. Comparison of the mean corrected stripe number between hemizygous females and hemizygous males at different ages. A 2-way ANOVA showed no significant variation in mean corrected stripe number with age (P=0.4517) or sex (P=0.9865). Error bars are standard errors of the mean (SEM). The numbers of adrenals in each group are shown in Fig. 6.6.

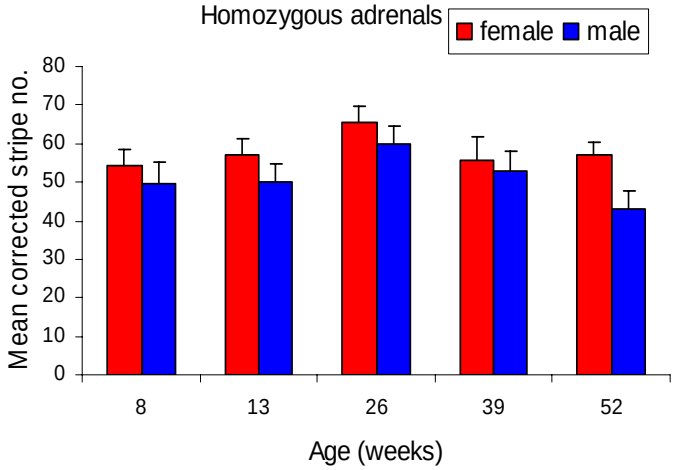

Fig. 6.8. Comparison of the mean corrected stripe number between homozygous females and homozygous males at different ages. A 2-way ANOVA showed no significant variation in mean corrected stripe number with age (P=0.1072) but there was a significant difference between males and females (P=0.0188). Unpaired t-tests revealed a significant difference between homozygous females and homozygous males at 52 weeks (P=0.0215) but not at other ages (P=0.5369, 0.1815, 0.3793, 0.7088 respectively for 8, 13, 26 and 39 weeks). Error bars are standard errors of the mean (SEM). The numbers of adrenals in each group are shown in Fig. 6.6.

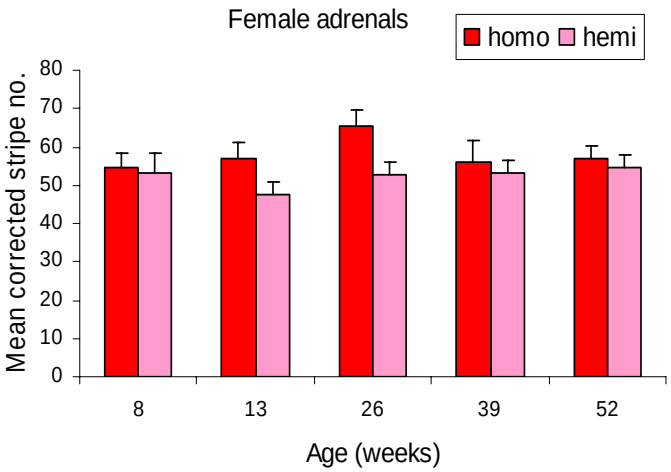

Fig. 6.9. Comparison of the mean corrected stripe number between hemizygous and homozygous females at different ages. A 2-way ANOVA showed no significant variation in mean corrected stripe number with age (P=0.6187) but there was a significant difference between hemizygotes and homozygotes (P=0.0314). Unpaired t-tests revealed a significant difference between homozygous females and hemizygous females at 13 weeks (P=0.0314) and 26 weeks (P=0.0215) but at other ages there was no significant difference (P=0.8472, 0.7513 and 0.6272 respectively for 8, 39 and 52 weeks). Error bars are standard errors of the mean (SEM). The numbers of adrenals in each group are shown in Fig. 6.6.

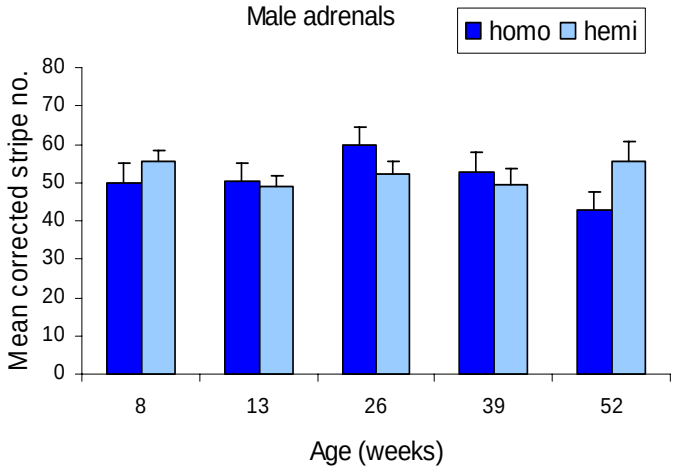

Fig. 6.10. Comparison of the mean corrected stripe number between hemizygous and homozygous males at different ages. A 2-way ANOVA showed no significant variation in mean corrected stripe number with age (P=0.570) or homozygous versus hemizygous genotype (P=0.1799). Error bars are standard errors of the mean (SEM). The numbers of adrenals in each group are shown in Fig. 6.6.

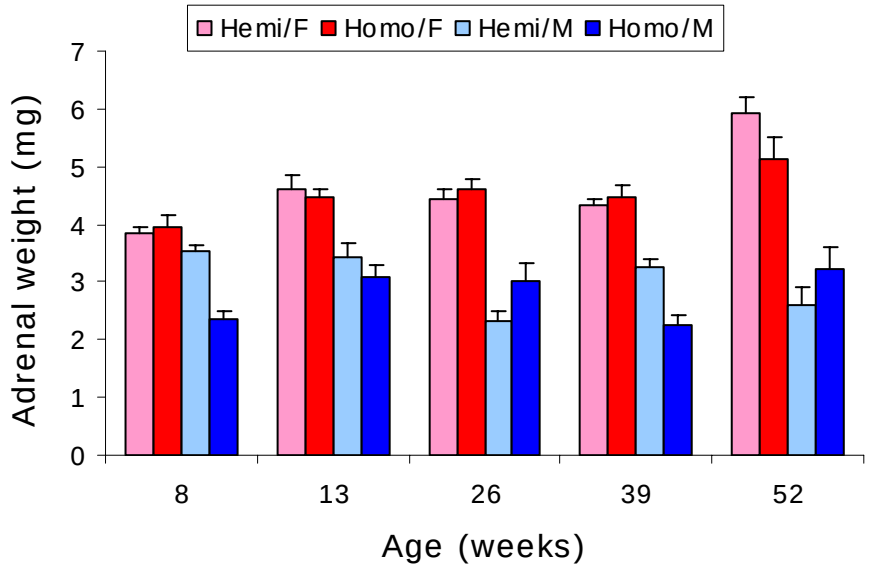

Fig. 6.11. Comparison of adrenal weights between four groups of *21OH/LacZ* transgenic mice at different ages. A 2-way ANOVA showed female adrenals were heavier than males for both homozygotes ($P<0.0001$) and hemizygotes ($P<0.0001$) but homozygous female adrenals were not significantly heavier than adrenals from hemizygous females ($P=0.5341$ by 2-way ANOVA). Female adrenals were heavier than male adrenals at each age. Abbreviations: F, female; M, male; hemi, hemizygous; Homo, homozygous. Error bars are standard errors of the mean (SEM). The numbers of adrenals in each group are shown in Fig. 6.6.

6.3.5 Comparison of the frequency of transgene inactivation in *21OH/LacZ* male and female homozygotes and heterozygotes at different ages

Mosaic *21OH/LacZ* transgene expression is probably due to random inactivation of the transgene in some progenitor cells at an early developmental stage but the mechanism of transgene inactivation is not understood and it is not known whether inactivation is exclusively an embryonic developmental event or continues throughout adult life. The percentage of β-gal-negative cells was compared in the four *21OH/LacZ* experimental groups at different ages to test whether transgene inactivation continues in the adult or whether a constant frequency of transgene inactivation is maintained (Fig. 6.12). One-way ANOVA showed no significant differences in the percentage of β-gal-negative cells at different ages for hemizygous females, hemizygous males or homozygous females (Fig. 6.12). The percentage of β-gal-negative cells in homozygous male adrenals differed significantly between ages and post-hoc tests indicated that this was due to a higher percentage of β-gal-negative cells at the 52 week time point only. Apart from this there was no other evidence that the percentage of β-gal-negative cells increased with age. For both male and female homozygotes the highest percentages of β-gal-negative cells occurred at 26 and 52 weeks. However this trend does not suggest progressive transgene inactivation with age because, in each case, the percentage of β-gal-negative cells was lower at 39 weeks than 26 weeks. The higher percentage of β-gal-negative cells at one specific age (26 weeks) in both sexes could be due to experimental variation in the samples analysed. Overall, the evidence implies that the *21OH/LacZ* transgene does not continue to inactivate beyond 8 weeks, the first time point tested, and it might be valuable in future to examine earlier time points, e.g. from postnatal week 3 when stripes resemble the adult pattern, to determine whether the level of transgene changes during postnatal adrenal growth.

There was no consistent difference in the percentage of β-gal-negative cells between males and females but homozygotes consistently had lower percentages of β-gal-negative cells (higher percentage of cells expressing the transgene) than hemizygotes. This difference is explored in more detail in the next section to see whether it provides any information about the mechanism of transgene inactivation.

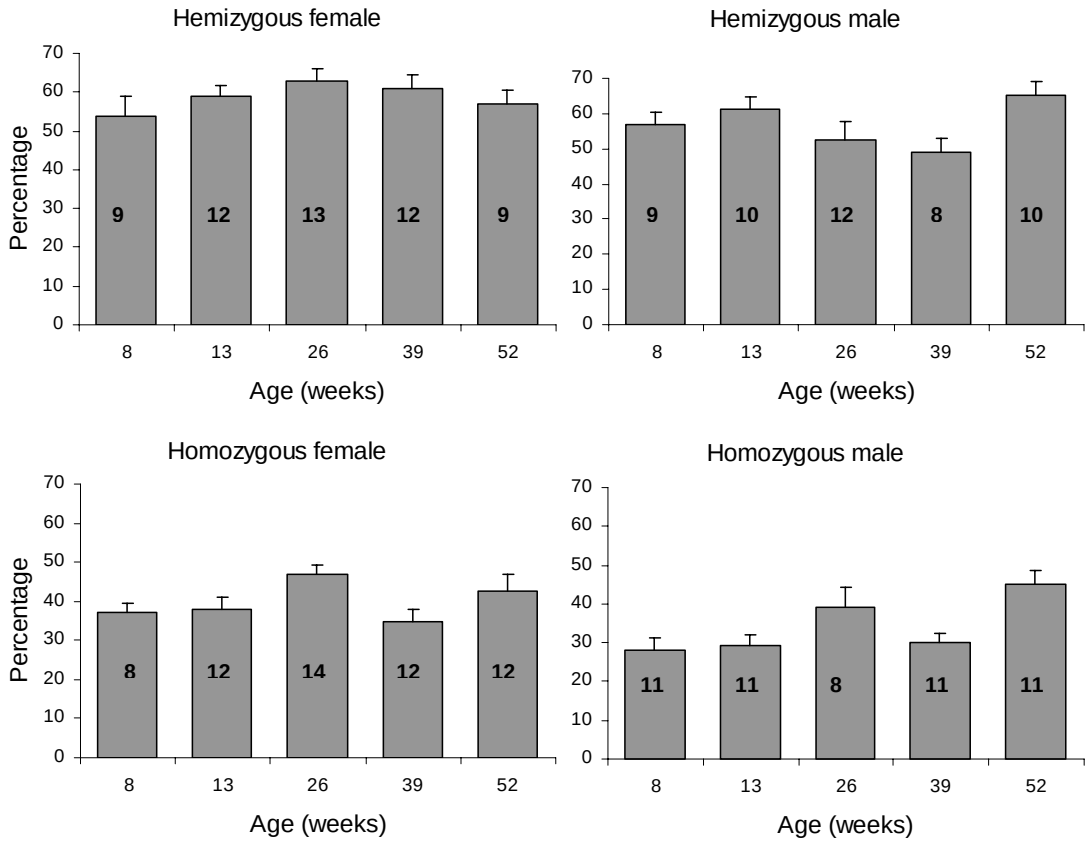

Fig. 6.12 Comparison of the percentage of β-gal-negative cells in the adrenal cortices of *21OH/LacZ* transgenics at different ages. The percentages of β-gal positive and β-gal negative cells were estimated from measurements along a measured circumference as described in section 2.5. No significant variation in percentage β-gal-negative cells with age was found by 1-way ANOVA for hemizygous females (P=0.4004), hemizygous males (P=0.0804) or homozygous females (P=0.0655). Variation among ages was significant for homozygous males (P=0.0012) and Scheffe's post hoc tests showed significant differences in percentage β-gal-negative cells between 8 and 52 (P=0.0124), 13 and 52 (P=0.0228) and 39 and 52 weeks (P=0.0382) but other comparisons were not significant. Error bars are standard errors of the mean (SEM). The numbers shown in the grey bars are the numbers of adrenals analysed in each group.

6.3.6 Comparison of the frequency of transgene inactivation in homozygous and hemizygous *21OH/LacZ* adrenals

In the previous section it was noted that *21OH/LacZ* homozygotes consistently had lower percentages of β-gal-negative cells than hemizygotes. This would be predicted if transgene silencing occurs at the chromosomal level but not if transgene silencing occurs at the cellular level (Fig. 6.13). The percentage of β-gal-negative cells was significantly lower in homozygotes than hemizygotes for both females (Fig. 6.14) and males (Fig. 6.15), as predicted if transgene silencing occurs at the chromosomal level (independent inactivation of both alleles) rather than at the cellular level (co-ordinated inactivation of both alleles).

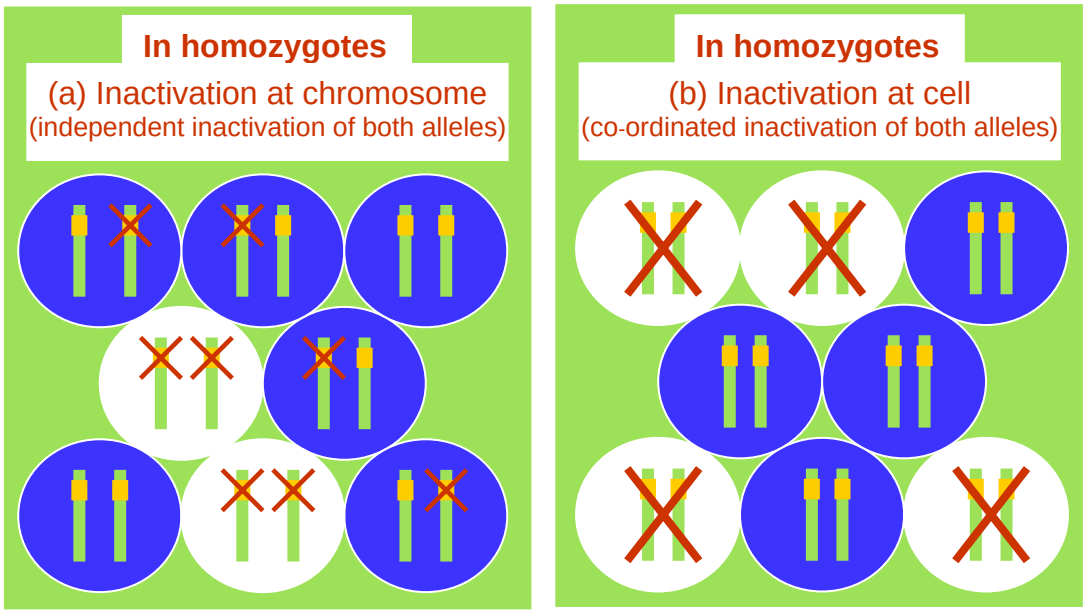

Fig. 6.13. Predictions for frequencies of transgene silencing in *21OH/LacZ* homozygotes by a chromosomal or cellular-based mechanism.
(a) If transgene inactivation occurred at the chromosomal level both copies of the transgene need to be separately inactivated to produce a β-gal-negative cell, so the chance of inactivating both transgene copies in a cell is less than the chance of inactivating a single copy. The cell will only be β-gal-negative if both copies are inactivated so the frequency of β-gal negative cells is expected to be lower in homozygotes than hemizygotes. (b) If transgene inactivation occurred at the cellular level either both or neither copies of the transgene are inactivated. The chance of inactivating both copies in a homozygous cell will be the same as inactivating the single copy in a hemizygous cell so the frequency of β-gal negative cells is expected to be the same in homozygotes and hemizygotes.

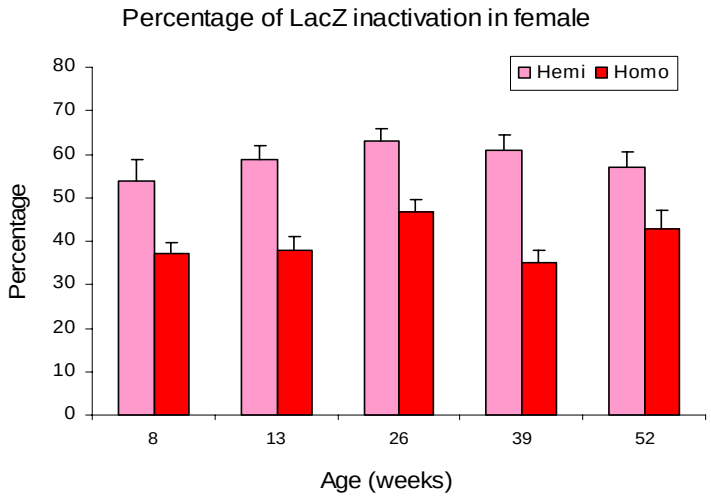

Fig. 6.14. Comparison of the percentage of β-gal-negative cells between homozygous and hemizygous females at different ages. A 2-way ANOVA showed significant variation in percentage β-gal negative cells for hemizygous versus homozygous genotype ($P<0.0001$) but not for age ($P=0.0662$). Error bars are standard errors of the mean (SEM). The numbers of adrenals in each group are shown in Fig. 6.12.

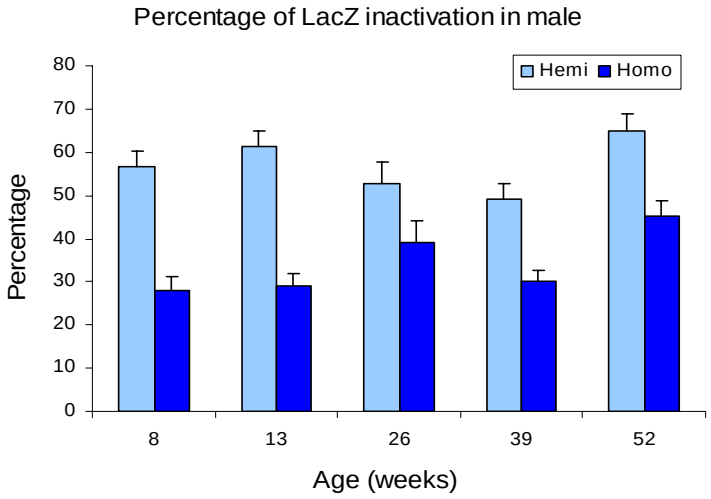

Fig. 6.15. Comparison of the percentage of β-gal-negative cells between homozygous and hemizygous males at different ages. A 2-way ANOVA showed significant variation in percentage β-gal negative cells for hemizygous versus homozygous genotype ($P<0.0001$). There was also a significant effect of age ($P=0.0013$). Scheffe's post hoc tests showed significant differences in percentage β-gal negative cells between 8 and 52 ($P=0.0126$) and 39 and 52 weeks ($P=0.0015$) but other comparisons were not significant (also see Fig. 6.12 for age effects). Error bars are standard errors of the mean (SEM). The numbers of adrenals in each group are shown in Fig. 6.12.

If the two transgene alleles are inactivated independently it is predicted that the probability of inactivating both alleles should be equal to the square of the probability of inactivating one allele. This prediction can be tested. The proportion of β-gal-negative cells in hemizygous adrenals (one allele inactivated) is designated p_n and the observed proportion of β-gal-negative cells in homozygous adrenals (both alleles inactivated) is designated $p_{N.}$ The proportion p_n should indicate the probability of inactivating the transgene on one chromosome. If both transgenes in homozygotes are inactivated independently (at the chromosomal level), the probability of inactivating the transgene in both chromosomes in a homozygous adrenals should be equal to $(p_n)^2$ and this should be equivalent to the observed proportion $p_{N,}$ in homozygotes.

To test whether the proportions of β-gal-negative cells in homozygotes fitted the expectations for independent inactivation at the chromosomal level, $(p_n)^2$ (calculated from p_n, the proportion of β-gal-negative in hemizygotes) was compared with $p_{N,}$ (the proportion of β-gal-negative in homozygotes) by ANOVA. As predicted, $(p_n)^2$ did not differ significantly from $p_{N,}$ for either females (Fig. 6.17) or males (Fig. 6.18). These results suggest that transgene silencing acts at the chromosomal level rather than cellular level.

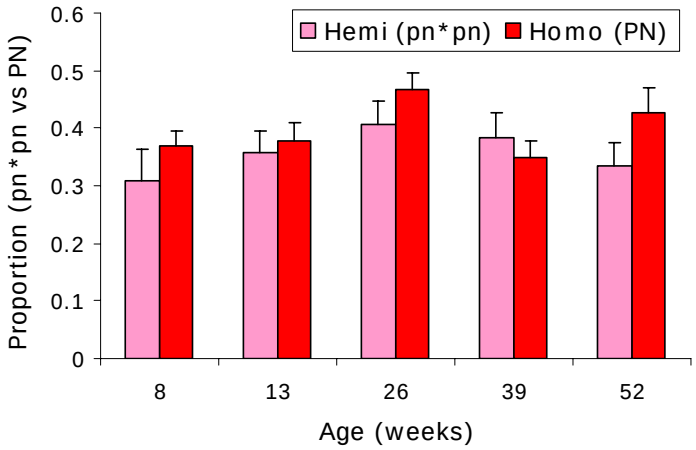

Fig. 6.16. Testing the prediction of transgene inactivation at the chromosomal level in females. A 2-way ANOVA showed that, as predicted, the proportion of β-gal-negative cells in homozygous females [p_N] was not significantly different from the square of the proportion of β-gal-negative cells in hemizygous females [$(p_n)^2$] (*P*=0.1055). Error bars are standard errors of the mean (SEM). The numbers of adrenals in each group are shown in Fig. 6.12.

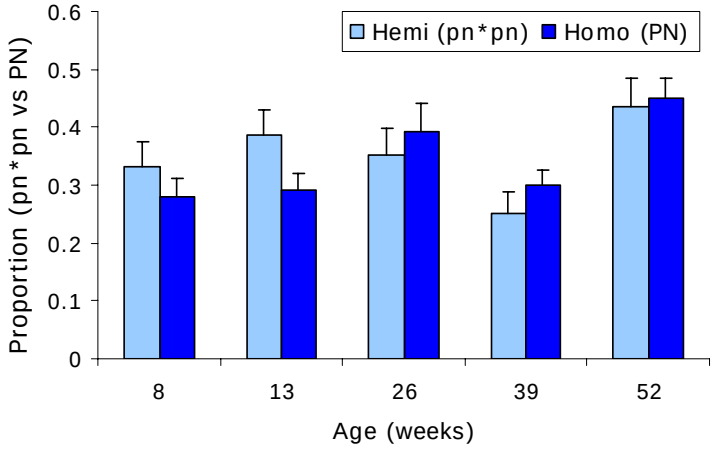

Fig. 6.17. Testing the prediction of transgene inactivation at the chromosomal level in males. A 2-way ANOVA showed that, as predicted, the proportion of β-gal-negative cells in homozygous males [p_N] was not significantly different from the square of the proportion of β-gal-negative cells in hemizygous females [$(p_n)^2$] (*P*=0.9680). Error bars are standard errors of the mean (SEM). The numbers of adrenals in each group are shown in Fig. 6.12.

6.4 Discussion

6.4.1 Qualitative observations on *21OH/LacZ* stripe patterns

In most cases, radial β-gal stripes cross the entire thickness of adrenal cortex. Almost all of those that are discontinuous can be explained as sectioning artefacts. However, careful analysis of several serial sections showed that in 3 of 200 adrenal glands a few stripes did not span the full thickness of the adrenal cortex. Although it seems more likely that these few discontinuous stripes were either experimental artefacts or morphological abnormalities (e.g. thick capsule), and the other points discussed below but, if proven, this finding would have significant implications for interpretations of how stem cells might maintain the adrenal cortex.

The finding of an 'undifferentiated' zone (Mitani et al., 2003) raises the possibility that this zone contains stem cells that maintain the adult adrenal cortex by bi-directional cell movement into the ZG and ZF. The presence of discontinuous stripes is compatible with maintenance by the undifferentiated zone (Fig. 1.11d) but not by the cell migration theory (Fig. 1.11a). If the undifferentiated zone contained stem cells that maintained the zona glomerulosa (to the outside) and also the zona fasciculata and zona reticularis (to the inside), the stem cells could be organised in several ways. There could be either a single population of stem cells maintaining both the ZG and ZF or two separate populations of stem cells, each of which maintains a distinct zone. If there are indeed two separate stem cell populations (e.g. separate populations of outer ZG and inner ZF/ZR stem cells) four types of stripes could be produced. Fig. 6.18, illustrates the two single colour stripes and one of the two possible alternative discontinuous stripes (containing both colours).

The stripe continuity may be relevant to identifying the origin of cortical cell progeny (location of putative stem cells) and distinguishing between the different hypotheses for the maintenance of adrenal cortex (chapter 1.4.3). The observation

that a few stripes do not span the entire cortex is compatible with maintenance by stem cells in the undifferentiated zone (Fig. 1.11d). However, this interpretation is placed into doubt by (1) the abnormal shape of the outer β-gal-negative region, which covers the width of many stripes (2) the failure to observe discontinuous β-gal-positive stripes in the ZG coupled with a β-gal-negative stripe in the ZF – only the opposite pattern was ever seen.

Previous published work has noted the existence of occasional hyperplasic extensions containing non-steroidogenic cells from the capsule into the cortex (Bielinska et al., 2003), which could disrupt the normal stripe pattern in the *21OH/LacZ* adrenal. Consequently further investigation is required to investigate the phenomenon of discontinuous stripes, for example by using zone- and capsule-specific markers in combination with β-gal staining to delineate the precise origin of such stripes.

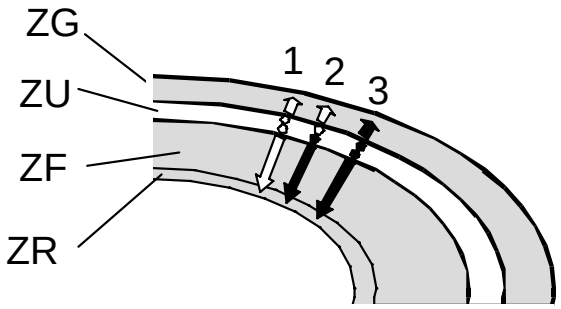

Fig. 6. 18. Possible production of a discontinuous mosaic pattern by two populations of adrenal stem cells in the ZU. This diagram represents a variant of the model shown in Fig. 1.11e, with two rows of stem cells in the undifferentiated zone (ZU). Three combinations of stem cells are shown in the ZU. An outer row of stem cells maintains the ZG and an inner row of stem cells maintains the ZF/ZR. At position 1 the outer and inner stem cells both produce β-gal-negative stripes. At position 2 the outer stem cell produces β-gal-negative stripe and the inner stem cell produces a β-gal-positive stripe. At position 3 the outer and inner stem cells both produce β-gal-positive stripes. At position 2 the β-gal-positive stripe does not span the whole cortex.

6.4.2 Effects on the mean corrected stripe numbers in the *21OH/LacZ* adrenal cortex

The corrected stripe number provides a form of clonal analysis that has been used previously in the corneal epithelium to compare stem cell function between different experimental groups of mosaic mice (Collinson et al., 2002). The observed number of stripes is affected by the proportions of β-gal-positive cells. Calculation of a corrected stripe number allows for variation that is attributable to differences in proportions of β-gal-positive cells. It therefore provides a means of comparing the numbers of clonal lineages in different groups. This was used here to compare stripe numbers in adrenals from different groups of *21OH/LacZ* transgenic mice. No consistent effect of gender, genotype (hemizygous versus homozygous) or age (8 to 52 weeks) on β-gal adrenocortical corrected stripe numbers was found.

The absence of an age-related effect suggests that the adult adrenocortical stripe pattern is fully established by 8 weeks of age, the earliest time point tested, It would perhaps also be informative to carry out a similar analysis at earlier ages, e.g. 2 or 3 weeks, when the data presented in Chapter 3 suggests that radial stripe patterns indistinguishable from adult are already emerging. The lack of evidence for an age-related decline in the mean of corrected β-gal adrenocortical stripe number differs from the results reported previously for the corneal epithelium (Collinson et al., 2002). In the corneal epithelium, a similar analysis of radiating stripes showed a decline in corrected stripe number with age which was suggested to reflect a decline in the number of active stem cell clones that maintain the adult corneal epithelium.

If mosaic stripes in the *21OH/LacZ* adrenal cortex are produced by stem cells that maintain the tissue, the results presented here provide no evidence for a decline in adrenocortical stem cell function equivalent to that reported for the corneal epithelium. This may be because (1) the stripes in the adrenal cortex are not produced by stem cells or (2) the two tissues are maintained differently. Although

the adrenal cortex has a significant regenerative potential, the rate of cell turnover is thought to be relatively low during normal tissue maintenance. The constant corrected stripe number between 8 and 52 weeks may indirectly reflect a relatively constant number of active stem cell clones responsible for the basic maintenance of adrenal cortex. The number of active stem cell clones might decline more rapidly in other tissues where cell turn-over is higher.

6.4.3 *21OH/LacZ* transgene expression and inactivation

The endogenous mouse steroid 21-hydroxylase A gene is expressed throughout the adrenal cortex but the β-gal staining in the *21OH/LacZ* transgenic adrenals displayed strikingly variegated patterns of mosaic patches and radial stripes respectively in fetal and adult stages (Morley et al., 1996). Such mosaic transgene expression is thought to involve some type of stochastic inactivation of the transgene in some progenitor cells early in development (Dobie et al., 1997). Transgene inactivation could occur throughout life or only early in development. If *21OH/LacZ* transgene inactivation occurs throughout life the proportion of β-gal-negative cells in *21OH/LacZ* adrenal cortices should increase with age. If transgene inactivation occurs only early in development, adult transgene expression patterns would be clonally maintained because new members of clonal cell lineages should inherit a stable state of transgene expression (either on or off). Therefore, the proportion of β-gal-negative cells should not change with age. The results presented here showed no significant increase in the level of transgene inactivation with age and so favour the hypothesis that transgene inactivation in the *21OH/LacZ* transgenic adrenal is established before 8 weeks (the first experimental time point tested) and is then stably inherited throughout adult life.

These results also indicated that *21OH/LacZ* homozygotes had significantly fewer β-gal-negative cells than hemizygotes. Comparison of the experimentally determined proportion of β-gal-negative cells in homozygotes with that predicted if transgene inactivation occurred at the chromosomal rather than cellular level, showed that these values did not differ significantly. These observations support

the hypothesis that the transgenes on homologous chromosomes are inactivated independently (i.e. the inactivation of the transgene on one chromosome does not influence whether the transgene on the homologous chromosome is inactivated or remains active). It also suggests that in homozygotes some β-gal-positive cells probably express both alleles of the *21OH/LacZ* transgene while other cells only express one allele.

At least two other studies have compared mosaic transgene expression in homozygotes and hemizygotes. In the first study, transgenic fish (tilapia) showed mosaic expression of a carp β-actin/*LacZ* transgene. *LacZ* expression in homozygotes was approximately twice that in hemizygotes, suggesting that both alleles are expressed in homozygotes (Rahman et al., 2000). Although the frequency of β-gal-positive cells was not specifically compared in homozygotes and hemizygotes the illustrations in the paper suggest that the homozygotes have a higher proportion of positive cells which would be more consistent with mosaicism caused by transgene silencing at the chromosomal rather than cellular level.

In the second study, two lines of transgenic mice carrying 20-30 copies of an ovine β-lactoglobulin (BLG) transgene showed mosaic expression (Opsahl et al., 2003). In one line (BLG/45) the homozygotes produced approximately twice as much β-lactoglobulin protein as the hemizygotes, suggesting both alleles were active. However, in the other line (BLG/7) the homozygotes produced only about 40% more protein than the hemizygotes. Further analysis showed that only one allele of the transgene was expressed in BLG/7 homozygotes, which shows that the control of transgene expression in this line is complex.

Further studies are needed to identify the molecular mechanisms involved in inactivation of the *21OH/LacZ* transgene. These could involve factors such as transgene copy number, transgene position in the chromosome (e.g. close to the centromere) and DNA modification (e.g. methylation).

6.5 Conclusions

Differences in the proportions of β-gal-positive cells in homozygous versus hemizygous *21OH/LacZ* adrenal cortices suggested that transgene inactivation occurs at the chromosomal rather than cellular level. The analysis of mosaic stripe patterns in the adrenal cortices of *21OH/LacZ* transgenic mice revealed no convincing evidence in favour of maintenance of the ZG and ZF/ZR by separate populations of stem cells. Quantitative analysis of the corrected stripe number in mosaic *21OH/LacZ* adrenal cortices did not show any age-related reduction that might have suggested an age-related decline in stem cell function.

7. General discussion

The adrenal cortex is a dynamic tissue which undergoes changes in proliferation pattern and tissue remodelling during perinatal growth and is maintained by a balance between cell proliferation, cell movement and apoptotic cell death during adult life. The main scientific question considered in this thesis is whether the adrenal cortex is maintained by a resident stem cell population. If so, it is important to ask when stem cells become activated and where they are located. The experimental aim of chapters 3 and 4 was to understand when and how the adult pattern of mosaic β-gal stripes forms in mosaic *21OH/LacZ* transgenic adrenals. This is relevant to the question of when stem cells are likely to become activated (if they exist). Chapters 5 and 6 considered how the adult adrenal cortex is maintained. This is relevant to the questions of whether stem cells are involved in adrenal cortical maintenance and, if so, where they are most likely to be located. The general discussion in the present chapter is divided into three sections. The first deals with emergence of stripes in the mosaic adrenal cortex, the second considers the evidence for stem cells in the adrenal cortex and the third deals with the possible stem cell mode of adrenocortical maintenance.

7.1 Mosaic β-gal stripe formation in the perinatal *21OH/LacZ* adrenal

The original study of mosaic patterns in *21OH/LacZ* transgenic adrenal cortices showed that the pattern changed from randomly orientated patches in the fetus to radial stripes in the adult (Morley et al., 1996). The experiments reported in this thesis explored when this change occurs and showed that the mosaic pattern changed from randomly orientated clusters at E14.5 to emerging radial stripes at P7 and to complete radial stripes by P14 -21. The complete radial stripe patterns described for P21 in this thesis and reported previously for juvenile stages (3 weeks and 4.5 weeks) in my MSc thesis (Chang, 2003) were the same as those in the adult.

Consideration of other mosaic tissues that form stripes can help guide the interpretation of how the mosaic β-gal stripes emerge in the *21OH/LacZ* transgenic adrenal cortices and whether this is relevant to the timing of stem cell activation. Stripes arise in both the retinal pigmented epithelium (RPE) and corneal epithelium of mosaic mice as discussed in section 1.5. Fig. 7.1 compares the likely changes in mosaic patterns in the RPE and corneal epithelium from fetal to adult stages.

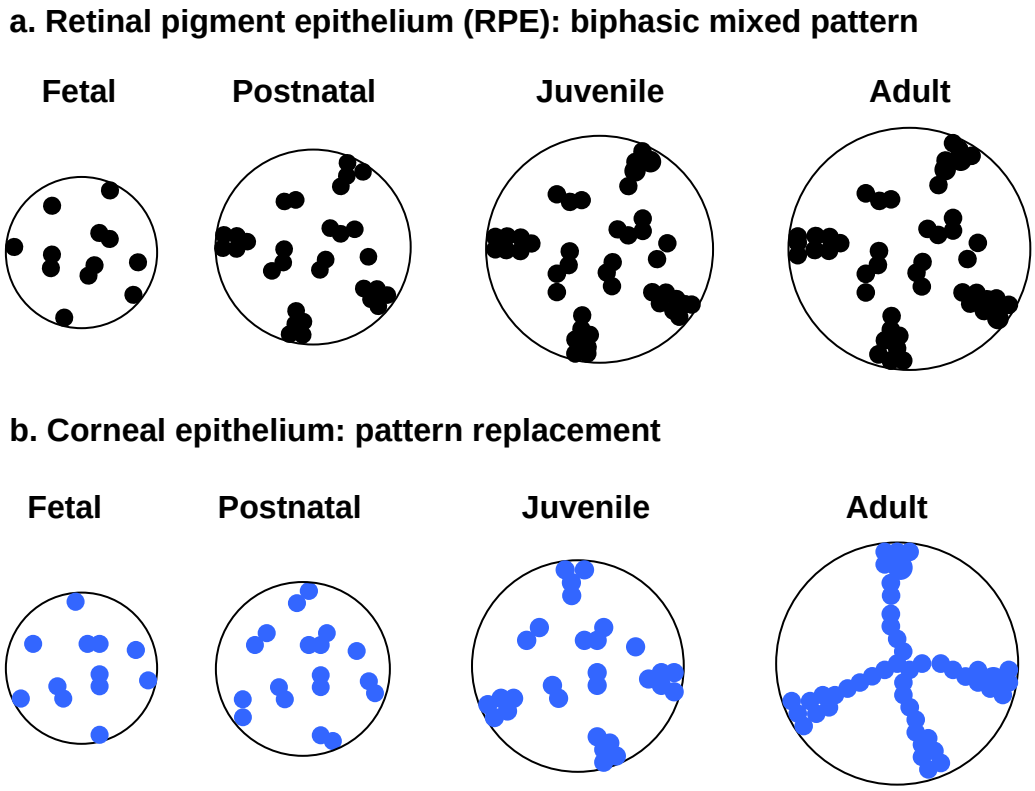

Fig. 7.1 Changes of mosaic patterns in the RPE and corneal epithelium from fetal to adult stages. (a) In the RPE, the mosaic pattern changes from randomly-orientated patches at the fetal stage to a mixed pattern of randomly orientated patches in the centre with radial stripes at the periphery from the early postnatal stage. The proposed explanation is that the pattern of proliferation switches from interstitial growth to edge-biased growth and this reduces cell mixing and initiates stripe formation. This mixed pattern appears to remain stable in the adult. (b) In the corneal epithelium, the mosaic pattern changes from randomly orientated patches to a mixed pattern of central randomly orientated patches with radial stripes at the periphery by the juvenile stage and then changes to complete radial stripes by the adult stage. It is proposed that the stripes emerge when the stem cells become activated in the corneal limbus and replace the original fetal mosaic pattern by early adult. See text for relevant literature references.

During the development of the RPE, the first part of the tissue to form produces the proximal (posterior) part of the RPE in the adult (shown as the central region in Fig. 7.1a) and the tissue formed later produces the distal or peripheral part of the adult RPE. So the RPE of adult mosaics has a patchy mosaic pattern in the centre but radial stripes at the periphery. The changes in pattern from patches to stripes has been explained by a change in proliferation pattern from interstitial growth to edge-biased growth (Bodenstein and Sidman, 1987a; Bodenstein and Sidman, 1987b). Computer simulation demonstrated that this change of proliferation pattern would cause a reduction in cell mixing, resulting in the formation of radial stripes during the later stages of tissue growth (Bodenstein, 1986; Bodenstein and Sidman, 1987c). Mosaic patterns in the adult RPE can be considered to be mixed and arise in a biphasic way, with the patches in the central region reflecting the early period of interstitial growth and the stripes at the periphery representing the later period of edge-biased growth.

A similar transition of mosaic pattern occurs in the corneal epithelium (Collinson et al., 2002). Fig. 7.1b shows that initially a randomly orientated mosaic pattern persists postnatally but this is then replaced by radial stripes which emerge from the periphery at about 5 weeks and reach the centre by 8-10 weeks. The corneal epithelium is about 5 cells thick so the mature pattern is not clear until the older more superficial layers are replaced. However the pattern of radial stripes is clear by about 12 weeks and then persists in the adult. This displacement of the early (fetal) mosaic pattern with centripetal stripes has been attributed to the activation of limbal stem cells (LCSs) at the periphery of the corneal epithelium. The LSCs produce clones of daughter TA cells that migrate inwards and replace older cells that leave the basal layer and then are lost by desquamation (Collinson et al., 2002). Unlike the RPE, the early pattern is not retained in the corneal epithelium but is completely replaced by the newly formed stripes.

It is useful to consider whether the changes in mosaic pattern described for the adrenal cortex in chapter 3 resemble the changes shown in Fig. 7.1 for either the RPE (biphasic mixed pattern) or corneal epithelium (pattern replacement). Fig. 7.2 shows two hypothetical possibilities of how stripes in the adult adrenal cortex may have formed from a pattern of randomly orientated patches in the fetus. In Fig. 7.2a it is proposed that edge-biased growth occurs from an early stage (similar to the RPE) to produce a pattern of radial stripes spanning most of the cortex. However, the stripes will not reach the medulla unless the older cells produced in the fetus die and are replaced by new cells. In Fig. 7.2b it is proposed that radial stripes are not formed until stem cells are activated in the early adult stage.

Fig. 7.2c shows the actual transition of the mosaic patterns observed in the adrenal cortex, as described in chapter 3. The radial stripes appear at the early postnatal stage (similar to Fig. 7.2a) and by the juvenile stage the fetal pattern has been completely replaced by a radial striped adult pattern. This may be explained by two different hypotheses. (1) Edge-biased growth generates stripes which replace the fetal pattern when the earliest cells die in the inner adrenal cortex. This does not require the existence of stem cells but if they are involved it is assumed that they are activated once the stripes are formed and maintain the original striped pattern. (Presumably stem cells would be specified within the stripes before they become activated.) (2) Stem cells may have become activated in the periphery at the early postnatal age and replace the fetal pattern when the adrenal grows. In this case, edge-biased proliferation may reflect division of stem cells or early TA cells near the periphery during the growth phase. In both cases, edge-biased growth and stem cells would produce a similar striped pattern so the time of stem cell activation cannot be identified from the mosaic pattern and distribution of proliferating cells.

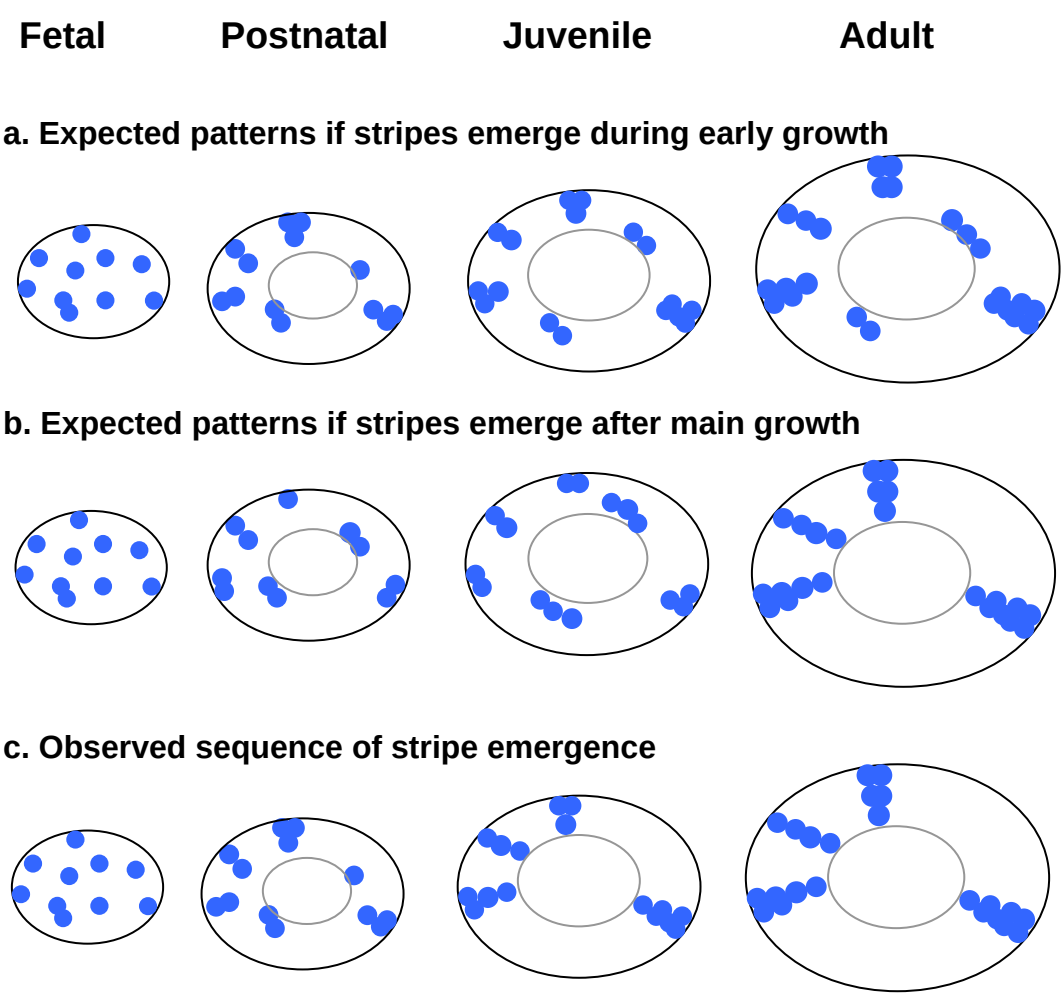

Fig. 7.2. Formation of stripes in the adrenal cortex. This shows two hypothetical possibilities (a and b) of how stripes in the adult adrenal cortex may form from a pattern of randomly orientated patches in the fetus and the actual transition that was observed experimentally (c). **(a)** This possibility shows radial stripes formed by edge-biased growth, beginning at the postnatal stage but they do not reach the medulla unless older cells die. **(b)** This possibility shows radial stripes formed when stem cells become activated at late juvenile age. **(c)** The actual observed transition from randomly-orientated clusters to radial striped pattern in the entire adrenal cortex occurs before the juvenile stage. This observed sequence probably involves edge-biased growth (a) but it is unclear whether stem cell activation (b) occurs (see text).

Other studies using computer simulations to explain how stripes could emerge in chimeric and mosaic adrenal cortices, predicted they could arise by edge-biased proliferation (Landini and Iannaccone, 2000). The finding (in chapter 3) that edge-biased proliferation preceded the time of stripe formation at the perinatal stage of adrenal growth supports this explanation of how stripes emerge.

Although stripes probably first emerge by edge-biased proliferation this does not explain the disappearance of the fetal pattern near the medulla. This is presumably a result of death of the older cells and net movement of cells from the proliferative regions. The evidence of the centripetal cell movement in postnatal adrenal (McNicol and Duffy, 1987; Mitani et al., 1999; Wright and Voncina, 1977) supports the displacement of the original fetal mosaic pattern with radial stripes. This is consistent with the activation of stem cells but the stripes could also be formed entirely by edge-biased growth followed by loss of the fetal pattern when older cells die. It, therefore, remains unclear whether stem cell activation is involved in the transition from the randomly orientated patches in the fetus to the radial stripes in the adult adrenal cortex. So far, the changes of mosaic pattern together with proliferation pattern are consistent with edge-biased proliferation or with pattern replacement involving stem cells function.

Although the analysis of perinatal patterns and cell proliferation showed that edge-biased growth occurs, there are some issues that need to be clarified to better understand how cell proliferation and death affect the mosaic adrenocortical stripe pattern.

First, it is unclear when edge-biased growth begins in the mouse but stripes probably emerge just after zonation commences (just before birth in the rat and probably also in the mouse). This suggests that the proliferative cells near the edge of the cortex are within the developing ZG. Evidence from studies in the rat indicate that at E16 proliferation is randomly distributed throughout the adrenal cortex (Mitani et al., 1999), which is consistent with interstitial growth at that stage, though proliferation becomes concentrated in the rat subcapsular region at later stages (Mitani et al., 1999). Cell proliferation should be analysed in the mouse adrenal cortex at earlier fetal stages (from E14.5) to determine when the expected switch from interstitial to edge-biased growth occurs.

Second, in the present study, it was shown that edge-biased growth had already begun by E18.5 but stripes were not detected until several days later (continuous stripes were first identified at P7, though their formation was not complete until P14-21). This may be because cell proliferation is relatively slow in the perinatal adrenal cortex so there is a lag before sufficient new cells are produced to generate a stripe, or it may be because cell divisions are randomly orientated when edge-biased growth begins. It would be useful to determine whether cell divisions are randomly orientated during interstitial growth but generally radial once edge-biased growth begins. The lag in identification of stripes may also be because the resolution of the methods used was insufficient to detect the earliest stripes, particularly when the proportions of β-gal-positive and β-gal-negative cells is similar, as is the case in the adrenal cortex of the *21OH/LacZ* strain used here. Other approaches, such as 3D reconstruction of serial sections or optical projection tomography, OPT (Sharpe et al., 2002) may provide better resolution of when and how stripes emerge.

Third, it would also be useful to identify how the initial randomly orientated mosaic pattern is replaced by the radial stripes. Some cells produced early may contribute to the X zone and others may die. It was anticipated that analysis of stripes during the early postnatal period would identify whether and when stripes extended to the boundary with the medulla by replacing the original tissue as it

dies. However, the limited resolution of the staining methodology and the complication of several cellular events going on at the same time (i.e. cortical growth, zonation, X zone and cortical-medulla resolution) made it difficult to follow the perinatal replacement of the original punctate pattern with mosaic stripes with certainty. Nevertheless, it was apparent that the time when the majority of stripes first spanned the cortex coincided with the first appearance of a morphologically distinct X zone (P10-P14) and further studies of this period may help us clarify the resolution of the fetal and definitive zones. Additional time points over the period P7-14, or improved imaging techniques (such as 3D reconstruction), particularly in chimeras or mosaics with a lower proportion of β-gal staining, may help to follow the progress of stripe formation. A study of the distribution of apoptotic cells during the emergence of stripes would also help to evaluate how the original fetal mosaic pattern is eliminated while the radial elongated patches begin to emerge in the outer cortex.

7.2 Stem cells in the adrenal cortex

The strongest evidence for the existence of stem cells in the adrenal cortex is provided by experiments showing adrenocortical regeneration after enucleation and experiments involving the regeneration of functional adrenal cortex cells from cloned cells (Perrone et al., 1986; Skelton, 1959; Thomas et al., 1997). In the enucleated adrenal gland, the remaining capsule and underlying subcapsular cells proliferate and expand towards the centre to regenerate a new cortex with normal histological appearance, cortical zonation and restored steroidogenic functions after approximately 30 days (Perrone et al., 1986; Skelton, 1959; reviewed in Kim and Hammer, 2007). Moreover, transplantation of cloned bovine adrenocortical cells under the kidney capsule of adrenalectomised SCID (severe combined immunodeficient) mice proliferated and after 36-41 days had formed a vascularised tissue mass with a normal adrenocortical histological appearance that performed the normal endocrine functions of the ZG and ZF and was able to replace the mouse's own adrenal cortex (Thomas et al., 1997). Both experiments suggest that stem cells, or at least cells which are able to dedifferentiate and function as adrenocortical progenitors, exist in the adrenal cortex and are probably located either close to or in the capsule.

Other authors have identified cells in the adrenal cortex that appear relatively undifferentiated as candidates for stem cells. As discussed in section 1.1.1, a zone of relatively undifferentiated cells, that do not express cortical zone-specific enzymes, has been reported to be located between the ZG and ZF of rats and mice, (Mitani et al., 2003; Mitani et al., 1994; Mukai et al., 2002) or in the inner zona glomerulosa (Vinson, 2003). In addition, spindle shaped cells (A cells), with limited steroidogenic capacity, occur near the capsule in older mice from some strains, proliferation of which can be induced by gonadectomy (Bielinska et al., 2003). These cells are reported to be able to proliferate and are proposed to produce steroidogenic cells (B cells). Production of both cell types (A cells and B cells) is thought to represent metaplasia of competent cells in the outer adrenal

cortex. The competent cells could be stem cells or progenitor cells in this region but they have not yet been identified.

In this thesis, I have tried to identify putative stem cells as label-retaining cells. This approach has been used previously to identify stem cells in other tissues as described in section 1.3.2. The basis of this approach is that many stem cells divide relatively infrequently. (This may help to retain their stem cell characteristics and higher proliferative potential and also avoid accumulating genetic errors.) The strategy used to detect label-retaining cells is to use prolonged exposure to a DNA label (such as BrdU), which will label cells that divide less frequently (including putative stem cells) as well as those that divide more frequently. This is followed by a long-term chase period. During the chase time most cells divide several times and dilute the label at each cell division but putative stem cells that divide less frequently will retain the label and can be detected as label-retaining cells at the end of the chase period.

However, not all label retaining cells are stem cells and cells may retain label for the following reasons. (1) Cells divide infrequently (some may be stem cells but some may be other cells). (2) Cells may become quiescent and stop dividing after they are labelled. These may include stem cells and other cells. (3) Cells may become differentiated and stop dividing after being labelled. These will not be stem cells. (4) Some cells within a lineage may permanently retain a specific DNA strand, using it repeatedly as the template for DNA replication, and if labelled this would lead to label retention. This is thought to happen in some stem cells and the idea that stem cells may retain one of the original DNA strands as a mechanism to minimise mutations in their genomes has been called the immortal strand hypothesis. It has been suggested that label-retaining cells in the small intestine retain the label for this reason reviewed in (Potten, 2004). However recent evidence (Barker et al., 2007; discussed in section 1.3.1.2) suggests they are more likely to be early TA cells (progenitor cells), where strand retention might also be a valuable strategy for protecting against mutations during rapid cycles of cell division.

Although some types of stem cells have been identified as label-retaining cells (see section 1.3.2), recent evidence suggests that at least some stem cells are not label-retaining cells. For example, few haematopoietic stem cells, HSCs (isolated by FACS sorting for expression of HSC markers) are label-retaining cells (Kiel et al., 2007). Also, as noted above, the *Lgr5*-positive crypt base columnar cells (which appear to be intestinal stem cells) are not label-retaining cells (Barker et al., 2007), but do pass the 'gold standard' test of gastrointestinal stem cells by being able to regenerate all small intestinal cell types (Humphries and Wright, 2008). Therefore, label retaining cells cannot always identify stem cells and stem cells need to be identified and tested in more specific ways (e.g. the ability to self-renew and produce more differentiated progeny, clonal maintenance within a tissue and the ability to regenerate a tissue).

One previous study used a label-retaining type of approach to investigate the mouse adrenal cortex (Kataoka et al., 1996). In this work, newborn mice were labeled with tritium for 30 days and chased for up to 200 days. However, the study was designed to look at cell movement in the adult adrenal cortex rather than to identify label-retaining cells and no specific label-retaining region was suggested by the results. The experiments described in chapter 5 of this thesis identified label-retaining cells in the outer part of the adrenal cortex, near the capsule. Although this location is consistent with some other evidence for the location of stem cells (discussed above) it is not clear whether these label-retaining cells really are putative stem cells. This is both because similar labelling patterns were found after single injections of BrdU and a 15 week chase period (see chapter 5) and because recent evidence (discussed above) suggests the label-retaining cell approach may not be as good as was previously thought for identifying stem cells.

Overall, the evidence (e.g. from the regeneration experiments) suggests that that the adrenal cortex is maintained by stem cells and the most likely location is the outer cortex (based on regeneration experiments and supported to some extent by the label-retaining cell study reported in this thesis). It remains possible (but less likely) that stem cells could be located near the inner ZG / outer ZF (based on the presence of relatively undifferentiated cells, that do not express cortical zone-specific enzymes).

7.3 Maintenance of adult mouse adrenal cortex

The results presented in Chapter 5 are consistent with the general hypothesis, that the adrenal cortex is maintained by cell proliferation in the outer cortex, centripetal movement and death in the inner cortex near the medulla (see section 1.4.3). These results showed that most cell proliferation occurs in the outer regions of the mouse adrenal cortex and cells move centripetally towards the medulla. However, there was insufficient time available during this thesis to investigate the location of apoptosis within the cortex. Also, the preliminary result, suggesting the possibility of outward movement within the outer 10% of the cortex, needs to be investigated further.

Consideration of the most likely locations of stem cells in the adrenal cortex (previous section) together with information on cell proliferation, movement and apoptosis provides the basis for evaluating different hypotheses of adrenal maintenance. Five ‘classical’ hypotheses for maintenance of the adrenal cortex were discussed in chapter 1 (section 1.4.3). These and some alternative models (Fig. 7.3c2, c3 and f) are shown in Fig. 7.3.

Fig. 7.3c2 and c3 shows zonal maintenance combined with centripetal movement. Fig. 7.3c2 shows a variant of the zonal hypothesis where it is assumed that each zone has a separate group of stem cells located in the outer part of the zone and is maintained by inward movement within each zone. Fig. 7.3c shows that the adrenocortical zones are separated into 2 areas (ZG and ZF/ZR) and they are maintained with inward movement in each area. (Justification for grouping the mouse ZF and ZR is based on their overlapping biochemical expression profiles.) Model (f) is a combined model (model a plus c3) which suggests that the adrenal cortex could be maintained in 2 ways.

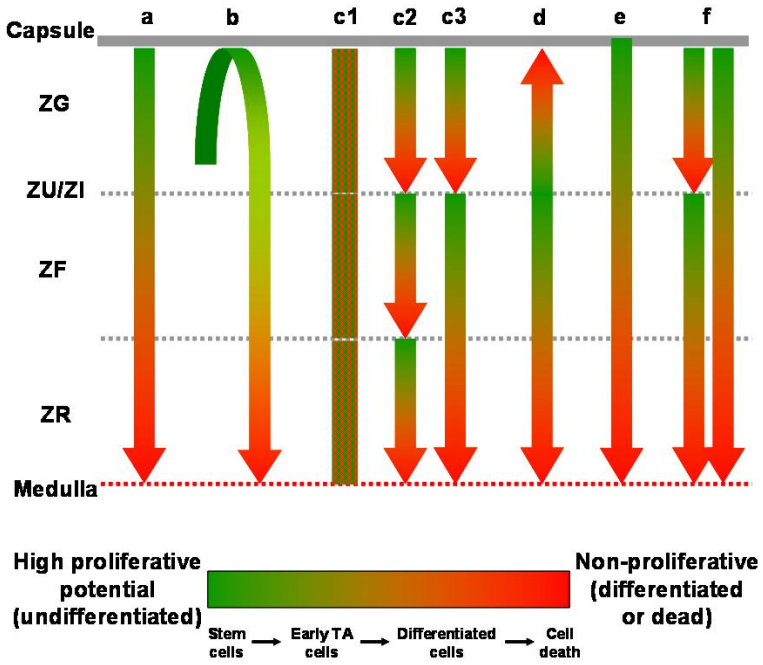

Fig. 7.3 Models of maintenance in the adrenal cortex. (a) Centripetal movement from the outer cortex. (b) Maintenance within "walking stick-shaped" unit. (c) Three versions of zonal maintenance. (c1) localised maintenance; (c2) separate maintenance within each zone combined with centripetal movement from 3 stem cell regions; (c3) separate maintenance of the ZG and ZR/ZF combined with centripetal movement from 2 stem cell regions. (d) Maintenance by stem cells in the zona intermedia. (e) Maintenance by stem cells in the capsule. (f) Combined model involving maintenance by models (a) and/or (c3) with stem cells in both the outer cortex (ZG) and outer ZF. (Models a, b, c1, d and e are based on previously published hypotheses and are described more fully in Fig. 1.11.)

Experimental evidence	Predicted outcome for models in Fig. 7.3							
	a	b	c1	c2	c3	d	e	f
Centripetal movement	√	√	×	√	√	√	√	√
Most proliferation in outer cortex	√	√	×*	×*	√	√	√	√
Most apoptosis in inner cortex	√	√			×?	×?	√	×?
Enucleated regeneration	√	√	×?	×?	×?	×	√	√
Continuous radial stripe	√	?	?	?	?	?	√	?

Table 7.1 Evaluation of models of maintenance in the adrenal cortex. The models in Fig. 7.3 are evaluated by experimental evidence showing that centripetal movement occurs, cell proliferation is mostly in the outer cortex (ZG/outer ZF), apoptosis is almost all in the inner cortex, the enucleated adrenal can regenerate the cortex (suggesting stem cells are in the outer cortex and/or capsule) and continuous radial stripes span the entire cortex in mosaic *21OH/LacZ* transgenic mice. (√ model is consistent with experimental evidence; × model is inconsistent with experimental evidence; ×? model is unlikely; ×* model is inconsistent with combination of two types of experimental evidence; ? not clear whether model is consistent with experimental evidence.)

Table 7.1 evaluates the models shown in Fig. 7.3 using various experimental criteria. Evidence of centripetal cell movement is grounds to reject the classical model of zonal maintenance (c1), in which cells are replaced locally without centripetal movement in each zone, but cannot exclude the alternative models of zonal maintenance combined with centripetal movement (c2 and c3). Centripetal cell movement is also consistent with models a, b, d, e and f. Further work is required to determine whether outward movement occurs in the ZG (chapter 5) which support model d and/or b.

Evidence for proliferation predominantly in the ZG/outer ZF does not exclude any of the models shown in Fig. 7.3. Although models c1 and c2 would be consistent with different levels of proliferation in different zones if the rate of cell turnover varied between zones, they are not consistent with proliferation being mostly in the outer two zones and apoptosis being mostly in the inner zone. The reports that apoptosis is concentrated almost entirely in the inner cortex near the medullary

boundary in young rats (Carsia et al., 1996; Mitani et al., 1999) and non-obese diabetic mice. (Breidert et al., 1998) is also inconsistent with models c3 and d (and possibly f) which predict a second major region of apoptosis. However, as apoptosis was not investigated in this thesis, models c3 and d are regarded as unlikely rather than disproved by the distribution of apoptotic cells.

Evidence from adrenal cortex regeneration after experimental enucleation excludes model d, when only the capsule and 2-3 subcapsular layers are left to regenerate the adrenal cortex. It also makes models c, c2 and c3 unlikely unless stem cells that normally only maintain the ZG can maintain all three zones after enucleation.

The significance of continuous radial β-gal stripes for the different models of adrenocortical maintenance is not clear because it is not known whether or not complete stripes are formed by edge-biased growth without any input from stem cells. If that was the case, then none of the models would be ruled out by the occurrence of radial stripes although the stripes may become less clear in model c1 if cell divisions were not radially orientated and there was no centripetal movement. Similarly, the stripes may be more intermingled in the ZG in model b, rather than being purely radially orientated. If, on the other hand, stem cells produced the stripes in a previously randomly orientated mosaic, discontinuous stripes might occur in models c2, c3, d and possibly f, if stem cells along a radial axis were not all phenotypically equivalent (all β-gal-positive or all β-gal-negative).

Consideration of all these factors (Table 7.1) favours models (a) and (e). These propose either that stem cells are in the outer cortex (model a) or the mesenchymal cells in the capsule (model e). In each case, stem cells would function to produce TA cells (progenitor cells) that move centripetally, proliferate mainly during the first part of the journey (in the ZG and outer ZF) before differentiating and eventually dying near the medullary boundary. This also

implies that the cells must change their pattern of gene expression and cell biochemistry as they pass through each zone.

The label-retaining cell experiment described in chapter 5 is also consistent with these two models. BrdU label-retaining cells were shown to be present in the outer cortex, close to the capsule or in capsule extension but, as discussed in section 7.2, the label-retaining cells might represent other kind of cells rather than stem cells. Some of these had oval rather than round nuclei and could be the spindle shaped cells associated with some adrenal tumours in tumour-susceptible mouse lines (Bielinska et al., 2003), but cell type-specific marker studies are needed to rule out other possibilities, such as differentiated endothelial cells of blood vessels.

An analysis of radiating stripes in the corneal epithelium showed an age-related decline in corrected stripe number that was interpreted as representing an age-related decline in limbal stem cell function (Collinson et al., 2002). The absence of a similar age-related decline in the mean corrected stripe number in the *21-OH/LacZ* mosaic adrenal cortex (chapter 6) could be either because the stripes are not maintained by stem cells in the same way as those in the corneal epithelium or because the age-related demands on stem cells are different in the adrenal cortex and corneal-limbal epithelium. Rando (2006) pointed out that stem cells are much more active in some tissues (e.g. the epidermis, which is classified as having high cellular turnover and high regenerative potential) than others that still have capacity to regenerate (e.g. the adrenal, which classified as having low cellular turnover and high regenerative potential). If cell turnover is lower, stem cells may be less active and any decline in stem cell function may occur more slowly and not be noticeable. (For example, TA cells may not be replenished by stem cells in the adrenal cortex as frequently as in the corneal epithelium.)

Further investigations using double-labelling experiments would be useful to evaluate the different models for adrenocortical maintenance in more detail. For example, double labelling with two markers of cell proliferation (e.g. BrdU and Ki67 or BrdU and iododeoxyuridine, IddU) used at different times could be used

to identify the direction and distance of cell movement between divisions more precisely. Double labelling with markers of proliferation and steroidogenic enzymes (zone-specific markers or general markers for steroidogenic differentiation e.g. SCC or SF-1) would help characterise the identity of the proliferative cells in different zones. A study of the distribution of apoptotic cells would also help to evaluate the models outlined in Fig. 7.3.

One of the limitations of the BrdU label-retaining study is that only some of the putative stem cells would be labelled in a 2 week chase period. An alternative transgenic approach to identify label-retaining cells more efficiently in mouse skin has been described (Tumbar et al., 2004). The retained label was a fluorescent histone-2B/GFP fusion protein (H2B-GFP) that was expressed specifically in the skin. H2B-GFP was incorporated into chromatin of all skin cells during development. Expression of the H2B-GFP in the skin was regulated by the tetOff system so could be switched off with doxycycline (a tetracycline analogue) for the chase period without the H2B-GFP label. Treatment with doxycycline for 4-16 weeks stopped expression of H2B-GFP, which was then diluted from the chromatin of proliferating cells, but retained in slow-cycling, putative stem cells. This allowed GFP label-retaining cells to be identified in the skin and then isolated by flow cytometry for further characterisation. If a similar H2B-GFP label-retaining system could be devised for the adrenal cortex it might be possible to isolate label-retaining cells by FACS sorting and characterise their properties as a first step towards isolating stem cells from the adrenal cortex.

7.4 Future directions

The work described in this thesis has involved analysing mosaic patterns and the distribution of cell proliferation to better characterise cellular aspects of organogenesis during growth of the mouse adrenal cortex (chapters 3 and 4) and its maintenance in the adult (chapters 5 and 6). Further work is required to complete and extend the specific experiments described. The experiments also raise wider questions, which could be addressed, for example, by experiments designed to identify the source of the cells that maintain the adrenal cortex.

7.4.1 Growth of the adrenal cortex

Experiments in chapters 3 and 4 suggest that stripes emerge in mosaic 21OH/*LacZ* adrenals by edge-biased growth. Further work required to characterise this more completely would include the following.

- Apoptosis should be studied during the period when stripes emerge to identify whether apoptotic cells are located in the positions predicted.

- Cell proliferation should be analysed at earlier fetal stages (from E14.5) to determine when the expected switch from interstitial to edge-biased growth occurs.

- Experiments should be designed to test whether cell divisions are randomly orientated during interstitial growth but generally radial once edge-biased growth begins. For example immunohistochemistry to detect the mitotic spindle could be used.

- Cell size measurements should be made to test whether embryonic and postnatal adrenal cortical growth involves increase in cell size (hypertrophy) as well as increase in cell numbers (hyperplasia) and whether cell shape changes occur during stripe formation to become radially elongated.

- The transition from mosaic patches to stripes should be re-analysed to identify whether stripes elongate at the outer edge of the adrenal as predicted. This could involve using a GFP mosaic model with better single-cell resolution, mosaics with lower proportions of labelled cells, or improved imaging techniques (e.g. 3D reconstruction of serial sections or optical projection tomography; Sharpe et al., 2002).

- Analysis of mosaic patterns at more time points between P7 and P14 should help follow the progress of stripe formation and identify whether stripes are exclusively in the definitive zone as predicted if the X zone is produced from a distinct set of fetal adrenal cortical cells.

- A combined analysis of mosaic patterns and zone-specific markers would help determine whether stripes have their origin in the ZG, ZI or outer ZF and if stripes are excluded from the X zone, as predicted above.

- A combined analysis of proliferative and zone-specific markers would help determine whether edge biased growth is associated with ZG emergence in the outer cortex and contributes to the emergence of zonation.

7.4.2 Maintenance of the adrenal cortex

Experiments in chapters 5 and 6 are consistent with the general hypothesis that the adrenal cortex is maintained by cell proliferation in the outer cortex, inward cell movement and apoptosis in the inner cortex near the cortical/medulla boundary. The following investigations would help to characterise this more completely:

- Double labelling (e.g. with BrdU and Ki67) should be used to investigate the rate and direction of cell movement between divisions and identify whether outward cell migration into the ZG occurs.

- Double labelling with BrdU and zone-specific markers would help delineate the proliferative region more precisely.

- Alternative approaches are needed to try to identify putative stem cells that maintain the adrenal cortex. One possibility would be to develop a label-retaining cell method based on labelling the chromatin protein rather than the DNA, similar to the fluorescent histone-2B/GFP fusion protein (H2B-GFP) used to identify label-retaining cells in the skin (Tumbar et al., 2004).

- Label-retaining cell experiments could be combined with double labelling and physiological interventions (such as unilateral adrenalectomy or administration of synthetic ACTH) to promote rapid proliferation. The first label (e.g. BrdU or H2B-GFP) would be followed by a chase period. Labelled cells would include putative stem cells and cells that terminally differentiate during the chase period. Use of the second label (e.g. IdU) during stimulation of cell proliferation would allow identification of label-retaining cells that were then stimulated to divide by the experimental intervention. This should help distinguish putative stem cells from terminally differentiated cells, which would not be expected to divide again and so would not incorporate the second label.

7.5 Conclusions

The adrenal cortex undergoes tissue remodelling during perinatal growth and is maintained by a balance of cell proliferation, movement and apoptosis in the adult, which may involve maintenance by stem cells. Edge-biased growth is likely to provide the initial impetus to the emergence of radial stripe patterns in *21OH/LacZ* adrenal cortices but this does not exclude the involvement of stem cells.

The study of BrdU-labelled cells reported here is consistent with the general hypothesis that the adrenal cortex is maintained by cell proliferation in the outer cortex, inward cell movement and apoptosis in the inner cortex near the cortical/medulla boundary. However, the possibility of outward cell migration into the ZG requires further investigation. Also, the detection of label-retaining cells following a long chase period suggests that putative stem cells might be located near or in association with the capsule, though it must be recognised that label retention may not be specific to stem cells. The adult β-gal stripe pattern does not show age-related changes similar to those seen in the corneal epithelium, which may reflect the relatively low cellular turnover in normal maintenance of the adrenal cortex.

Although it remains uncertain whether adrenal cortical stem cells exist and, if so, when they become specified and activated during development, the evidence reviewed here suggests that it is most likely that such stem cells do exist and they are located in the periphery

Bibliography

Badea, T. C., Wang, Y., and Nathans, J. (2003). A noninvasive genetic/pharmacologic strategy for visualizing cell morphology and clonal relationships in the mouse. *J Neurosci* **23,** 2314-22.

Ba-Omar, T. A., and Downie, J. R. (2006). Microscopic study of cell death in the adrenal glands of mouse and chick embryos. *Tissue Cell* **38,** 243-50.

Barker, N., van Es, J. H., Kuipers, J., Kujala, P., van den Born, M., Cozijnsen, M., Haegebarth, A., Korving, J., Begthel, H., Peters, P. J., and Clevers, H. (2007). Identification of stem cells in small intestine and colon by marker gene Lgr5. *Nature* **449,** 1003-1007.

Barrandon, Y., and Green, H. (1987). 3 clonal types of keratinocyte with different capacities for multiplication. *Proc Natl Acad Sci USA* **84,** 2302-2306.

Beebe, D. C., and Masters, B. R. (1996). Cell lineage and the differentiation of corneal epithelial cells. *Invest Ophthalmol Vis Sci* **37,** 1815-25.

Belloni, A. S., Mazzocchi, G., Meneghelli, V., and Nussdorfer, G. G. (1978). Cytogenesis in the rat adrenal cortex: evidence for an ACTH-induced centripetal cell migration from the zona glomerulosa. *Arch Anat Histol Embryol* **61,** 195-205.

Bez, A., Corsini, E., Curti, D., Biggiogera, M., Colombo, A., Nicosia, R. F., Pagano, S. F., and Parati, E. A. (2003). Neurosphere and neurosphere-forming cells: morphological and ultrastructural characterization. *Brain Res* **993,** 18-29.

Bielinska, M., Parviainen, H., Porter-Tinge, S. B., Kiiveri, S., Genova, E., Rahman, N., Huhtaniemi, I. T., Muglia, L. J., Heikinheimo, M., and Wilson, D. B. (2003). Mouse strain susceptibility to gonadectomy-induced adrenocortical tumor formation correlates with the expression of GATA-4 and luteinizing hormone receptor. *Endocrinol* **144,** 4123-33.

Bielohuby, M., Herbach, N., Wanke, R., Maser-Gluth, C., Beuschlein, F., Wolf, E., and Hoeflich, A. (2007). Growth analysis of the mouse adrenal gland from weaning to adulthood: time- and gender-dependent alterations of cell size and number in the cortical compartment. *Am J Physiol Endocrinol Metab* **293,** E139-46.

Bland, M. L., Desclozeaux, M., and Ingraham, H. A. (2003). Tissue growth and remodeling of the embryonic and adult adrenal gland. *Ann N Y Acad Sci* **995,** 59-72.

Bodenstein, L. (1986). A dynamic simulation model of tissue growth and cell patterning. *Cell Differ* **19,** 19-33.

Bodenstein, L., and Sidman, R. L. (1987a). Growth and development of the mouse retinal pigment epithelium. I. Cell and tissue morphometrics and topography of mitotic activity. *Dev Biol* **121,** 192-204.

Bodenstein, L., and Sidman, R. L. (1987b). Growth and development of the mouse retinal pigment epithelium. II. Cell patterning in experimental chimaeras and mosaics. *Dev Biol* **121,** 205-19.

Bodenstein, L., and Sidman, R. L. (1987c). Cell patterning in vertebrate development: models and model systems. *Curr Top Dev Biol* **21,** 1-29.

Booth, C., and Potten, C. S. (2000). Gut instincts: thoughts on intestinal epithelial stem cells. *J Clin Invest* **105,** 1493-9.

Breidert, M., Bottner, A., Moller, S., Herberg, L., and Bornstein, S. (1998). Apoptosis in the adrenal gland of non-obese diabetic (NOD) mice. *Exp Clin Endocrinol Diabetes* **106,** 478-83.

Budak, M. T., Alpdogan, O. S., Zhou, M., Lavker, R. M., Akinci, M. A., and Wolosin, J. M. (2005). Ocular surface epithelia contain ABCG2-dependent side population cells exhibiting features associated with stem cells. *J Cell Sci* **118,** 1715-24.

Carsia, R. V., Macdonald, G. J., Gibney, J. A., Tilly, K. I., and Tilly, J. L. (1996). Apoptotic cell death in the rat adrenal gland: an in vivo and in vitro investigation. *Cell Tissue Res* **283,** 247-54.

Chang, S. P. (2003). Patterns of clonal growth in the adrenal cortex and ovary revealed by transgenic and mosaic mice. Masters Thesis, University of Edinburgh

Chen-Pan, C., Yamamoto, Y., Ito, Y., Pan, I. J., and Hayashi, Y. (1996). A new type of cell death, the protruded type, observed in the adrenal gland of normal rats. *J Vet Med Sci* **58,** 373-6.

Collinson, J. M., Hill, R. E., and West, J. D. (2004). Analysis of mouse eye development with chimeras and mosaics. *Int J Dev Biol* **48,** 793-804.

Collinson, J. M., Morris, L., Reid, A. I., Ramaesh, T., Keighren, M. A., Flockhart, J. H., Hill, R. E., Tan, S. S., Ramaesh, K., Dhillon, B., and West, J. D. (2002). Clonal analysis of patterns of growth, stem cell activity, and cell movement during the development and maintenance of the murine corneal epithelium. *Dev Dyn* **224,** 432-40.

Cotsarelis, G., Cheng, S. Z., Dong, G., Sun, T. T., and Lavker, R. M. (1989). Existence of slow-cycling limbal epithelial basal cells that can be preferentially stimulated to proliferate: implications on epithelial stem cells. *Cell* **57,** 201-9.

Deane, H., Shaw, J., and Greep, R. (1948). The effect of altered sodium or potassium intake on the width and cytochemistry of the zona glomerulosa of the rat's adrenal cortex. *Endocrinol* **43,** 133–153.

Dobie, K., Mehtali, M., McClenaghan, M., and Lathe, R. (1997). Variegated gene expression in mice. *Trends Genet* **13,** 127-30.

Eguchi, Y. (1960). Experimental studies on the adrenal cortex of the mouse-fetus. I Effects of maternal adrenalectomy on the adrenal of the fetus based on histology and volume determination. *Develop Growth Differ* **5,** 206-218.

Ehrhart-Bornstein, M., Hinson, J. P., Bornstein, S. R., Scherbaum, W. A., and Vinson, G. P. (1998). Intraadrenal interactions in the regulation of adrenocortical steroidogenesis. *Endocr Rev* **19,** 101-43.

Estivarez, F. E., Lowry, P. J., and Jackson, S. (1992). Control of adrenal growth. *In* "The Adrenal Gland. 2nd edition, " (V. H. T. James, Ed.), pp. 43-70. Raven Press, New York

Ganong, W. F. (1997). "Review of medical physiology." Appleton & Lange, Stamford, Conn.

Gardner, R. L., and Papaioannou, V. E. (1975). Differentiation in the trophectoderm and inner cell mass. *In* "The Early Development of Mammals. The Second Symposium of the British Society for Developmental Biology." (M. Balls and A. E. Wild, Eds.), pp. 107-132. Cambridge University Press, Cambridge.

Gottschau, M. (1883). Structur und embryonale entwickelung der Nebennieren bei Säugethieren. *Arch Anat Physiol. (Leipzig)* **9,** 412-458.

Hajkova, P., and Surani, M. A. (2004). Programming the X chromosome. *Science* **303,** 633-634.

Hatano, O., Takakusu, A., Nomura, M., and Morohashi, K. (1996). Identical origin of adrenal cortex and gonad revealed by expression profiles of Ad4BP/SF-1. *Genes Cells* **1,** 663-71.

Hinson, J., Raven, P., and Chew, S. L. (2007). "The endocrine system." Churchill Livingstone, New York.

Holgert, H., Dagerlind, A., and Hokfelt, T. (1998). Immunohistochemical characterization of the peptidergic innervation of the rat adrenal gland. *Horm Metab Res* **30,** 315-22.

Howard-Miller, E. (1927). A transitory zone in the adrenal cortex which shows age and sex relationships. *Am J Anat* **40,** 251-293.

Hu, M. C., Chou, S. J., Huang, Y. Y., Hsu, N. C., Li, H., and Chung, B. C. (1999). Tissue-specific, hormonal, and developmental regulation of *SCC-LacZ* expression in transgenic mice leads to adrenocortical zone characterization. *Endocrinol* **140,** 5609-18.

Humphries, A., and Wright, N. A. (2008). Colonic crypt organization and tumorigenesis. *Nat Rev Cancer* **8,** 415-424.

Huszar, D., Sharpe, A., Hashmi, S., Bouchard, B., Houghton, A., and Jaenisch, R. (1991). Generation of pigmented stripes in albino mice by retroviral marking of neural crest melanoblasts. *Development* **113,** 653-60.

Iannaccone, P. M. (1987). The study of mammalian organogenesis by mosaic pattern analysis. *Cell Differ* **21,** 79-91.

Iannaccone, P. M., and Weinberg, W. C. (1987). The histogenesis of the rat adrenal cortex: a study based on histologic analysis of mosaic pattern in chimeras. *J Exp Zool* **243,** 217-23.

Iannaccone, P., Morley, S., Skimina, T., Mullins, J., and Landini, G. (2003). Cord-like mosaic patches in the adrenal cortex are fractal: implications for growth and development. *FASEB J* **17,** 41-3.

Ikeda, Y., Shen, W. H., Ingraham, H. A., and Parker, K. L. (1994). Developmental expression of mouse steroidogenic factor-1, an essential regulator of the steroid hydroxylases. *Mol Endocrinol* **8,** 654-62.

Jackson, K. A., Majka, S. M., Wulf, G. G., and Goodell, M. A. (2002). Stem cells: a minireview. *J Cell Biochem Suppl* **38,** 1-6.

Kataoka, Y., Ikehara, Y., and Hattori, T. (1996). Cell proliferation and renewal of mouse adrenal cortex. *J Anat* **188 (Pt 2),** 375-81.

Keegan, C. E., and Hammer, G. D. (2002). Recent insights into organogenesis of the adrenal cortex. *Trends Endocrinol Metab* **13,** 200-8.

Kelly, S. J. (1975). Studies of the potency of the early cleavage blastomeres of the mouse. *In* "The Early Development of Mammals. The Second Symposium of the British Society for Developmental Biology." (M. Balls and A. E. Wild, Eds.), pp. 97-106. Cambridge University Press, Cambridge.

Kerr, J. F. (2002). History of the events leading to the formulation of the apoptosis concept. *Toxicology* **181-182,** 471-4.

Kiel, M. J., He, S., Ashkenazi, R., Gentry, S. N., Teta, M., Kushner, J. A., Jackson, T. L., and Morrison, S. J. (2007). Haematopoietic stem cells do not asymmetrically segregate chromosomes or retain BrdU. *Nature* **449,** 238-242.

Kim, A. C., and Hammer, G. D. (2007). Adrenocortical cells with stem/progenitor cell properties: recent advances. *Mol Cell Endocrinol* **265-266,** 10-16.

Kopp, H. G., Avecilla, S. T., Hooper, A. T., and Rafii, S. (2005). The bone marrow vascular niche: Home of HSC differentiation and mobilization. *Physiology* **20,** 349-356.

Landini, G., and Iannaccone, P. M. (2000). Modeling of mosaic patterns in chimeric liver and adrenal cortex: algorithmic organogenesis? *FASEB J* **14,** 823-7.

Levin, S. (1998). Apoptosis, necrosis, or oncosis: What is your diagnosis? A report from the Cell Death Nomenclature Committee of the Society of Toxicologic Pathologists. *Toxicol. Sci.* **41,** 155-156.

Levy, A., and Lightman, S. L. (1997). "Endocrinology." Oxford University Press, Oxford.

Majchrzak, M., and Malendowicz, L. K. (1983). Sex differences in adrenocortical structure and function. XII. Stereologic studies of rat adrenal cortex in the course of maturation. *Cell Tissue Res* **232,** 457-69.

Majno, G., and Joris, I. (1995). Apoptosis, oncosis, and necrosis. An overview of cell death. *Am J Pathol* **146,** 3-15.

Marshman, E., Booth, C., and Potten, C. S. (2002). The intestinal epithelial stem cell. *BioEssays* **24,** 91-98.

McCarthy, M., Turnbull, D. H., Walsh, C. A., and Fishell, G. (2001). Telencephalic neural progenitors appear to be restricted to regional and glial fates before the onset of neurogenesis. *J Neurosci* **21,** 6772-81.

McNicol, A. M., and Duffy, A. E. (1987). A study of cell migration in the adrenal cortex of the rat using bromodeoxyuridine. *Cell Tissue Kinet* **20,** 519-26.

Mesiano, S., and Jaffe, R. B. (1997). Developmental and functional biology of the primate fetal adrenal cortex. *Endocr Rev* **18,** 378-403.

Mintz, B. (1967). Gene control of mammalian pigmentary differentiation. I. Clonal origin of melanocytes. *Proc Natl Acad Sci U S A* **58,** 344-51.

Mitani, F., Mukai, K., Miyamoto, H., Suematsu, M., and Ishimura, Y. (1999). Development of functional zonation in the rat adrenal cortex. *Endocrinol* **140,** 3342-53.

Mitani, F., Mukai, K., Miyamoto, H., Suematsu, M., and Ishimura, Y. (2003). The undifferentiated cell zone is a stem cell zone in adult rat adrenal cortex. *Biochim Biophys Acta* **1619,** 317-24.

Mitani, F., Suzuki, H., Hata, J., Ogishima, T., Shimada, H., and Ishimura, Y. (1994). A novel cell layer without corticosteroid-synthesizing enzymes in rat adrenal cortex: histochemical detection and possible physiological role. *Endocrinol* **135,** 431-8.

Moog, F., Bennett, C. J., and Dean, C. M., Jr. (1954). Growth and cytochemistry of the adrenal gland of the mouse from birth to maturity. *Anat Rec* **120,** 873-91.

Moore, K. A., and Lemischka, I. R. (2006). Stem cells and their niches. *Science* **311,** 1880-1885.

Morley, S. D., Chang, S. P., Tan, S. S., and West, J. D. (2004). Validity of the 21-OH/LacZ transgenic mouse as a model for studying adrenocortical cell lineage. *Endocr Res* **30,** 513-9.

Morley, S. D., Viard, I., Chung, B. C., Ikeda, Y., Parker, K. L., and Mullins, J. J. (1996). Variegated expression of a mouse steroid 21-hydroxylase/beta-galactosidase transgene suggests centripetal migration of adrenocortical cells. *Mol Endocrinol* **10,** 585-98.

Mukai, K., Nagasawa, H., Agake-Suzuki, R., Mitani, F., Totani, K., Yanai, N., Obinata, M., Suematsu, M., and Ishimura, Y. (2002). Conditionally immortalized adrenocortical cell lines at undifferentiated states exhibit inducible expression of glucocorticoid-synthesizing genes. *Eur J Biochem* **269,** 69-81.

Nesbitt, M. N. (1974). Chimeras vs X inactivation mosaics: Significance of differences in pigment distribution. *Develop Biol* **38,** 202-207.

Nicolas, J. F., Mathis, L., and Bonnerot, C. (1996). Evidence in the mouse for self-renewing stem-cells in the formation of a segmented longitudinal structure, the myotome. *Development* **122,** 2933-2946.

Norton, A. J., Jordan, S., and Yeomans, P. (1994). Brief, high-temperature heat denaturation (pressure cooking): a simple and effective method of antigen retrieval for routinely processed tissues. *J Pathol* **173,** 371-9.

Nyska, A., and Maronpot, R. R. (1999). Adrenal gland. *In* "Pathology of the mouse. Reference and atlas." (R. R. Maronpot, G. A. Boorman, and B. W. Gaul, Eds.), pp. 509–536. Cache River Press, Vienna, IL.

Okamoto, M., and Takemori, H. (2000). Differentiation and zonation of the adrenal cortex. *Curr Op Endocrinol Diabetes* **7,** 122-127.

Opsahl, M. L., Springbett, A., Lathe, R., Colman, A., McClenaghan, M., and Whitelaw, C. B. (2003). Mono-allelic expression of variegating transgene locus in the mouse. *Transgenic Res* **12,** 661-9.

Pellegrini, G., Dellambra, E., Golisano, O., Martinelli, E., Fantozzi, I., Bondanza, S., Ponzin, D., McKeon, F., and De Luca, M. (2001). p63 identifies keratinocyte stem cells. *Proc Natl Acad Sci USA* **98,** 3156-3161.

Perrone, R. D., Bengele, H. H., and Alexander, E. A. (1986). Sodium Retention after Adrenal Enucleation. *Am J Physiol* **250,** E1-E12.

Pignatelli, D., Ferreira, J., Vendeira, P., Magalhaes, M. C., and Vinson, G. P. (2002). Proliferation of capsular stem cells induced by ACTH in the rat adrenal cortex. *Endocr Res* **28,** 683-91.

Potten, C. S. (2004). Radiation, the ideal cytotoxic agent for studying the cell biology of tissues such as the small intestine. *Radiat Res* **161,** 123-36.

Preston, S. L., Alison, M. R., Forbes, S. J., Direkze, N. C., Poulsom, R., and Wright, N. A. (2003). The new stem cell biology: something for everyone. *Mol Pathol* **56,** 86-96.

Race, G. J., and Green, R. F. (1955). Studies on zonation and regeneration of the adrenal cortex of the rat; effects of sodium restriction, potassium intoxication, corticotropin, and orchiectomy when studied with colchicine. *AMA Arch Pathol* **59,** 578-86.

Rahman, M. A., Hwang, G. L., Razak, S. A., Sohm, F., and Maclean, N. (2000). Copy number related transgene expression and mosaic somatic expression in hemizygous and homozygous transgenic tilapia (*Oreochromis niloticus*). *Transgenic Res* **9,** 417-27.

Rando, T. A. (2006). Stem cells, ageing and the quest for immortality. *Nature* **441,** 1080-6.

Reynolds, B. A., and Rietze, R. L. (2005). Neural stem cells and neurospheres--re-evaluating the relationship. *Nat Methods* **2,** 333-6.

Roach, S. A. (1968). "The Theory of Random Clumping." Methuen, London.

Ross, M. H., Kaye, G. I., and Romrell, L. J. (1995). "Histology: a text and atlas." Williams & Wilkins, Baltimore ; London.

Salmon, T. N., and Zwemer, R. L. (1941). A study of the life history of cortico-adrenal gland cells of the rat by means of trypan blue injections. *Anat Rec* **80,** 421-429.

Schlotzer-Schrehardt, U., and Kruse, F. E. (2005). Identification and characterization of limbal stem cells. *Exp Eye Res* **81,** 247-64.

Schmidt, G. H., Wilkinson, M. M., and Ponder, B.A.J (1986). Non-random spatial arrangement of clone sizes in chimaeric retinal pigment epithelium. *J Embryol Exp Morphol* **91**: 197-208.

Schmidt, M. V., Enthoven, L., van der Mark, M., Levine, S., de Kloet, E. R., Oitzl, M. S. (2003). The postnatal development of the hypothalamic-pituitary-adrenal axis in the mouse. *Int J Dev Neurosci* **21**, 125-132.

Schulte, D. M., Shapiro, I., Reincke, M., and Beuschlein, F. (2007). Expression and spatio-temporal distribution of differentiation and proliferation markers during mouse adrenal development. *Gene Expr Patterns* **7,** 72-81.

Sharpe, J., Ahlgren, U., Perry, P., Hill, B., Ross, A., Hecksher-Sorensen, J., Baldock, R., and Davidson, D. (2002). Optical projection tomography as a tool for 3D microscopy and gene expression studies. *Science* **296,** 541-5.

Skelton, F. R. (1959). Adrenal Regeneration and Adrenal-Regeneration Hypertension. *Physiol Rev* **39,** 162-182.

Smith, A. (2006). A glossary for stem-cell biology. *Nature* **441,** 1060-1060.

Spencer, S. J., Mesiano, S., Lee, J. Y., and Jaffe, R. B. (1999). Proliferation and apoptosis in the human adrenal cortex during the fetal and perinatal periods: Implications for growth and remodeling. *J Clin Endocrinol Metab* **84,** 1110-1115.

Sucheston, M., and Cannon, M. S. (1968). Development of zonular patterns in human adrenal gland. *J Morphol* **126,** 477-491.

Swann, H. G. (1940). The pituitary-adrenocortical relationship. *Physiol Rev* **20,** 493-521.

Tam, P. P., Williams, E. A., and Tan, S. S. (1994). Expression of an X-linked *HMG-lacZ* transgene in mouse embryos: implication of chromosomal imprinting and lineage-specific X-chromosome activity. *Dev Genet* **15,** 491-503.

Tan, S. S., Williams, E. A., and Tam, P. P. (1993). X-chromosome inactivation occurs at different times in different tissues of the post-implantation mouse embryo. *Nat Genet* **3,** 170-4.

Tanaka, S., and Matsuzawa, A. (1995). Comparison of adrenocortical zonation in C57BL/6J and DDD mice. *Exp Anim* **44,** 285-91.

Teitelbaum, H. A. (1942). The innervation of the adrenal gland. *Quart Rev Biol* **17,** 135.

Thomas, M., Keramidas, M., Monchaux, E., and Feige, J. J. (2003). Role of adrenocorticotropic hormone in the development and maintenance of the adrenal cortical vasculature. *Microsc Res Tech* **61,** 247-51.

Thomas, M., Northrup, S. R., and Hornsby, P. J. (1997). Adrenocortical tissue formed by transplantation of normal clones of bovine adrenocortical cells in *scid* mice replaces the essential functions of the animals' adrenal glands. *Nat Med* **3,** 978-83.

Tumbar, T., Guasch, G., Greco, V., Blanpain, C., Lowry, W. E., Rendl, M., and Fuchs, E. (2004). Defining the epithelial stem cell niche in skin. *Science* **303,** 359-63.

Van Cruchten, S., and Van den Broeck, W. (2002). Morphological and biochemical aspects of apoptosis, oncosis and necrosis. *Anat, Histol, Embryol: J Vet Med Ser C* **31,** 214-223.

Vinson, G. P. (2003). Adrenocortical zonation and ACTH. *Microsc Res Tech* **61,** 227-39.

Watt, F. M., Hogan, and B. L. M. (2000). Out of Eden: Stem cells and their niches. *Science* **287,** 1427-1430.

West, J. D. (1976). Clonal development of the retinal epithelium in mouse chimaeras and X-inactivation mosaics. *J. Embryol. Exp. Morphol.* **35,** 445-461.

West, J. D. (1978a). Analysis of clonal growth using chimaeras and mosaics. *In* "Development in Mammals" (M. H. Johnson, Ed.), Vol. 3, pp. 413-460. Elsevier, Amsterdam.

West, J. D. (1978b). Clonal growth versus cell mingling. *In* "Genetic Mosaics and Chimeras in Mammals" (L. B. Russell, Ed.), pp. 435-444. Plenum Press, New York.

West, J. D., Hodson, B. A., and Keighren, M. A. (1997). Quantitative and spatial information on the composition of chimaeric fetal mouse eyes from single histological sections. *Dev Growth Differ* **39,** 305-17.

Wilkie, A. L., Jordan, S. A., and Jackson, I. J. (2002). Neural crest progenitors of the melanocyte lineage: coat colour patterns revisited. *Development* **129,** 3349-57.

Wilson, A., and Trumpp, A. (2006). Bone-marrow haematopoietic-stem-cell niches. *Nat Rev Immunol* **6,** 93-106.

Winter, J. S. D. (1985). The adrenal cortex in the fetus and neonate. *In* "Adrenal Cortex" (D. C. Anderson and J. S. D. Winter, Eds.). Butterworths, London.

Wotus, C., Levay-Young, B. K., Rogers, L. M., Gomez-Sanchez, C. E., and Engeland, W. C. (1998). Development of adrenal zonation in fetal rats defined by expression of aldosterone synthase and 11beta-hydroxylase. *Endocrinol* **139,** 4397-403.

Wright, N., and Voncina, D. (1977). Studies on the postnatal growth of the rat adrenal cortex. *J Anat* **123,** 147-56.

Wyllie, A. H., Kerr, J. F., and Currie, A. R. (1973a). Cell death in the normal neonatal rat adrenal cortex. *J Pathol* **111,** 255-61.

Wyllie, A. H., Kerr, J. F., Macaskill, I. A., and Currie, A. R. (1973b). Adrenocortical cell deletion: the role of ACTH. *J Pathol* **111,** 85-94.

Zajicek, G., Ariel, I., and Arber, N. (1986). The streaming adrenal cortex: direct evidence of centripetal migration of adrenocytes by estimation of cell turnover rate. *J Endocrinol* **111,** 477-82.

Zhou, S., Schuetz, J. D., Bunting, K. D., Colapietro, A. M., Sampath, J., Morris, J. J., Lagutina, I., Grosveld, G. C., Osawa, M., Nakauchi, H., and Sorrentino, B. P. (2001). The ABC transporter Bcrp1/ABCG2 is expressed in a wide variety of stem cells and is a molecular determinant of the side-population phenotype. *Nat Med* **7,** 1028-34.

Zubair, M., Ishihara, S., Oka, S., Okumura, K., and Morohashi, K. (2006). Two-step regulation of *Ad4BP/SF-1* gene transcription during fetal adrenal development: initiation by a Hox-Pbx1-Prep1 complex and maintenance via autoregulation by Ad4BP/SF-1. *Mol Cell Biol* **26,** 4111-21.

Zwemer, R. L., Wotton, R. M., and Norkus, M. G. (1938). A study of corticoadrenal cells. *Anat Rec* **72,** 249-263.

Appendix 1

Statistical modelling used by Dr Robert Elton (Medical Statistics Consulting, Edinburgh) to analyse adrenal weights

(This appendix is based on a longer written report provided by Dr Elton.)

A1.1 Effects of sex and adrenal position (left versus right)

The $\log_{10}$-transformed adrenal size data was analysed by Dr Robert Elton to test for effects of sex and adrenal position (left versus right) on adrenal size and to investigate the shape of the growth curve. General linear modelling (a mixture of analysis of variance and regression) was used to fit factors such as litter, sex and side (left versus right) and covariates such as age.

To test for sex effects, models were fitted with age, sex and litter group as factors. For length this gave a significant result (P=0.014) with females tending to have larger adrenals after adjusting for age and litter. The 95% confidence limits for the mean difference on the log scale (to base 10) were 0.003 to 0.025, which translates on taking antilogs to female adrenals being between 0.7% and 5.9% longer on average at a given age, compared to males. For width (omitting the P5 data, which may be aberrant for reasons discussed in section 4.4.1), the sex effect was not significant (P=0.53, confidence limits -1.8% to +3.5%). However, the sex effect on the ratio of length to width was also not significant, so it is not clear whether the contrasting results between males and females for width and length indicate a genuine difference in the magnitude of any sex effects.

A similar analysis indicated that left-sided adrenals tended to be larger than right-sided ones. This was not quite significant for length (P=0.08, -0.2% to +4.2% for L versus R), but was highly significant for width (P<0.001, +1.9% to +6.4%), and once again the test for side (L versus R) effects on the ratio was not significant.

To test whether differences between sexes and adrenal position only applied to later stages (after P5), Dr Elton performed an interaction test for age and sex in

the analysis of length, which fits the product of age and sex as an extra term in the multiple regression and examines whether the sex effect is related to age. This was non-significant (P=0.26), showing no evidence that the magnitude of the sex effect changes with age.

A1.2 Shape of the adrenal growth curve

The initial impression was that the adrenal growth curve (on unlogged measurements) might be triphasic with a plateau phase, where size increased only slowly, from around E16.5 until P5. Dr Elton was asked if he could test whether the growth curve was likely to be tri-phasic.

Cubic Model: The relationship between adrenal size and age is not straightforward to test for several reasons. First, the impression of extra variation over and above a smooth trend was confirmed by fitting parametric curves to the data. The most sensible model for a 'plateau' or temporary slow-down in the growth curve would be a cubic model, which is simple to fit and the right sort of shape at least over the range of ages measured. Therefore the model was fitted with age as a cubic (in addition to sex, side, but not litter this time) and this was compared to the fit of a model entering age as a factor (i.e. not assuming any particular smooth shape for the curve). This gives an F-test which yielded $F(9,162) = 3.15$ ($P<0.01$) for length and $F(8,151) = 4.92$ ($P<0.001$) for width. Thus both measurements are more variable from day to day than would be expected from variation around the most complex smooth curve that it is sensible to fit. *The result for both length and width is that the cubic fits very little (and not significantly) better than the straight line, suggesting that evidence for a plateau in the growth curve somewhere over the period E16.5 and P5 is weak.*

Quadratic Model: Although the cubic model provided no statistical support for a plateau it was still possible that the curve was non-linear (e.g. with faster rates of growth after P5). To address this Dr Elton tried one more set of analyses by fitting quadratics, rather than cubics, - this to test for a smooth increase in slope of the

$\log_{10}$-transformed growth data with age, which may be more biologically plausible than a sudden change at a particular point. This also avoids having to choose where that point is - if it's chosen informally, by inspection of the graph, that may cause a bias in favour of finding a significant change.

The analyses were performed for length, width and volume (on the log scale, omitting P5 for the last two, adjusting for sex, side and litter as before). The P-values for the quadratic terms were 0.52, 0.23 and 0.21 respectively. Thus there is little evidence for a steadily increasing slope (of logged values). This may seem surprising given the apparent pattern in the plots but this probably reflects the need for larger or more tightly controlled experiments to pin down the exact shape of these curves. *Thus there is no evidence that the growth curve (for the logged values) is non-linear.*

Summary:

- There seems to be unexplained variation from day to day, possibly caused by experimental error or small sample size.
- Females of a given age have longer adrenals than males.
- Left-sided adrenals of a given age are wider than right-sided ones.
- There is little evidence for a plateau in the growth curve.
- There is little evidence for a steadily increasing slope (of logged values).